The Effect of Manipulated Flows on Fish Kinematics and Behaviour at Migratory Barriers

Guglielmo Sonnino Sorisio

Cardiff University

Supervised by:

Prof. Catherine A.M.E Wilson and Prof. Jo Cable

This thesis is submitted in partial fulfilment of the requirements for the degree of

Doctor of Philosophy (Ph.D.)

2024

Abstract

Anthropogenic structures in rivers have caused the current state of the world's freshwater bodies to become highly fragmented. This has caused an overall decline in biodiversity and has majorly impacted migratory fish populations by blocking their migration pathways. Fish passes are therefore required to allow fish to migrate past these obstructions and complete their life cycle, but each obstruction presents its own challenges and requires a separate solution. In this thesis, emerging threats and current fish protection measures are assessed and new passage solutions are tested through the consideration of fish behaviour and kinematic in response to the manipulated hydrodynamics produced by the passage solutions. The experiments were carried out in laboratory recirculating open channel flumes. The current European eel (*Anguilla anguilla*) screening regulations were tested with different screening materials, screen angles, and flow velocities (Chapter 2). The current regulations did not produce any impingement or entrainment of eels through the screens at velocities allowed by the regulations but started to occur when velocity was increased showing that the regulations give appropriate velocity ranges. Eel tiles were investigated as a possible solution for high velocity barriers, the hydrodynamic analysis (Chapter 3) revealed that over a range of flow conditions the tiles produced low velocity flow around them and shear layers when in contact with the open channel. Juvenile eels had higher passage rates with the presence of the tiles (Chapter 4) and were able to pass upstream with reduced swimming effort compared to eels not using the tiles. Three-spined sticklebacks (*Gasterosteus aculeatus*) similarly benefitted from the tiles and shoaling sticklebacks had significantly higher passage rates (Chapter 5). The shoaling dynamics of sticklebacks were therefore investigated (Chapter 6) and these analyses revealed that there is a hydrodynamic benefit to stickleback shoaling. The effects of shoaling on rainbow trout (*Oncorhynchus mykiss*) interacting with different hydrokinetic turbine configurations presented bolder behaviour towards the turbine in the trout and increased the fish's usage of the turbine wake to reduce swimming effort (Chapter 7). By using colour to increase the contrast of turbine blades with the background, and unwanted turbine interactions that could potentially lead to impact with the rotor were decreased (Chapter 8). The overall findings from this thesis show that hydrodynamic conditions and behavioural factors are important when evaluating fish passage.

Acknowledgements

Contents

List of publications and conferences

Journal articles

Müller, S., Muhawenimana, V., **Sonnino Sorisio, G.**, Wilson, C. A. M. E., Cable, J., & Ouro, P. (2023). Fish response to the presence of hydrokinetic turbines as a sustainable energy solution. Scientific Reports, 13(1), 7459. https://doi.org/10.1038/s41598-023-33000-w

Sonnino Sorisio, G., Müller, S., Wilson, C. A. M. E., Ouro, P., & Cable, J. (2023). Colour as a behavioural guide for fish near hydrokinetic turbines. Heliyon, e22376. https://doi.org/10.1016/j.heliyon.2023.e22376 (Chapter 8)

Sonnino Sorisio, G., Wilson, C. A. M. E., Don, A., & Cable, J. (2024). Fish passage solution: European eel kinematics and behaviour in shear layer turbulent flows. Ecological Engineering, 203, 107254. https://doi.org/10.1016/j.ecoleng.2024.107254 (Chapter 4)

Conference proceedings

Sonnino Sorisio, G., Don, A., Cable, J., & Wilson, C. (2023). Eel tile hydrodynamics: mitigation at entraining flows. IFM First International Fish Impingement and Entrainment Conference. Liverpool, UK (Chapters 3 and 4)

Sonnino Sorisio, G., Robison-Smith, Wilson, C., C. Don, A., & Cable, J. (2024). Evaluation of current eel screening regulations and eel dynamics at exclusion screens and bypasses. IFM 2nd International Eel Science Symposium. Liverpool, UK (Chapter 2)

Conference presentations

Jones, D., **Sonnino Sorisio, G.,** & Wilson, C. (2024). Performance, degradation and regeneration of instream woody barriers over time.12th IAHR International Conference on Fluvial Hydraulics. Liverpool, UK

Sonnino Sorisio, G., Don, A., Cable, J., & Wilson, C. (2022). Slow and Steady? The Effect of Flow over Eel Tile and its Instabilities on Eel Kinematics. APS Division of Fluid Dynamics Meeting. Indianapolis, USA (Chapters 3 and 4)

Sonnino Sorisio, G., Don, A., Cable, J., & Wilson, C. (2023). European Eel kinematics over Eel Tiles under different hydrodynamic conditions. 40th IAHR World Congress. Vienna Austria. (Chapters 3, 4, and 5)

Sonnino Sorisio, G., Don, A., Cable, J., & Wilson, C. (2023). Eel tile hydrodynamics: mitigation at entraining flows. IFM First International Fish Impingement and Entrainment Conference. Liverpool, UK (Chapters 3 and 4)

Sonnino Sorisio, G., Lenton, K., Don, A., Cable, J., & Wilson, C. (2021). Slowing the Flow: the Hydrodynamics of Benthic Protrusions and their Impact on European Eel (*Anguilla anguilla*) Kinematics. APS Division of Fluid Dynamics Meeting. (Chapter 3)

Sonnino Sorisio, G., Robison-Smith, Wilson, C., C. Don, A., & Cable, J. (2024). Evaluation of current eel screening regulations and eel dynamics at exclusion screens and bypasses. IFM 2nd International Eel Science Symposium. Liverpool, UK (Chapter 2)

List of figures

List of tables

Abbreviations

ADV	Acoustic doppler velocimetry
AIC	Akaike information criterion
BAEP	Best achievable eel protection
BL	Body length
CFD	Computational fluid dynamics
CO	Co-rotating
CRB	Counter-rotating backwards
CRF	Counter-rotating forwards
EA	Environment Agency
FBF	Fin beat frequency
FFT	Fast Fourier transform
FPS	Frames per second
GLM	Generalised linear model
GLMM	Generalised linear mixed model
HK	Hydrokinetic
HPP	Hydropower plant
IUCN	International union for conservation of nature
KH	Kelvin-Helmholtz
LP	Large protrusions
NACA	National Advisory Committee for Aeronautics
PCA	Principal component analysis
PDF	Probability density function
PIT	Passive integrated transponder
PIV	Particle image velocimetry
RAS	Recirculating aquaculture system
Re	Reynolds number
rms	Root mean square
RPM	Rotations per minute
RSS	Reynolds shear stress
SE	Standard error
SP	Small protrusions

SVAT	Single vertical axis turbine
TBF	Tailbeat frequency
TI	Turbulent intensity
TKE	Turbulent kinetic energy
TL	Total length
TVAT	Twin vertical axis turbine
SL	Standard length
UK	United Kingdom
UN	United nations
USA	United States of America
VAT	Vertical axis turbine
Ve	Escape velocity
Vs	Sweeping velocity

Nomenclature

Greek symbols

α	Angle to the longitudinal direction
ΔS	Spacing between protrusions
$\emptyset$	Solid volume fraction
λ	Tip speed ratio
μ	Dynamic viscosity
ρ	Density
τ_{uv}	Horizontal Reynolds shear stress
τ_{uw}	Vertical Reynolds shear stress
υ	Kinematic viscosity
ω	Rotational velocity

Latin symbols

BL	Fish body length
C_D	Coefficient of drag
D	Turbine diameter
d	Stem or protrusion diameter
f	frequency
H	Total flow depth
h	Flow depth
M	Fish mass
n	Manning's n value
Q	flowrate
R	Hydraulic radius
Re	Reynolds number
Re_d	Protrusion Reynolds number
Re_R	Flume Reynolds number
St	Strouhal number
U	Bulk or average streamwise velocity
$\bar{u}$	Time averaged streamwise velocity
u	Streamwise velocity
u'	Streamwise velocity fluctuation

V	Bulk or average lateral velocity
v	Lateral velocity
$\bar{v}$	Time averaged lateral velocity
v'	Lateral velocity fluctuation
Ve	Escape velocity
Vs	Sweeping velocity
W	Bulk or average vertical velocity
w	Vertical velocity
$\bar{w}$	Time averaged vertical velocity
w'	Vertical velocity fluctuation

Chapter Contributions

The following list details contributions to each data chapter of this thesis.

Chapter 2: Conceptualisation and methodology by Prof. Jo Cable, Prof. Catherine Wilson, Andy Don, and Guglielmo Sonnino Sorisio. Data collection by Guglielmo Sonnino Sorisio and Charlotte Robison-Smith. Analysis, visualisation, and writing by Guglielmo Sonnino Sorisio and editing by all of the above. Advice and input from Chris Bell and Chris Grzesiok.

Chapters 3, 4, and 5: Conceptualisation and methodology by Prof. Jo Cable, Prof. Catherine Wilson, Andy Don, and Guglielmo Sonnino Sorisio. Data collection by Guglielmo Sonnino Sorisio, Kathryn Lenton and Nia Davies. Analysis, visualisation, and writing by Guglielmo Sonnino Sorisio and editing by all of the above. Advice and input from Petr Denissenko, Chris Bell and Chris Grzesiok.

Chapter 6: Conceptualisation and methodology by Prof. Jo Cable, Prof. Catherine Wilson, and Guglielmo Sonnino Sorisio. Data collection by Guglielmo Sonnino Sorisio. Data processing by Guglielmo Sonnino Sorisio and Joseph Johnson. Analysis, visualisation, and writing by Guglielmo Sonnino Sorisio and editing by all of the above.

Chapter 7: Conceptualisation and methodology was by Prof. Jo Cable, Prof. Catherine Wilson, Dr. Stephanie Müller, Dr. Pablo Ouro, Dr. Valentine Muhawenimana, and Guglielmo Sonnino Sorisio. Data collection by Guglielmo Sonnino Sorisio and Dr. Stephanie Müller. Analysis, visualisation, and writing by Guglielmo Sonnino Sorisio and editing by all of the above.

Chapter 8: Conceptualisation and methodology was by Prof. Jo Cable, Prof. Catherine Wilson, Dr. Stephanie Müller, Dr. Pablo Ouro, and Guglielmo Sonnino Sorisio. Data collection by Guglielmo Sonnino Sorisio and Dr. Stephanie Müller. Analysis, visualisation, and writing by Guglielmo Sonnino Sorisio and editing by all of the above.

Chapter 1. General Introduction

1.1 State of rivers

Rivers and other freshwater bodies are an important and valuable resource and are home to diverse ecosystems throughout the world. These resources currently face a multitude of challenges and are among some of the most threatened and overexploited habitats (Seliger & Zeiringer, 2018). This section gives an overview of the current state of rivers with particular focus on one of the major threats to riparian wildlife, the anthropogenic fragmentation of freshwater systems. Freshwater is exploited by humans for many uses, each impacting rivers. Overall, estimates of river fragmentation vary depending on methods used and location. Globally, only 23% of rivers have no obstructions and 37% have uninterrupted lengths of 1000 km or more (Grill et al., 2019); 48% of river volume is impacted by fragmentation (Grill et al., 2015). Fragmentation and connectivity vary regionally, with Europe highly impacted having an overall 68% of river length impacted and over 200,000 km of rivers affected but up to 95% for the Mediterranean basin (Duarte et al., 2020) and 97% in Great Britain (Jones et al., 2019; Parasiewicz et al., 2023). Even outside Europe, rivers can be highly fragmented, in New Zealand, for example over 50% of the river network is upstream of migration barriers for fish (Franklin et al., 2022). Other regions, despite currently being less fragmented, are at risk of becoming highly fragmented, a range of planned dams, particularly in the Amazon basin, could see the global percentage of fragmented river volume rise from 48% to 93% (Grill et al., 2015). These estimates are often derived from national and international databases which feature most large structures like dams, but many of these exclude smaller scale anthropogenic features like culverts, weirs, and low-head dams and small tributaries. This leads to an underestimation in migration barrier number and density by between 61% and 68% respectively (Belletti et al., 2020; Jones et al., 2019).

Estimates of the barrier number and density can therefore be imprecise unless they are ground-truthed. A conservative estimate of the number of barriers in Europe is 1.2 million barriers with a density of 0.74 barriers per km (Belletti et al., 2020). The type of barrier fragmenting the river is also relevant to understanding and mitigating the problem of fragmentation. Most attention has previously been given to dams built for varying purposes such as hydropower, flood mitigation, and water abstraction (Seliger & Zeiringer, 2018).

Large dams are typically defined as having a head drop of at least 15 m (Belletti et al., 2020; Seliger & Zeiringer, 2018), and globally 58,400 of these have been identified (Seliger & Zeiringer, 2018) with a large increase in the past six decades (Grill et al., 2015) and many more planned, especially in areas that are currently unobstructed (Belletti et al., 2020; Seliger & Zeiringer, 2018). These large dams, despite being well documented, make up less than 1% of the barriers in Europe (Belletti et al., 2020), whereas smaller hydropower structures are more common with 21,800 in the European Union alone (SETIS, 2013). Small hydropower represents 73% of the anthropogenic modifications in the USA with more than 50,000 known dams, most of which are mid-sized and account for 48% of water impoundment (Spinti et al., 2023). Worryingly, the regions with the best river connectivity like the Balkans in Europe (Belletti et al., 2020; Carolli et al., 2023), have the most new or planned dams (Carolli et al., 2023), and despite accounting for a small percentage (9.6% in Europe) of barriers (Belletti et al., 2020), very few river basins remain unaffected by them (van Puijenbroek et al., 2019). Belletti et al. (2020) produced one of the most complete inventories of barriers in Europe to date, and found that 68% of barriers have a head drop of 2 m or less, which also are the barriers most commonly left out of the databases. This inventory also reveals estimates for the proportion of barrier types, with weirs at 30.5%, ramps and bed sills at 31.5%, and culverts at 17.6% followed by dams, sluice gates, and fords.
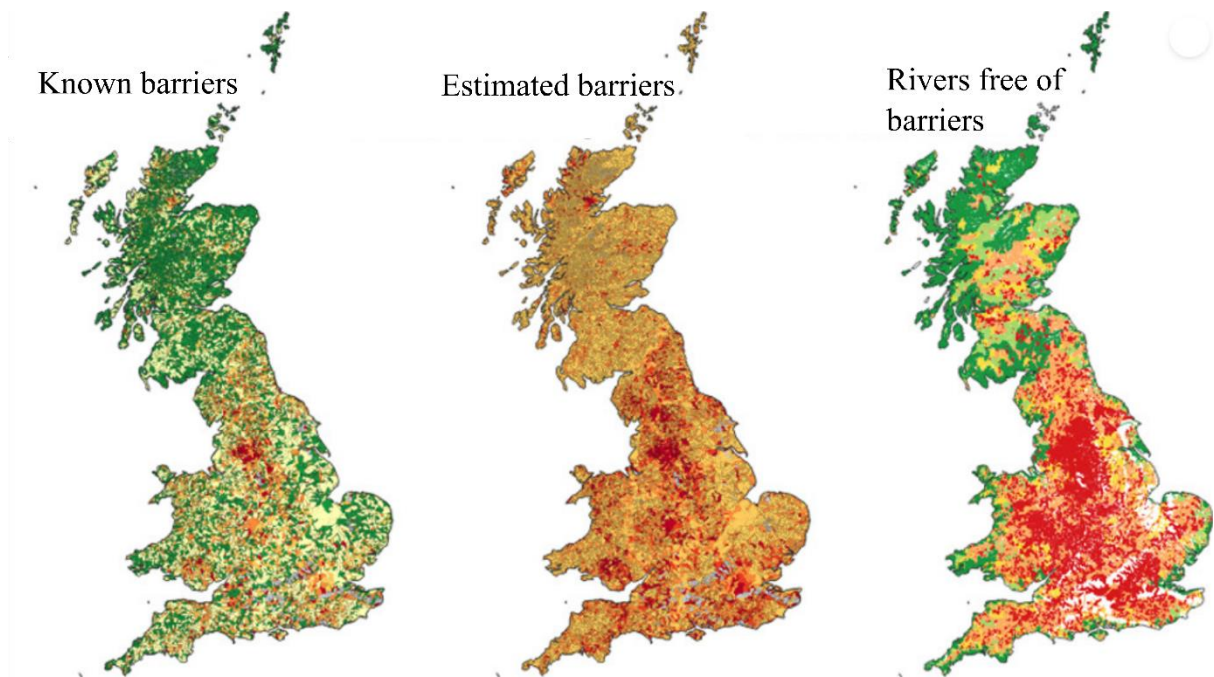
Figure 1.1. Maps of river fragmentation in the Great Britain detailing current and estimated barrier densities from national and international databases and field validation. Green represents the lowest density and red the highest except for the rightmost plot where green signifies the largest amount of free flowing rivers and red the least. Adapted from Jones et al., (2019).

All these barriers are known to fragment rivers, cutting off habitats but also preventing the natural transport of sediments (El Aoula et al., 2021; Kondolf & Schmitt, 2018; Leandro Velázquez-Luna et al., 2016) and causing chemical and thermal pollution in some cases (Raptis et al., 2016). The effect of fragmentation is most obvious for migratory fish that navigate between different habitats within freshwater or between fresh and saltwater to complete their life cycle. But fragmentation also has a strongly negative effect on overall biodiversity, species richness and abundance, and genetic diversity (Fahrig, 2003). Furthermore, the riparian flora species richness is linked to more free-flowing rivers (Andersson et al., 2000). In Europe, 37% of freshwater fish species are classified as threatened and a further 4% critically endangered, unsurprisingly therefore, this is one of the most at risk taxonomic groups globally with levels of extinction calculated as 1000 times over the natural level (Seliger & Zeiringer, 2018). This follows the trend of a global decline in freshwater biodiversity, and especially migratory fish populations since the 1980's. Hydropower dams have the potential to cause 100% morality of fish passing through them (Larinier & Travade, 2002) but small barriers, which are much more abundant, have recently

3

been identified as an even larger problem for freshwater fish (Belletti et al., 2020; Consuegra et al., 2021; Jones et al., 2019). Making remediation of this array of different barriers harder is the different passage requirement for each species and life stage (Jones et al., 2020). Fish species differ in swimming speed and style (Clough et al., 2004; Jones et al., 2020), and passage solutions have been focused on keystone migratory species like salmonids that have some of the highest swimming speeds, making passage even more difficult for other fish (Clough et al., 2004; Clough & Turnpenny, 2001; Taguchi & Liao, 2011). Although remediations can help reduce the effects of fragmentation (Erkinaro et al., 2017), variable fish passage efficiencies and flow conditions make fragmentation hard to evaluate (Shaw et al., 2016), and the effects of fragmentation are likely to be underestimated (Fuller et al., 2015) despite having a larger effect on migratory fish than other stressors (Dean et al., 2023).

The direct effects of these barriers must be considered with the indirect effects such as thermal pollution for example. This can cause an increase in water temperature of more than 5°C measured on a yearly average basis which is concerning since fish are very sensitive to temperature (Raptis et al., 2016). Other anthropogenic effects on rivers are the high levels of pollution (predicted to rise significantly), with many of these pollutants still poorly understood (Wen et al., 2017), biotic stressors such as parasites that often interact with environmental stressors, and climate change. The latter has caused reduced river flowrates and more extreme weather events from drought to flood (WMO, 2023) to which fish can be susceptible and which can reduce their ranges (Herrera et al., 2020). The effects of climate change also affect human populations with in turn puts further pressures on rivers by the construction of the necessary mitigation measures. Extreme floods affect more than 33 million people in Asia alone (WMO, 2023) and 3 billion people will potentially suffer water scarcity by 2050 (Wang et al., 2024) putting even more pressure of freshwater systems.

1.2 State of freshwater fish

This section briefly expands on the current status of freshwater fish populations following the various pressures faced listed in the previous section with particular focus on the three species featured in this thesis: The European eel (*Anguilla anguilla*), the rainbow trout (*Oncorhynchus mykiss*), and the three-spined stickleback (*Gasterosteus aculeatus*). Fish that spend at least part of their life in freshwater are a highly threatened group. Populations of migratory freshwater species have declined by an overall 81% according to databases

considering 284 species and 1864 separate populations (Deinet et al., 2024). The highest declines are found in Europe, Latin America and the Caribbean, and North America (75%, 91%, and 34% respectively) (Deinet et al., 2024). Data for Asia and Africa are still deficient making the estimated decline of 28% for Asia a conservative estimate, since focused analyses of the Mekong River revealed that 19% of the native fish in that river basin face extinction (Hughes, 2024). Overall, 92 freshwater fish species are now extinct, and 3303 out of 15830 assessed species are threatened with over 700 of these being critically endangered (IUCN, 2024). Dams and anthropogenic barriers are consistently classified as one of the top three threats to fish populations (IUCN, 2024; Muhlfeld et al., 2019). Species that face specific threats are in greater decline than those not threatened, but encouragingly, species with management plans in place declined less than others (Deinet et al., 2024).

The European eel (*Anguilla anguilla*) is a critically endangered catadromous fish native to Europe and Northern Africa (IUCN, 2024). Taking the European eel stocks of 1960 to 1979 as a baseline, this species has experienced a decline of over 95% (Dekker, 2003) with recent recruitment numbers as low as 0.6% in the North Sea and 5.5% elsewhere in Europe in 2021 (ICES, 2022). Although estimates from provisional data for 2022 show a partial recovery to 9.7% in Europe excluding the North Sea (ICES, 2022), eels still face many challenges in the freshwater stages of their life. General pollution and poor ecological status of rivers, the invasive parasite *Anguillicola crassus*, overfishing and illegal trafficking, and habitat fragmentation are all reasons for decline of this fish in freshwaters (ICES, 2022; Kirk, 2003; Pujolar et al., 2012). The life cycle of the eel is complex (Fig. 2). They start life in the Sargasso Sea as larvae known as Leptocephali and migrate over 5000 km to Europe using ocean currents (Cresci, 2020). They mature into glass eels, spend time in estuaries, sometimes remaining there indefinitely, before migrating into rivers. When glass eels first enter freshwater, they are not strong swimmers (McCleave, 1980; Vezza et al., 2020) and they use the tide - selective tidal stream transport (STST) - to help them enter the river (Harrison et al., 2014). They position themselves mid-flow depth during the flood tide and then remain closer to the banks and riverbed during the ebb tide to exploit the lower velocity of water in the boundary layer (Harrison et al., 2014). Notably, eels of all life stages swim near the riverbed to exploit the lower velocities (Haro et al., 2000). They only increase their upstream swimming behaviour against the tide when they are sufficiently upstream that the effect of the tide is lessened (Harrison et al., 2014). They also show increased shoaling behaviour in the upper estuaries (Harrison et al., 2014), a technique which can reduce energy

expenditure (de Bie et al., 2020). Juvenile eels are attracted by the freshwater flow from rivers, especially during high discharge (Cresci, 2020; Harrison et al., 2014), and all eel life stages are photophobic (Elvidge et al., 2018), migrating more in the first few hours of darkness (Bolland & Wright, 2009; Brown & Castro-Santos, 2009; Harrison et al., 2014; Lenihan et al., 2019). Juvenile eels will even abstain from migrating upstream during the full moon (Harrison et al., 2014). Temperature and turbidity also impact upstream migration. Below 6°C, reduced eel activity has been observed and critical temperatures at which migration occurs vary between 10 and 15°C, glass eels have been observed swimming up to 24.5°C (Boubée et al., 2001; Harrison et al., 2014). Turbidity is positively correlated with eel migration (Harrison et al., 2014). Conditions favourable for upstream migration are disrupted by barrages and other obstructions (Bult & Dekker, 2007), but strategies have been implemented to facilitate elvers passage over certain barriers such as weirs, dams, culverts, locks and gates. The European eel regulations of 2007 require that 40% overall escapement of silver eel should be obtained, and that each member country produce an eel management plan and as part of this, structures that prevent this objective to be reached should be equipped with appropriate measures (EC 1100/2001, European Commission. EU 2020). It is further required that connectivity is restored by "structural measures to make rivers passable".
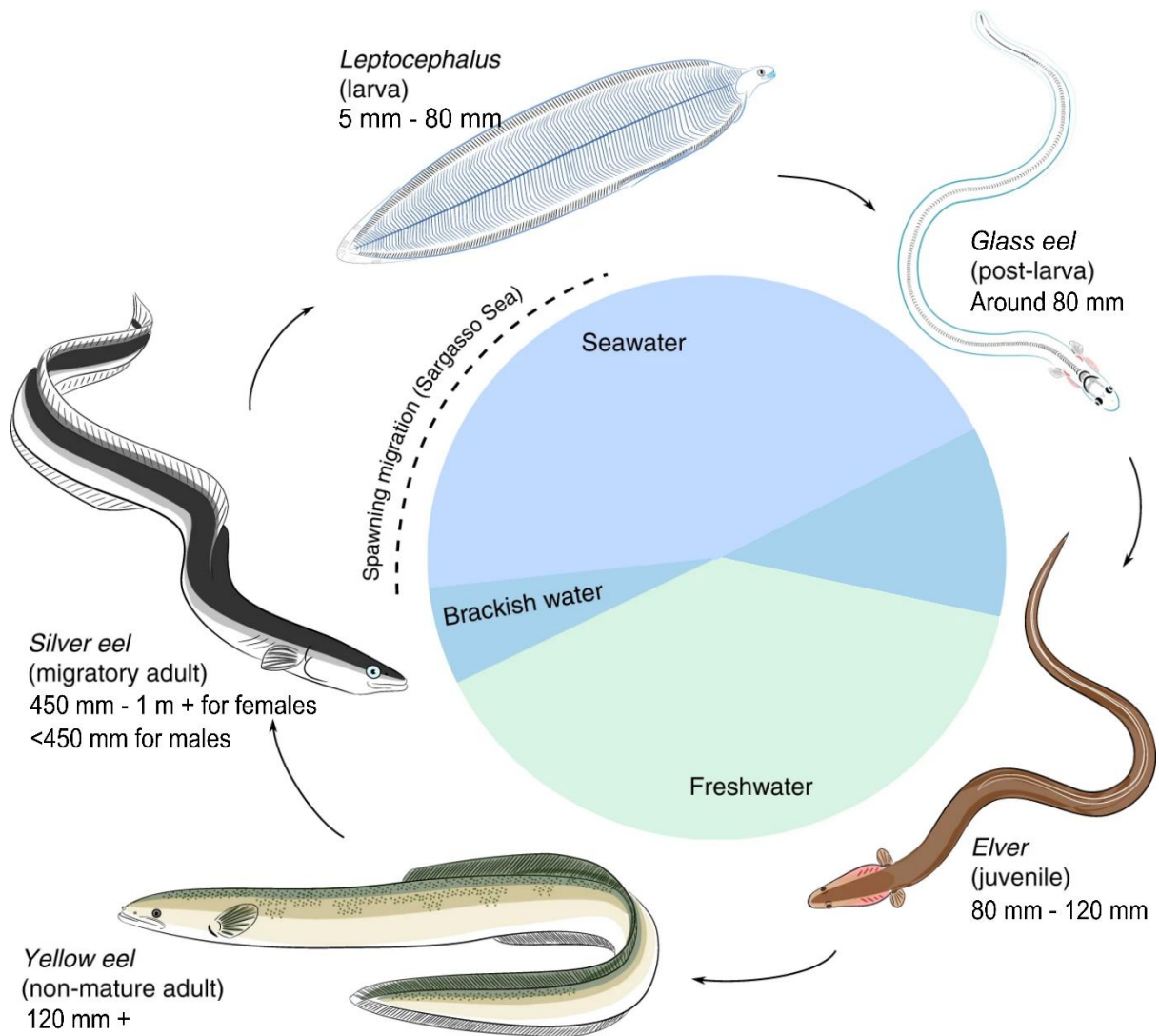
Figure 1.2. The migration pattern and life stages of the European eel (*Anguilla anguilla*). European eels perform two 5000 km migrations in their life, the first as leptocephali and the second as silver eels after having developed in the freshwater systems of Europe. Adapted from Cresci (2020).

As eels mature, they change from elvers to yellow eels, the latter being the form in which they will be present within the freshwater system without engaging in a major migration but will be obstructed when travelling both up and downstream. Slowly the yellow eels undergo silvering (Van Ginneken et al., 2007) at which point they are ready to migrate back to the sea. The seaward migration of eels occurs at different times all over Europe (Bruijs & Durif, 2009), which allows all individuals to reach the Sargasso Sea at the same time. In the UK, the migration takes place from October to January (Bruijs & Durif, 2009) and similarly the upstream migration can be influenced by many factors. Silver eels migrate within the first

hours of darkness (Brown & Castro-Santos, 2009), there is a close correlation between silver eel mass migration and river discharge (Fjeldstad et al., 2018; Jansen et al., 2007). Most silver eels migrate one to two days after high discharge events (Teichert et al., 2020), it has even been theorised that a controlled shutdown of hydropower facilities during the days over which eels migrate could save many individuals that would otherwise incur injury or death resulting from impacts with turbine blades (Teichert et al., 2020). As with juveniles, moon phase can also influence migration (Behrmann-Godel & Eckmann, 2003). The main obstacles faced by seaward migrating silver eels are water abstraction and hydroelectric facilities (Brown and Castro-Santos 2009; Dainys et al. 2018). Here, eels may become entrained and impinged, potentially causing severe injury and death (Dainys et al. 2018). Other migration barriers include dams, tidal gates, flaps and locks and weirs, which impede the downstream passage of eels, these may not cause high mortality or injury but can severely delay the migration of eels trapped upstream and cause unnecessary energy expenditure (Verhelst et al., 2014). The European eel is studied in this thesis as a critically endangered species of high conservational value in Europe and the UK. It is also unlike most other freshwater fish species in its kinematic gait and undulatory swimming characteristics which remain largely unstudied in applied fish passage scenarios.

The three-spined stickleback (*Gasterosteus aculeatus*) is a freshwater fish native to North America and Europe (IUCN, 2024) and, like rainbow trout, exist in both river resident and anadromous populations (Dalziel et al., 2012) leading to genetically distinct populations. Compared to trout, however, these fish are much smaller and have lower swimming abilities (Blake et al., 2005; Dalziel et al., 2012; Tudorache et al., 2007). They are well known to live in large shoals and to live in habitats with high amounts of vegetation for cover (Gagnon et al., 2019). They are currently classified as Least Concern (IUCN, 2024) but populations are fragmented, leading to genetic diversity arising between populations (Scharsack et al., 2012). This is has led to sticklebacks being popular in studies on evolution and genetic diversity caused by different pressures. Their natural tendency to live in shoals has also been used by researchers to investigate shoaling dynamics under different stressors such as disease (Stewart et al., 2018; Ward et al., 2005), and shoal size and familiarity (Barber & Ruxton, 2000; Mehlis et al., 2015). Its range is so extended that it has been considered for use as an environmental sentinel (Pottinger et al., 2002). This species represents a small-bodied fish with migratory and river resident populations. Combined with its limited swimming capacity in comparison to other species and its labriform form of locomotion,

this fish enables the evaluation of fish passage solutions to be tested for a non-target species. Its diverse nature compared to eels has the potential to offer insight into different aspects and scales of fish passage.

Salmonid fish are native to the northern hemisphere but have now been widely introduced in the southern hemisphere (Williams et al., 2015) and the status of species belonging to this family (various salmon species in particular) are closely monitored due to their value as food and sport fish. Many salmonids are migratory, either anadromous or potamodromous (McDowall, 1992). Some species like brown trout and sea trout (*Salmo trutta*) and rainbow trout and steelhead trout (*Oncorhynchus mykiss*) have both diadromous and potamodromous populations known by different names. These fishes are generally found in temperate regions and are therefore particularly susceptible to global warming which may restrict their range (Williams et al., 2015) and as migratory fish, river fragmentations also poses a significant threat to them. Currently, 73% of trout and char species are threatened with global extinction (Muhlfeld et al., 2019), with the top threats being invasiveness of other species (like rainbow trout, which is invasive throughout most of its range), and anthropogenic barriers (Muhlfeld et al., 2019). The rainbow trout is also an ideal model species for flume testing of emerging technologies as there is an extensive body of literature examining it in diverse flow scenarios and much is known about its swimming preferences and responses to turbulence. Combined with its conservational value in its native range where many hydrokinetic turbine installations have been proposed, this species was well placed as a model to use in the evaluation of this technology as a potential threat to fish populaitons.

1.3 Abstractions and Screening

Water abstractions from surface waters exist for a wide range of purposes, from public water supply, to agriculture, to electricity generation and pumping stations used to regulate water levels in channels. In England and Wales alone, around 20,000 abstraction licences exist for surface waters (DEFRA, 2022; Holleran, 2023; NRW, 2024), and these are not traditionally classified as migration barriers or sources of fragmentation when assessing river connectivity or barrier abundance (Belletti et al., 2020; Jones et al., 2019). Although water abstractions do not necessarily block the river width in its entirety or act as a gravity barrier, these abstractions do pose a threat to fish that may swim into them and get damaged by pumps, turbines, or other processes (Carter & Reader, 2000; Seaby, 2023). To prevent fish

from being harmed in abstractions, there are requirements for these to be screened (Environment Agency, 2020). This is often done by the placement of a physical screen to prevent fish from passing into the abstraction (Turnpenny & O'Keefe, 2005) but the screens currently in use still produce injury and mortality through impingement and entrainment. Impingement occurs when a fish is stuck on the screen surface as a result of the immediate flow field at the screen such that the fish cannot swim away, this causes mortality and increased predation (Hadderingh et al., 1992; Rytwinski et al., 2017) whereas entrainment occurs when fish are able to pass through the gaps in the screen and into an area which is potentially harmful for them (Carter & Reader, 2000). Several factors affect the screening efficiency; material (Lemkecher et al., 2022; Meister, 2020; Rose & Mesa, 2012), spacing (Beck, 2020; Carter et al., 2023; Ebel, 2016), inclination and angle (de Bie et al., 2021; Harbicht et al., 2022; Russon et al., 2010), and hydrodynamic conditions (Meister, 2020; Raynal et al., 2013). All these factors must be corrected to achieve the best fish protection (Environment Agency, 2020). Wherever possible, a bypass should be present to take the fish to a safer area and allow them to progress their migration.

Other screening strategies are available at water abstractions, these can even feature an active element to the design in which the screen moves in contrast with the passive function of the most deployed simple screens described above. These alternatives are described below but their performance has largely not been evaluated.

(i) Spillway screens allow water to be abstracted from the downstream weir wall that forms the spillway, this is achieved by replacing the weir wall with a screen so that water may flow into a channel below (Dorratcague et al., 1986).

(ii) Rotary disc screens are usually employed for smaller abstractions and consist of a series of vertical cylinders. Each cylinder is made of stacked discs with spacing between them, placed flush to the riverbank that rotate. These discs mesh with discs on the adjacent shaft (National Oilwell Varco, 2016). Little information is available on the performance of these screens in terms of fish exclusion and injury. These screens were initially designed to be self-cleaning (National Oilwell Varco, 2016).

(iii) Sub gravel intakes can be used for very small abstractions, in which water is filtered through a layer of gravel placed on top of a screen. This has minimal effect on the flow and any fish, preventing impingement (Turnpenny & O'Keefe, 2005).

(iv) Cylindrical wedge wire screens are an enclosed cylinder of wedge wire mesh with their axis aligned with the river flow (Kempema & Ettema, 2016), usually located close to the bank. This allows flow to enter the cylinder through the cylindrical grid section whilst also keeping fish out (Turnpenny & O'Keefe, 2005) and is particularly suitable for larval stages and other smaller fish (Sheridan et al., 2011). They rely on the sweeping current to carry impinged and debris safely downstream (Black, 2019) and can reduce mortalities, but they are particularly susceptible to ice formation and debris accumulation, which impede function (Kempema & Ettema, 2016).

(v) Fish recovery and return systems involve a system of buckets on a conveyor belt arrangement driven by motors serving as a fish lift (Black, 2019). A water jet is used to wash them into a return channel where they can be safely re-introduced to the river (Turnpenny, 2013). Buckets attached to screens should be capable of retaining the fish and preventing escape while also holding enough water with low turbulence (Black, 2019). The fish are washed out of the buckets by a low-pressure jet of water into the fish return system, which consists of a channel that leads back to the river and must be supplied with sufficient flow to keep the eels covered and moving. Electrification of bar racks can be effective for eels but also cause injury (Meister, 2020). Electric field strength can be used to selectively exclude some species of fish and longer fish are generally more affected by the electric field (Miller et al., 2024).

There are also alternatives to increase screening efficiency that rely on behavioural traits of fish to deter them from the abstraction. These have the advantage of being less intrusive on the flow of the river but the disadvantage is that every species might have a different behavioural response to each stimulus. Behavioural screens range from lights, acoustic, odour, and bubble curtains. Light can be used to dissuade fish from danger zones (Elvidge et al., 2018) as some species are photophobic (Harrison et al., 2014). Strobing light emitting diode (LED) arrays and other light sources have been successfully used as deterrents for various fish species (Ford et al., 2018, 2019). Continuous light can also deter eels (Hadderingh et al., 1992) as exemplified by studies on artificial light at night where European eels were more likely to pass in darkness (Vowles and Kemp, 2021) and, for other fish, has been used to illuminate physical screens to prevent impingement (Turnpenny & O'Keefe, 2005). Design considerations include the placement, intensity, strobe rate, colour and depth of the light source, and for all low turbidity is desirable.

Acoustic deterrents are another common form of behavioural deterrent and have been installed in front of intakes at several locations within the UK to deter many fish species (Turnpenny & O'Keefe, 2005) but are not always efficient for all species. In a flume study, silver eels were not influenced in their choice of route within an acoustic maze (Deleau, 2018), but in an *in situ* experiment they showed slightly greater avoidance in the presence on a screen when sound was played between 60 and 1000 Hz (Deleau et al., 2020b). In a forebay to a hydroelectric plant, a 12 Hz sound source was tested, under this treatment passage was similar to control but eels showed greater avoidance around the acoustic device (Piper et al., 2019).

Odour can be used an attractant to passes and bypasses rather than a deterrent, functioning to guide eels (Briand et al., 2002). In a field study, glass and yellow eels counts at the top of an eel ladder were 140% of the normal levels when water from a holding tank containing eels was directed to the top of the pass (Briand et al., 2002).

Bubble curtains are generated by releasing a stream of air from the riverbed along a line to form a curtain of bubbles, usually achieved by pumping air into a perforated tube (Turnpenny & O'Keefe, 2005). This is commonly used to reduce sound produced by underwater construction operations like drilling (Würsig et al., 2000). These have also been used as acoustic, visual and hydrodynamic screens (Zielinski & Sorensen, 2016). Bubble curtains have been successfully deployed for several carp species reducing passage by up to 80% (Zielinski and Sorensen 2016) and work better in darkness with reduced effectiveness in daylight (Flores Martin et al., 2021); however other studies have found their efficacy is poor (Mussalli et al., 1980; Sheridan et al., 2011). Factors that affect the effectiveness of bubble screens are the density and size of bubbles.

1.4 Hydropower plants

One of the dangers faced by seaward migrating fish are hydropower plant (HPP) facilities (Teichert et al., 2020), especially those which occupy the whole width of the river, which is the case for most of the larger installations and especially for silver eels migrating downstream. Here, fish may become entrained and impinged and facing severe injury and death (Carr & Whoriskey, 2008), or migration can be severely delayed if they are trapped upstream (Behrmann-Godel & Eckmann, 2003; Kerr et al., 2015; Trancart et al., 2020; Verhelst et al., 2014). Most studies conducted to evaluate route selection and behaviour used

in situ Passive Integrated Transponder (PIT) tagging, this involves catching fish and implanting them with a PIT tag, so the fish can then be tracked at PIT monitoring stations set up along the river (Baker et al., 2020; Wright et al., 2015). Although there have been many publications covering downstream eel passage at hydroelectric facilities, a knowledge gap still exists in finding an effective method to allow safe passage to migrating fish such as silver eels (Bolland & Wright, 2009). In the UK, fish passes are required at new obstructions in rivers where migratory fish such as salmonids and eels are present under the SAFFA and Eel Regulations (Armstrong et al., 2020; The Eels (England and Wales) Regulations 2009 No. 3344, 2009).

Screens are present before turbine inlets to prevent fish from swimming into the turbines (Gosset et al., 2005), however migrating fish are attracted by strong flows and will often enter the inlets nonetheless (Carr & Whoriskey, 2008). Turbines can severely injure or kill fish, and eels are more likely to be injured due to their elongated shape. There is commonly more than one Hydropower Plant (HPP) on a single river, just the High Rhine has 11 of these and there are many more before the sea is reached (Dębowski et al., 2020). Fish commonly show searching and circling behaviour in the forebay to a HPP (Brown & Castro-Santos, 2009) or perform rejections and swim back upstream (Brown & Castro-Santos, 2009), which can cause delays of days or weeks (Behrmann-Godel & Eckmann, 2003; Kerr et al., 2015; Trancart et al., 2020; Verhelst et al., 2014). This increases their energy expenditure, which could impact their migration (Van Den Thillart et al., 2004). The passes featured at these sites are usually tailored to salmonids and thus harder for other fish species to locate and navigate since the entrances are often located near the surface (Brown & Castro-Santos, 2009).

For low head installations, such as Archimedes screws, migration delays can be as low as 15 minutes (Kibel, 2008), but for other types of hydropower they can be days (Gosset et al., 2005; Pedersen et al., 2012), more than a week (Behrmann-Godel & Eckmann, 2003), multiple weeks (Haro et al., 2000; Pedersen et al., 2012) or more than a month (42 days) (Brown & Castro-Santos, 2009). Since on many rivers there are multiple HPPs, cumulative delays of 68 days have been measured (Piper & Wright, 2017) and this figure is likely to be larger for the worst-case scenario if delays of more than a week occur at >10 consecutive plants. Most studies found that European and American eels migrate into the forebays during the night (Bolland & Wright, 2009; Brown & Castro-Santos, 2009; Gosset et al., 2005; Haro

et al., 2000; Silva et al., 2016) but other studies suggest European silver eels arrive at forebays independent of time of day (Behrmann-Godel & Eckmann, 2003). Speed of downstream migration swimming has been reported in two studies to be 0.3 or 1.2 m/s (Behrmann-Godel & Eckmann, 2003; Brown & Castro-Santos, 2009). Silver eel migrations often show positive correlation with high flows and rain (Boubée & Williams, 2006; Brown & Castro-Santos, 2009; Buysse et al., 2014; Gosset et al., 2005). European and American Silver eels display rejections at trash racks and screens when they make contact with them (Behrmann-Godel & Eckmann, 2003; Brown & Castro-Santos, 2009) after which (if they are not impinged) they show searching and circling behaviour looking for exits (Behrmann-Godel & Eckmann, 2003; Brown & Castro-Santos, 2009; Carr & Whoriskey, 2008), but at this stage they will swim through the whole water column (Brown & Castro-Santos, 2009). Some American eels return upstream and are not recorded again (Brown & Castro-Santos, 2009). Most will attempt to pass downstream, most frequently through the turbines (Behrmann-Godel & Eckmann, 2003; Brown & Castro-Santos, 2009; Bruijs & Durif, 2009; Calles et al., 2010; Pedersen et al., 2012).

Different routes, each with different potential outcomes taken by fish at HPPs are listed below:

(i) They become impinged in the screen or trash and suffer injury or death (Baker et al., 2020; Boubée & Williams, 2006; Bruijs & Durif, 2009).

(ii) They pass the trash rack (Calles et al., 2012) and are injured by the turbine (Berg, 1986; Behrmann-Godel and Eckmann, 2003), this can occur in a number of ways, contact with the turbine, barotrauma (by rapid decompression) and shear stress (Brown et al., 2023; Koukouvinis & Anagnostopoulos, 2023), these injuries can cause delayed mortality due to scale loss, scratches, burst or damaged swim bladder or other injuries (Koukouvinis & Anagnostopoulos, 2023).

(iii) They pass through the turbine unharmed (Berg, 1986; Kibel, 2008), certain turbine designs are more fish friendly than others (Brown et al., 2023; Koukouvinis & Anagnostopoulos, 2023; Larinier, 2008).

(iv) They pass through the turbine and die because of contact with the turbine blades (Berg, 1986; Boubée et al., 2001; Larinier and Travade, 2002; Behrmann-Godel and Eckmann, 2003; Gosset et al., 2005; Bolland and Wright, 2009; Brown and Castro-Santos, 2009; Bruijs

and Durif, 2009; Calles et al., 2010; Pedersen et al., 2012; Buysse et al., 2014; Fjeldstad et al., 2018). Elongated fish and small turbines have higher mortality rates (Boubée et al., 2001).

(v) They use the spillway when flows are high enough (Larinier and Travade, 2002; Boubée and Williams, 2006; Silva et al., 2016; Piper et al., 2017; Baker et al., 2020) and are more likely to use the spillway than a bypass (Boubée & Williams, 2006; Piper et al., 2017). Spillways that drop 50-60 m can cause 100% mortality (Larinier and Travade, 2002) but spillways are still a safer option than the turbine route as evaluated in a laboratory flume study (Silva et al., 2016). If the upstream section of the spillway is sloped (30-45º) rather than a vertical wall (90º), European eels are more likely to pass over them (Silva et al., 2016). The ramp guides the eels from the riverbed and causes smoother acceleration whilst avoiding recirculation zones, which eels avoid, and this can increase passage from 58% to 95% (Silva et al., 2016). Significant delays have been found in fish passage caused by spillways and dams (Baker et al., 2020; Trancart et al., 2020) or where fish were unable to use the spillway (Trancart et al., 2020). Mortality is between 0-37% for spillways 30-60 m high (Larinier and Travade, 2002). Fish can be injured by the shear, abrasion to the surface (which can be mitigated by different surfaces), pressure changes, contact with baffles or turbulence in the basin below (which should be kept to a minimum). Large fish, such as adult European eels, need to stay within the descending water column to avoid reaching high terminal velocities (Larinier and Travade, 2002).

(vi) They use a bypass or fish pass (Boubée & Williams, 2006; Gosset et al., 2005). Surface sluices are the most common in HPPs (Larinier, 2008) but these prove hard to find for bottom dwelling fish and have low efficiency for European and American eels (Brown & Castro-Santos, 2009; Pedersen et al., 2012). Bottom sluices are 42-53% efficient compared to 8-14% efficiency for a surface sluice under similar flow conditions (Gosset et al., 2005). Piper et al. (2017) found that the overshot bypass (over a weir) was the chosen route for a large percentage of European eels compared to the undershot bypass (through redundant HPP turbines). The route to the undershot bypass was less commonly used, due to rejections made at a debris boom and the entrance was also screened by a bar rack. To reduce rejections, the entrance to the bypass should have a bellmouth design to create a smoother flow acceleration (Sheridan et al., 2011).

The type and design of turbine present at a HPP can affect the injuries suffered by European eels (Larinier, 2008). Kaplan turbines are extremely common in Europe (Bruijs & Durif, 2009), but cause a wide range of eel mortality rates as shown in Table 1.1. Dainys et al. (2018) compared a Kaplan turbine to a CINK crossflow turbine but found that it had four times (100% vs 25%) the mortality rate of the tested Kaplan turbine.

The Archimedes screw is generally considered to have the best potential for allowing European eels to pass unharmed (Kibel, 2008; Buysse et al., 2014; Buysse et al., 2015; Piper et al., 2018). The mortality rate for these turbines ranges according to size, general design and use but is consistently low in comparison with the high maximum percentages of deaths of the other common types of turbines. Mortality rate of Archimedes screws ranges from 0% (Piper et al. 2018) to 19% (Buysse et al., 2015) making this the most eel friendly option, it has been found however, that other fish such as bream (*Abramis brama*) can suffer higher mortality rates than this (Pauwels et al., 2020).

Recently, there has been an increasing attention on producing 'fish friendly' turbines and pumps that allow fish to escape through the other side unharmed. These designs aim to minimise the risk of injury through barotrauma, blade strike, pinching between the blades and the housing, and shear stress and turbulence (Koukouvinis & Anagnostopoulos, 2023). New designs vary but incorporate the following design criteria; reducing the number of blades, low rotational speeds, larger radiuses on the blade leading edge, swept leading edge, and large openings for the fish to go through (Brown et al., 2023; Koukouvinis & Anagnostopoulos, 2023; Río et al., 2024). Many of these designs, however, are not currently in widespread operation and most HPPs still rely on the more harmful Francis and Kaplan designs.

Most large river basins have cumulative effects from several HPPs (Bruijs & Durif, 2009; Larinier, 2008). In fact, the escapement of silver eels from the High Rhine is 7% (Brujis and Durif, 2009) and this does not account for delays and energy expenditure. Calculations of mortality rate based on telemetry data potentially underestimate the number of deaths since fatally injured European eels can remain active for up to 48 hours after turbine passage (Heisey et al., 2019). Furthermore, surviving eels may be injured and even if they are not, increased energy expenditure means they are less healthy than control eels that have not passed through Kaplan turbines (Ben Ammar et al., 2021).

Table 1.1 A review of mortality rates experienced by seaward migrating silver eels. The species of eel being studied depends on whether the experiment was conducted in North America (*Anguilla rostrata*) or Europe (*Anguilla anguilla*). The flowrates given are the total flowrate through all the turbines and varies largely as does the capacity of the hydropower plant and size of the plant, where the flowrate is given as a single number, this is the annual average. Mortality rate is given as the percentage of fish that died out of all fish entering the turbine, this means passage rate can be higher than implied by the mortality rate if the eels are using other routes to migrate downstream. Although the rate of mortality varies widely for every turbine type, the Archimedes screw is overall the most fish friendly. *Denominates where more than one HPP and location was considered to produce the data and +denominates where the flowrate data is not included.

Location	Species	Mortality (%)	Flowrate (m^3s^{-1})	Turbine	Reference
River Mosel, Germany	*A. anguilla*	20-90	*	Kaplan	(Behrmann-Godel & Eckmann, 2003)
Neckarzimmern	*A. anguilla*	50	40-80	Kaplan	(Berg 1986)
Cabot station, Massachussets	*A. rostrata*	25	262	Francis	(Brown & Castro-Santos, 2009)
River A'tran	*A. anguilla*	74	20-230	Francis	(Calles et al., 2010)
*	*A. anguilla*	100	*	Pelton	(Larinier & Travade, 2002)
*	*A. anguilla*	15-30	*	Kaplan	(Larinier & Travade, 2002)
*	*A. anguilla*	50-100	*	Kaplan	(Larinier & Travade, 2002)
Meuse and Vecht Rivers	*A. anguilla*	5-25	*	*	(Hadderingh & Bakker, 1998)
Tange hydropower station	*A. anguilla*	58	21	Francis	(Pedersen et al., 2012)
*	*A. anguilla*	15-20	*	*	(Larinier & Travade, 1998)
Linne hydropower station	*A. anguilla*	30	30-100	Kaplan	(Hadderingh et al., 1992)
Neckarzimmern	*A. anguilla*	38	40-80	Kaplan	(Berg 1986)
Dettelbach	*A. anguilla*	22	+	Kaplan	(Holzner, 1999)
Obernau	*A. anguilla*	20	+	Kaplan	(Von Raben, 1957)

Beauharnois	*A. rostrata*	24	+	Kaplan	(Desrochers, 1995)
Raymondville	*A. rostrata*	37	+	Kaplan	(Franke et al., 1997)
Avrijevaart canal	*A. anguilla*	97	8	Kaplan	(Buysse et al., 2014)
Leopold canal	*A. anguilla*	19	14	Archimedes	(Buysse et al., 2014)
Leopold canal	*A. anguilla*	17	14	Archimedes	(Buysse et al., 2014)
Leopold canal	*A. anguilla*	14	14	Archimedes	(Buysse et al., 2015)
Leopold canal	*A. anguilla*	19	14	Archimedes	(Buysse et al., 2015)
Slupia River	*A. anguilla*	5	15	Francis	(Dębowski et al., 2020)
River Meuse	*A. anguilla*	16-34	*	*	(Winter et al., 2007)
Magaguadavic River	*A. rostrata*	100	+	Kaplan	(Carr & Whoriskey, 2008)
River Dart	*A. anguilla*	0	+	Archimedes	(Kibel, 2008)
River Stour	*A. anguilla*	0	3	Archimedes	(Piper et al. 2018)
Connecticut River	*A. rostrata*	10	*	Francis	(Heisey et al. 2019)
River Rhine	*A. anguilla*	19	*	Kaplan	(Heisey et al. 2019)
Nemunas River	*A. anguilla*	24	375	Kaplan	(Dainys et al. 2018)
Siesartis River	*A. anguilla*	52	5	Kaplan	(Dainys et al. 2018)
Streva River	*A. anguilla*	100	0.8	CINK	(Dainys et al. 2018)
Albert canal	*A. anguilla*	3	9-15	Archimedes	(Pauwels et al., 2020)
River Meuse	*A. anguilla*	8	+	Kaplan	(Ben Ammar et al., 2021)
River Meuse	*A. anguilla*	20	+	Kaplan	(Ben Ammar et al., 2021)

An effective method to allow more eels to pass safely through a HPP is to temporarily shut down the turbines during a period of migration at night (Haro et al., 2003; Piper & Wright, 2017; Smith et al., 2017; Teichert et al., 2020) but this comes at the expense of energy production (Smith et al. 2017; Teichert et al. 2020). The predictability of eel migration is a

limiting factor (Gosset et al., 2005) but new research has developed a framework to calculate shut down timing to maximise escapement and minimise the production loss by considering several factors (Teichert et al., 2020; Smith et al., 2017).

1.5 Culverts

Culverts can impede upstream passage due to their higher velocities, variable flow regimes (Boubée et al., 1999; Shiau et al., 2020; Warren & Pardew, 1998), smooth surface roughness and low flow depths (Katopodis, 1992; Shiau et al., 2020). Culverts are generally built in the same direction and angle as the river and the culvert floor should connect to the riverbed to avoid the entrance being too high during low flow (Boubée et al., 1999), although one of the most common problems arises when the high velocity downstream of the culvert scours the downstream entrance causing an overhang. Flow velocity in the culvert (barrel velocity) should be below 0.3 m/s based on swimming performance of several species, if this cannot be achieved, corridors on the side of the culvert should have this velocity or lower (Boubée et al., 1999), and all junctions should be rounded to benefit climbing species such as elvers. Many types of culvert exist, however arch culverts are recommended as they retain the natural riverbed (Boubée et al., 1999; Larinier, 2002b) and they should be as wide as the river to avoid excess erosion of the riverbed (Boubée et al., 1999). Pipe culverts should be wide enough such that the natural flow characteristics of the river are maintained (Larinier 2002b) and they sometimes feature transverse iron corrugation to slow down the flow, but this can also cause increased turbulence in the flow (Boubée et al., 1999). Box culverts are the least recommended solution (Boubée et al., 1999; Larinier, 2002b) because they have higher velocities and low water height (Boubée et al., 1999). A pool can be made immediately downstream of the entrance of the culvert to provide fish with a resting area before they enter the culvert (Larinier, 2000b).

Baffles can be employed to ease passage upstream (Newbold et al., 2014) as they provide lower flows and resting areas for the fish (Boubée et al., 1999). There are many designs and configurations of baffles (for more detail see Katopodis (1992)) but the baffles should not cover the whole floor of the culvert to allow flow through the culvert even at low flows (Boubée et al., 1999; Katopodis, 1992). Corner baffles, which are sloped produced 100% passage success and corner baffles, which are vertical plates achieved 92% success, whilst the control efficiency was 40% for yellow eels (Newbold et al., 2014). Baffles have been

shown to work for other fish species such as brown trout (Olsen & Tullis, 2013) but have the drawback of causing debris accumulation (Larinier 2002b). It is advised that weirs and baffles are features on weir structures with 0.5-5% gradient (Larinier 2002b). Tiles such as the ones used for elver passes (see section 4.7.5) are another possible solution to increase passage by using them to line the bed of the culvert, specifically the studded substrate shows promise for this application (Jellyman et al., 2017).

1.6 Technical fishways

Technical fishways are a common upstream passage solution for anadromous fish (Larinier, 2002c). They include numerous designs with the common feature being a series of pools or chambers separated by weirs or baffles (Katopodis, 1992) that allow low velocity flows to facilitate upstream passage of certain fish. A successful fishway will allow the target species to pass upstream with no delays or injury (Larinier, 2002c), influenced primarily by establishing the correct flow velocity and regime for the target species (Larinier, 2002). These passes are mainly designed for salmonid passage (Fjeldstad et al., 2018) so they feature flow velocities too high for elvers (Barbin & Krueger, 1994; McCleave, 1980), even silver eels cannot easily navigate these passes when swimming upstream (Tamario et al. 2019). This is because silver eels have typically slower swimming velocities than salmonids, in a flume experiment it was determined that eels have a maximum swimming velocity of 2.12m/s (Russon & Kemp, 2011) compared to 8.08m/s for salmonids. Silver eels still use these passes nonetheless (Porcher, 2002; Solomon & Beach, 2004a), however certain designs are more navigable than others, such as nature like fishways, exist for eels (Tamario et al., 2018). What follows is a short list of some of the most commonly adopted fish passage solutions.

1.6.1 Pool fishways

These consist of a descending series of pools separated by vertical slots, gaps or weirs which control the discharge. The pools provide low velocities areas for the fish to rest, with short bursts of speed required to pass from pool to pool (Larinier, 2002). The slope is typically 10-15% (Larinier, 2002) and they can be used for longer stretches than types of fishway that do not provide resting zones. There are different designs for this type of fishway:

Vertical slot fishways have a vertical space in the weir between pools through which the flow descends into the pool (Katopodis, 1992). There exist many variations where the vertical slots are positioned directly in line (as in Figure 1.3A) or on alternating sides (Katopodis, 1992). These slots produce a main jet of water between each other with recirculation zones of lower flow (Larinier, 2002) that dissipate the energy of the flow and have a high shear with the main jet. The flow velocity is uniform within the water column (Katopodis, 1992) but these features can be manipulated by changing the geometry to suit the target species. Nevertheless, all variations require a high flow to operate (Larinier, 2002) and have high turbulent kinetic energy values (Puzdrowska & Heese, 2019). This type of fishway is well suited for silver eels (Fjeldstad et al., 2018; Solomon & Beach, 2004a).

A   Vertical slot fishway
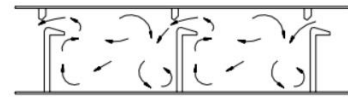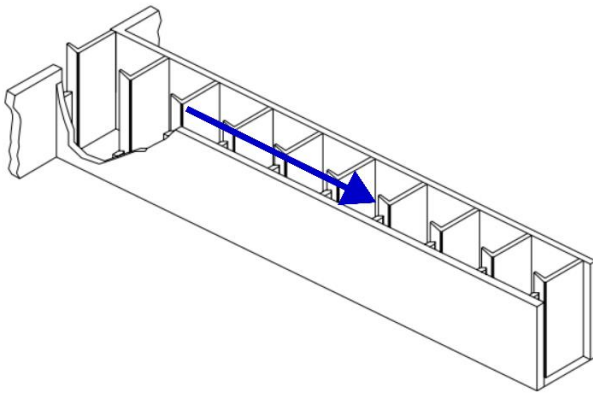
Plan view
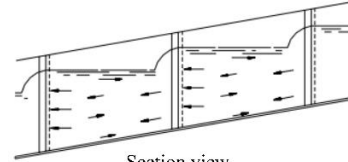
Section view

B   Weir fishway
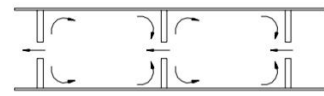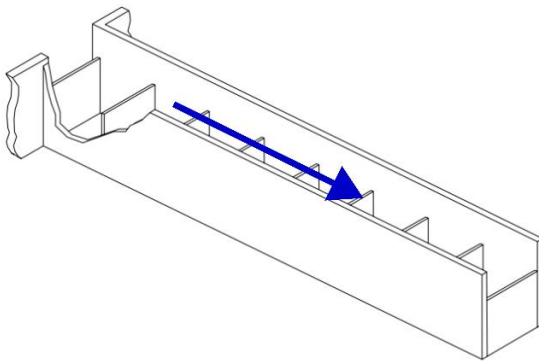
Plan view
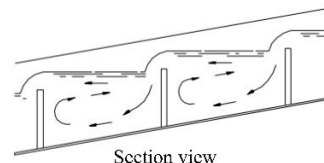
Section view

C   Denil fishway
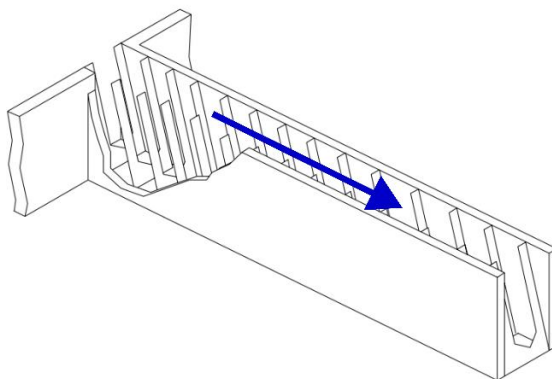
Plan view
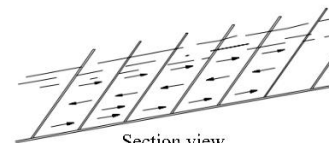
Section view

Figure 1.3. Schematics of: A – a vertical slot fishway, B – a weir fishway, and C – a Denil or baffle fishway. The dividing baffles between pools form low velocity areas where the fish

22

can rest. In all plots the blue arrow in the plot on the left represents flow direction and the black arrow on the plots to the right display the flow pattern. Adapted from Katopodis (1992).

Pool and weir passes simply function as a series of consecutive weirs (Larinier, 2002) and operate under two main flow conditions: plunging and streaming flow (Katopodis, 1992). Plunging flows have a lower water height over the weir and have strong recirculation zones with high turbulent shear stress between the recirculation zone and the top layer of flow moving downstream which fluctuates in velocity, being slowed by the shear over the pool and being faster over the weir. With streaming flow, a larger component of the flow passes over the weir and is not drawn into the recirculation zone which results in a more consistent velocity in the top layer with smaller recirculation zones with less shear (Katopodis, 1992). The recirculation zones are shown in Figure 1.3B.

Weirs with notches and orifices are very similar in function to pool and weir fishways, the difference being that they also feature a notch in the weir or an orifice on the bottom (Larinier, 2002). For eels, the most relevant feature as a bottom dwelling species is the orifice (Fjeldstad et al., 2018). These designs have the advantage of being able to maintain appropriate conditions for passage with changing discharge of the river (Larinier, 2002). If the passes rely exclusively on the bottom orifice for the flow to pass downstream then they will be especially susceptible to debris accumulation (Larinier, 2002).

Bolt fishways are a series of pools divided by rows of adjacent cylindrical structures with a gap in them which connects the pools and alternates from side to side with each successive pool (Puzdrowska & Heese, 2019). They have lower turbulent kinetic energy values than vertical slot and pool and weir fishways so they are easier to navigate for slower diadromous fish, so they show promise for eels but no specific study has been conducted to explore this possibility.

1.6.2 Denil or baffle fishway

These feature baffles, either on the sides, floor, or both (as shown in Figure 1.3C) and were originally developed for salmonids exclusively (Larinier, 2002a). As with the pool fishways, they come in a number of configurations. These fishways are generally steeper (20% slope) and shorter than pool fishways (Larinier, 2002a). They have a hydraulic operating range

beneath which the required turbulence is not formed so the pass does not work as intended and above which the flow slowly becomes supercritical and the baffles do not fulfil their intended role. Baffles must be carefully dimensioned to produce the correct lengthscale of turbulence for the target species. It is however advisable to use the smallest baffles possible. The entrance should be submerged enough to not cause a flow acceleration. No jumping should be necessary to pass between sections, fish should swim at a constant velocity and must pass in a single attempt. If the fishway is too long then resting pools should be provided every 1.2-1.5 m of drop to allow fish to rest (Larinier, 2002a). Denil fishways have highly turbulent flow, the recirculation zones between baffles produce a decelerating shear on the main flow so flow velocity is lower but is faster towards the surface (Katopodis, 1992). These fishways may need added maintenance when installed on rivers with large rocks on the bed as these can enter the pass and disrupt the flow (Larinier, 2002), they are commonly used with an adjacent elver pass (Environment Agency, 2009; Solomon & Beach, 2004). Baffle passes are considered better for eels because with slots or notches the eel needs to attain a higher maximum swimming speed for a short length of time instead of a constant but lower speed (Solomon & Beach, 2004).

Side baffle fishways produce a helical current on either side of the main flow to dissipate energy and to decelerate the main flow (Katopodis 1992). This design is more suited than other baffle designs to be effective under a wider range of discharges (Larinier, 2002a). The main drawback and reason they are not as widespread as other designs though is that they become easily clogged by debris (Larinier, 2002a).

Bottom baffle fishways are less likely to be affected by debris but are not able to adapt to wide ranges of discharge (Larinier, 2002a). Perhaps the best-known version of this is the Larinier fishway also known as the super active bottom baffle design, which features V-shaped bottom baffles. It allows for strong attraction flows because several Vs can be placed adjacent to each other provided that a plate separating them of the same height of the Vs is present (Larinier, 2002a). Eels are able to use a Larinier pass at 1.3-1.4 m/s (Solomon and Beach, 2004).

1.6.3 Nature-like fishways

Artificial natural channels or nature-like fishways are often the recommended methods for eel passage (Fjeldstad et al., 2018; Tamario et al., 2019). They are made near one of the

banks from natural materials and mimic the properties of a natural stream that circumvent a migration barrier (Tamario et al., 2018). These fishways have the potential not only to restore connectivity (Sheppard & Block, 2013), but they also provide additional habitats (Tamario et al., 2018) even though they are narrower and shallower than the natural habitats, these installations however, are able to adapt to varying discharges well (Fjeldstad et al., 2018). Nature-like fishways feature natural obstacles, such as rock ramps (Environment Agency, 2009), which are placed at intervals as shown in Figure 1.4, or weirs to mimic a natural river (Larinier, 2002c), these should be permeable to prevent high turbulence from being produced in their wake (Zheng et al., 2020) and therefore creating the same problems that make some technical fishways impassable by certain species. One of the major advantages of this passage solution is that it is suitable for multiple species (Larinier, 2002c; Fjeldstad et al., 2018) and can be more than 90% efficient (Fjeldstad et al., 2018) and can faciliate both up and downstream passage (Fjeldstad et al., 2018). One year old elver recruitment was increased by 86% by the building of a nature-like fishway (Sheppard & Block, 2013). In a comparative analysis, nature-like fishways were the only passage solution that did not negatively affect the probability of juvenile eels being found upstream in contrast to technical fishways (Tamario et al., 2019). To better accommodate eels, the fishway should be kept shallow (Tamario et al., 2018) even within the already shallow range of angles available for this fishway (Larinier, 2002c). The drawbacks of this fishway are that it takes up more space than other passage solutions (Larinier, 2002c; Fjeldstad et al., 2018) and maintenance is still required to keep the fishway operating at maximum efficiency (Fjeldstad et al., 2018).
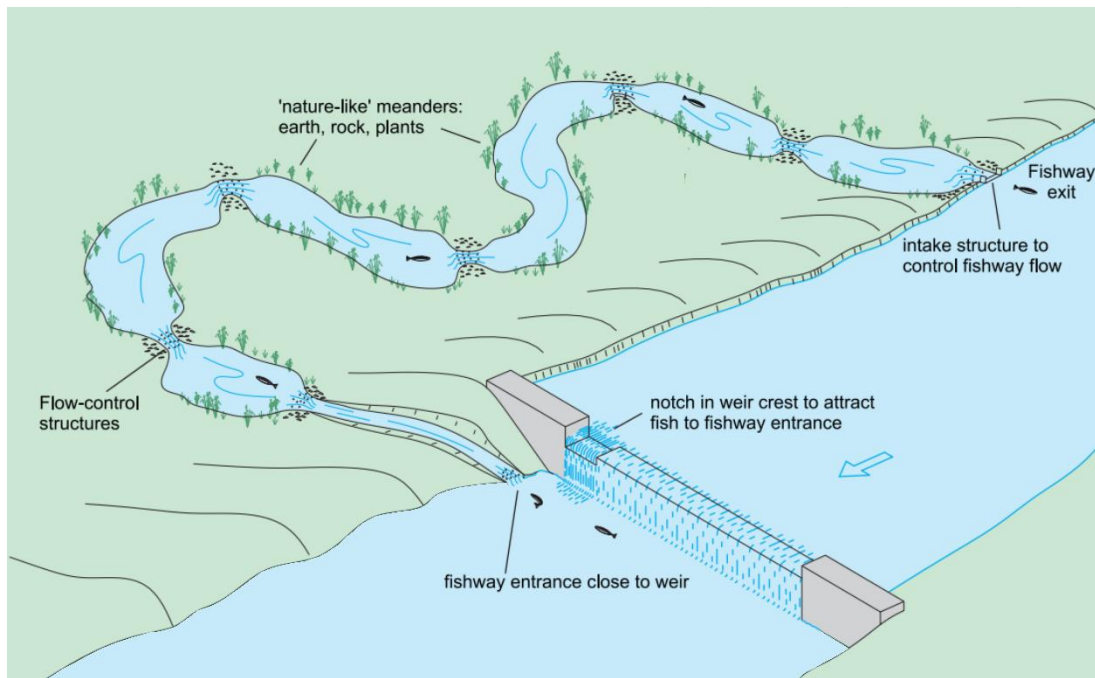
Figure 1.4. Nature-like bypass around a migration barrier. These fishways are suitable for most fish and provide added habitat but have the drawback of being more complex and expensive both spatially and financially. Adapted from Thorncraft & Harris (2000).

1.10 Elver pass

Elver and glass eels have very specific requirements for passage, they are slow swimmers (Barbin & Krueger, 1994; Tamario et al., 2019) with low endurance (McCleave, 1980) but are able to climb if necessary (Solomon & Beach, 2004; Watz et al., 2019). For this reason, elver passes are built, usually near a technical fishway (Environment Agency, 2009; Solomon & Beach, 2004) with a target efficiency of 90% (Fjeldstad et al., 2018). When designing an elver pass the following factors should be taken into consideration: (i) placement at the entrance in relation to the barrier and river cross-section; (ii) attraction flow; (iii) the length and width of the pass; (iv) means to avoid predation; (v) bed slope; (vi) and climbing substrate.

Design optima include passes mounted near the banks that reach down to the riverbed to be more accessible to juveniles and should start near the obstruction as this is a stopping point for the migrating fish (Fjeldstad et al., 2018; Solomon & Beach, 2004). Elver passes function well when there is enough flow to achieve a water depth capable of submerging the elver completely, most passes having flows between 66 and 230 $Lmin^{-1}m^{-1}$ width of the pass

(Solomon & Beach, 2004). This will not produce a strong or effective enough attraction flow since a flow velocity of 2.43 m/s impedes the passage of elvers (Kerr et al., 2015; Padgett et al., 2020) through computational fluid dynamics (Ansys Fluent 17.2), evaluated that passage success for elvers was maximized when the pass featured shallow slopes and low discharge. An artificial flow is therefore a good option to improve performance, and plunging flow can be twice as efficient than a streaming flow (Piper et al., 2012). Predation is avoided by covering the top of the pass to exclude predators, this serves the double function of shielding from light sources which might dissuade the elver from entering the pass (Solomon & Beach, 2004). Slopes of 30° or less are more effective for a range of substrates (Jellyman et al., 2017; Watz et al., 2019). Many weirs have a bed slope of 45° (Vowles et al., 2017) and a reduction in passage has been found for slopes greater than 50° (Jellyman et al. 2017) and in general steeper slopes are harder for the elver to climb with 70° showing low passage success (Jellyman et al., 2017). Furthermore, a smooth surface roughness, regardless of the bed slope can be impossible for elvers to climb (Vowles et al., 2015).

The type of substrate for an eel pass is a crucial design consideration, the most common type in the UK being bristles (Environment Agency, 2009; Solomon & Beach, 2004), followed by plastic tiles with protrusions, otherwise known as studded tiles (Watz et al., 2019). Bristles and studded climbing substrates are available in different configurations of size and separation, other substrates like an open weave are randomly assembled fibres, these three substrates are present in Figure 1.5 (Watz et al., 2019). Another option is to mimic natural substrates of gravel and rocks (Jellyman et al., 2017; Solomon & Beach, 2004a). In a flume experiment, a studded substrate was used more frequently by elvers (40%), than bristles (21%) or open weave (5%), and elvers climbed more quickly (26% faster) on the studded substrate; these laboratory results were validated by trials conducted in the field (Watz et al., 2019). The size and spacing of the studs can also impact performance. In a flume, eel passage increased from 0% with a smooth bed to 67% with studs, which were tested in two configurations: a larger diameter stud substrate and a smaller diameter one with studs spaced in proportion to their size, the smaller studs accounted for 59% of all the total passes (Vowles et al., 2015). However, preference on spacing may change depending on the slope (Solomon and Beach, 2004). The vertical/horizontal orientation of the studded tile on which the substrate is presented also impacts passage efficiency. In a flume experiment, vertically oriented tiles produced a passage efficiency of 67%, horizontally oriented tiles achieved 93% efficiency (Vowles et al., 2015). These climbing substrates can be placed directly on

the weir or used to line an overpass or a bypass to the obstruction where an artificial flow is supplied, this is usually decided on a case-by-case basis (Environment Agency, 2009; Solomon & Beach, 2004). The drawback of devices for the upstream passage of elvers is that they can easily become clogged by debris brought by the river and thus become impassable (Larinier, 2002c; Solomon & Beach, 2004), there are also instances where larger debris has damaged one of the channels lined with tiles used to allow passage of elver over the hydrological device therefore dropping the elvers into potentially unsafe areas or impeding their further passage (Solomon & Beach, 2004). *In situ* evaluations of the effectiveness of the elver passes agree with flume studies (Watz et al., 2019) and show that these passes can be beneficial measures for elver passage rivers (Drouineau et al., 2015).
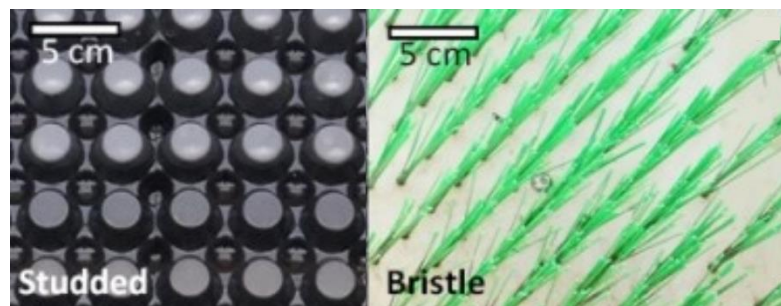
Figure 1.5. The two more commonly found substrates used for elver passes adapted from Watz et al. (2019), the studded substrate comes in various forms, in this example it has studs and depressions and generally performs best. Bristle substrates, however, are currently still the most commonly used.

Table 1.2. The effectiveness of different configurations of elver pass. Effectiveness is measured as percentage of successful upstream passes out of the total elvers attempting passage. The pass type can be where the tiles are directly attached to the weir or where a separate arrangement of channels (overpass) supplied with flow (given as flowrate) and lined with tiles that pass over the barrier. *Flowrate and width for the pass in Pas-Du-Bouc not given.

Location	Species	Effective-ness (%)	Flow rate (ls^{-1})	Angle of incline (°)	Width of pass (m)	Length (m)	Substrate	Pass type	Reference
Pas-Du-Bouc, France	*A. anguilla*	39	*	45	*	6	Bristle	Overpass	(Drouineau et al., 2015)
Laholm, Sweden	*A. anguilla*	40	0.07	30	0.32	2	Studded	Overpass	(Watz et al., 2019)
Laholm, Sweden	*A. anguilla*	21	0.07	30	0.32	2	Bristle	Overpass	(Watz et al., 2019)
Laholm, Sweden	*A. anguilla*	5	0.07	30	0.32	2	Open weave	Overpass	(Watz et al., 2019)
Lab flume	*A. anguilla*	67	1	18	0.3	1.25	Studded	Weir	(Vowles et al., 2015)
Lab flume	*A. australis*	87	0.1	30	0.1	1.5	Studded	Overpass	(Jellyman et al. 2017)
Lab flume	*A. australis*	57	0.1	50	0.1	1.5	Studded	Overpass	(Jellyman et al. 2017)
Lab flume	*A. australis*	13	0.1	70	0.1	1.5	Studded	Overpass	(Jellyman et al. 2017)
Lab flume	*A. australis*	80	0.1	30	0.1	1.5	Gravel (2-15 mm)	Overpass	(Jellyman et al. 2017)
Lab flume	*A. australis*	13	0.1	50	0.1	1.5	Gravel (2-15 mm)	Overpass	(Jellyman et al. 2017)
Lab flume	*A. australis*	4	0.1	70	0.1	1.5	Gravel (2-15 mm)	Overpass	(Jellyman et al. 2017)
Lab flume	*A. anguilla*	67-93	90	18	1.37	1.74	Studded	Weir	(Vowles et al., 2017)

29

1.11 Tidal gates, flaps and sluices

Hydraulic devices are often used in estuaries and at the sea/freshwater interface, these include tidal gates, flaps and sluices that are used to prevent high tides from flooding areas of the estuary where the land is needed, to create a reservoir of fresh water or to allow docks to be constructed (Larinier, 2002b). These can cause problems to the migrations of catadromous fish by blocking access to estuaries and rivers (Environment Agency, 2009). The upstream migration of glass eels is most affected (Bult & Dekker, 2007; Environment Agency, 2009; Larinier, 2002b) since in estuaries they move mostly through selective tidal stream transport (STST) (Bult & Dekker, 2007) and do not have sufficient swimming ability (Environment Agency, 2009). Gates, flaps and sluices of this kind are likely to be opened only a few times a day when low tide conditions allow it (Environment Agency, 2009) so when they are open the flowrate is large and the velocity too high for the glass eels to swim through (Environment Agency, 2009). Tidal flaps are particularly problematic because they have narrow openings and high velocities, hinged tidal gates are preferable as they allow a wider gap and therefore provide a better opportunity for glass eels (Larinier, 2002b). A potential problem faced by both up and downstream migrants is the sudden change in salinity at these devices where it would naturally be gradual (Larinier, 2002b).

A passive solution is to leave a small gap in the gates as the tide rises (Environment Agency, 2009). The seawater passing into the gate was not significant so this is potentially a cheaper and easier solution that might also benefit downstream migrants (Mouton et al., 2011). Fish passes have also been installed at tidal sluices (Larinier, 2002b) but they are not appropriate for glass eel passage. For downstream migrating silver eels, these obstacles are less problematic, although eels can be delayed by several hours when the gate is closed, 98.3% of tagged eels escaped in a study by Wright et al. (2015). It was also found that passage increased with darkness and gate opening angle and that a pass for the eels eliminated some of the delay (Wright et al., 2015).

1.12 Attraction flow

Every passage solution will have a flow either going into it, exiting from it, or both. Attraction flow is the flow leading up to a fish pass as viewed from upstream or downstream, it can be manipulated to be more attractive to the targeted species (eels for example, see Piper et al. (2012)). A successful attraction flow design will increase the number of fish that

approach the pass and although at times the natural flow of the pass is sufficient to attract fish, occasionally this is augmented by additional flows, either artificial (Piper et al., 2012) or nearby natural flows (Fjeldstad et al., 2018). The attraction flow must work with the deterrents to guide the fish towards the bypass entrance (Enders et al., 2009). Fish follow flows and have preferences for specific flow conditions (Fjeldstad et al., 2018; Russon et al., 2010) that are species-specific.

Upstream migrating elvers commonly use elver passes, which feature a small internal flow, low in comparison to that of the river (Solomon & Beach, 2004) so artificial attraction flows helps the juvenile eels find the entrance (Piper et al., 2012). Plunging flow (an artificial vertical flow from above and plunging into the river at the entrance to the elver pass) can be twice as efficient than a streaming flow in attracting elvers to the pass (Piper et al., 2012).

For fishways other than an elver passes it is widely suggested that the flow should comprise at least 2-5% of the total river flow (Larinier, 2002d) but can be required to be as much as 9% of the total river flow for some species (Enders et al., 2009). This flow should be pointed into the main flow at an angle if it is small in proportion, but kept parallel to the main flow if it is large in proportion to the main flow (Fjeldstad et al., 2018; NOAA, 2015). If additional flow is needed for the attraction flow, which cannot come through the fishway, the pass can be located next to another strong flow or more water can be released near the entrance (Fjeldstad et al., 2018). Accelerations in flow can deter fish (Piper et al., 2015) so when using physical barriers to guide fish to the pass entrance it is important to ensure the accelerations in the flow are smooth (Sheridan et al., 2011).

Eels display erratic behaviour in response to flow accelerations and follow laminar flow (Piper et al., 2015). As eels tend to swim near the riverbed (Harrison et al., 2014), a gradual transition from the natural bed to the pass bed should be made to prevent sudden changes in flow regime (Fjeldstad et al., 2018). With lower flow accelerations, eels have been seen to reject the area less and search more (Piper et al., 2015) thus making them more likely to find the pass. Downstream swimming eels also predominantly swim near the sides of the river (Piper et al., 2012) and the bed (Brown & Castro-Santos, 2009), they prefer high turbulent intensities in their route selection (Russon et al., 2010). In all cases, the site hydrodynamics must be studied to efficiently plan the attraction flow criteria. There is little work covering the flow preference of seaward migrating eels.

1.13 Removal of the barrier and fish pass dangers

The removal of dams, weirs and other obstacles remains the most effective solution to restore connectivity and the river's normal flow. If these structures are obsolete, then this is a viable option to restore connectivity. However, most migration barriers are still in use and needed, so another passage solution must be adopted where relevant. It may be noted that fish passes carry their own set of risks that can detract from the passage benefits they create. Fish passes can create predation hotspots by multiple predator types (Agostinho et al., 2012). Ecological traps can also be created by inadequate fish pass implementation, the two main mechanisms for this to occur are the presence of upstream passage where no downstream passage is available (Ohms et al., 2022), and by allowing fish to settle in low quality habitats (Raut et al., 2019). These effects are typical of anthropogenic alterations to habitats (Battin, 2004) and care must be taken to evaluate habitat quality before a fish pass is constructed. Fish passage efficiencies are highly variable and a low efficiency pass may act as a hidden barrier (Kemp, 2016).

1.14 Fish locomotion

Fish have a very large morphological variation between different taxa, and are all adapted to moving through water in different ways. Most fish primarily swim with their caudal fin, oscillating it from side to side to create thrust (Videler, 2019). The extent to which the rest of the body moves with the caudal fin characterises different caudal fin swimming modes. Thunniform swimmers (named after tuna), keep a stiff body and move only the most posterior portion of their body with the caudal fin, carangiform swimmers oscillate slightly more of their body (like a mackerel), subcarangiform swimmers (like trout) use even more of their body and may reach a wavelength of 1 meaning they occasionally have a full waveform on their body while swimming, and finally anguilliform fish (like eels) use the majority of their body to swim reaching a wavelength of 0.6 body lengths, so they have more than one wave on their body whilst swimming (Gray, 1936; Lindsey, 1978; Smits, 2019; Videler, 2019; Webb, 1984). Anguilliform swimmers tend to have lower top swimming speeds but good efficiency whilst thunniform fish can reach very high speeds. Interestingly, some anguilliform fish are able to also swim backwards (Videler, 2019). The frequency with which fish beat their caudal fin (also known as tailbeat frequency) is the kinematic variable

that most reliably influences swimming speed (Tytell, 2004a, 2004b), but different swimming modes and body morphologies of fish still produce thrust in different ways (Tytell, 2005; Tytell et al., 2010). The different swimming modes, however, display similar midline kinematics and have similar values of the ratio of the head amplitude to the tail amplitude (Santo et al., 2021), casting doubt over whether the classification of the swimming modes is a useful tool. Most fish swim using their body and caudal fin, but some use primarily their pectoral fins for propulsion (Blake, 1979; Walker & Westneat, 2002). Even within this more restricted group of species there is a high level of variability in pectoral fin shape and actuation (for example, up and down or front to back) (Blake, 1979). Fish that primarily use their pectoral fins (also known as labriform), commonly start to engage the caudal fin at higher swimming speeds. Fish that use their caudal fin will, at high swimming speeds, stop swimming steadily and start engaging in burst and coast.

Fish swimming in shoals to save energy, and this has been found to be the case across different morphologies and swimming styles (Johansen et al., 2010; Ligman et al., 2024; Wei et al., 2023; Weihs, 1973; Zhang & Lauder, 2024). The exact mechanism by which this occurs has not yet been fully determined but several models exist that show energetic benefits of swimming in groups (Cushing & Jones, 1968; Harvey et al., 2022; Zhang & Lauder, 2024).

1.15 Thesis aims and objectives

This thesis aims to address knowledge gaps in fish passage research and fish behaviour associated with anthropogenic structures in rivers. This is achieved through a series of laboratory studies in which the focus was put on the behavioural aspect but also on the fine details of fish response to hydrodynamic stimuli and the consequent kinematic response. Fish locomotion has been studied for some species, including all those studied in this thesis, but generally the kinematics of swimming are evaluated for very well defined and discrete flows such as uniform flow conditions in a bare flume (Tytell, 2004b) or flow in the presence or well-defined and discrete turbulent structures (Harvey et al., 2022; Liao et al., 2003). Shoaling is another aspect of fish behaviour which has many functions (Larsson, 2012), but that is often not specifically evaluated in studies on fish at anthropogenic barriers in rivers. This thesis attempts to quantify the benefits of shoaling and determine the primary functions of the shoal in differing flow conditions. Of the myriad of barriers that exist in rivers, here

mainly high velocity barriers are considered, but all three of the anthropogenic modifications studied (hydrokinetic turbines, water abstractions, and high velocity barriers) act differently and pose different threats despite being high velocity.

Any water abstraction from surface freshwater above 20 m^3 per day requires screening in the UK (Environment Agency, 2020) but the screens need to be effective in preventing the entrainment or impingement of fish whilst not overly restricting water entry or being vastly expensive. This balance must be found if efficient fish screens are to be implemented, especially for critically endangered species like the European eel that is particularly vulnerable during its juvenile life stages to impingement as a result of low swimming speeds and to entrainment due to their long body but comparatively small head. In Chapter 2, current eel screening regulations for the UK are tested with eels at different flow velocities and different screen configurations to evaluate the mechanics of impingement and the fine scale hydrodynamics of the screens as well as overall performance.

Structures like culverts produce fast, shallow flows that are difficult to traverse for many species, this risks halting fish migrations (especially if the cumulative effect is considered), as well as reducing their energy budget and creating predation hotspots. These structures need to be made passable by a variety of different species with different swimming abilities and morphologies and ideally without creating a large backwater effect during storm events and at a low cost considering the pervasiveness of these structures. Eel tiles were originally developed for elver passage at gravity barriers and consist of 0.5 m by 0.5 m bases with two sizes of cylindrical protrusions, could be a possible solution so their hydrodynamics are quantified and tested in a laboratory flume with eels and sticklebacks in Chapters 3, 4, 5, and 6.

Thought to cause less fragmentation and be cheaper and simpler than traditional hydropower dams, instream hydrokinetic turbines for rivers are being planned all over the globe to generate renewable power but their effect on fish movement is not well understood. Turbines have the potential to reduce fish movement (Hammar et al., 2013) as well as cause blade strikes that injure the fish. Fish behaviour around these devices needs to be better understood and ways of mitigating the potentially harmful impacts of these devices should be found. The behaviour and passage of a shoal of rainbow trout is evaluated for several turbine configurations and a single rainbow trout is tested to find if the colour of the turbine blades can affect fish behaviour in Chapters 7 and 8. Each data chapter of this thesis includes a self-

contained literature review in the introduction to provide more in-depth information on the specific topic of that chapter or field and to allow for the future publication of each chapter to relevant engineering or biological journals despite each chapter remaining interdisciplinary.

The aim of this thesis is to investigate existing (screens) and new (eel tiles) solutions and assess emerging threats (hydrokinetic turbines) at velocity barriers in rivers by considering a range of species, fish sizes, fish kinematics and locomotion techniques, and shoaling. Specific objectives are listed below:

1. Analyse the behavioural and hydrodynamic effects and advantages of shoaling applied to fish passage research and hydrodynamic conditions spanning uniform flow, to more complex canopy-like flow, to flow manipulated by an actively rotating set of devices (Chapters 5, 6, and 7)

2. Combine hydrodynamic, behavioural, and kinematic responses of fish at migration barriers to analyse fine-scale movement of fish (Chapters 2, 3, 4, 5, 6, 7, and 8)

3. Evaluate eel tiles as a potential solution for multi-species fish passage at high-velocity barriers (Chapters 3, 4, and 5)

4. Test current eel screen regulations and develop an understanding of the fundamental hydrodynamic and kinematic mechanisms of impingement and escape (Chapter 2)

5. Quantify high spatial resolution hydrodynamics of fish passage and protection measures (Chapters 2 and 3)

6. Evaluate vertical axis hydrokinetic turbines as a potential emerging threat and explore mitigation solutions (Chapters 7 and 8)

Chapter 2. The Role of Screen Angles and Velocity in Fish Impingement and UK Eel Screening Regulations

Conceptualisation and methodology by Prof. Jo Cable, Prof. Catherine Wilson, Andy Don, and Guglielmo Sonnino Sorisio. Data collection by Guglielmo Sonnino Sorisio and Charlotte Robison-Smith. Analysis, visualisation, and writing by Guglielmo Sonnino Sorisio and editing by all of the above. Advice and input from Chris Bell and Chris Grzesiok.

Summary

Water abstractions in inland watercourses have the potential to harm European eels (*Anguilla anguilla*) if they are not correctly protected, potentially contributing to further declines of this critically endangered species. Current regulations aim to prevent eel impingement and entrainment at intakes and outfalls by specifying mitigation screening techniques such as screen types, screen apertures, and maximum approach velocities to the screens. These aim to prevent eels from being injured and allow them to bypass the abstraction, but they have yet to be empirically tested. In this laboratory study, screens with 3 mm apertures of horizontal and vertical wedge-wire and a Hydrolox screen were evaluated under the current UK regulations. We measured the hydrodynamics of the screens and then observed eel behaviour and swimming dynamics upstream of the screens. The screens had minor effects on the upstream flow fields and produced suitable velocities and turbulence levels for eel escapement. At the regulation velocities, no eels impinged on the screens, validating the current regulations but significant impingement started to occur at higher velocities, so the regulation velocities should not be exceeded. Screens at smaller angles to the flow caused significantly fewer eel impingements and therefore are preferable. The current screen regulations for 3 mm wedge-wire screens are appropriate for eels of the size tested in this study and do not cause impingement or entrainment.

2.1 Introduction

Water is a limited, diminishing but heavily abstracted resource, with a significant portion, 87% in England and 73% in Wales, abstracted from freshwaters (Holleran, 2023; NRW, 2024). In these countries, there are an estimated 17,100 abstraction licences from surface

waters (DEFRA, 2022; NRW, 2024), which removed 10.4 billion cubic metres of water in 2018 with a potential increase to 12.7 billion cubic metres in 2023 (DEFRA, 2022; Holleran, 2023; NRW, 2024). The main abstractors of water are from electricity generation and public water suppliers, followed by agriculture, aquaculture, and other industries (Holleran 2023; NRW 2024). Such abstractions have the potential to entrain fish (Turnpenny and O'Keefe 2005) causing them delays at best and death at worst (Carr & Whoriskey, 2008; Carter & Reader, 2000; Dainys et al., 2018; Larinier & Travade, 2002). These abstractions add to the millions of barriers already fragmenting the rivers of Europe and blocking fish migration pathways (Belletti et al., 2020; Jones et al., 2019). Fish screens are typically employed to mitigate these risks but a poorly designed screen can still cause entrainment for some fish and impingement for others (Hanson, 1977; Hadderingh et al., 1992; Turnpenny and O'Keefe, 2005; Bromley et al., 2013; Seaby, 2023).

The European eel (*Anguilla anguilla*) is a catadromous fish that migrates upstream from the sea into Europe's rivers. It is currently classified as critically endangered (Jacoby and Gollock, 2015; Pike et al., 2020), having undergone four decades of dramatic decline in recruitment, now <5% of pre-1980 levels (Dekker, 2003; ICES, 2020). This decline is caused by a variety of factors, including river fragmentation and the associated deaths and migration delays (Halvorsen et al., 2020; Piper et al., 2017, 2018b; Warren & Pardew, 1998). This is exacerbated by the high prevalence of the parasite *Anguillicola crassus* which affects eel swimming behaviour (Kirk, 2003; Newbold et al., 2015) probably making migration barriers harder to overcome (Hanson, 1977; Hadderingh et al., 1992; Bromley et al., 2013; Rytwinski et al., 2017; Seaby, 2023). Juvenile eels are especially vulnerable because they have a low swimming performance (Clough et al., 2004; Clough & Turnpenny, 2001; Turnpenny et al., 2001; Vezza et al., 2020), and are therefore more likely to go through the screen, known as entrainment, if the aperture is large, or impinge on the screen if it is small.

Following the 2007 European Union Eel Regulation (The Council of The European Union 2007) and the subsequent UK application of this into England and Wales (UK Government, 2009), the European eel is protected in its migrations. These regulations stipulate a target of 40% biomass escapement of eels to the sea, measured relative to escapement in an unmodified and healthy catchment. Efficient screening techniques can reduce mortalities and help to achieve the required escapement levels, but screening regulations must balance several practical challenges. The screen aperture should prevent entrainment, the approach

velocities should not cause impingement, the screen material should not cause injury to the fish, and the screen must achieve this whilst allowing the required volume of water through without being prohibitively expensive. Current Environment Agency (2020) guidelines define Best Achievable Eel Protection (BAEP) as the standard for eel protection at intakes and specify the allowable range of screen aperture, approach velocity, and angles for each size range of fish. For eels 121-300 mm they specify approach velocities of 0.15 ms^{-1} for screens at 90° and 31.5°, and 0.3 ms^{-1} for screens at 26.5° and 20°.

Several screening techniques and guidelines have been developed to increase the efficiency of fish escapement. For most species, screen aperture should be around 10% of the fish's length to exclude them, however because of the eel's elongated body, the recommended size is 3% of their length (Ebel, 2016; David et al., 2022). For eels 60-80 mm and 100-160 mm long, respective 1 mm and 2 mm apertures cause no entrainment (Carter et al., 2023), but for silver eels (~ 660 mm), 12 mm (Russon et al. 2010), and 15 mm (David et al., 2022) aperture is effective. Apertures up to 30 mm can also function to guide eels to bypasses (Meister, 2020; Motyka et al., 2024), but this aperture does not guarantee exclusion and behavioural screening techniques have been used to supplement the physical screen. Electrification of bar racks causes avoidance but can cause injuries and some eels still entrained (Meister, 2020).

Acoustic and infrasound deterrents marginally increased avoidance but the effect was small (Deleau et al., 2020a, 2020b; Piper et al., 2019). Light-based deterrents show the most promise for eels (Hadderingh et al., 1992), but efficiency differs amongst species and fish ages. The screen material must be an appropriate balance of fish protection, hydraulic performance, and cost. Bar racks orientated vertically or horizontally are a widespread solution (Meister et al., 2020b; Meister, 2020; de Bie et al., 2021; Lemkecher et al., 2022), larger apertures are usually used, but round bars are prone to 'gill' fish (Turnpenny and O'Keefe, 2005), a variation of this design are foil shaped bars, designed to reduce head losses from the screen (Meister et al., 2020a). Wire mesh and perforated plates can easily clog and be hard to clean, whereas wedge wire screens (Figure 2.1) present a smooth surface to the fish and are less prone to debris accumulation whilst also decreasing the blocked area within the screen due to their triangular profile, which does not compromise rigidity (Turnpenny and O'Keefe, 2005; Bromley et al., 2013).
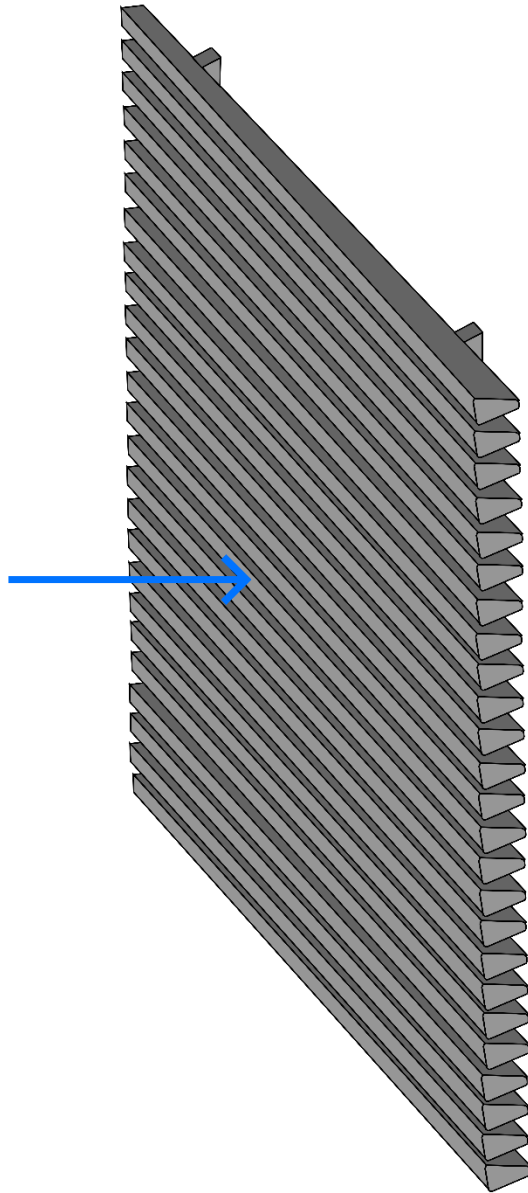
Figure 2.1. An illustration of a Wedge Wire screen oriented horizontally. In the present study, the Wedge Wire made from stainless steel was 3 mm thick with 3 mm gaps between each bar. Flow direction in this diagram is indicated by the blue arrow with the thicker section of the wedge wire on the upstream face and the tapered trailing end on the downstream face.

The orientation of the screening material (referred hereafter as vertical or horizontal) is often linked to the axis on which the screen is angled and the location of the bypasses such that the screening material guides towards the bypass. Vertical screens are often the preferred orientation if inclined with respect to the bed and guide to a surface bypass (Raynal et al., 2013; David et al., 2022). However, a vertical or horizontal screen can be positioned across the river channel at an angle to the main flow direction and this is the more common

approach, and often leads to a fish bypass at the downstream end of the screen (de Bie et al., 2018; Meister, 2020; David et al., 2022; Harbicht et al., 2022; Motyka et al., 2024) or in rare cases located at the upstream end (Russon et al., 2010). Flume studies with screens directly perpendicular to the flow direction show high impingement rates and less efficient guidance towards the bypass (Carter et al., 2023; Russon et al., 2010), whereas angled screens have a greater ability to guide fish. Comparing vertical and horizontal screens, some studies on fish species other than eels have found horizontal screens were up to 20% more effective for guidance, whereas others found little difference (de Bie et al., 2018; de Bie et al., 2021; Harbicht et al., 2022). The location and type of bypass has a large impact on the overall effectiveness of installation; a badly designed bypass can delay migrating eels by days, weeks, or months (Behrmann-Godel & Eckmann, 2003; Brown & Castro-Santos, 2009; Carr & Whoriskey, 2008; Gosset et al., 2005; Haro et al., 2000; Pedersen et al., 2012). Eels primarily swim near the bed, and this is also true in the presence of fish screens (Russon et al., 2010). Surface and pipe bypasses for fish have consequently been found to be a poor design for eels, with down to 0% passage (Calles et al., 2012; Egg et al., 2017; Boes et al., 2022), and bottom bypasses are generally preferred (Calles et al., 2012; Egg et al., 2017; Environment Agency, 2020). Full depth bypasses have the best passage rates in flume trials but are not always practical in the field (Russon et al., 2010; Boes et al., 2022; Harbicht et al., 2022). Passage rate is also influenced by other factors; flowrate, should be 2-5% of the total flow (Environment Agency 2020), and velocity gradient should be mild to attract the eels without being too high and abrupt as this can cause rejections (Boes et al., 2022; de Bie et al., 2018; Piper et al., 2015). More specifically, a 20% velocity increase towards a bypass increased passage whereas a 40% increase decreased it (Beck, 2020; Beck et al., 2020a). Variables external to screen design can also influence eel behaviour and passage rates, low dissolved oxygen levels are associated with higher impingement rates (Shepherd et al., 2016), temperature affects fish swimming abilities (Clough et al., 2004; Muhawenimana et al., 2021), and silver eel body mass has been linked to passage success (Motyka et al., 2024).

Approach velocity to the screen can significantly impact impingement and is fish species and life stage specific, therefore it needs to be low enough for the weakest swimmer (Russon et al., 2010; Stocks et al., 2019). For juvenile eels, for example, 0.2 m/s caused up to 100% impingement rates (Carter et al., 2023). Another important parameter to consider is how fish screens affect the flow, potentially impacting both the abstraction and the fish. With any blockage of the flow, there will be a loss of velocity head. The most influential parameters

on head loss are screen angle, where a low angle to the flow direction creates a lower head (Lemkecher et al., 2022), and rack aperture (Albayrak et al., 2020), while the bar shape had less significant effects (Meister, 2020). In terms of the local flow field, the effect of screens on the upstream velocity profile is small compared to the change in main component of velocity, and a sweeping flow component is generated along the screen surface but screen angle and bar orientation did not significantly affect this (Rajaratnam et al., 2010; Lemkecher et al., 2018; Beck et al., 2020b; Meister et al., 2020b; Lemkecher et al., 2022).

At present, most studies evaluating screening technology for eels have concentrated on the seaward migration of the silver eel and there is little evidence available for the best screening approaches to protect elvers and yellow eels. In particular, screen orientation and angle have yet to be evaluated for the current set of EA regulations (Environment Agency, 2020). So here we test the effect of screen type (vertical or horizontal wedge wire and a Hydrolox screen), screen angle and approach velocity. As the effect of screen angle on velocity profile for Wedge Wire Screens angled to the main flow direction (but not the bed) has yet to be experimentally evaluated, we conduct here a hydrodynamic investigation which can be utilised to validate the results of previous Computational Fluid Dynamics (CFD) studies. The effect that screen angle has on impingement is also poorly understood; steeper angles can reduce impingement, and the current regulations allow higher approach velocities at angles below 26.5° to the longitudinal flow direction, but the underlying mechanisms of impingement are unknown. This study aims to experimentally evaluate the effect of screen type, angle and approach velocity and analyse near screen interactions for eels between 121 and 300 mm. Eel swimming kinematics are evaluated to provide further details of eel interactions with the screens and this data will be combined with hydrodynamic data to gain a better understanding of fish screen behaviour.

2.2 Methods

2.2.1 Fish origin and maintenance

European eels, *Anguilla anguilla* (N=32), were collected from the River Taff downstream of Blackweir (51.495050, -3.195827) on 22/06/2023 with water temperature of 15 °C, by electrofishing conducted by Natural Resources Wales (NRW). The eels were transported to Cardiff School of Engineering and acclimatised to the holding tank temperature (17 °C) at a rate of 2 °C/h. The holding tank was 1.3 m in diameter with a water depth of 0.35 m, giving

a volume of 460 L. The tank contained water dechlorinated with Tetra Aquasafe and filtered and cooled through a Aquamanta EFX 600 External Canister Filter and D-D Aquarium Solution DC 750 connected in series (at a flowrate of approximately 0.75 Ls^{-1}). The tank was provided with tubes and rocks to create refugia for the eels and an automatic light kept a 16:8 light:dark cycle in keeping with the sunlight hours at the time of the experiment. The fish were fed bloodworm daily each morning before the trials and the water quality was checked every other day to ensure that pH, ammonia and nitrites were in the recommended margins (ammonia 0-0.2 mg/L; nitrite 0-0.25 mg/L; and pH 7-8). The tank was kept shut with a plexiglass sheet to ensure no eels were able to escape. Fish size averaged 168 mm in keeping with the specific section of the eel screen regulations being tested, for full measurement details, see Table 2.1 in the supplementary materials. After the trials were completed, all eels were measured with calipers and weighed, then returned to the location of their capture. All work was approved by Cardiff University Animal Ethics Committee and linked to UK Home Office PP816714.

2.2.2 Experimental setup

The trials were conducted in an open channel recirculating flume 10 m long, 1.2 m wide and 0.3 m deep with a bedslope of 1/1000. The experimental area consisted of a screen mounted at either 90º, 31.5º, 26.5º, or 20º to the flow direction (Figure 2.2), and 4 m upstream of the screen left with a bare flume bed (PVC) and walls (glass). At the upstream end of the flume and downstream of the fish screen, flow straighteners were used to prevent the eels from escaping the designated area. The screens were attached to the flume walls with G clamps and sections of screen were joined together by G clamps and zip ties to produce different screen lengths to achieve the correct screen length for the angle required. When a bypass was present, a 130 mm wide gap was left at the downstream end of the screen between the screen and the wall and the screen was then supported by a wooden arm attached to the flume wall and screen end. For a full depth bypass, the gap was left unobstructed whereas for surface and bottom bypasses, a blanking plate was used to block the bottom and top half of the flow depth respectively. Attention was taken to never leave gaps between screen sections or the walls or bed and to present a smooth screen surface. Three screen types were tested, horizontal and vertical wedge wire screens with 3 mm wire and 3 mm gaps (supplied by the Environment Agency) as well as a plastic Hydrolox screen section from a rotating band screen consisting of a plastic panel with a grid of holes (Hydrolox 2024). The flume water was dechlorinated with Prime Dechlorinator and cooled to 17 $\pm$ 2 ºC with a D-D

Aquarium Solution DC 2200. The experiments were recorded with three cameras; a wide-angle camera recording the entire experimental area, a handheld GoPro Hero 9 camera used to record interactions with the screen through the glass flume wall, and a high speed camera recording the screen surface and the adjacent area. The high speed camera had a sampling rate of 80 frames per second to capture the eel's interactions with the screens from above and to conduct kinematic analyses. The flow conditions (shown in Table 2.1) were established in the flume without screens to have constant flow depth for the length of the working area.

Table 2.1. Experimental treatments showing all combinations of screen type, angle, and bulk velocity that the eels were exposed to in the flume. For the treatment names, the first letter denotes screen type (H = Horizontal Wedge Wire, V = Vertical Wedge Wire, P = Plastic Hydrolox), the number denotes the angle of the screen to the streamwise direction, and any subsequent letter denotes bypass type (FB = Full depth Bypass, BB = Bottom Bypass, SB = Surface Bypass).

Treatment	Screen type	Angle to flow	Bulk Velocity (ms^{-1})	Flow depth (mm)	Bypass
H90	Horizontal	90°	0.15, 0.3	130, 168	No
H31.5	Horizontal	31.5°	0.15, 0.3	130, 168	No
H26.5	Horizontal	26.5°	0.3, 0.45	168, 144	No
H26.5FB	Horizontal	26.5°	0.3, 0.45	168, 144	Yes
H26.5BB	Horizontal	26.5°	0.3, 0.45	168, 144	Yes
H26.5SB	Horizontal	26.5°	0.3, 0.45	168, 144	Yes
H20	Horizontal	20°	0.3, 0.45	168, 144	No
V90	Vertical	90°	0.15, 0.3, 0.56	130, 168, 130	No
V31.5	Vertical	31.5°	0.15, 0.3	130, 168	No
V26.5	Vertical	26.5°	0.3, 0.45	168, 144	No
V20	Vertical	20°	0.3, 0.45	168, 144	No
P90	Hydrolox	90°	0.15, 0.3	130, 168	No

2.2.3 Hydrodynamics

Particle Image Velocimetry (henceforth PIV) was used to quantify the flow dynamics of the setup and the screens. PIV was conducted for all screen configurations in both a side view and a top view. The area illuminated by the laser sheet measured 400 mm wide and up to 600 mm long. Where the screen was angled, the equipment was moved across the flume following the screen surface at four locations. For side view PIV, the entire water column was captured, and for top view PIV, three readings were taken, one 20 mm above the bed,

one mid-depth, and one 20 mm below the surface water. For all screens and inclinations, the bulk velocities tested for PIV were 0.15 ms^{-1}, 0.3 ms^{-1}, and 0.45 ms^{-1}, approach velocity is defined at 100 mm from the screen surface. To conduct PIV, a Baumer VLXT-50M.I camera with a Kowa LM8JC10M 8.5cm lens was used, recording at 120 frames per second. To produce the laser sheet and synchronise it to the camera, a Rigol 1032Z wave generator was used in conjunction with a Polytec BVS – II Wotan Flash stroboscope at 15% intensity and a STEMMER IMAGING CVX Triggerbox. The flow was seeded at 0.063 gL^{-1} of AXALTA Talisman 30 White 110 particles. All other light sources were temporarily shut off during the PIV recording. The PIV images were recorded as TIFF files and stored on an external hard drive then analysed with PIVlab version 2.63 in MATLAB R2023a. Custom MATLAB scripts were then utilised to further analyse the results of the PIV exported from PIVlab. The streamwise velocity was defined as *u,* the vertical velocity as *w*, and the lateral velocity as *v*, the bulk velocity (spatially and temporally averaged *u*) was called *U,* and the temporal fluctuations in streamwise velocity and lateral velocity termed *u' and v' respectively.* The resultant velocity was termed R ($\sqrt{u^2 + v^2}$), the screen angle as α to the longitudinal direction, and the horizontal Reynolds Shear Stress (RSS) was calculated as $\tau_{uv} = -\rho\overline{(u'v')}$. The sweeping velocity (*Vs*) defined as the component of the velocity parallel to the screen and the escape velocity (Ve) defined as the component of the velocity perpendicular to the screen were calculated as:

$$Vs = (\sqrt{u^2 + v^2}) \cos(\alpha - \tan^{-1}\frac{v}{u}) \qquad\qquad (2.1)$$

$$Ve = (\sqrt{u^2 + v^2}) \sin(\alpha - \tan^{-1}\frac{v}{u}) \qquad\qquad (2.2)$$

2.2.4 Experimental procedure

The trials were conducted in daytime hours for increased visibility of the camera recordings and the light sources were kept constant throughout the trials. Of the 32 eels collected, 30 were chosen for the trials and all eels completed all treatments randomly. The eels were acclimated to the flume water for one hour before being exposed to a flow of 0.15 ms^{-1} for 15 minutes prior to the beginning of the trial. At the start of the each trial, the eels were placed upstream of the screen in the release area (Figure 2.1) at 0.15 ms^{-1} for 5 minutes and then at 0.3 ms^{-1} for a further 5 minutes for screen angles of 90° and 31.5°, whereas for angles 26.5° and 20°, the first 5 minutes were spent at 0.3 ms^{-1} and the following 5 minutes at 0.45

ms^{-1}. Any trial was interrupted if an eel became impinged, this was defined as a state of exhaustion in which the eel was unable to detach from the screen and swim upstream and was tested by starting a 60 s timer every time an eel rested on a screen. If after 60 s the eel was still in contact with the screen, the back of the screen was tapped to dislodge the eel if it had the strength to swim away, if it remained impinged, it was declared impinged and moved to a recovery tank. If the eel moved away from the screen within the 60 s or after the screen was tapped, it was considered as resting during that time and the experiment was allowed to continue. Any subsequent contact with the screen started a new 60 s timer. If the full 10 minutes of the experiment elapsed with no impingement, the eel was removed and placed in a recovery tank. In the event of an eel passing downstream of the screen, it was placed upstream again with a fish net, the escape noted, and the experiment was continued. For the vertical wedge wire screen and the Hydrolox screen at 90 °, a third bulk velocity of 0.56 ms^{-1} was tested for a further 5 minutes if the fish had not impinged prior, this was done to test the maximum velocity the flume could achieve with those conditions to evaluate if 0.56 ms^{-1} was sufficient to reliably impinge the eels in a short time for use in fish recovery and return systems, a full list of treatments and velocities is specified in Table 2.2. After all trials, each eel was inspected visually for external injuries sustained during the trial. Water temperature of the flume was monitored throughout the day and remained within the specified margin.
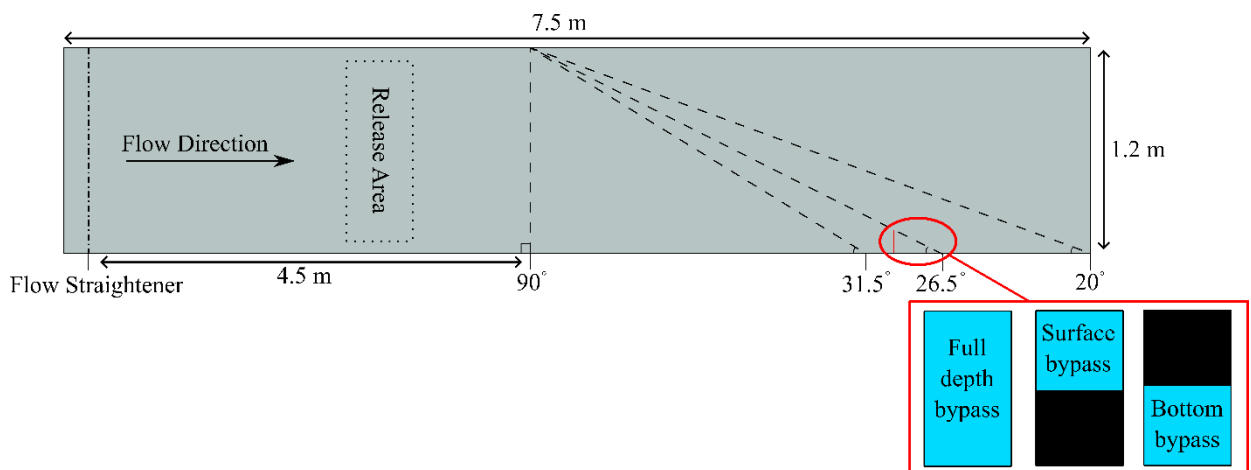
Figure 2.2. A schematic showing the flume (grey rectangle) with the different angles of channel spanning screens. In treatments where a bypass was present, it was located at the downstream end of the 26.5° screen. The bypass position is indicated by the red line and was 130 mm wide and the three bypass configurations shown below with the blue areas marking the unobstructed part of the bypass.

2.2.5 Kinematic analysis of the eel screen interaction

Kinematic videos recorded at 80 frames per second (fps) were analysed in Kinovea (Charmant, 2022). The videos were subjected to a frame-by-frame manual analysis which produced robust data despite small surface wave interference that prevented automated tracking. The full list of tracked parameters is available in Table 2.2. For a subset of clips, a minimum of equidistant 10 points were tracked along the length of the eel's body to fully visualise the swimming gait and evaluate swimming amplitude.

Table 2.2. The kinematic parameters were measured in Kinovea for 80 fps clips. Frame-by-frame analysis was used to track the eels near the screen. The reference direction was always to the longitudinal flow direction and a screen perpendicular to the flow is considered at 90° to the flow.

Variable	Description	Schematic
Tailbeat frequency (Hz)	Frequency of the oscillation of the caudal fin	
Swimming speed (BLs^{-1})	The ground speed of the fish plus the flow velocity normalised by fish length when swimming in the upstream direction	
Swimming orientation (deg)	The direction of alignment of the fish's body	
Swimming direction (deg)	The direction of movement of the fish	
Escape angle (deg)	The angle of the fish's body to the screen at the moment of escape from the screen	

Attached proportion (-)	Proportion of the fish's body length touching the screen directly before escape	

2.2.6 Statistical analysis

The behavioural and kinematic data were analysed in RStudio R version 4.2.2 (R Core Team 2022). To perform analyses with generalised linear mixed models (GLMM), the nlme and lme4 packages used (Carey and Wang, 2001; Bates et al., 2015). For generalised linear models (GLM), the MASS package was used (Venables and Ripley, 2002). For all variables, the effect of the same fish being used in each treatment was evaluated by running a null GLMM and then finding the R^2 value to determine if a GLMM was necessary following established methods (Sonnino Sorisio et al., 2024). This approach revealed that fish id had no effect and GLMs were therefore used because of better model fits. In all models, experimental order was also included. To find the best model, the AIC values and the residuals were inspected, and the best fitting model was chosen. For all models considering the impingement rate and passage rate, a binomial GLM with a cloglog link was used. The analysis of the number of rejections from the eels to the bypass, a poisson GLM was used with a log link. The remainder of the statistical models for behavioural and kinematic variables were gaussian GLMs with identity links except for passage time of eels with bypass design, which was an inverse gaussian GLM with a $1/mu^2$ link.

2.3 Results

2.3.1 Hydrodynamics

The flow in the flume with fish screens was characterised by Reynolds numbers between 16,000 and 60,000 (based on hydraulic radius) and was dominated by the streamwise component of the velocity. With a 90° screen, the vertical and lateral velocity components to the velocity were unaffected and the effect of the screen on the flow only reduced the longitudinal velocity within 50 mm upstream of the screen surface. This occurred uniformly across the channel width, only being affected by the wall effects on either side, and these findings remain true for both horizontal and vertical wedge-wire screens. At lower velocities, for both the Hydrolox screen and wedge-wire screens, the impact of the screen on the flow field were similar but at higher velocities there was a more marked deceleration of the flow in proximity of the Hydrolox screen but not to the extent of modifying the screen

performance. At screen angles between 31.5° and 20° to the flow, the velocity remained uniform and there were minor deviations of the flow in the direction of the screen within 30-50 mm of the screen surface, introducing a lateral velocity component, as can be seen in Figure 2.4. Where the screen meets the flume wall (where no bypass is present), there is a reduction in velocity magnitude that is higher with screen angles 20° and 26.5° and lower at a screen angle of 31.5°. Despite the velocity reduction, the velocity gradients remain low, with no harsh transitions in flow regime being present in any screen configuration without a bypass. Consequently, Reynolds Shear Stress (RSS) magnitudes were never elevated, with slightly higher values in higher velocities but no areas of consistently high RSS (Figure 2.4).
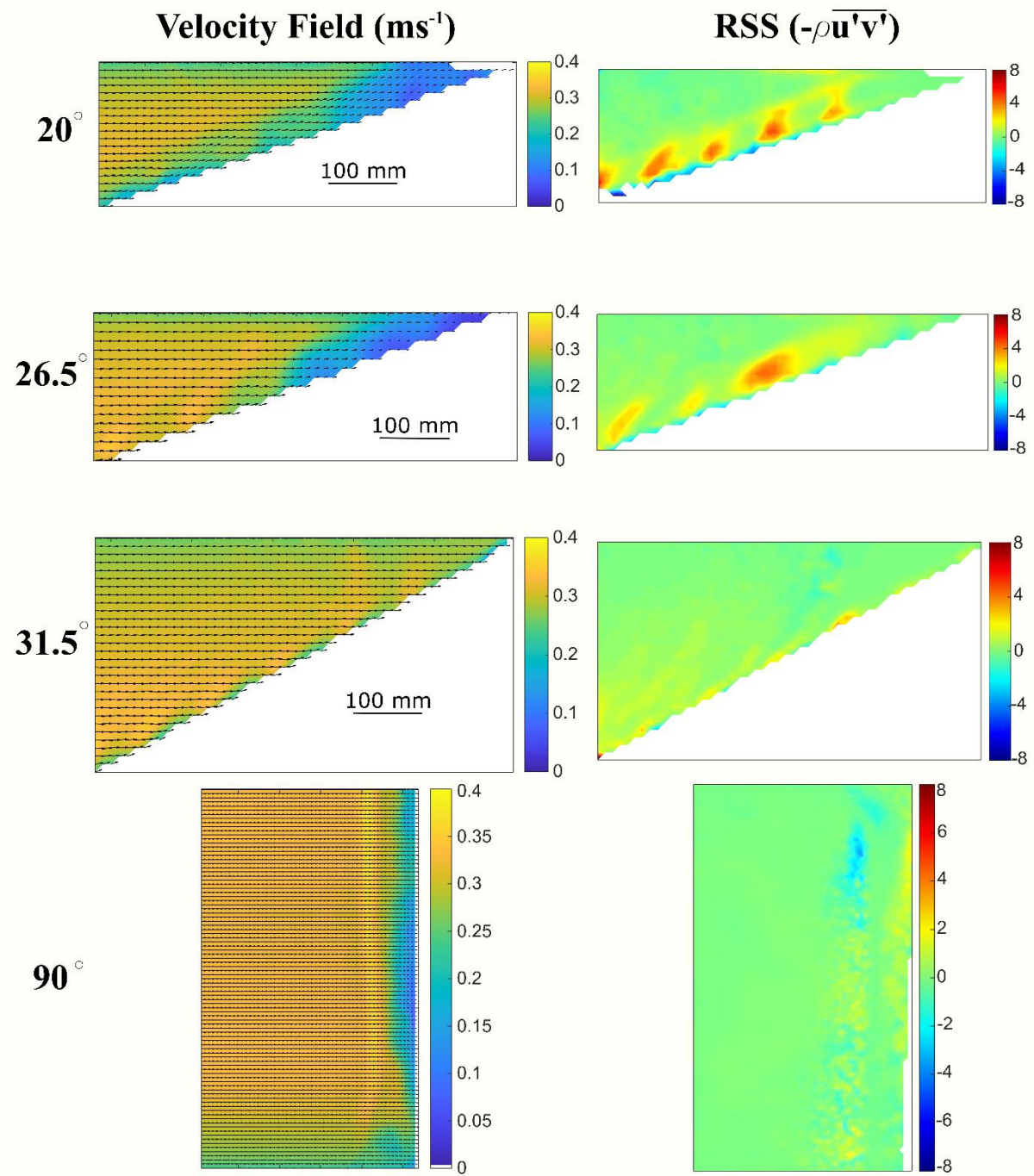
Figure 2.3. Top view contour plots showing the resultant velocity, vectors composed of the streamwise and lateral velocity components (ms^{-1}) and horizontal Reynolds Shear Stress (RSS; kgm^{-1}s^{-1}). All plots are from conditions with 0.3 ms^{-1} bulk velocity and for a horizontal wedge-wire screen without bypass. Measurements are taken at mid depth, white areas on plots indicate that no data was available, the streamwise velocity is left to right and the plots are not to scale. For the top six plots, the top boundary is the left hand side flume wall and

in the 90° plots top and bottom are both flume walls. Plots for all other flow conditions and screens are in the supplementary materials.

With a bypass present (with a screen at 26.5° to the flow), the flow fields upstream of the opening remained unaffected, whilst the velocity increased when approaching the bypass. The full depth bypass showed a mild velocity gradient leading to the opening and a wake with a few turbulent vortices and lower vorticity values compared to the other bypass types. The bottom and surface bypasses both showed sharper flow accelerations at mid flow depth as a result of half of the flow depth being blocked for the width of the opening. With these two bypasses, enhanced vertical velocities were generated that contributed to the increased velocity gradient. In the wake of the bottom and surface bypasses, for all flow conditions tested, a vortex street was shed from the trailing edge of the screen with areas of high vorticity. Plots and videos showing these wake characteristics are present in the supplementary materials.
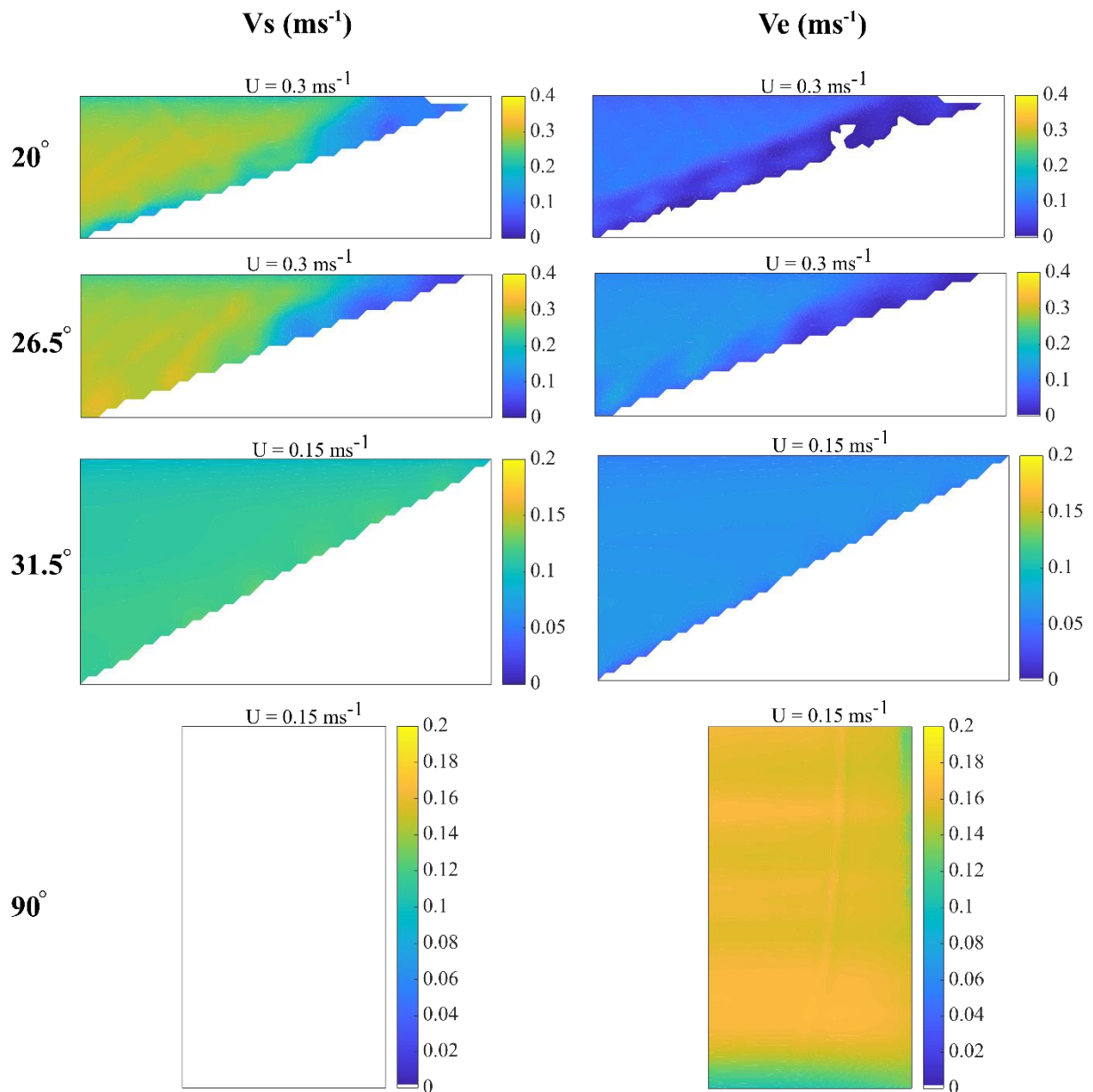
Figure 2.4. Top view contour plots of sweeping velocity (Vs) and escape velocity (Ve) for a horizontal wedge-wire screen at the four angles tested. For each angle, the plots portray Vs and Ve for the bulk velocity that represents the maximum allowable velocity at the screen according to Environment Agency regulations (0.15 ms^{-1} for screens at 90° and 31.5°, and 0.3 ms^{-1} for screens at 26.5° and 20°). Measurements are taken at mid depth, white areas on plots equate to values equal to 0 or where no data was available. Plots for all velocities tested and screen types are available in the supplementary materials.

The sweeping and escape velocities (Vs and Ve respectively) as defined in the methods are a measure of how well a screen can guide fish downstream and how difficult it is for fish to swim away from the screen. An analysis of these components of the velocities in Figure 2.4

51

shows how sweeping velocities are greatest for smaller screen angles and decrease to zero for perpendicular screens. The escape velocity, however, shows the opposite trend, being very low at 20° and steadily increasing to a maximum at 90°, where it is approximately the same as the streamwise velocity component. The magnitude of these velocities was driven less by the flow being deviated by the screen (Figure 2.3) and mostly by the screen angle as shown by the closeness of the data points in Figure 2.5 to plots of sine and cosine, indicating that for the flow conditions tested screen angle governs Vs and Ve magnitude. When normalised by the bulk velocity, there is little variation in Vs and Ve between different bulk velocities and screen angles, again pointing to the screen angle being dominant over other flow characteristics produced by the screen, making these velocities predictable if screen angle and bulk velocity is known for a uniform cross-sectional channel such as a laboratory flume.
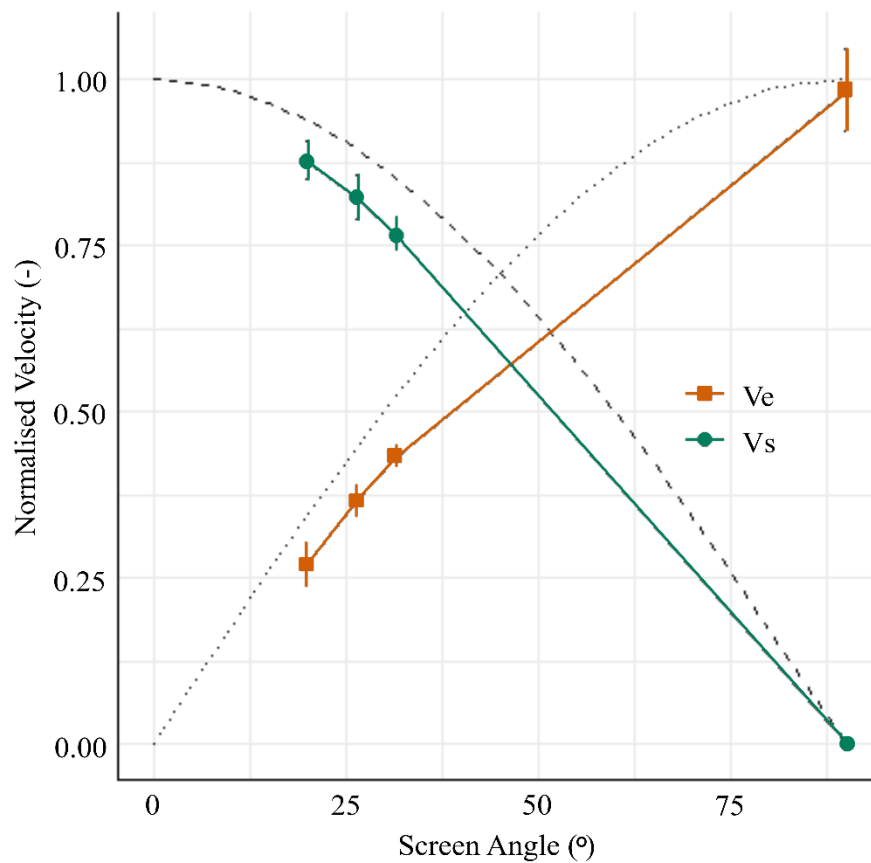
Figure 2.5. A plot of the average sweeping (Vs) and escape (Ve) velocities normalised by bulk velocity (U) against screen angle based on a sampling area within 300 mm of the screen surface. For each angle, data from all flow conditions and screen types are combined, their

variation is represented by the whiskers on each data point. The dotted and dashed lines represent sine and cosine functions respectively.

2.3.2 Impingement and passage

For all screens at the maximum permissible flow velocity for that angle according to regulation (0.15 ms^{-1} for screens at 90° and 31.5°, and 0.3 ms^{-1} for screens at 26.5° and 20°), there was no impingement and this independent of screen type (GLM, p>0.4). Impingement was recorded only in velocities exceeding the regulation velocity, which were set as an ulterior 0.15 ms^{-1} beyond the regulation velocity. Higher bulk velocities significantly increased impingement (GLM, p<0.02), and impingement probability increased with velocity, reaching a maximum for the 0.56 ms^{-1} condition as shown in Figure 2.6A. It should be noted in Figure 2.6A that the 0.3 ms^{-1} data includes all angles including angles for which 0.3 ms^{-1} was the lower velocity and at which no impingement occurred. Impingement was also significantly higher with higher angles (GLM, p<2e-16), with screens perpendicular to the flow having the highest impingement rates. For fish that impinged, it took longer to impinge with the 90° screen (GLM, p<0.035), potentially due to the lower velocities in that treatment at the start of the trials. Despite the low impingement numbers (maximum 20%, minimum 3%, overall 9.6%), 68% of fish made contact with the screen at least once but could swim upstream in the majority of these contacts.

Throughout the trials, no entrainment occurred through the 3 mm screen gaps, showing that it is an appropriate opening for the size of eels. However, during pre-trial tests if any small gaps were left between the two sections of the screen (since they were made up of between one and three different sections) or between the screen and the flume bed, eels commonly found these gaps and passed downstream.
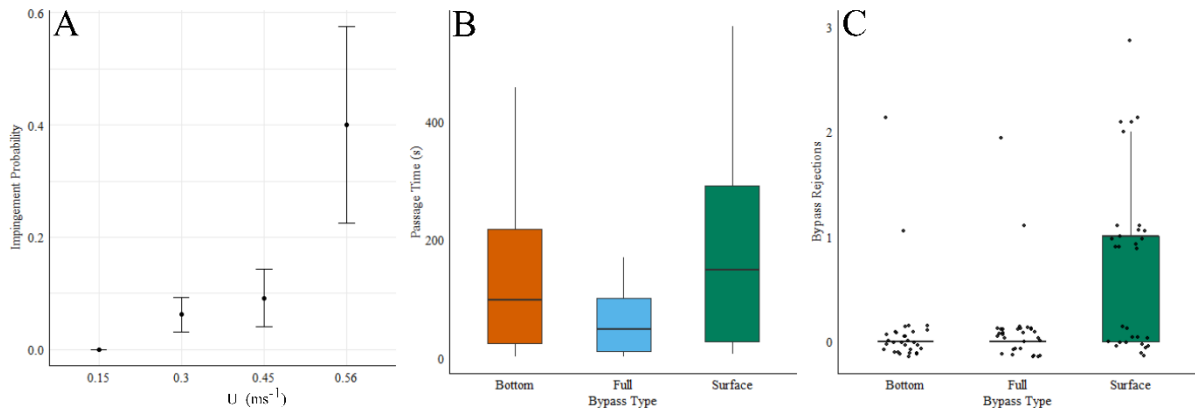
Figure 2.6. A – Impingement probability with bulk velocity (U) with error bars. It should be noted that in this plot, the 0.3 data contains all angles including those at which 0.3 ms^{-1} was the lower velocity were no impingement occurred. B – Time taken by the fish to pass downstream using the bypass for each bypass type. C – Number of times each fish rejected the bypass according to bypass type.

In the trials with the different bypass arrangements, there was no significant difference in overall passage rate between bypass types (GLM, p>0.38). Passage time, however, was quicker for the full depth bypass (GLM, p<0.05) but not significantly different between surface and bottom bypasses (GLM, p=0.52) despite the mean passage time being lower for the bottom bypass as shown in Figure 2.6B. Fish rejected the surface bypass significantly more often (GLM, p<0.002) than the other bypasses in which very few rejections occurred (Figure 2.6C). Fish length did not impact bypass passage nor impingement (GLM, p>0.05).

2.3.3 Kinematics

Behaviour was analysed for all video clips where an eel rested on and escaped from the screen before swimming upstream. The escape angle (Table 2.2) was significantly higher with higher screen angles (GLM, p=1.8e-15) as the eels point themselves into the flow. The proportion of the body in contact with the screen immediately before escape, however, showed no correlation with screen angle. When approaching the screens, fish were significantly more likely to make contact with the screen head-first when the screen was perpendicular to the flow and tail-first with all other screen angles (GLM, p=2e-16).
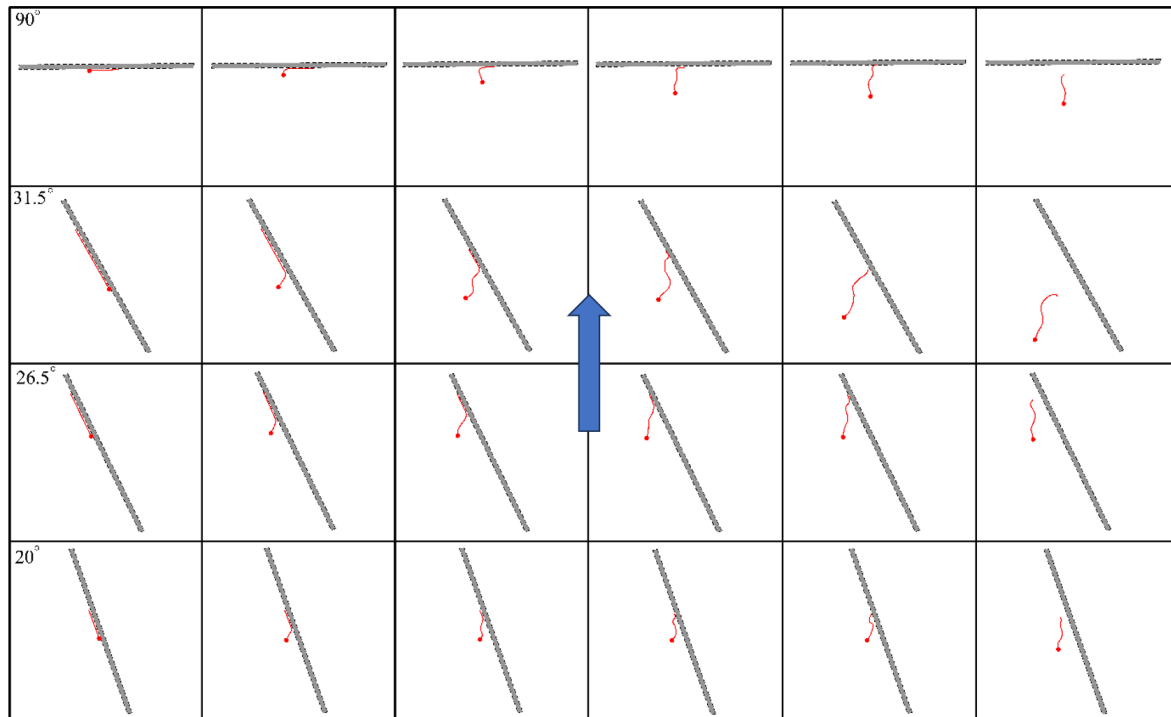
Figure 2.7. Four series of frames showing six stages of fish releasing from the screen at each screen angle tested. The frames are in succession from left to right, starting with the fish flat against the screen. The screen is represented by the grey bar and the fish by the red line with the red circle representing the head. All swimming events portrayed on this plot were taken from trials at 0.3 ms^{-1} (flowing from bottom to top) for the purposes of comparison and are representative of the manner in which the eels escaped themselves from the screen.

Screen angle impacted the body movements made by the eels to escape from the screen after contact or a period of resting. As shown in Figure 2.7, the angle the eel must produce between its body and the screen to point itself into the flow is smaller, the smaller the screen angle. The trajectory of the eel post-escape shows how the eels are able to move in a cross-flow direction with the lower angled screens but at 90° they must propel themselves directly against the flow and therefore push off the screen.

The distance the fish swam from the screens correlated with the orientation angle the eels were swimming at (GLM, p=4.7e-15). The swimming direction was also related to the orientation angle of fish swimming (GLM, p=2e-16), the orientation angle being smaller than the overall direction of movement of the fish as they contend with the oncoming flow. The degree to which the eels swam directly against the flow increased in proportion to how large the angle to the flow their trajectory was (GLM, p=6.7e-9), and this appeared to cause

the fish to increase their tailbeat frequency (GLM, p=0.02), suggesting increased energy expenditure.
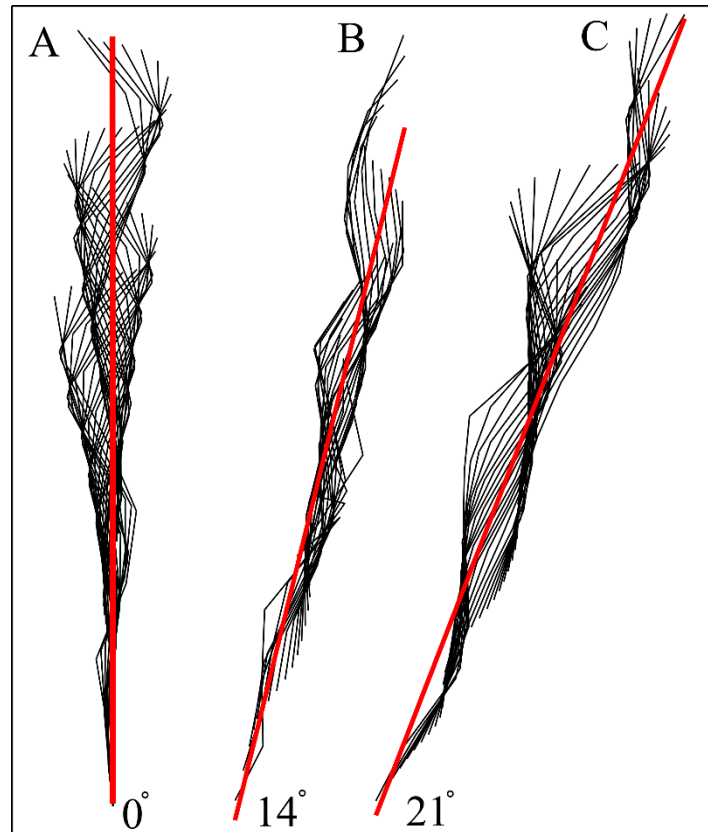
Figure 2.8. Three plots showing the swimming trajectories and body positions of eels swimming at progressively larger angles to the flow direction. Each black line is the midline of the eel body and successive black lines show progression frame-by-frame, with the head of the eel facing the bottom of the plot and the water flowing from bottom to top. The red lines show the overall path of the eel. All swimming events portrayed on this plot were taken from trials at 0.3 ms^{-1} and away from the screens.

A detailed analysis of the swimming gait of the eels swimming at different angles (Figure 2.8) revealed how the amplitude is asymmetric when swimming at an angle to the flow. In Figures 2.8B and 2.8C where the eel is swimming at increasingly larger angles to the flow, the swimming amplitude on the downstream side of the red trajectory line (left side of Figures 2.8B and 2.8C) is larger than the upstream. The head amplitude is also increased in 2.8B compared to the fish swimming in 2.8A and is largest in 2.8C. This is consistent with the previous findings of the eel orientation having a smaller angle to the flow than the swimming direction. By comparison, Figure 2.8A shows a symmetrical gait with a low head

amplitude. The eel is therefore swimming asymmetrically to move at an angle and traverse the flow while still making upstream progress.

2.4 Discussion

This study found that the current UK regulations create an effective protection for eels in the tested size range of 121-300 mm if all guidelines are followed. Importantly however, when velocity was increased, impingement started to occur, and whenever in the pre-trials there was a small gap between screen panels, there were high levels of entrainment. The levels of impingement found in this study are lower than found in a previous study concerning eels with a similar size range, where impingement occurred at a lower velocity (Carter et al., 2023). This difference in impingement rates can be attributed to differences in methodology and how impingement was defined in the two studies, with this study considering the eels as 'resting' if they could subsequently (and within the allowed time of 60 seconds) escape from the screen whilst they would be considered impinged in the aforementioned study. Using a similar definition of impingement to Carter et al. (2023) would result in impingement rates of 68% instead of 9.6%. The water temperature could also be a contributing factor to the lower impingement, temperature increases swimming speed in fish, allowing them to escape from a screen more easily if the temperature is high (Clough et al., 2004; Muhawenimana et al., 2021). This study found no difference between the two bar orientations of wedge-wire screens, similar to studies using bar racks (de Bie et al., 2021), however, other studies have found differences between horizontal and vertical screens and racks, vertical wedge wire screens have previously been found to produce a higher velocity gradient towards a bypass and therefore decrease chub (*Squalius cephalus*) passage (de Bie et al., 2018). Hydrodynamically, the vertical and horizontal wedge wire produced similar flow fields on a flume scale (Lemkecher et al., 2022).

Screens with smaller angles to the flow reduced impingement rate but for the fish that did impinge, the time before impingement was shorter for perpendicular screens. This can probably be explained by considering that the 90° screen had lower flow velocities than 20° and 26.5° but can also point to the difficulty of releasing from a 90° screen. The kinematics reveal how the eel must first point itself into the oncoming flow, which requires them to turn more for perpendicular screens and less for screens closer to the flow, and then they must push off of the 90° screen directly into the flow whereas with an angled screen they can

allow themselves to drift in a crossflow direction before engaging a steady swimming gait (as established by Tytell (2004) and shown in Figure 2.8), a manoeuvre which depends less on generating a forward momentum whilst contending with a lower drag force. This hypothesis can potentially explain why fish took longer to impinge with a 90° screen but did so more often; the lower flow velocities allowed the eel to swim upstream of the screen without needing rest for longer, but once they did make contact with the screen, it was harder to escape from it. To some extent, this phenomenon can also be visualised by considering escape velocity, which is lowest at the smallest angle (shown in Figure 2.6). The sweeping and escape velocities, calculated from equations 1 and 2, are highly dependent on flow in the streamwise direction due to the screens not generating comparatively high crossflow velocity components. The sine and cosine lines on Figure 2.6 would predict Vs and Ve if there was no crossflow (v) component, however the screens deviate the flow enough for the measured Ve and Vs values to be slightly different but not enough to impact on the fish kinematics. Figure 2.8 shows how the eels adapted their swimming gait to diagonal swimming by pointing their bodies at a smaller angle to the flow than their overall movement direction, also meaning that their swimming amplitude is larger on the downstream end of the red line in Figure 2.8. This data shows that despite the flow being slightly deviated by the screens, the eels still had to swim against the main longitudinal velocity component (U) as well as moving sideways. Where a bypass is present, de Bie et al. (2018) found that Vs and Ve increase towards the bypass location, whereas the opposite trend was found in this study when there is no bypass and the screen meets the flume wall. This is due to the flow accelerating towards an open bypass but decelerating if the downstream end of the screen is present (Meister et al., 2020b). The velocity field found at the screens in this study match well with previous literature using ADV (Beck et al., 2020; Meister, 2020; Raynal et al., 2013), and through the use of PIV, measurement of velocity fields was measured with higher spatial resolution over a larger sampling area, allowing for the flow to be measured very close to the screen surface. These detailed readings are particularly useful when considering the flow experienced by impinged fish of small size.

Eels are well known to prefer bottom and full depth bypasses (Calles et al., 2012; Egg et al., 2017; Meister, 2020; Harbicht et al., 2022), although even these can be ineffective. This study found very high passage rates (91% overall) across all bypass designs, possibly as a result of the modest size of an experimental flume compared to a full scale river meaning that the eels could easily and quickly explore the entire working area. Despite the high

passage, there was a distinct difference between passage time for the full depth bypass and the surface and bottom bypasses. This may be attributed to the increased velocity gradient towards the surface and bottom bypasses as half of the flow area is blanked and there is therefore an increase in acceleration towards the open flow area in comparison to the full bypass where the entire area is open. Moderate velocity gradients have been found to increase passage counts whilst harsh ones decrease it (Beck, 2020; Egg et al., 2017; Piper et al., 2015). As a result of the higher velocity present, the surface and bottom bypasses generate a vortex street in the bypass which may deter fish that interact with the vortices (Muhawenimana et al., 2019). The preferred bypass arrangement is therefore the full depth, however this is not always practical to implement in the field. Between the surface and bottom bypasses, the bottom bypass is the best performing option as the eels rejected it far less than the surface bypass (Figure 2.6C), this may be due to eels preferring to swim towards the bed of watercourses. This study did not evaluate other negative effects of fish screening such as descaling or predation.

2.5 Conclusion

Lower flow velocities and lower angles to the flow both decrease impingement for 3 mm wedge-wire screens, for which no entrainment occurred, whilst screen orientation did not affect impingement. The angled screen is directly beneficial to the sweeping and escape velocities and allows eels to escape from the screen more easily. This is shown by the kinematic analysis that evidences how the screen angle allows eels to use the sweeping velocity and drift sideways into the open flow instead of needing to overcome the drag on the perpendicular screen. For the three bypass types tested surface, bottom, and full depth bypasses, the full depth is preferable to the bottom bypass, which in turn is better than the surface bypass. The recommended screening techniques in Environment Agency (2020) are appropriate to the tested fish sizes and flow velocities and satisfy the need for fish protection whilst not requiring extremely fine screen aperture, stipulate velocities that are too slow, or the use of very small screen angles, all of which drive screen and installation price (Clough et al., 2013) thus making these solutions accessible. Of the tested screen types, all materials and orientations performed equally well, however horizontal wedge-wire may be preferable to vertical due to the ease of cleaning as the sweeping velocity could push trash downstream

if the screen direction aligns with the velocity. This chapter addresses objectives 2, 4, and 5 of this thesis.

Chapter 3. Eel Tile Hydrodynamics and Canopy Flow Analyses

Conceptualisation and methodology by Prof. Jo Cable, Prof. Catherine Wilson, Andy Don, and Guglielmo Sonnino Sorisio. Data collection by Guglielmo Sonnino Sorisio and Kathryn Lenton. Analysis, visualisation, and writing by Guglielmo Sonnino Sorisio and editing by all of the above.

Summary

Eel tiles have been proposed as a solution for fish passage at high velocity barriers, such as culverts, where the altered flow renders upstream passage challenging. The tiles feature cylindrical protrusions set in a staggered array composed of two array densities and protrusion diameters which make them similar to rigid vegetation canopies present in nature. The aim of the study was to quantify and analyse the impact of the tiles on the flow field in the surrounding area and within the tiles for submerged conditions and to evaluate their potential to produce favourable conditions to fish passage. Tiles were mounted in a recirculating flume in two different configurations near the flume wall, leaving part of the channel smooth. Particle image velocimetry was employed to acquire hydrodynamic data for ten flow conditions varying in both bulk velocity and flow depth. The tiles produced a large reduction in streamwise velocity within them as well as around them and did so consistently for all flow conditions. The Reynolds shear stress produced by the tiles was similar to canopy flow turbulence but the turbulent structures were not as discrete. The hydrodynamics of the tiles appear appropriate for fish passage due to the induced slow flow and moderate turbulence.

3.1 Introduction

European rivers are severely fragmented by manmade structures (Belletti et al., 2020). These dams, weirs, culverts and other such structures disconnect rivers resulting in decreased biodiversity (Fuller et al., 2015; Wu et al., 2019). Each of these barriers poses a unique challenge for fish passage. Flumes used to measure open channel flows and culverts in rivers can channel the flow into smooth sections which cause steep velocity gradients. These sections are often smaller than the river width (Shiau et al., 2020) and this accelerates the bulk velocity of the river, which prevents or delays fish being able to swim upstream. This

problem can occur wherever anthropogenic modifications to the river result in high flow velocities without providing adequate mitigation features to allow fish to pass upstream. Migratory species such as the critically endangered European eel (*Anguilla anguilla*) must migrate upstream during their life cycle and barriers have contributed to their declining populations and Critically Endangered IUCN status (Jacoby & Gollock, 2015; Pike et al., 2020). Relative to other fish, eels have a poor maximum swimming speed (Fjeldstad et al., 2018) but can overcome obstacles by crawling or climbing (Tamario et al., 2019). This ability cannot be used when swimming through enclosed, smooth walled and fast flows; such structures must therefore be modified to allow passage.

One solution that has been applied to weirs to facilitate eel passage is the use of 'eel tiles', each tile is composed of multiple closely spaced cylindrical protrusions (Fig. 1). The tiles are mounted on the inclined surfaces of anthropogenic structures and are designed for the flow depth to not significantly exceed the top of the tile protrusions (Padgett et al., 2020). Juvenile eels can use the protrusions as an effective substrate for climbing the weirs (Jellyman et al., 2017; Watz et al., 2019) and therefore these tiles have already been installed at several locations in the UK to provide passage for eels navigating fast flows and help steer them to passage facilities (Environment Agency personal communication).

Capture trap and videographic evidence from these sites indicates that some eels do indeed use the tiles to navigate upstream but how they are used and how the tiles affect the flow when fully submerged is not yet understood.
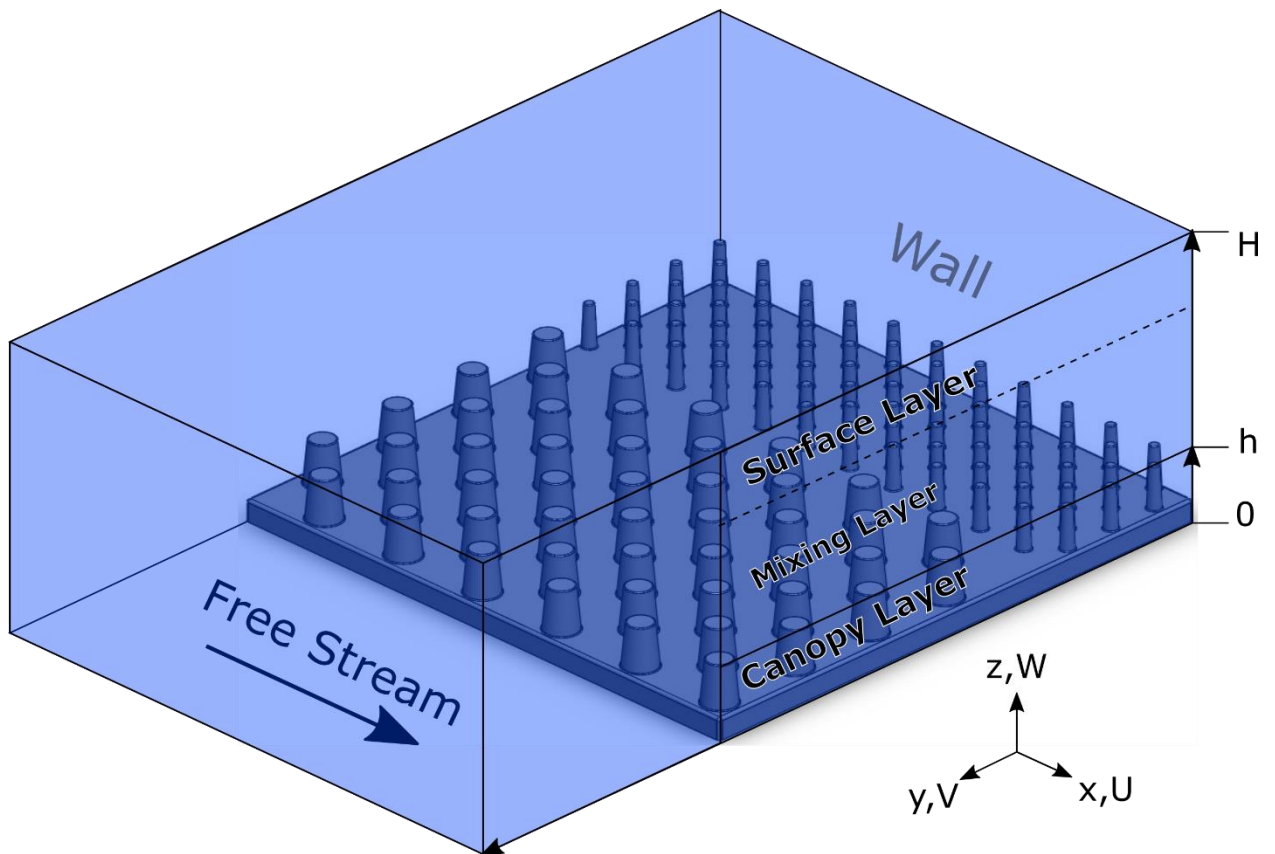
Figure 3.1. The eel tile and the protrusions designed to help eels ascend instream obstructions. Here, h represents the height of the protrusions and H is the depth of the flow from the flume bed. The layer of flow below and above h are termed the canopy layer and surface layer, respectively. The mixing layer is the area of flow that includes the top portion of the canopy layer and reaches the surface layer. The small protrusions are adjacent to the wall of the flume in this figure whilst the large protrusions end along the channel centreline and are therefore next to free stream flow.

The tile's cylindrical protrusions create a structure that bears similarities with some vegetation types present in freshwater streams (Caroppi et al., 2018; White & Nepf, 2008). The shedding and turbulent structures in submerged vegetation, defined as when the vegetation top is below the water surface, is often analysed as canopy flow; this type of flow occurs in nature in a multitude of scenarios, including air flow over trees or water flow over corals. Initially flow through submerged vegetation was analysed as a surface roughness layer but following on from Raupach et al.'s (1996) assertion that canopy flow is more similar to a mixing layer rather than a surface roughness layer when considering parameters such as velocity profiles, turbulent kinetic energy and Reynolds shear stress, it has been viewed as a mixing layer. Thus, analysis of the largest length scale instabilities and turbulent

63

structures can be more accurately modelled as the shear layer between two free stream layers of flow travelling parallel to each other at different velocities (Raupach et al., 1996). The difference in bulk velocity between the layers of flow creates an instability, known as the Kelvin-Helmholtz (KH) instability, which was first used to understand how wind creates waves in the ocean (Brown & Roshko, 1974; Drazin, 2002; Kelvin, 1871). Batchelor (1967) provided a mathematical description of this phenomenon, wherein he also detailed some of the turbulent structures and fully formed eddies within the vortex sheet arising from the interaction between the two flow layers. In submerged vegetated flows, the KH vortices will reach the scale of the canopy height unless they are suppressed by low water depth (Ghisalberti, 2002).

Canopy flow caused by vegetation in channels is often experimentally represented by vertically placed cylinders of various diameters and spacing with similar geometries to the eel tiles. In the case of a fully submerged array of vertically oriented objects, canopy flow is characterized by different scales of turbulence, the smaller scale is that of the individual cylinder diameter (sometimes known as stem-scale turbulence; Nepf, 2012; Lou et al., 2021). The spacing and density of the canopy can also influence the stem-scale size of the turbulence. If the distance between individual cylinders is smaller than their diameter, then the length scale of the vortices will be of the spacing and not the diameter (Tanino & Nepf, 2008). The density of the array also determines how the individual stem-scale vortex streets will interact, sparse arrays with relatively small diameter cylinders can produce distinctly identifiable vortex streets, whilst more densely packed arrays of larger diameter cylinders are more likely to produce wakes that interact with each other and form more homogeneous and less discrete turbulent flow; turbulence intensity increases with increasing density regardless of these effects (Tanino & Nepf, 2008). The density also impacts the average velocity within the canopy layer, with higher densities being associated with lower velocities (Rominger & Nepf, 2011). Stem scale turbulence is important in understanding sediment and nutrient transport in channels (Lou et al., 2021; White & Nepf, 2008) but for fish larger than the protrusion diameter, the stem scale turbulence may be too small to affect swimming (Muhawenimana et al., 2019).

Turbulence of larger scale in canopy flow results from instabilities created by the shear between the canopy layer and the layers on top and on the side of the array (in the case of a vegetation patch not covering the entire width of the channel; Figure 3.1). Vegetation that

can be approximated as an array of vertically oriented cylinders generally grows in shallow water, therefore the canopy is submerged but the flow at the water surface may be influenced by the turbulent structures formed by the canopy (Ghisalberti & Nepf, 2006). This has the effect of potentially limiting the scale of the vortices produced by the instability between the canopy layer and the top flow layer (for a submerged canopy) or free stream layer of the flow (for a vegetation patch), but it also means that the layer above the canopy is not greatly affected by the boundary layer turbulence (Nepf & Ghisalberti, 2008). Larger scale turbulence is shed because of the instability created by the difference in velocity profiles between the canopy layer and the free stream and is only present if there is sufficient difference to cause an inflection in the vertical profile of streamwise velocity to produce a KH instability (Brown & Roshko, 1974; Nepf & Ghisalberti, 2008). These vortices penetrate the canopy layer of the flow and thus contribute to mixing between the two layers of flow (Nepf, 2012). In the horizontal plane (e.g. vegetation patch), the instability also produces KH vortices (Rominger & Nepf, 2011), which penetrate the canopy array. In both vertical and horizontal planes, the maximum Reynolds stress is offset a small distance into the array, away from the protrusion tops (vertical plane) or canopy edge (horizontal plane) (Caroppi et al., 2018; Ghisalberti & Nepf, 2006; Rominger & Nepf, 2011). The frequency of the shedding of KH vortices has been evaluated for vegetated flows and the values in previous studies range from 0.01-0.11 Hz (Ghisalberti, 2002). Canopy flow is therefore a useful lens through which to view and analyse the effect of eel tiles on the flow as it already covers many of the hydrodynamics associated with the eel tiles.

Typically, eel tiles are mounted close to the bank of a stream or channel to favour their use by the eels (and potentially other fish) as they exploit the favourable lower flow conditions of the banks and maximise cover. The interaction between the flow in the two adjacent areas of protrusions of different densities and diameter is also an unknown. It is important to understand the flow within and around the tiles because, like all fish, eels appear to prefer certain flow regimes (Fjeldstad et al., 2018; Russon & Kemp, 2011). For these tiles to be an effective passage solution they need to produce a flow that can be easily used by eels, this would also enable them to be used as a guidance system to other hard to find fish passes as eels often do not easily find the pass entrance (Brown & Castro-Santos, 2009). Another important factor in assessing these tiles for use in fast flows is to evaluate the level of turbulence and the forms this takes to determine the suitability of the tiles as a swimming aid for eels. Certain types of turbulence, at a scale similar to the dimensions of the fish, and

certain orientations can destabilise fish (Muhawenimana et al., 2019; Tritico & Cotel, 2010) so it would be beneficial to know if the turbulence produced by the tiles has the potential to impair eel swimming behaviour.

The aim of this study was to evaluate the effect that differing flow depths and velocities for two tile orientations. We tested the hypotheses that tiles would reduce the flow velocity in their vicinity to facilitate fish passage and produce turbulence similar to submerged vegetated canopies. Eel tiles were mounted near the wall of a flume with either the small or large protrusion side adjacent to the wall, but leaving more than half of the channel width uncovered. Tested flow ranged from 0.12 to 0.46 ms^{-1} and the relative submergence from 2.08 to 4.17 with Reynolds numbers (Re) based on the hydraulic radius ranging between 16,000 and 61,000. Thus, we investigated the effect of the tiles in a smooth channel on flow velocity. To identify the turbulent structures, we measured Reynolds shear stress and velocity profiles present in the flow and how they varied between different conditions. We analysed the flow surrounding and inside the tile protrusion layer to assess the vertical and horizontal gradients of Reynolds shear stress, turbulent structures produced and associated flow regime. The interaction between adjacent areas of protrusions of different densities were analysed, and the effect of the wall on the canopy flow. The turbulent structures were identified and the velocity profiles, the shear layers, the Reynolds shear stresses and other flow parameters were considered both vertically and horizontally across the tiles and in the smooth channel region.

3.2 Theory

The solid volume fraction ($\emptyset$) of the canopy can be calculated with

$$\emptyset = \left(\frac{\pi}{4}\right) ad \quad (3.1)$$

where $\emptyset$ is the solid volume fraction, d is the stem (or protrusion) diameter and

$$a = \frac{d}{\Delta S} \quad (3.2)$$

where ΔS is the spacing between protrusions (Nepf & Ghisalberti, 2008; Tanino & Nepf, 2008). The tiles have protrusions with a smaller diameter at the top than the bottom so for this calculation a height-averaged value of diameter was calculated for small and large protrusions and the solid volume fraction calculated for each tile density area then combined

in proportion of the size of the area they cover to obtain the overall tile solid volume fraction. The small protrusion and large protrusion regions have a solid volume fractions of 0.06 and 0.11 repsectively, giving an overall value of 0.09. These values suggest a canopy that is dense enough to generate stem scale and canopy scale turbulence which can theoretically penetrate to the flume bed (Nepf, 2012). Using this overall value and the protrusion Reynolds number (Re_d) an approximation of the coefficient of drag (C_D) can be found following the equation in (Zhao & Nepf, 2021) based on the numerical modelling work of (Etminan et al., 2017):

$$C_D = \left(\frac{1-\emptyset}{1-\sqrt{2\emptyset/\pi}}\right)^2 \left[1 + 10Re_d^{-2/3}\left(\frac{1-\emptyset}{1-\sqrt{2\emptyset/\pi}}\right)^{-2/3}\right] \quad (3.3)$$

The predicted value of C_D for test 4/C (see Table 3.1) is 1.64 for the combined tile however it should be noted that this value will change with flow velocity as the Reynolds number will change. The hydraulic resistance produced by the tiles can also be expressed as a Manning's n value by using the equations in Nepf (2012) that allow these values to be approximated for partially-vegetated channels where the canopy does not cover the full width of the channel:

$$n = \sqrt{\frac{C_*}{2}}(1 - B_x)^{-3/2} \quad (3.4)$$

where C_* is a value 0.05-0.13 and B_x=wh/(WH), w and h being the width and height of the tiles and W and H being the channel width and the flow depth. In the case of a single row of tiles mounted laterally across the channel:

$$n = \sqrt{\frac{C_*}{2}}(1 - \frac{0.025}{WH})^{-3/2} \quad (3.5)$$

since the tile width and height is fixed. This implies that the Manning's n value will decrease with increasing flow depth and will therefore not be constant which is typical for open channel flows and vegetated flows.

3.3 Methods

Eel tiles manufactured from high density co-polymer (Berry & Escott, 2023) were supplied by the Environment Agency. Each tile is 505 x 505 mm, comprised of two different areas with protrusions (height (h) 50 mm) of different diameter and density.
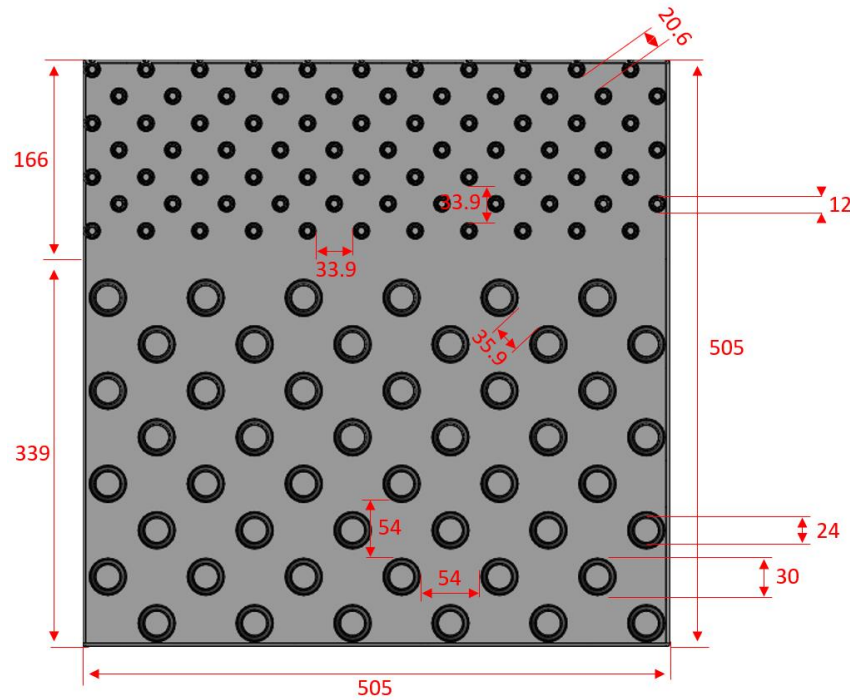
Figure 3.2. Top view schematic of a Berry & Escott eel tile with dimensions shown in millimetres. The overall height of the tile is 75 mm, the base is 25 mm tall and all protrusions are 50 mm tall. Protrusions have a reduced diameter at the top, as shown in the schematic.

The tiles were mounted with screws to the bed of a recirculating flume in the hydraulics laboratory at Cardiff University. The flume is 10 m long, 1.2 m wide and 0.3 m deep with a honeycomb flow straightener at the upstream end. The working area was a 2 m long section starting at 5 m and ending at 7 m from the downstream end. One tile edge was mounted flush to the glass sidewall and oriented as shown in Figure 3.1. Two orientations were tested: the small protrusions adjacent to the wall (orientation named SP) and the large protrusions adjacent to the wall (orientation named LP). The top view area, monitored by an overhead high speed PIV camera, was 400 mm long and 600 mm wide, whilst the section view (with the camera mounted on the side of the flume) was 400 mm long and the height equivalent to the flow depth. The view area was located 5.42 to 5.82 m from the downstream end, where the flow over the tiles was fully developed. By analysing time averaged flow properties across the field of view the flow was tested to verify it was fully developed at that location. Water in the flume was kept at 18±1°C. Different flow conditions were tested by changing the flowrate and adjusting the weir at the end of the flume to vary bulk velocity (whilst flow depth was kept constant) and flow depth (whilst bulk velocity was kept constant) (Table 3.1).

Table 3.1. Recirculating flume flow conditions tested in the current study varied in both flow depth and bulk velocity. Two series of flow condition were produced: 1 to 6 where the bulk velocity was varied and flow depth kept constant, and A to E where the velocity remained constant and flow depth varied. Condition 4/C is shared by the flow depth varying series and the bulk velocity varying series of conditions. The Reynolds number (Re_R) is based on hydraulic radius (R) and bulk velocity (U). H is the flow depth, h is the protrusion height and H/h is the relative submergence of the protrusions.

Tile Orientation	Test Name	Bulk Velocity, U (ms^{-1})	Flowrate, Q (Ls^{-1})	Re_R (-)	Water Depth, H (m)	H/h (-)
SP and LP	1	0.12	26	16,165	0.181	3.12
SP and LP	2	0.21	46	28,218	0.1805	3.11
SP and LP	3	0.29	64	38,773	0.180	3.10
SP and LP	A	0.35	54	35,280	0.129	2.08
SP and LP	B	0.35	65	40,931	0.155	2.60
SP and LP	4/C	0.35	76	46,608	0.181	3.12
SP and LP	D	0.35	88	51,962	0.208	3.66
SP and LP	E	0.35	98	55,630	0.2335	4.17
SP and LP	5	0.42	90	55,026	0.1805	3.11
SP and LP	6	0.46	99	60,901	0.1825	3.15

For all conditions in Table 3.1, uniform flow conditions were maintained. Flow depth was measured with a pointer gauge with a vernier scale (± 0.1 mm), flowrate was measured with a flowmeter (± 0.1 Ls^{-1}) and the bulk velocity was measured with PIV.

Particle Image Velocimetry (PIV) was used to analyse the flow around the eel tiles using a high speed camera (Baumer VLXT-50M.I) with a Kowa LM8JC10M 8.5 cm lens. The camera was mounted above the flume for top view recordings and on the side of the flume for section view recordings. The images were sampled at a rate of 120 frames per second, the image size captured was 1952 x 950 pixels and 2048 x 1000 pixels for the top view and section view, respectively. Streampix single-camera software was used to log the images and

establish the field of view. A Rigol 1032Z wave generator was used to trigger the Polytec BVS – II Wotan Flash stroboscope operating at 15% intensity and the high speed camera (through a STEMMER IMAGING CVX Triggerbox). The Stroboscope emits the laser pulse through optics to produce a sheet of light 300 mm wide. The flow was seeded with AXALTA Talisman 30 White 110 particles at a density of 0.0632 g/L.
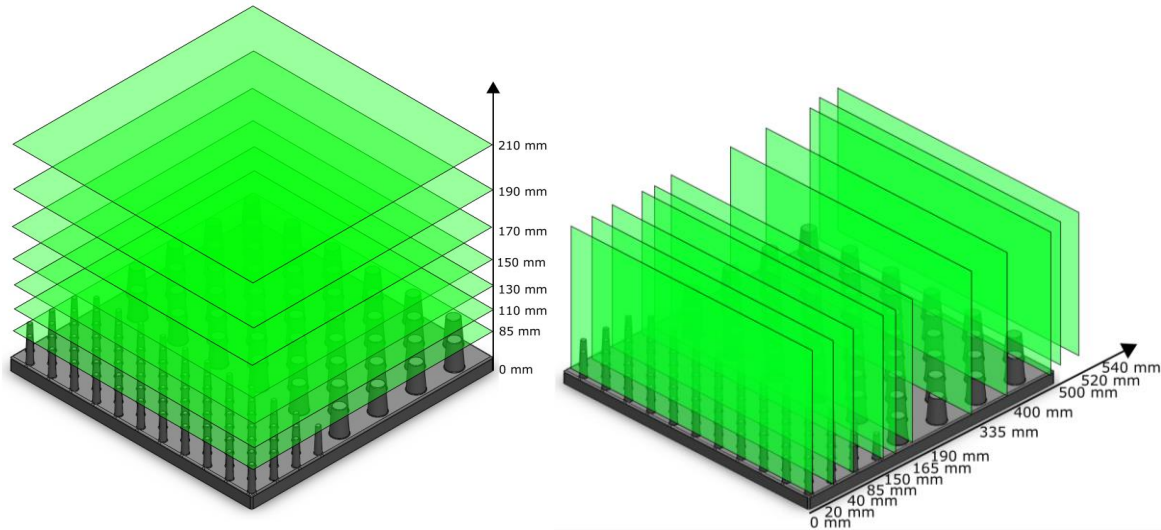
Figure 3.3. Schematic outlining locations of PIV measurements in and above the tile protrusions. For PIV recordings, the flume was set to one of the pre-established conditions (Table 3.1), a minimum of 120 s was given for the flow to reach a steady state condition after which the room lights were turned off so recordings could be made in the dark. The Rigol wave generator was then triggered and the flow was recorded for 10 s. This length of time was chosen in accordance with a sensitivity analysis of the time averaged streamwise velocity profiles and root mean square fluctuations of the streamwise velocities that was conducted by examining different lengths of time. This analysis confirmed that for a sampling rate of 120 Hz in all tested flow conditions, 10 s was sufficient to obtain a stable profile.

PIV was recorded for the tiles in both top and section views (Figure 3.3.). In top view, the laser was placed horizontally on the side of the flume near the glass wall and the camera was positioned above. Starting from the layer of flow immediately above the tiles, the laser was moved upwards in 20 mm increments until the surface layer of flow was reached. As flow depth varied, the number of top views was not the same for all conditions. In the section view, the laser was mounted vertically above the flume and oriented so that the 300 mm long pulse was visible from the side of the flume where the camera was mounted. The laser was

moved from near the glass wall across the flume width taking 11 readings (moved by 15-145 mm for each reading).

The images were analysed with PIVlab version 2.55 on MATLAB R2021b. Calibration was carried out using images of the flume with objects of known length at the correct distance from the camera for each position of the laser, variation of calibration values across the frame was checked to verify that particles at the extremities of the frame were not significantly more distant than particles at the centre of the frame. MATLAB scripts were written to use PIVlab outputs to calculate turbulent parameters not included in the PIVlab package. For turbulent kinetic energy (TKE), since only two velocity components were available for any calculation, the non-streamwise component was used twice as a substitute for the missing velocity.

To further visualise the flow field and the vortex structures around and within the tiles, flow visualization was conducted using dye injection. Dye (Cole-Palmer Fluorescent Red 00298-16) was placed into syringes and injected into the flow whilst a Nikon D5100 with a NIKKOR AF-S 10-24 lens was used to capture images and video of the flow from above the flume or from the side.

3.4 Results

3.4.1 Velocity profiles and attenuation

The hydrodynamics of the channel without tiles were first analysed to provide a baseline for all other conditions. This bare channel was designated the control condition and the hydrodynamics within this revealed a steady flow characterised by no identifiable turbulent structures and constant flow velocity (Figure 3.4). With the eel tiles in place, the vertical profiles of the streamwise velocity (u) revealed that velocity was reduced both within and above the tiles compared to the control condition. Within the tiles this increased near the top of the tiles and especially in the mixing layer above the tiles until it equalled or surpassed the velocity in the control condition in the upper parts of the water column as illustrated in Figure 3.4 for both SP (small protrusions near the wall) and LP (large protrusions near the wall) configurations. The vertical profiles of the vertical velocity (w) show that there were comparatively low velocities in the control condition compared to the increased levels in conditions with tiles. Nevertheless, the magnitude of the vertical velocities with the tiles was

moderate, reaching a maximum in the mixing layer. The horizontal velocity profiles over the tiles also exhibited a reduction of streamwise velocity with the presence of the tiles. With the tiles mounted in SP (small protrusions near wall), the streamwise velocity is low at the wall and increases for a short distance from the wall (as may be expected) before dropping to a minimum near the intersection of the two protrusion areas. Over the less porous large protrusions, the velocity increases again and an even more pronounced increase is present where the tile meets the open channel flow. When the large protrusions were mounted near the wall (LP), the velocity was lower across the top of the tiles compared to SP but the same small peak is present at a short distance from the wall. The velocity further decreases over the small protrusions, only becoming higher near the open channel. The cross-streamwise velocity (v) in both SP and LP was higher than the control but markedly higher in LP compared to SP.
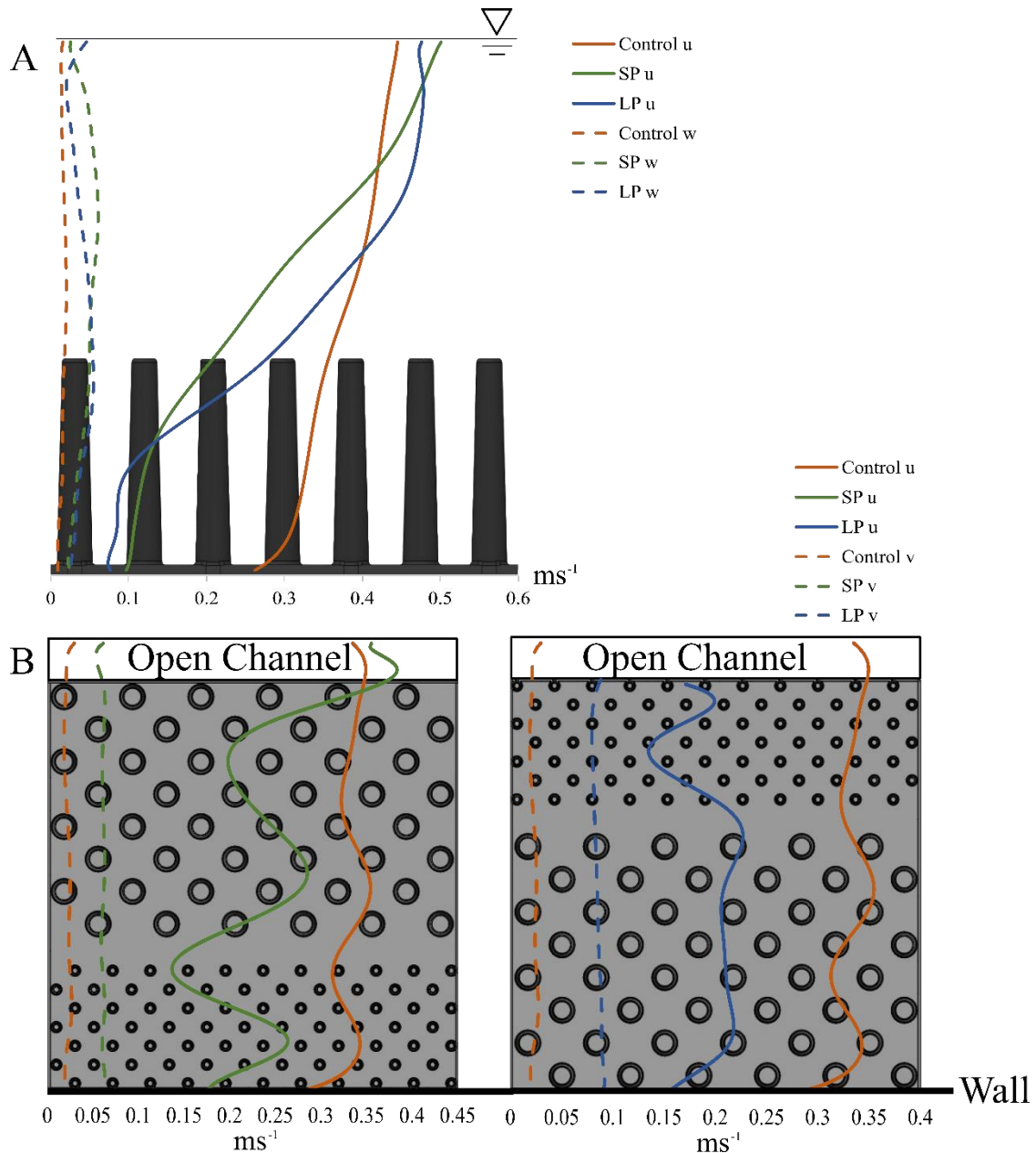
Figure 3.4. Exemplar plots showing temporally and spatially averaged streamwise velocity (u) profiles from a side view (plot A) and a top view (plots B). The data shown is from treatment 4/C and measurements were taken 85 mm from the wall for A and 85 mm from the bed for B. All velocities are in ms^{-1}. In plot A the dashed lines represent the vertical velocity (w) and in plot B they represent the cross-streamwise velocity (v). In B, the plot to the left shows velocity profiles for the tiles mounted in the SP configuration whereas the plot to the right shows the tile in the LP configuration.

The relative velocity reductions of SP and LP configurations compared to the control were calculated to visualise the proportion of velocity being attenuated by the tiles throughout the

water column for each flow condition in Figure 3.5, where values larger than zero indicate a reduction in velocity compared to control whilst a negative value shows an increase. Figure 3.5A compares the relative reduction for all treatments in the SP configuration (small protrusion adjacent to the wall) for the spatially-averaged profile with increasing bulk velocity and constant flow depth, the envelope of all plotted lines is narrow, particularly in the upper portion of the plot. On average, the crossover point above the tiles where the velocity starts to be attenuated instead of being accelerated is around $z/H = 0.72$ (or 72%) of the way up the water column below which there is a steep increase in attenuation until it reaches a maximum of up to 95% in the near-bed region. Overall, the attenuation (shown by relative velocity reduction) is similar across these test conditions. In Figure 3.5B, the same is shown for the series of flow conditions varying in flow depth where bulk velocity remained constant. Interestingly, the crossover point of the y axis, separating the attenuation region from the acceleration region, remains approximately the same independent of flow depth, the attenuation is similar across treatments with the exception of the region below the protrusion top where generally there is an increased attenuation for higher flow depths. Figure 3.5D shows the same data as in Figure 3.5B for the large protrusion configuration (LP), the trend is similar to small protrusion configuration (SP; Figure 3.5B) and the y intercept is the same for each flow depth regardless of the configuration. The shallower flow conditions (H=129 mm; H=155 mm) appear to be less effective in attenuating flow in the lower 50 mm of the water column but a flow velocity reduction of over 50% is still present in all cases in this region. Figure 3.5C for the relative reduction of increasing bulk velocities in the LP configuration exhibits a tight grouping of all the plotted lines and is similar to the SP configuration (Figure 3.5A) except for being less effective at attenuating velocity in the canopy layer of the flow, where for the LP configuration the attenuation remains constant for the lower 50 mm of the water column. The SP configuration appears to be more effective at slowing the flow in the canopy layer of the flow whereas the LP configuration is marginally more effective in the region immediately above the protrusion tops but overall the velocity reduction created by the tiles is significant and has the potential for fish to exploit these lower velocities for passage.
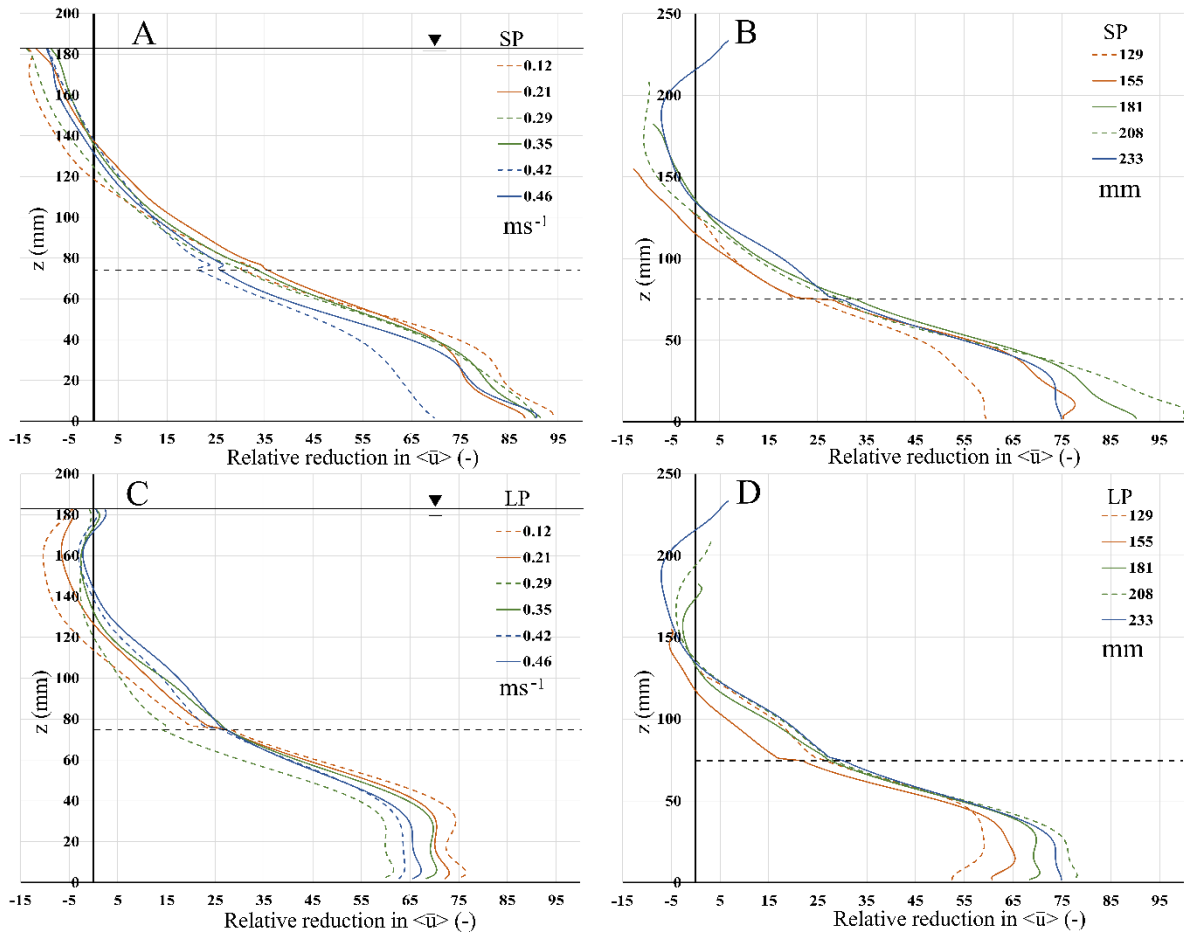
Figure 3.5. Percentage relative reduction in spatially-averaged streamwise velocity throughout the water column. A and C (H = 180 mm) show the velocity reduction for increasing bulk velocity treatments whereas B and D show the velocity reduction for treatments with increasing flow depth. Each line is the average percentage velocity reduction across the tile, A and B show the results for the tiles mounted in configuration SP (small protrusions adjacent to flume wall) and C and D for configuration LP (large protrusions adjacent to flume wall). The horizontal dotted lines show the tops of the protrusions.

3.4.2 Eel tile roughness, shear layers and turbulent parameters

Previously Ghisalberti (2002) established that 10 h downstream of the leading edge, the canopy scale vortices remain the same size and have the same horizontal penetration into the canopy. In the case of the tiles, this is roughly equivalent to the length of one tile from the leading edge. Predictions can be made for the penetration depth into the canopy based on C_{Dah} (Nepf, 2012), in this case ($C_{Dah} = 0.56$), $C_{Dah} > 0.23$ indicates that the penetration will be less than the height of the tiles, which is further compounded by the shallow flow

(H/h<2) over the tiles reducing the size and strength of these large scale vortices (Nepf, 2012).

In the vertical plane, the vertical Reynolds shear stress (RSS, -ρuw) peaks just below the top of the canopy layer, in the shear layer created by two adjacent flow regions moving at different velocities. Reynolds shear stress decreases constantly from the peak towards both the water surface and bed. As would be expected for control conditions, the profile remains low throughout the water column and increases for increasing flow velocities as Reynolds number increases. The vertical Reynolds shear stress for the SP and LP configurations also increases with velocity, being close to control conditions at a bulk velocity of 0.2 ms^{-1} but steadily increases with increasing bulk velocity. The SP configuration has higher peak values of vertical Reynolds shear stress than the LP configuration but the profile remains unchanged throughout the different test cases, suggesting that the protrusion size and density affects turbulent momentum magnitude while protrusion height determines the peak of the vertical RSS curve. The horizontal Reynolds shear stress data (-ρuv) is less clear, there is a peak in both SP and LP configurations where the tiles meet the open channel, confirming the presence of a shear layer. Above the protrusions, in SP configuration there are two major peaks, one above the small protrusion section and one above the large seen in Figure 3.6, however at the intersection between the two protrusion densities which may be expected to have a peak, there is no presence of a peak in either SP or LP configuration. The overall magnitude of horizontal Reynolds shear stress is smaller than in the vertical, possibly due to the limited water depth or to measurement location.

The vertical turbulent intensity (TI) remains always low in the control conditions, while in the tests with tiles it increases in magnitude with increasing bulk velocity and peaks just below the level of the protrusion tops (similar to the Reynolds shear stress) reaching a minimum at the bed, as shown by Figure 3.6 . In the horizontal plane, the turbulent intensity also increases with bulk velocity but is relatively constant over the width of the tile.

Following the trend of the Reynolds shear stress and turbulent intensity profiles, the turbulent kinetic energy (TKE) reaches a maximum in the vertical shear layer and a minimum in the canopy layer. Examining the vertical and horizontal planes (XZ and XY respectively), the increase of magnitude of TKE with bulk velocity is pronounced compared to the increases seen in other metrics. In the horizontal plane, the TKE profile increases with distance from the wall for the higher velocity conditions.

These results show the primary shear layers created by the tiles; most notably, where the fast-moving flow above and beside the tile and these meets the slow moving flow within the tiles. The velocity differential between the large and small protrusions is not sufficiently large to generate a shear layer in this location, favouring the use of the tile by fish.
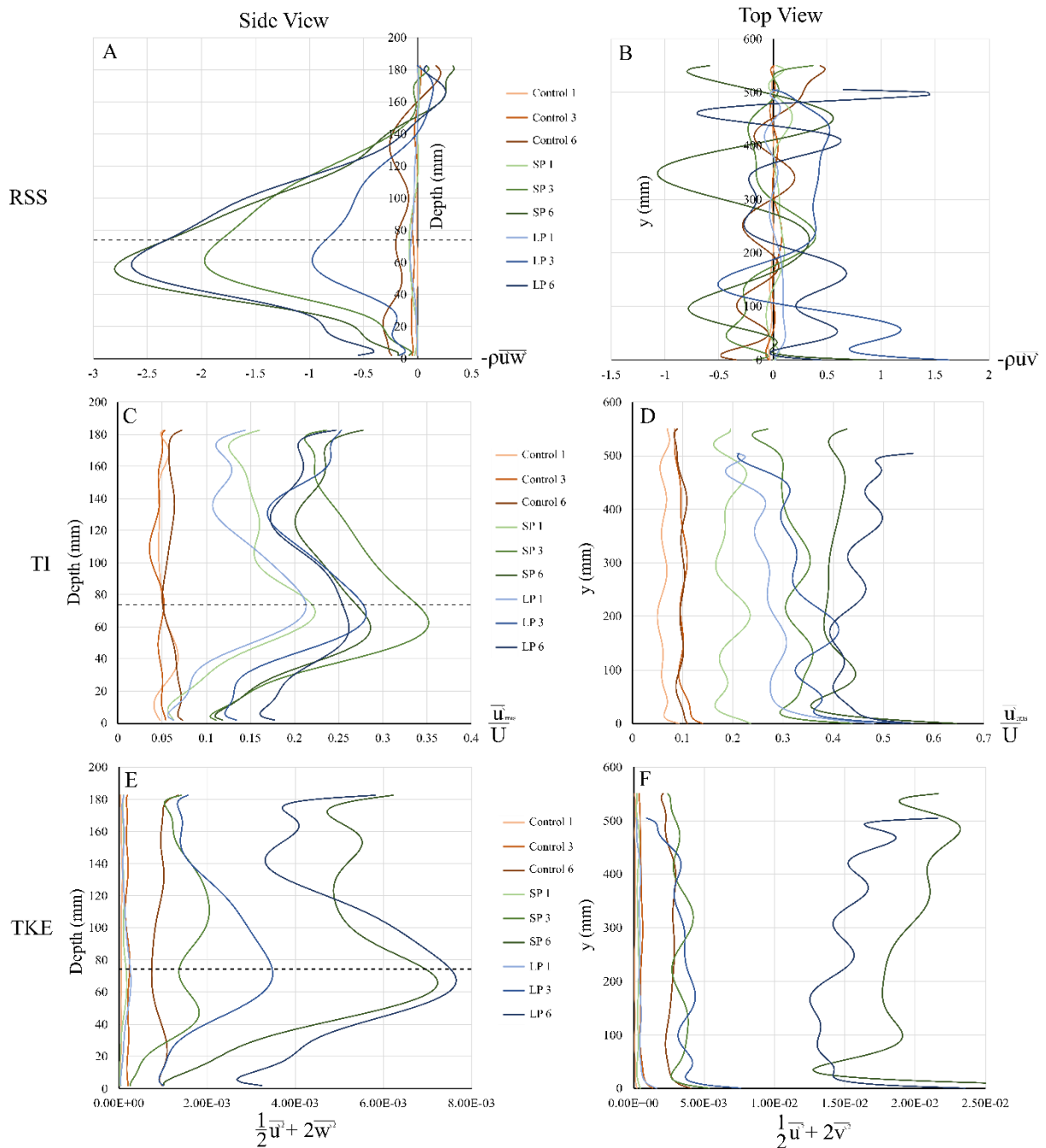
Figure 3.6. Plots showing three turbulence parameters of the flow from a side view and a top view (where y=0 is the flume wall). A and B show data for vertical and horizontal Reynolds shear stress (RSS - ρuw, ρuv), C and D show turbulent intensity (TI) and E and F show turbulent kinetic energy (TKE). Only three tests per tile configuration (control, SP, and

LP) are displayed, tests 1, 3, and 6, this approach was taken to show the overall trend without overcrowding the plot. Each flume condition is represented by a colour, getting darker with increasing bulk velocity of the test. The data for the plots was in all cases taken at 85 mm from the wall for the side view and 85 mm from the bed for the top view (10 mm above the top of the tiles). Horizontal dotted lines represent the tops of the protrusions.

3.4.3 Turbulent structures

By inspecting PIV images and video and flow visualisation images, we identified turbulent structures. Vertical turbulent structures were identified from PIV images taken through the side of the flume and were characterised by periodic upwards and downwards oscillations in the flow mainly affecting the vertical (w) component of the velocity. These vertical oscillations did not appear as fully formed vortices and the vorticity levels within them were the same as the background vorticity. The oscillations were present in all treatments but more pronounced at higher velocities. The scale of this turbulence was similar to that of the canopy (canopy scale) and analysis of the flow depth varying treatments revealed it to be restricted by the available flow depth. At increased flow depths (and therefore increased space in the above protusion region) the oscillations became larger to fill the available space. The upwelling phase of the oscillation originated at the interface between the mixing layer and the canopy layer (Figure 3.1), but in some cases for the SP configuration within the small protrusions the downwelling phase penetrated the canopy layer by up to 50% of the protrusion height. The penetration depth of the turbulence was inconsistent across different instances and across treatments; there was also no observable difference in the oscillations across the tiles except for immediately adjacent to the wall where they were less frequent. In the LP configuration where the penetration was observed primarily into the large protrusions, the penetration depth was up to 75% due to the sparser canopy density. A fast Fourier transform (FFT) was performed on the PIV data to identify any dominant frequency in the oscillations but no identifiable frequency was found suggesting that these oscillations may occur as an interaction of other turbulent phenomena beyond just the instability arising from the surface layer and the canopy layer moving at different speeds.

In the horizontal plane (XY plane) where the measured velocities were the streamwise velocity (u) and the cross-streamwise velocity (v), turbulent structures were also identified. Similar to the vertical plane (XZ plane), no discrete or fully formed vortices were present.

78

Oscillations, however, occurred at the interface between the canopy and the open channel with a wavelength of approximately 180 mm which classifies them as canopy scale. These oscillations were not always present and a FFT analysis was unable to identify any prevailing frequencies. These fluctuations occur in the mixing layer above the tiles and overlap heavily over the tiles with an amplitude of the same scale as the wavelength.

3.4.4 Stem scale

Within the tiles there were vertically oriented recirculation zones directly behind the individual small and large protrusions. There were, however, no indications of discrete vortices being shed in the horizontal plane from the cylindrical protrusions and no von Karman vortex street formed as a result. This may be due to the interfering turbulence from upstream and adjacent protrusions since the flow measurements were taken on one of the downstream tiles where the flow was fully developed. Velocity fluctuations were present behind the protrusions despite no stem vortices being present and these could affect small fish. The velocity within the canopy layer remained low in all tested flow conditions, regardless of bulk velocity which could further evidence the lack of high levels of coherent turbulence structures. There were no significant differences between the turbulent structures shed by the protrusions in the SP or LP configurations.

3.4.5 Effects on the channel

The flow in the untiled section of the channel adjacent to the tiles was not highly affected by their presence; the velocities on the bare section of the channel were unaffected by the tiles beyond the horizontal mixing layer, suggesting that for the flow conditions tested, the conveyance capacity of the channel was not severely impacted by the presence of the tiles despite 42% of the channel width being occupied by the tiles. This is particularly true of the SP series whereas for the LP configuration the velocities in the smooth channel section were marginally increased which may be problematic for fish that may not choose to use the tiles for passage.

3.5 Discussion

Eel tiles are effective at reducing velocities but they also create moderate levels of turbulence. This is encouraging when viewed through the lens of potential fish passage. The flow in this study features multiple shear layers and combined with the dual protrusion density of the tile makes for a complex flow. The established field of vegetated canopy flow in open channels is a helpful tool for analysis of the hydrodynamics under investigation because vegetation is often modelled as arrays or clusters of rigid cylinders in a flume which resembles the current experimental setup. Furthermore, the overall solid volume fraction of the submerged tile ($\emptyset$ =0.09) matches $\emptyset$ values investigated in previous studies between 0.02 to 0.1 (Nepf & Ghisalberti, 2008; Unigarro Villota et al., 2023; White & Nepf, 2007). The vertical velocity profiles through the tiles are similar to those found in submerged vegetation canopies, with slow flow within the canopy rapidly increasing at the interface and reaching a more constant higher value at the top of the water column. This is typical of canopy flow and the inflection point in the profile points to the potential presence of a Kelvin-Helmholtz (KH) instability (Ghisalberti & Nepf, 2005; Nepf & Ghisalberti, 2008; White & Nepf, 2007). Although less well characterised, the cross channel velocity profile also has similarities to canopy flow. Plots of horizontal Reynolds shear stress are also closely matched, the peak being slightly below the top of the canopy and confirming the presence of a shear layer (Nepf & Vivoni, 2000).

The turbulent structures identified in previous work have been extensively studied, the KH instability generates coherent canopy scale vortices that, according to the relative submergence, the canopy density and other factors, will penetrate within the canopy to different depths (Ghisalberti & Nepf, 2005; Nepf & Ghisalberti, 2008; Nepf, 2011, 2012). Conversely, in the current study, the large scale turbulent structures recorded were non coherent ejections and fluctuations that were not strictly periodic. Ghisalberti and Nepf (2006) found that vortices were shed at the shear layer at 0.11 Hz so there is a possibility that the primary shedding frequency of the fluctuations in the current study was not detected because the sampling time was too short to detect it. Penetration of the turbulent structures was correctly predicted by Nepf (2012) such that the turbulence was penetrating the canopy but the depth of the turbulence was less than the height of the protrusions, having a solid volume fraction of above 0.23 and being damped by the shallow water depth (H/h<3). This may have implications for swimming stability of fish.

A potential issue of the tiles is that the low velocities may cause sediment deposition, causing them to become blocked. Deposition will largely depend on the sediment load of the water approaching the tiles, bed shear stress, and the flow velocity. During low flows the base of the tiles should provide a barrier to the lowest velocities depositing sediment and higher flows may initiate it into resuspension. Some studies have found that the turbulence generated by canopies can enhance sediment mobility and create scour within the canopy, especially with higher levels of turbulent kinetic energy which could potentially keep the tiles clean (Chen et al., 2012; Liu et al., 2021; Nepf, 2012). There is also the opportunity to lessen the scour downstream of the tiles due to the lower velocities immediately of the tiles which could help with preventing overhangs forming between the downstream end of culverts and the river bed. Anecdotal evidence from practitioners who have installed these tiles report that they are easy to maintain sediment free, especially when compared to other available solutions like elver brushes.

The tiles need to create favourable conditions for fish passage at high speed barriers, primarily for eels but also for as many other species, to maximise habitat restoration and connectivity. The tiles produce significant velocity reductions within them and in their vicinity and do so consistently under varied flow conditions. This comes at the expense of generating turbulence which can be detrimental to swimming fish. Many studies have attempted to characterise fish responses to turbulence and have found that in specific situations, fish can utilize turbulence to their benefit if the turbulence is discrete, in the correct plane and shed at the correct frequency (Harvey et al., 2022; Liao, 2007; Liao et al., 2003; Stewart et al., 2016). Other studies have found that vortices can destabilise fish, causing them to 'spill' (Muhawenimana et al., 2019; Smith et al., 2014; Tritico & Cotel, 2010; Webb & Cotel, 2011; Zha et al., 2021) depending on the orientation of the eddy. With regards to the European eel, Russon et al. (2010) argued that they are often found in turbulent regions as they are prone to swim in the proximity of river beds and banks. The size of the vortices is important to fish stability, eddies the same length scale as the fish are more likely to cause spills (Muhawenimana et al., 2019). Reviewing the findings of studies on fish stability, the canopy scale turbulence produced by the tiles should not be strong, coherent or periodical enough for most fish to be either destabilised by it or to benefit from it. The stem scale turbulence however, would be the correct length scale for small fish (0-50 mm) to be destabilised if it were strong and discrete enough. Overall, the flow in and around the tiles seems suitable for fish passage and any fish species which find the conditions suboptimal

will have the remainder of the channel to pass upstream as the tiles only partially cover the channel width. Furthermore, the tiles in SP configuration have very little influence on the rest of the channel, benefitting other species that may not need the tiles and reducing the impact of the tiles on the flow through a culvert or similar structure. The recommended mounting for the tiles is therefore to place the small protrusions next to the stream bank or culvert vertical wall. The next step is to directly evaluate the suitability of the tiles for fish passage.

3.6 Conclusion

In summary, this study found that eel tiles do attenuate flow within and around the tiles without producing excessive drag levels and severely modifying the flow in the rest of the channel. The turbulence produced by the tiles aligns with findings from analyses of vegetated canopy flow, in particular the velocity profiles formed between open channel flow and canopy layer. The lack of strength of the shear layers and multiple shear layer interactions led to the turbulent structures present in the flow to not be cohesive or discrete. This, along with the lower velocities and the structure of the protrusions should allow for the upstream passage of fish, and eels in particular, in line with findings from fish stability literature and observed results from sites where the tiles are deployed. The eel tiles therefore seem to be a potentially effective solution and should be evaluated with fish trials and should be mounted with the small protrusions near the channel wall. This chapter met objectives 2, 3, and 5.

Chapter 4. Eel tiles as a passage solution for eels at high velocity barriers

Conceptualisation and methodology by Prof. Jo Cable, Prof. Catherine Wilson, Andy Don, and Guglielmo Sonnino Sorisio. Data collection by Guglielmo Sonnino Sorisio. Analysis, visualisation, and writing by Guglielmo Sonnino Sorisio and editing by all of the above. Advice and input from Petr Denissenko, Chris Bell and Chris Grzesiok.

Summary

High velocity barriers pose a risk to upstream migrating European eels (*Anguilla anguilla*) as the flow can be too fast for them to swim against. These barriers delay or even prevent migration, exacerbating population declines of this critically endangered species. Eel tiles are an emerging solution for this application, already successfully deployed to increase passage at gravity barriers. Here, eel tiles mounted to the bed of an open channel recirculating flume were assessed in terms of eel passage, behaviour and kinematics relative to movement in the absence of the tiles. The tiles significantly increased passage and allowed the eels to rest without the need to swim back downstream. The tiles also significantly reduced the amount of energy needed to travel upstream. For the first time eel swimming was examined in a flow with multiple shear layers and turbulent structures of varying lengthscale. Swimming kinematics were analysed for complex turbulent flows and revealed a new swimming gait in the shear layer beside the tile. By allowing the eels to continuously move upstream, the tiles potentially decrease accumulation of eels at resting hotspots. Overall, the tiles were effective in helping eels migrating upstream.

4.1. Introduction

The European eel (*Anguilla anguilla*) has been in a population decline since before the 1980s, leading to the species being classified as critically endangered by the IUCN in 2013 (Jacoby & Gollock, 2015; Pike et al., 2020). This catadromous fish that begins its life in the Sargasso Sea (Wright et al., 2022) is transported by oceanic currents to the coastlines of Europe (Anderson, 2022; Pike et al., 2020). Recruitment of this fish is around 1 - 5% of pre-1980 levels (ICES, 2020) and this decline has occurred throughout the eel's geographical

range. There are multiple causes for this decline. Ocean currents in the Atlantic are shifting as a result of global warming, altering the path larval eels (leptocephali) take to reach fresh water (Baltazar-Soares et al., 2014). When eels arrive in estuaries, they face polluted waters and chemical barriers as well as fishing pressures and infections, including from *Anguillicoloides crassus,* a common parasite that affects the swim bladder (Kirk, 2003; Righton et al., 2021; Teunen et al., 2021) and impacts eel swimming behaviour (Newbold et al., 2015). Other threats to the upstream migration are the significant number of physical barriers due to anthropogenic alterations to rivers that make upstream journeys difficult or even impossible (Belletti et al., 2020; Halvorsen et al., 2020; Piper et al., 2017; Warren & Pardew, 1998).

River barriers fragment, disconnect, and reduce habitat availability, this affects many diadromous species but also river resident fish (Belletti et al., 2020; Fuller et al., 2015; Jones et al., 2019; van Puijenbroek et al., 2019). Of these potential 5 million physical barriers in Europe, 1.3% are sluices and tidal gates, 9.8% are dams, 30.5% are weirs, and 17.6% are culverts (Belletti et al., 2020). Each of these obstacles offers a unique challenge for eels, and fish passes are now commonly implemented at most hydraulic structures. Culverts and river flumes are not gravity barriers but they are velocity barriers (unless they have an overhang), often constricting the flow into a narrow section and typically they have smooth walls; both aspects lead to increases in flow velocity without offering any refugia (Jones et al., 2021; Warren & Pardew, 1998). The high velocities can be too fast for juvenile eels to navigate and the lack of resting opportunities exacerbates energy expenditure by requiring the fish to swim in fast flows over long distances. Fish that attempt these crossings can be exhausted as a consequence of the fast flows and seek to rest immediately upstream of the structure if successful, or immediately downstream if unsuccessful. If many fish are all using the same areas to rest this can create predation hotspots (Cairns et al., 2014). Unfortunately, fish that are successful in swimming upstream are soon likely to encounter other barriers and the cumulative effects of navigating multiple barriers can reduce their energy budgets and make them less likely to successfully complete their life cycle.

Eel tiles are a potential solution to velocity barriers. Each tile, made from high density co-polymer, is 0.505 m wide and 0.505 m long with a 25 mm base and 50 mm high cylindrical conical protrusions of two densities to accommodate different eel sizes (Fig. 4.1). The tiles were originally designed to be used on the downstream faces of weirs and similar inclined

structures where they might facilitate elvers to pass upstream by climbing (Jellyman et al., 2017; Watz et al., 2019). Elvers can climb upwards using the substrate provided by the protrusions in the tiles. Tiles used in this manner will have flow going through the protrusions, which in normal operating conditions will not exceed the height of the protrusions. These tiles have been tested against other commonly used substrates, such as bristle passes at various inclinations, and in all trials they improved eel passage (Jellyman et al., 2017; Watz et al., 2019). The tiles are sturdy, cheap relative to other passage solutions, and are quick and easy to install, making them an ideal solution for not only streambed inclines but also velocity barriers to potentially create flow conditions more suitable for eels, as well as providing resting areas.

The flow over and around eel tiles has been investigated with the use of particle image velocimetry for a wide range of flow conditions, covering diverse flow velocities and flow depths (Chapter 3). The analysis revealed that the tiles are effective in decreasing flow velocities both within the protrusions and around them without severely affecting the flow carrying capacity of the channel. Two main shear layers are present: a vertical shear layer forms between the tiles and the flow above them and a horizontal shear layer generated in the lateral region adjacent to the tiles and the 'free stream' flow towards the centre of the channel. Where the areas of slower flow meet the faster flow in the rest of the channel, a mixing layer exists with elevated levels of Reynolds shear stress that create a Kelvin-Helmholtz instability that generates large scale fluctuations that can potentially destabilise swimming fish, which is undesirable for efficient passage (Chapter 3). This phenomenon occurs in both the vertical (τ_{uw}) and horizontal planes (τ_{uv}); in the vertical the size of the turbulence is limited by the flow depth as the relative submergence of the tiles (ratio of flow depth to protrusion height) was never above 2.07 in the flume experiments (Chapter 3). The vertical shedding penetrates into the protrusions but velocities in the protrusion sublayer stay low. In the horizontal plane, the turbulent length scale is not bounded by the size of the channel and is of the scale of the spanwise extension of the protrusions and is strongest immediately above the tiles (Chapter 3).

Understanding the flow interaction between a tiled region, the free stream flow, and the eel's behaviour, including how they adapt to the conditions, is important when evaluating passage solutions. Eels primarily swim during hours of darkness and near the bottom of channels (Cresci, 2020; Harrison et al., 2014) and the way they swim has been observed and often

defined as undulatory or anguilliform (Lauder & Tytell, 2005; Müller et al., 2001; Tytell, 2004a, 2004b; Tytell & Lauder, 2004). The swimming amplitude envelope of eels is similar to that of other fish with different morphologies, it is symmetrical about the centerline, with a small head amplitude which increases along the body, reaching the maximum at the caudal fin (Gillis, 1998; Lauder, 1995; Tytell, 2004b, 2004a; Videler, 2019). Eels do not typically make significant usage of their pectoral fins during swimming. However, the number of wavelengths formed by their body is typically higher than fish with a lower body length to height/width ratio as they are comparatively more slender than other species and therefore less 'rigid' (Borazjani & Sotiropoulos, 2009; Gillis, 1998; Tytell, 2004a). This makes them efficient swimmers but they lack the high swimming speeds of more powerful fish like salmonids (Clough et al., 2004; Clough & Turnpenny, 2001; McCleave, 1980; Van Den Thillart et al., 2004). Generally, head amplitude will remain small at sustained and constant swimming speeds, and increases during acceleration and at burst velocities (Tytell, 2004a). Strouhal number has been used to compare tail velocity and swimming velocity (Triantafyllou et al., 2000). The Strouhal number for eels is generally constant at a value of 0.32, thought to be an efficient swimming mode (Read et al., 2003; Triantafyllou et al., 2000), but this value increases at lower swimming speeds (Tytell, 2004a). However, these observations have been made for eels swimming in stationary water or in an uniformly distributed velocity field, and much less is known about their swimming kinematics in turbulent flow and how they respond to different turbulent structures and shear layer flow. Their crawling gait has been investigated, and on sand, eels were found to adopt a gait with a much more uniform amplitude along the body, with a large amplitude from the head to the caudal fin (Gillis, 1998).

This study evaluates eel tiles as a potential passage solution for eels at velocity barriers. The hypotheses that the tiles help the eels move upstream compared to a non-tiled condition and that with the tiles the eels would prefer the tiles and use them to move upstream more easily are tested. To do this, eels were exposed to flow conditions of increasing flow depth (and therefore tile submergence) and we evaluated their behaviour, kinematics and energetics. These were compared with the hydrodynamic data for these tiles (Chapter 3) to find how the eels react to different types of shear layer flow. Finally, passage statistics were analysed to determine how tiles impact passage of European eels.

4.2. Methods

4.2.1 Fish Origin and Maintenance

European eels (*Anguilla anguilla*, N=29) were caught by electrofishing from the Ely Bridge on the Ely River (51.483802, -3.231746) on 29/07/2022 by Natural Resources Wales. The river temperature was 17°C. The eels were transported (approximately 20 minutes from the time they were taken from the river) to the School on Engineering at Cardiff University in water containing Stress coat™ and oxygenated via a battery powered air pump. In all instances where the eels were transferred from one body of water to another, they were acclimated to the temperature of the water they were being moved into at a rate of 1°C per 30 minutes.

Eels were housed in a large (diameter = 1.3 m, water depth = 0.35 m, volume = 460L) circular black tank with water dechlorinated with Tetra Aquasafe. A water cooler (D-D Aquarium Solution, DC 750) maintained the temperature at 17±1°C. After being cooled the water passed through a water filter (Aquamanta, EFX 600 External Canister Filter) and returned to the tank. Both hoses bringing water in and out of the tank were covered in mesh to prevent the eels swimming into them and the hose returning the water to the tank (flowrate <0.75L/s) was angled to create a small amount of flow. The water quality was monitored every other day with a water quality test kit to ensure ammonia, nitrite and pH were within safe limits (ammonia 0-0.2 mg/L; nitrite 0-0.25 mg/L; and pH 7-8). A 12:12 h light:dark cycle with lights on at 06:00 am was maintained throughout the experiment and the eels were fed thawed bloodworm once a day. Plastic tubes, ceramic pots and rocks were added to the tank as enrichment and refugia for the eels. The tank was covered in a plexiglass sheet to prevent the eels from escaping. Experiments began after one week acclimation period. On completion of the experiments, the eels were health checked, measured, weighed and transported back to their exact site of collection to be released on the 10/08/2022. No eel was damaged or displayed symptoms of ill health during the experiment and all were returned to their site of collection.
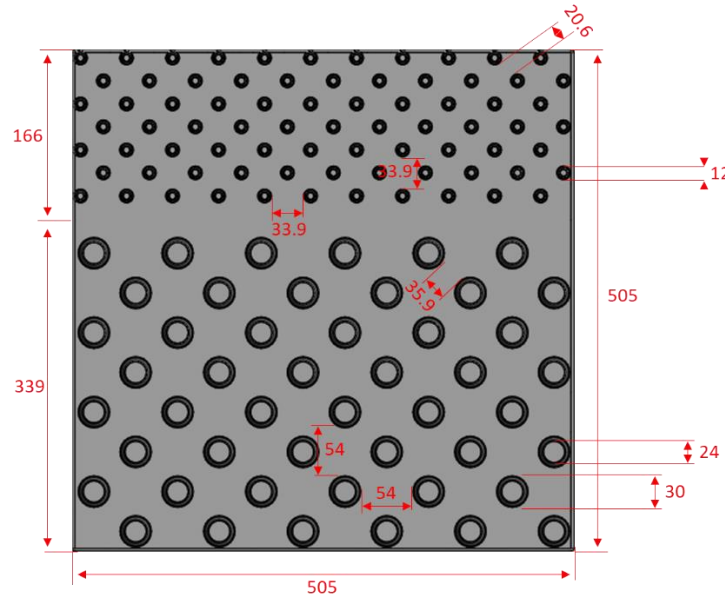
Figure 4.1. Top view of a dual density eel tile. In the diagram, the small protrusion section of the tile is at the top and the large protrusion section at the bottom. The tiles are made from a high-density co-polymer and have a 25 mm tall base and 50 mm tall protrusions. Units are in millimetres.

A recirculating open channel flume was used to conduct experiments where eels were exposed to tiles. The flume was 10 m long, 1.2 m wide and 0.3 m tall with a fixed bedslope of 1/1000. The bed of the flume was plastic and the walls were glass. The working section was 6 m long, and was bounded by flow straighteners. Eel tiles measuring 505 mm length by 505 mm width by 75 mm tall shown in Figure 4.1 produced by Berry and Escott Ltd. (Berry & Escott, 2023) were sourced by the Environment Agency. The tiles were mounted in the flume with the small protrusions near the flume wall. A third flow straightener was used to separate a 0.8 m long section at the downstream end of the working section in which no eel tiles were mounted and which was used to acclimate the eels to the flow conditions as shown in Figure 4.2. The flume was filled with water dechlorinated with Prime Dechlorinator and kept at 17±2°C with a D-D Aquarium Solution, DC 2200 cooler. The treatments chosen for this experiment had a fixed bulk velocity while varying flow depth, this resulted in the shallowest condition having the tiles exceed the water depth (emergent) and other conditions fully submerging the tiles (submerged).
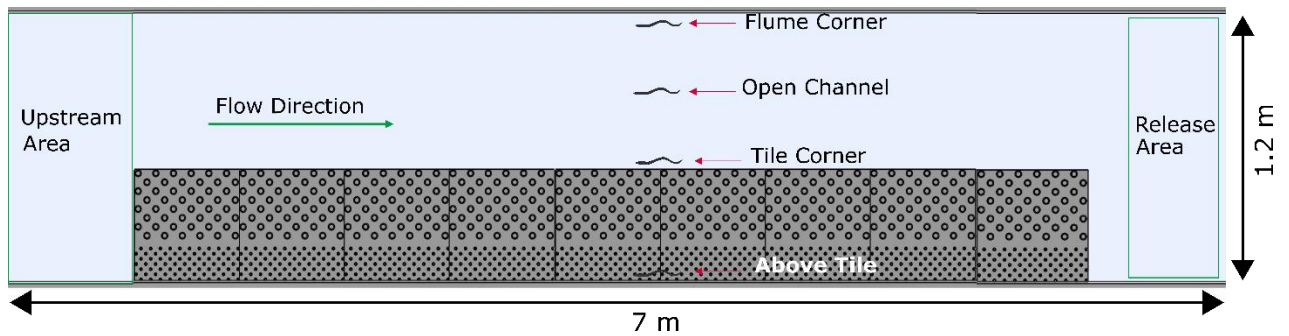
Figure 4.2. Diagram of the layout of the working section of the flume including the four main areas where the eels swam. Nine tiles were attached to the flume bed with the small protrusions nearest to the wall, the fish were released downstream of the tiles and allowed to swim upstream. In the control treatments no tiles were present. The flume used was 10 m long, 1.2 m wide and 0.3 m tall.

Table 4.1. The flow conditions used for the experiment. Bulk velocity (U) was kept constant while flow depth (H) was varied by adjusting the flume's weir at the downstream end and changing the flowrate (Q). The flume's Reynolds number (Re) was calculated based on the hydraulic radius of flow cross-section. The height of the tiles (h) and the flow depth (H) were used to calculate the relative submergence (H/h).

Treatment	Tile Presence	U $[ms^{-1}]$	H [mm]	Q $[Ls^{-1}]$	Submergence (H/h) [-]	Flume Re [-]
T56	Tiles	0.35	56	17.50	0.77	1.79×10^4
T75	Tiles	0.35	75	26.25	1.00	2.33×10^4
T129	Tiles	0.35	129	45.15	1.72	3.71×10^4
T155	Tiles	0.35	155	54.25	2.07	4.31×10^4
C56	Control	0.35	56	17.50	0.77	1.79×10^4
C75	Control	0.35	75	26.25	1.00	2.33×10^4
C129	Control	0.35	129	45.15	1.72	3.71×10^4
C155	Control	0.35	155	54.25	2.07	4.31×10^4

All experiments were conducted between the hours 19:00 to 03:00 in darkness, a Testo 540 lightmeter measured between 0-4 Lx throughout the working area. During the experiment, one eel was tested at a time and the same eel was allowed to recover for at least 24 hours

before being tested again. All 25 used eels were tested in random order for each treatment once and were fed after flume trials.

Before the eels were exposed to flow conditions of the flume, they were allowed to acclimate in flume water for 60 minutes. The eels were introduced into the acclimation section of the flume and exposed to the flow conditions for 15 minutes (Meister, 2020). At the end of the 15 acclimation minutes, the eel was moved into the working section of the flume with a net. The eel was allowed to swim freely throughout the working area for 5 minutes during which the experimental data were recorded. The eel was removed from the flume either after impinging on the downstream flow straightener for 60 seconds (after which the back of the flow straightener was gently tapped to verify the impingement), when the eel stayed upstream for 120 seconds and did not re-enter the working section with the tiles or when 5 minutes had expired.

A Baumer VLXT-50M.I high speed camera recorded the eels swimming at 80 frames per second in the fourth tile and fifth tiles from the downstream end of the working area. This camera was manually triggered whenever an eel entered the field of view. The tiles in question were painted white to increase the contrast between the eel and the background. Different colours have been shown to affect fish behaviour (Chapter 8) so behavioural data was analysed to validate the use of the white tiles for a kinematic analysis representative of the tiles in their normal colour. The analysis revealed no differences.

4.2.2 Behavioural analyses

To monitor the behaviour of the eels, three Swann Swpro-735cam cameras were set up to cover the entire working area (shown in Figure 4.2), these cameras recorded in infra-red due to the absence of light. Behaviour was quantified with JWatcher (Blumstein et al., 2000; Blumstein & Daniel, 2007). Using the videos of the entire working section, the behaviours recorded quantified whether the eel was swimming forward, backwards, holding station, crawling, or resting. The position where each of these behaviours occurred was also tracked by indicating the streamwise position of the nearest tile (or equivalent streamwise position within the channel) and whether the eel was with the small or large protrusions, above them, immediately to the side of the tile, in the open channel, or in the corner formed by the flume wall and the bed. In addition to these behaviours, the number of passage attempts was scored based on how many times the eels started making progress from the downstream area from

the tiles, impingement was recorded with the criteria specified above, and successful passage was recorded as the eels having swam past all nine tiles and reached the upstream area.

4.2.3 Kinematic analysis

High speed videos were converted to avi files using a custom Matlab (MathWorks, 2022) script. Tracking for kinematic analysis was performed with the free software Kinovea (Charmant, 2022), this allowed for semi-automatic tracking of points on the eel's body with manual inputs or corrections. To do this, a coordinate system was set and calibrated for each video, then a tracker was added for each point on the eel's body that was to be tracked. For all clips of the eels swimming in the field of view of the high-speed camera, the head and tail were tracked and for 12% of clips (spread evenly over different areas), the entire body was tracked with 13 points on average. From the coordinates of each point on every frame, kinematics parameters were extracted. Amplitude was evaluated by calculating the maximum range of movement from the centreline of each tracked point, head amplitude and tail amplitude were evaluated for every clip. Tailbeat frequency (Hz) was also calculated in all cases. The swimming velocity was calculated by adding the swimming speed of the fish evaluated from the tracking data to the flow velocity at the location of the swimming fish. All parameters with units, including metres, were normalised by body length (BL) to make a comparison with fish of different sizes. Stride length was calculated by dividing the normalised overall swimming speed by the tailbeat frequency (i.e. one "stride"), tailspeed was calculated by multiplying tailbeat frequency by tail amplitude. For full body kinematics data, a centreline was calculated from the tracked points along the body and successive centrelines for each frame for the duration of approximately one tailbeat were levelled at the head to form a diagram of the amplitude envelope of the whole body.

For the energetic analysis, full body tracking was used. The tracked points were imported into Matlab where a polynomial spline was applied to the centreline of the body for each frame to best fit the shape of the body of the eel. The curvature of the centreline was then computed and the difference in curvature between each successive frame was found. Following the method from Harvey et al. (2022), the moment of area of the muscle cross section from 15 sections along the body of the eel (measured with Fusion 360), the rate of change of curvature was then multiplied by the moment of area and integrated along the length of the eel, excluding the head and the caudal fin. This calculation yields a comparative measure of the energy used by the eel while swimming but does not provide measurements

of energy usage in Joules. These data were then analysed in RStudio (R Core Team, 2022) and modelled with tailbeat frequency, the relationship was found to be very significant (p < 1E-11) and the R squared value was 0.79 for the model. Because of the close relationship between the two variables, the energy expenditure was estimated from the tailbeat frequency data, thus using all available clips of swimming eels to evaluate comparative energy usage. The energy expenditure for the crawling gait could not be analysed by the same method since the act of pushing against a solid surface may involve different muscles compared to when moving freely within a fluid.

Comparisons of kinematics were made to hydrodynamic data defined as: Reynolds Shear Stress in the horizontal and vertical respectively, $-\rho u'v'$ and $-\rho u'w'$, and turbulent intensity, $\frac{u'_{rms}}{U}$.

4.2.4 Statistical analyses

All statistical analyses were performed in RStudio R version 4.2.2 (R Core Team, 2022). The packages nlme (Carey & Wang, 2001) and lme4 (Bates et al., 2015) were used for generalised linear mixed models (GLMM) and MASS package (Venables & Ripley, 2002) was used for generalised linear models (GLM). GLMMs were used wherever it was necessary to consider the pseudoreplication caused by using the same eels for each treatment. Null GLMM models were run to determine the magnitude of the effect of the random variable on each model and if the effect was considered small (R squared value below 0.01) then GLMs were also run and the model with the best residuals plots and AIC was selected. To compare the passage of the eels between treatments with and without tiles, length, and flow depth a binomial GLMM was used. A poisson GLMM was used to compare the number of passes between treatments, with length, and with flow depth. Negative binomial GLMMs were used to compare the number of attempts of upstream passage per fish between treatments, fish length, and flow depth. For the passage time variable, a gaussian GLM (identity link) was used. To analyse the time spent by eels in different areas of the flume, a combination of gaussian, inverse gaussian and Gamma GLMs were used with identity links in all cases. The amount of time spent crawling, and time spent in the flume corner was compared between treatments with a gaussian GLM with an identity link whereas for the time swimming in, and above the tiles, an inverse gaussian GLMs with 1/mu^2 links were utilized. For the total time spent in the tiles, a Gamma GLM with identity link was used. Gamma GLMs with identity links were also used to compare time spent in each area

of the flume within treatments. For the kinematic analysis, generalised additive models were trialed but rejected on the basis that their performance was similar or inferior to that of GLMs for the same variables. Gamma GLMs with identity links were used for tailbeat frequency with normalised velocity, and all turbulence parameters, whereas a gaussian GLM was used for amplitude, head amplitude, amplitude ratio, amplitude and location, tail speed and Strouhal number, tailbeat frequency and Strouhal number, length, stride length and location, normalised points of contact and protrusion type, fish length, and direction. The confidence interval used throughout the study was 95%.

4.2.5 Animal Ethics

All work was approved by the Cardiff University Animal Ethics Committee, NRW, EA, and conducted under UK Home Office licence PP8167141.

4.3. Results

4.3.1 Passage and behaviour

The tiles increased overall upstream passage of the eels (GLMM, p=0.02) by 16% overall but up to 35% for the shallowest condition in which the tiles were emergent (T56). Total fish length did not significantly impact the probability of an eel passing (GLMM, p=0.11) and neither did flow depth, passage not increasing or decreasing steadily with depth (GLMM, p=0.24). The number of attempts to pass was not associated with eel length (GLMM, p=0.86) and there was no difference for any of the flow conditions between number of attempts with and without tiles (p=0.07). The passage time was significantly higher with the tiles than in the control (without tiles) (GLMM, p<0.0001) and between corresponding treatments (GLMM, p<0.014) but not with fish length (GLMM, p=0.77). In the presence of tiles, all eels made some progress upstream, even though not all passed upstream whereas in the control conditions, a quarter of the eels were impinged on the downstream flow straighteners compared to no impingements for treatments with tiles.

The time spent in the open channel section of the flume was much higher in the control treatments (GLM, p<0.0001) but not significant in relation to fish length or flow depth (GLM, p>0.18). Across all individual treatments, the time in the open channel was higher for control treatments (GLM, p<0.031). Similarly, the time spent in the flume corner was higher in the control conditions (GLM, p=0.001), but only treatments C129 and C75 were

significantly higher than T129 and T75 (GLM, p<0.035). Within the tiled treatments, there was no significant difference in time spent crawling in the large protrusions (LP) between treatments (GLM, p>0.05). There was also no correlation between the eel size and which protrusion type they spent more time on as usage was uniform across eel sizes. Fish in treatment T155 (the treatment with the highest relative submergence) spent significantly more time crawling in the small protrusions (SP) than any other treatment (GLM, p<0.02) but there was no difference between other treatments. There was also no difference in time spent swimming in the protrusions (GLM, p>0.46), possibly due to the low number of occurrences of this behaviour. Similarly, there was no difference between T129 and T155 in time spent swimming above the protrusions, a comparison to other treatments cannot be made because the flow depth was too shallow and there was no layer of flow above the tiles. The total time spent in the tiles was significantly higher (GLM, p<0.02) for T155 than other treatments (among which there were no differences). Interestingly, the time spent crawling increased with flow depth and protrusion submergence (GLM, p=0.0005), most prominent with the T155 treatment. There was no difference however, with regard to time spent in the tile corner (GLM, p>0.49), eels exhibited similar usage of this space across the tiled treatments. The eels spent significantly more time resting downstream in the control treatments (GLM, p=0.025) and fish were significantly less likely to pass the more they rested downstream (GLM, p=0.022).
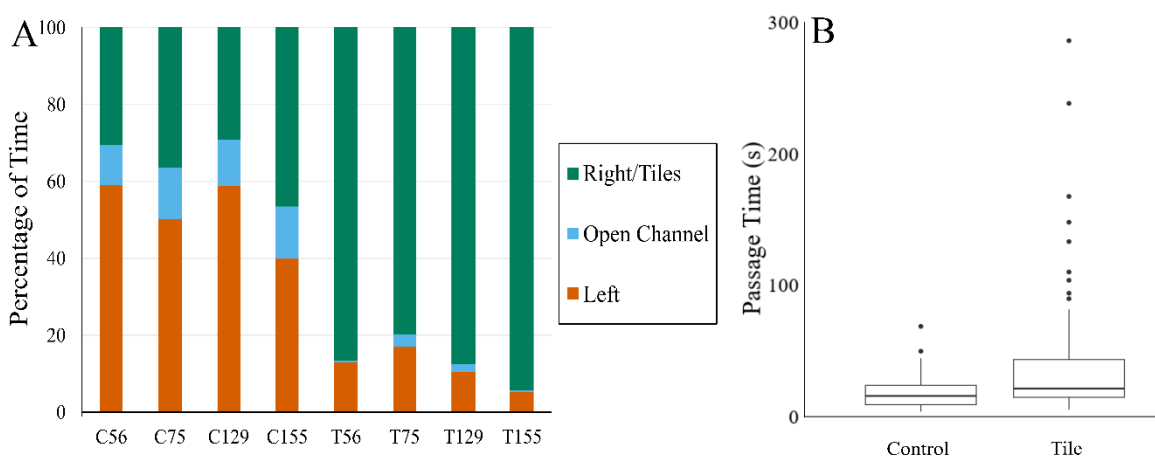
Figure 4.3. Eel behavioural plots. A) Proportion of time spent on right hand side (where tiles are present in treatments denoted with T and absent in treatments denoted with C), left hand

side and in the open channel region. Right and left refer to the side of the flume looking downstream and comprise of the corner formed between wall and bed and the 150 mm adjacent to that. B) Boxplot of the time eels took to pass upstream in the control conditions compared to when the tiles were present, the control data includes all control treatments and the tile data includes all tile treatments. The boxes show interquartile range, the whiskers 95% interval levels and the dots represent the outliers.

Within all treatments with the tiles, most time was spent within or around the tiles and significantly more than the open channel and flume corner (GLM, p<0.05). However, for the control experiment for the shallowest condition (C56), there was no differences in time spent between sides of the flume but more time was spent at rest and in the corners than in the open channel (GLM, p<0.02). The same was true of C75 and C129 but in C155 significantly more time was spent at rest than anywhere else (GLM, p<0.018).

4.3.2 Kinematics

The tailbeat frequency of swimming fish increased linearly with normalised swimming speed (GLM, p<0.0001). The relationship between tailbeat frequency and swimming speed of the eels was area specific, in the above tile area, eels had the lowest swimming speeds but also the steepest increase in tailbeat frequency with speed whereas eels within the open channel area consistently utilised fewer tailbeats per body length per second. In the tile corner and flume corner areas, eel kinematics showed a similar relationship of tailbeat frequency and swimming speed as seen in Figure 4.4. The amplitude of the caudal fin is linearly correlated with head amplitude (GLM, p<0.0001), with an increased head amplitude at higher caudal amplitudes and swimming speeds. Caudal amplitude, however, was not linked with an increase in swimming speed. The overall amplitude ratio (the ratio of head amplitude to tail amplitude) however, had a strong correlation with swimming speed (GLM, p=0.0001). The caudal amplitude did not significantly vary between areas of the flume, showing that this may be decoupled from swimming speed and turbulence. While tailspeed increased with increasing Strouhal number (GLM, p<0.0001), the tailbeat frequency decreased. The average Strouhal number was 0.49, but this varied by location, as the equation involves swimming speed directly; it was at a maximum where the swimming speed was at a minimum which was above the tile (GLM, p<0.0001). This however, implies that tailbeat frequency did not decrease at the same rate as swimming velocity in this area, something that is also evident in Figure 4.4. Stride length variation by area further confirms

this, the lowest value being in the above tile area and the highest in the open channel. The eel's stride length necessarily increased with local streamwise flow velocity, showing that the eels were using more a powerful gait in high velocity areas.
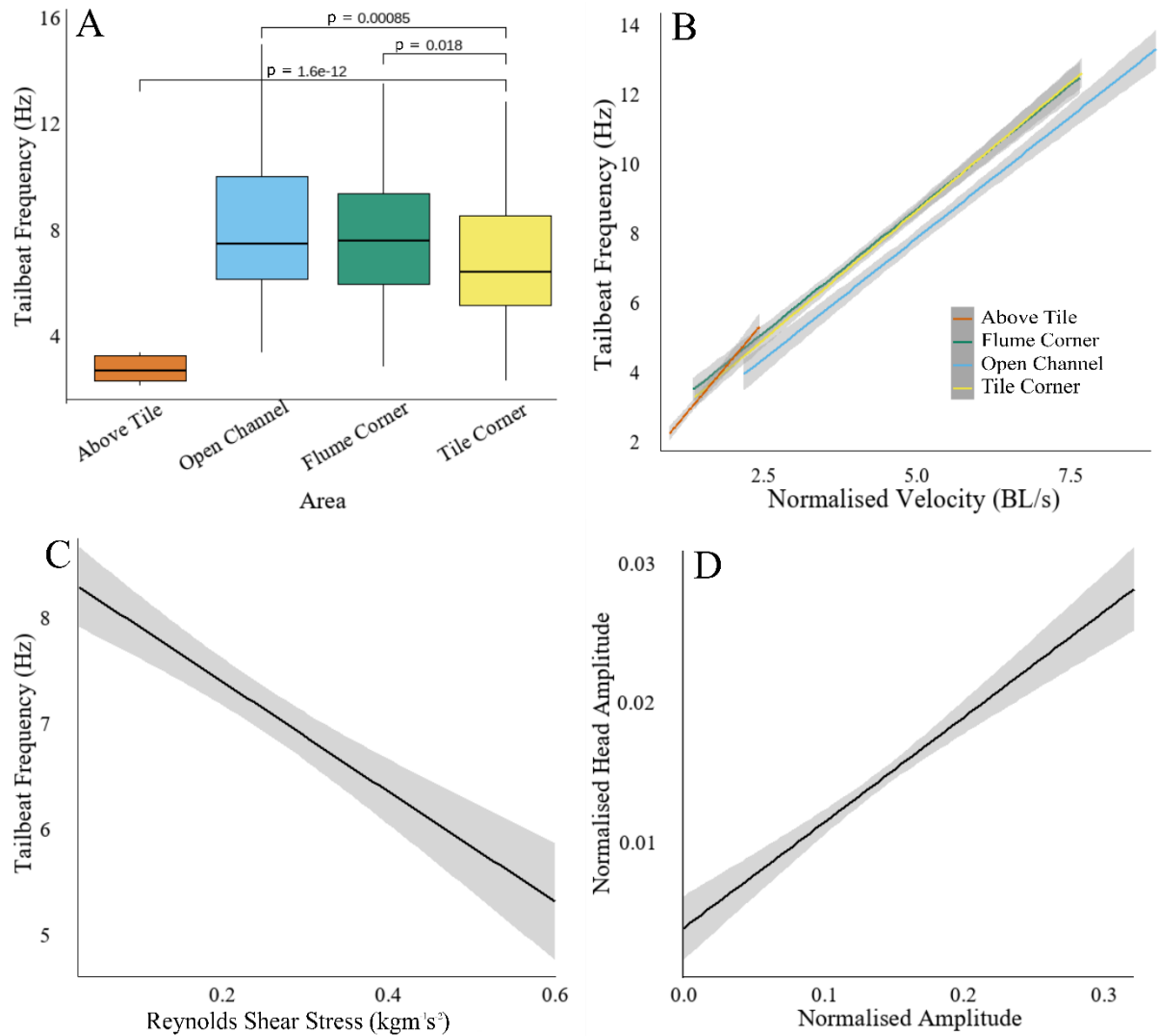
Figure 4.4. Kinematics parameters from the eel swimming data. A) Tailbeat frequency in different areas of the flume with p values to show significance between areas; B) Linear regressions with 95% confidence intervals for the relationship between tailbeat frequency and normalised swimming speed for different areas; C) Regression plot of the relationship between tailbeat frequency and Reynolds shear stress in the horizontal plane (τ_{uv}); and D) Relationship between head and tail amplitudes.

An analysis of turbulent parameters of the flow combined with kinematics data revealed that the horizontal Reynold's shear stress (RSS, τ_{uw}) had a significant effect on tailbeat frequency (GLM, p=0.003) while vertical RSS (τ_{uv}) and horizontal and vertical turbulent intensity (TI)

had non-significant effects. Tailbeat frequency decreased with increasing horizontal RSS (τ_{uw}). Notably, the normalised swimming speed of the eels negatively correlated with fish length as did the normalised caudal amplitude.

Crawling kinematics were highly varied in both amplitude envelopes, crawling speed, and all other pre-established kinematics parameters. Some distinctions and observations were made however, the number of points of contact between the eel and the tiles was normalised by eel length and was found to increase with flow depth (GLM, $p<0.05$). The points of contact also increased in the small protrusions (GLM, $p<0.0001$) but did not significantly differ on the direction of motion of the eel.

By associating the energy expenditure to the tailbeat frequency, the tailbeat frequency can be used as a proxy for energy usage for this data. Tailbeat frequency analysis by area shows that above the tiles the fish expended the least amount of energy, followed by the tile corner, then the flume corner and finally the open channel, where expenditure reached a maximum (GLM, $p<0.018$). The crawling energetics cannot be calculated in the same manner but if the method were used the expenditure would be much lower than any swimming gait due to the relatively slow movements when crawling. All analyses agree however that the slower swimming permitted by the flow attenuation of the tiles reduced energy expenditure.
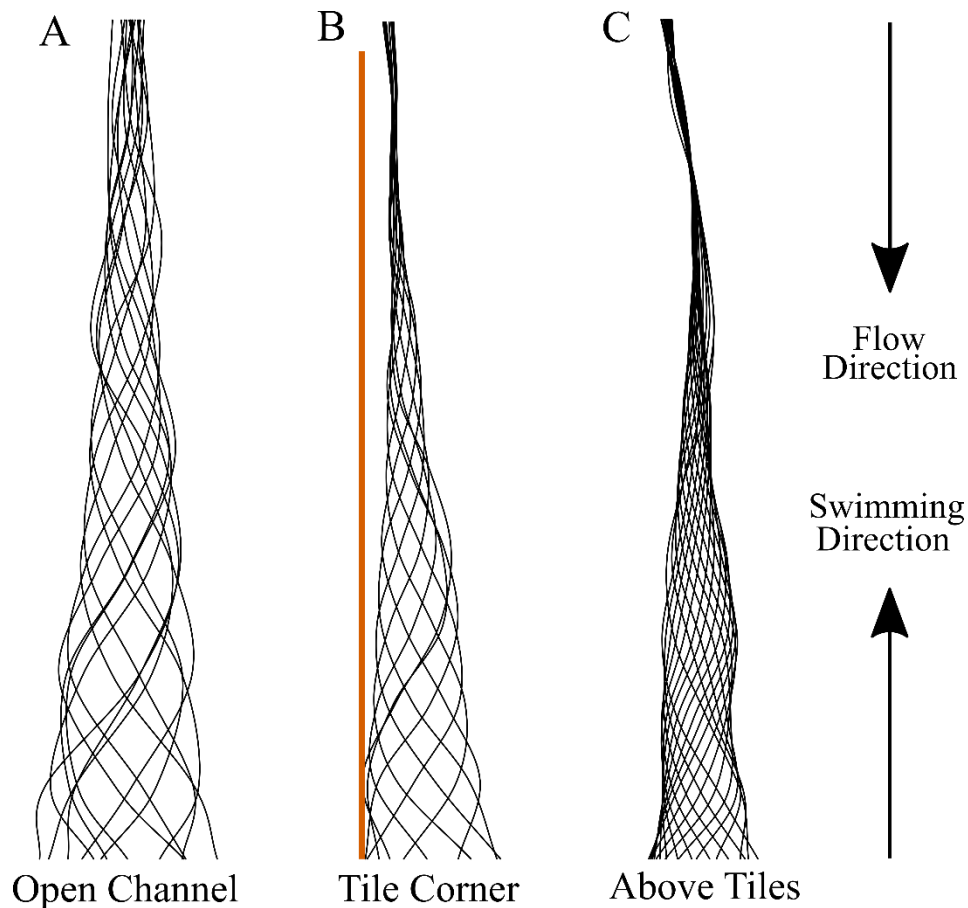
Figure 4.5. Eel amplitude envelopes for different areas of the flume. The head of the eel is at the top and the caudal fin at the bottom of the diagram. Each line represents the centreline of an eel for one frame (12.5 ms) and each envelope consists of many centrelines so that the full swimming gait of the eel may be visualised. A) Eel is swimming in the centre of the open channel; B) Eel is swimming along the edge of the tile shown by the orange line; C) Eel is swimming above the tiles with the flume wall to its left.

The swimming gait is best visualised by the amplitude envelope of the eels seen in Figure 4.5. Figure 4.5A shows a typical gait for open channel swimming, the eel is swimming with a high velocity compared to other areas and the amplitude is therefore large throughout the body and especially at the head, increasing steadily throughout the length of the body. The profile of the gait is also symmetrical against an imaginary centreline. In Figure 4.5B, the swimming gait in the tile corner is characterised by a much smaller head amplitude which steadily increases towards the caudal fin where it reaches a maximum. The reduced head amplitude is to be expected due to the reduced swimming speed of the eel in this area. The profile of the gait, however, is asymmetrical and shows how the eel is maintaining the head towards the left (which in this case is near the edge of the tiles). The skewed alignment of

the head and the rest of the body while oscillations are made asymmetrically into the open channel, suggests that the eels are attempting to maintain the majority of their body within the lower velocity zone near the tiles for as much of the time as possible. The eel in Figure 4.5B is benefitting from the low velocity from the tile while not swimming within the protrusions. In contrast to A and B, Figure 4.5C shows a more complex gait. The head amplitude remains small and the amplitude stays small along more of the body compared to A and B, due to the comparatively low swimming velocity. The amplitude does not increase steadily from head to tail nor is it symmetrical, although the maximum amplitude is at the caudal fin. Not all examples for swimming above the tile exhibited the same peaks and troughs as in the envelopes shown here but the eels had very similar gaits, suggesting the gait was unstable but exhibited the same typical features.

4.4. Discussion

Overall, the eel tiles increased fish passage, but that was not the only benefit they provided to the eels. While an increase in passage is the primary objective of the tiles, the eels used the tiles and increased passage even at a velocity where most eels were still able to pass upstream without tiles and the hydrodynamic data from the tiles suggests that even at higher flow velocities the tiles produce favourable conditions so the increase in passage is expected to be even greater at higher flow velocities since the tiles also allow the eels to rest and crawl. Despite not all eels passing upstream with the tiles, they were always able to progress onto the tiles and move upstream. Real world passage is likely to be even higher than the present results suggest as the tiles (and the small protrusions especially) were used for resting, which would allow even small eels with poor swimming performance to pass upstream over an appropriate length of time and without losing the upstream progress made. The current study was constrained by time and the eels may not have had long enough to pass upstream, but given more time and the ability to rest in the tiles more eels could potentially pass upstream, and even be able to pass long culverts. The tiles give the eels the ability to rest at any point in their navigation upstream and therefore not lose any progress already made. In the absence of the tiles, an exhausted eel would be swept back downstream and therefore be unlikely to pass upstream for as long as the velocity remains high. Even eels that are successful in passing upstream without the tiles may be more exhausted leading to resting immediately upstream of the tiles. These behaviours could cause resting hotspots up and downstream of the tiles, creating potential predation hotspots driven by 'density-dependent predation' which could exacerbate the passage issues of the velocity barrier

(Jepsen et al., 2010; Wright et al., 2015), whereas with the tiles the eels are able to rest at any point, avoiding the creation of hotspots. A gathering of many eels in one place is also likely to deplete resources faster and to increase the transfer of directly transmitted parasites (de Leaniz, 2008). Tiles can therefore be useful for any length of velocity barriers by allowing continuous progression upstream. The passage time was significantly higher with the tiles but this should not be considered a downside as the difference in passage time is in the order of seconds and minutes which is unlikely to impact an upstream migration and conversely, the added resting time can allow the eel to pass upstream more easily and with less effort. Baffle type passes used for similar applications do not always feature resting spots (Solomon & Beach, 2004), but some bristle passes do employ the use of resting pools to allow elvers to rest between sections (Solomon & Beach, 2004).

Behaviourally, the eels showed a strong preference for the tiles when they were present and not only spent more time within them than in the flume corner, but the time swimming in the open channel was reduced. The current study did not evaluate attraction to the tiles as the tiles occupied 42% of the channel width and were therefore easily found by the eels. This study reinforces the idea that in a box culvert or flume the eels will spend most of the time swimming near the bank as in the control conditions this is overwhelmingly where they swam, therefore suggesting that this would be the best place to mount tiles as eels are likely to be present here.

The kinematic analysis revealed further benefits that the tiles offer. The swimming speeds of the eels were slower when they swam in the vicinity of the tiles (and above them in particular), reducing the need for the eels to swim in bursts. The crawling speed was an order of magnitude lower than any swimming, which is also encouraging in terms of reducing energy expenditure and the crawling kinematics were widely diverse. Crawling showed a level of similarity with terrestrial locomotion in terms of the amplitude being similar along the body (Gillis, 1998). The relationship between tailbeat frequency and swimming speed was dependent on the area in which the fish were swimming however, in all cases the swimming speed correlated very closely with the tailbeat frequency (Gillis, 1998; Tack et al., 2021; Tytell, 2004b) but it appears that eels swimming in the open channel area needed significantly fewer tailbeats to achieve the same speed compared to those moving in the flume corner and tile corner. Although this may suggest more efficient swimming in the open channel and potential disturbances from the turbulence elsewhere, which according to the

relative swimming speeds in each area agrees with the findings of cost of transport being reduced at higher speeds (Tack et al., 2021). Energetically, the comparative energy expenditure of eels was highest in the open channel (in the control conditions) due to their higher swimming speeds, and lowest in the above tile and tile corner areas. The tiles reduced the energy expenditure of the eel while in motion as well as providing habitat for resting. The most energy efficient mode of locomotion however, is likely to be crawling due to the slow movements and very low flow velocities within the tiles. The crawling energetics, however, could not be calculated so the comparative energy expenditure is unknown. The tiles not only provide energy savings for the eels by allowing them to move upstream with locomotion methods that reduce energy expenditure, but by allowing the eels to rest, should they need to, they do not need to go downstream to rest so any progress they make is conserved.

Eel swimming speeds and tailbeat frequencies were not different amongst the flume corner and the tile corner but the tile corner indicated a lower energy usage. A mechanism for this reduction of energy consumption in the tile corner may be found in the analysis of the amplitude envelope of the eels in different areas. The open channel swimming gait show good agreement with the findings of previous studies concerned with eel kinematics, especially when examining higher swimming speeds (Gillis, 1998; Lauder & Tytell, 2005; Tack et al., 2021; Tytell, 2004b) but previous studies generally have been concerned with swimming in more simplified velocity field or tank (no flow) conditions and not in a high complexity flow of turbulence and shear layers as studied here. In the tile corner, the eels consistently swam asymmetrically by keeping the majority of their body close to the tiles for most of the time. This meant that the eels were exposed to lower flow velocities with most of their body, which is likely to reduce drag. This is the first time this behaviour has been studied and offers new insight into eel swimming strategy. This behaviour was not seen in the flume corner and this may be due to the smoother change in velocity, whilst in the tile corner there is a mixing layer driving the slow flow of the tiles and the fast flow of the open channel, making this transition more abrupt and easier to sense and exploit by the eels. This finding is unlikely to be the only way eels adapt their gait but is the first step in beginning to understand the plasticity of their gait in complex flows and shear layers which are more representative of flow conditions in nature. The above tile amplitude envelope however, shows a complex gait that defies easy characterisation. The above tile gait is irregular and this may be explained by the turbulence in that area being at its highest and therefore

interfering with the swimming stability of the fish. This, however, did not seem to negatively impact passage or to cause any major destabilization or 'spill' as defined in previous studies (Muhawenimana et al., 2019; Tritico & Cotel, 2010). This is not surprising since the turbulence shed by the tiles is not coherent enough, or the correct length scale to destabilise fish of these lengths (Muhawenimana et al., 2019; Tritico & Cotel, 2010), this may also be in part due to the different aspect ratio of eels compared to hitherto tested fish species. The kinematics data linked lower tailbeat frequencies with elevated turbulence parameters and specifically with Reynolds shear stress in the horizontal plane (τ_{uv}) but the effects of velocity and turbulence on tailbeat frequency cannot be disentangled as the highest levels of turbulence were present in the lower velocity areas. The relationships between other kinematic parameters were also found to match the literature, such as amplitude increasing with swimming speed (Tack et al., 2021; Tytell, 2004b) and tailspeed (Tytell, 2004b). Strouhal number decreased at higher swimming speeds and the average values matched the peak values found by previous work (Tytell, 2004a). The tiles increased passage while reducing energy expenditure, allowing eels to rest within the tile protrusions, and not significantly affecting the hydrodynamics in the rest of the channel. For these reasons they appear as a good solution for eel passage at high velocity barriers that do not require high swimming speeds at any point. Tiles are a proven technology for gravity barriers (Vowles et al., 2017) so should such a barrier be present at the downstream end of a culvert, where typically there can be a 'step', the tiles can be employed without the use of two different solutions for the gravity and high velocity barriers. While the tiles are cost-effective for both purchase and retrofitting, it is crucial to exercise caution during installation to ensure that no gaps are left between them. These gaps could potentially provide a passage for eels to swim beneath the tiles, encouraging them to establish residency within the tiles, rather than facilitate their upstream movement.

4.5. Conclusion

Eel tiles have been evaluated as a passage solution for eels and the findings conclude that an increase in passage is produced by adding the tiles to a high velocity barrier. The tiles bring the additional benefits of allowing the eels to rest and preserve any upstream progress and enabling them to crawl, swim in reduced flow velocity or swim normally. They also allow the eels to expend less energy in their upstream passage, something that is useful considering the multitude of barriers eels encounter in their migration. The kinematics of eels were analysed for the first time in flows with hydrodynamic complexity (e.g. multiple shear layers

and turbulent structures of varying lengthscale) and revealed new mechanisms of drag reduction through asymmetric swimming gaits exploiting a shear flow layer. Overall, the tiles appear to be a suitable solution for upstream passage of eels at high velocity barriers and have potential to work for other species of fish while not modifying the flow in the rest of the channel for fish species which may not require the tiles. This chapter confirmed some benefits of eel tiles meeting objective 3 of this thesis and also produced new knowledge of eel kinematics applied to complex flow meeting objective 2.

Chapter 5. Evaluation of Eel Tiles for Passage of the Three Spined Stickleback (*Gasterosteus aculeatus*)

Conceptualisation and methodology by Prof. Jo Cable, Prof. Catherine Wilson, Andy Don, and Guglielmo Sonnino Sorisio. Data collection by Guglielmo Sonnino Sorisio and Nia Davies. Analysis, visualisation, and writing by Guglielmo Sonnino Sorisio and editing by all of the above.

Summary

Culverts are high velocity barriers that pose a challenge for fish navigation. The high velocities generated within culverts have the potential to halt migrations and fragment habitats. Passage solutions for small, river resident, freshwater fish are scarce and eel tiles present a possible multi-species solution. In this study, moulded tiles designed to promote eel passage were mounted in a recirculating open channel flume, and we assessed whether a sentinel species, the three-spined stickleback (*Gasterosteus aculeatus*) could navigate fixed flow conditions in the presence and absence of tiles, either alone or in shoals of three fish. The tiles significantly decreased impingement on the downstream flow straightener and exhaustion. Shoaling significantly increased passage, but in harsher local velocity conditions fish in shoals did not maintain cohesion. The tiles benefitted the fish by providing lower flow velocities but produced turbulence that in some cases destabilised the swimming fish. Despite this the tiles improved the swimming ability of fish in areas where they would have otherwise become quickly exhausted.

5.1 Introduction

The rivers of Europe are amongst the world's most fragmented. Anthropogenic barriers are ubiquitous in many freshwater systems and are present in headwater streams to large rivers (Belletti et al., 2020; Jones et al., 2019). The number of barriers is unknown but estimates range from 1.2 to 3.7 million barriers in Europe alone, 61% of which are unreported (Belletti et al., 2020). Many of these unreported barriers are small installations with little to no head drop in the river but they still pose a threat to diadromous and potamodromous fish and general habitat connectivity. Of the estimated total number of barriers, 17.6% are culverts (Belletti et al., 2020). These can cause discontinuity in habitats and impair the ability of fish

to swim upstream by constricting the flow, creating high velocity flows due to their smooth uniform boundaries (Bouska & Paukert, 2010; Erkinaro et al., 2017; Gibson et al., 2005; Rodgers et al., 2017; Shiau et al., 2020; Warren & Pardew, 1998), and cause a reduction in fish passage especially for smaller bodied fish (Jones et al., 2021). Fish pass designs that are often implemented at barriers are designed for migratory fish, such as salmonids, some of the most powerful freshwater swimmers (Clough et al., 2004; Clough & Turnpenny, 2001; Kemp & O'Hanley, 2010) because of the migratory needs or status of endangerment.

Fish pass efficiencies are widely variable (Kemp, 2016; Shaw et al., 2016), but little is understood about the passage of so-called "non-target species" such as the Three-spined stickleback (*Gasterosteus aculeatus*). These form an important component of aquatic food webs and therefore fragmentation of habitats can cause detrimental pressure on these ecosystems. Smaller, resident riverine fish, especially those that are non-migratory and/or benthic, are typically less powerful swimmers and cannot reach the same swimming speeds as salmonids (Blake et al., 2005; Clough & Turnpenny, 2001; Tudorache et al., 2007). Such fish are impacted by all types of barriers and this is a contributing factor in the decline of freshwater biodiversity (Fahrig, 2003). A move away from species focused passage designs is therefore necessary to help restore ecosystems; passes should be navigable by multiple fish species of different morphologies and sizes. The design and implementation of fish passage solutions that are effective across a range of fish morphologies, sizes and swimming characteristics is currently an under-researched area and a clear knowledge gap (Jones et al., 2020, 2021). Textured substrates have been shown to be effective for smaller bodied fish in ramps (Franklin et al., 2021), and baffle designs can be adapted to match the passage needs of small fish (Magaju et al., 2021). Despite velocity barriers being a known hinderance to the migration of small fish, literature has shown some potential for existing solutions to benefit these species (Knapp et al., 2019).

Sticklebacks are present in water bodies throughout Europe and parts of North America. These fish, typically between 30 and 50 mm in length when fully grown, are usually found in ponds and streams, away from high velocity flow and in the shelter of vegetation. This species is marked as "least concern" in the IUCN Red List of Threatened Species but anthropogenic migration barriers have been found to drive genetic diversification and isolation in populations of these fish in Germany (NatureServe, 2019; Scharsack et al., 2012). This is compounded by an increase in migration between salt and freshwater habitats

due to increased saltwater pollution (Scharsack et al., 2012). Three spined sticklebacks are primarily labriform swimmers, meaning they primarily propel themselves forward with their pectoral fins, their caudal fin only is engaged when swimming in bursts and when maneuvering, but most often is compressed (Blake et al., 2005). Populations of this species can have diverse life cycles, some live their whole lives in freshwaters and never migrate, others migrate between freshwater, brackish and saltwater. Migrating sticklebacks can attain higher swimming speeds than river-resident individuals, swimming as fast as 0.43 ms^{-1} whereas the non-migratory fish can only reach 0.34 ms^{-1} (Tudorache et al., 2007). Sedentary populations of sticklebacks have been suggested as effective environmental sentinels for the UK, being a robust species found all over the country (Pottinger et al., 2002). Sticklebacks are a shoaling species (Barber & Ruxton, 2000; Mehlis et al., 2015), this benefits their social interactions, foraging, and defense from predators. Many studies have also shown the hydrodynamic advantage of shoaling and this should not be discounted when considering fish movement (Johansen et al., 2010). Shoaling dynamics can adapt to flow conditions to benefit the fish (Mayer, 2010), with some fish species shoaling more consistently when flow was present in a laboratory setting (De Bie, 2017; de Bie et al., 2020). Some of the mechanisms behind the hydrodynamic benefits of shoaling are well understood (Daghooghi & Borazjani, 2015). Shoaling in labriform fish is still poorly understood, and the balance of hydrodynamic and social benefit of shoaling under the presence of flow is a knowledge gap.

Eel tiles are a passage solution that have the potential to allow fish passage through high velocity barriers such as culverts and restore connectivity; they comprise a base from which cylinders protrude. The tiles were originally designed to help juvenile eels to climb past structures like weirs (Vowles et al., 2017) as surface-mounted climbing substrate, irrigated by relatively small flows passing through the protrusions. However, they can also be effective in barriers such as culverts (Chapter 4). They are fixed to the bed of the river or structure and are usually fully submerged. They provide cover for fish and reduce the flow velocity within the protrusions as well as creating low velocity areas above and horizontally adjacent to them (Chapter 4). The Berry and Escott tiles (Berry & Escott Ltd., 2023) consist of dual density protrusions, which have the advantage of creating areas with different characteristics, potentially allowing fish to select to swim in the area best suited to their ability. Analysis of the hydrodynamics around the tile revealed that there is the potential for different fish species to exploit them. Streamwise velocities generated within the tiles are in the region of 0.06 ms^{-1}, this equates to five times slower velocities than control conditions

without tiles on the channel bed (Chapter 4). The individual protrusions can generate vortex shedding which may have some destabilizing effects on fish (Muhawenimana et al., 2019; Tritico & Cotel, 2010). In addition, the shear layer created between the slow flow of the protrusion layer and faster flow in the adjacent free stream regions above and beside the tiles has the potential to roll up into Kelvin-Helmholtz vortices, thus creating the potential for multiple interacting turbulent structures. Particle image velocimetry analysis and flow visualization revealed that periodical vertical and horizontal fluctuations occur at these boundaries of high Reynolds shear stress. In experimental trials with eels, the tiles successfully increased passage, and turbulence above the tiles was only destabilising for the fish to a minor degree (Chapter 4). For the tiles to be used by other species, it is important to know if fish with different swimming styles, and swimming strengths can make similar use of the tiles or at least to check if they have no detrimental impact. Eel tiles are a promising solution to fish passage due to their ease of installation and low cost relative to other fishways. They also have flexibility for a range of different installations, including lining sections or one side of the channel while keeping the remainder free. If this species specific passage solution is to be introduced at velocity barriers, there is an opportunity to evaluate and optimise their use to benefit a wider range of species.

This study aims to evaluate eel tiles as a potential passage solution for the small-bodied, labriform species: the three spined sticklebacks and draw learnings that apply to other small bodied fishes. The effect of the presence of shoalmates was investigated as an added variable that determines passage strategy and potential success. The hypothesis that the presence of tiles and the presence of shoalmates would increase passage was tested. Single or shoals of non-migratory sticklebacks were placed in a laboratory flume with and without tiles to investigate the impact of shoaling in swimming conditions approaching the limit of their capabilities (Tudorache et al., 2007).

5.2 Methods

5.2.1 Fish origin and maintenance

Three spined sticklebacks (*Gasterosteus aculaetus*, n=320; hereafter referred to as sticklebacks) were caught with hand nets from the St Fagans ponds (Grid Reference: 51.48742630926287, -3.270094010847469), Cardiff, UK on the 22/03/2023. Water temperature on the day of collection was 12°C. The fish were transported to Cardiff School of Engineering on the same day with Stress Coat (API Stress Coat +) added to their water,

and were slowly acclimated to the temperature and water chemistry of their holding tank. The fish were maintained in a circular (1.5 m in diameter) tank filled to a water depth of 0.3 m with a volume of 530 L. Tank water was dechlorinated with Tetra Aquasafe and maintained at 15°C with a D-D Aquarium Solution, DC 750 cooler. The water was filtered by an Aquamanta, EFX 600 External Canister Filter and checked every day to ensure the water chemistry was suitable (Ammonia 0-0.2 mg/L; nitrite 0-0.25 mg/L; and pH 7-8). The fish were kept under a 12:12 hour light:dark regime (lights on at 07:00 am) and enrichment was provided to the fish in the form of ceramic pots, rocks and tubes to provide refugia. The tank was subdivided into two sections by a plastic mesh that allowed water mixing but restricting the sticklebacks so that after the first day of experiments fish already tested in the flume would not be used again. The fish were allowed to acclimate to the holding tank for a minimum of 24 hours before being used in the experiment and they were not fed for those initial 24 hours. Starting from the second day of captivity, the fish were fed thawed bloodworm every morning before the experiments began. After the experiments, a subsample of the fish underwent an external health check that revealed no visible injuries, then returned to their place of origin, ensuring to re-acclimate to their habitat by introducing pond water to the container they were in before releasing them. Fish total length averaged 34.2 ($\pm$ 0.5, range 18-59) mm and was not significantly different between treatments (GLM, $p > 0.89$), detailed in Table 5.1. Shoalmates were size matched ($\pm$ 2 mm). Despite originating from a lentic system, sticklebacks from similar populations have been found to have lower but comparable swimming performance (Tudorache et al, 2007), making them suitable for this study.

Table 5.1. Fish total length per treatment and details of the treatments, average length did not vary significantly between treatments or between focal fish and shoalmates (GLM, p > 0.89). The treatment codes refer to the flume setup (C = no tiles, T = tiles) and the number of fish in the flume (1 = one fish, 3 = shoal of three fish). For each treatment, 30 repeats were performed and all fish were only used once.

Treatment	Number of Fish	Tiles/Control	Fish	Mean mm	Minimum mm	Maximum mm
C1	1	Control	Focal	34	23	55
C3	3	Control	Focal	34	22	57
C3	3	Control	Shoalmate 1	35	20	59
C3	3	Control	Shoalmate 2	35	18	53
T1	1	Tiles	Focal	34	21	55
T3	3	Tiles	Focal	34	22	54
T3	3	Tiles	Shoalmate 1	34	25	52
T3	3	Tiles	Shoalmate 2	34	21	55

5.2.2 Flume setup and flow conditions

The experiment was carried out in an indoor recirculating open channel flume with rectangular cross-section 1.2 m wide and 0.3 m deep. The length of the flume was 10 m. The flume had a fixed bedslope of 1/1000 and a weir at the downstream end to control the water surface profile. The bed of the flume was lined with plastic and the walls of the flume were made of glass. The flume water was dechlorinated (Prime Dechlorinator) and kept at 15 ±2°C by a cooler (D-D Aquarium Solution, DC 2200 cooler). Nine Berry and Escott dual density eel tiles were mounted to the plastic bed of the flume with the small protrusions section of the tile adjacent to the flume wall (Figure 5.1). Each tile measured 505 mm by 505 mm (width and length) and 75 mm tall (h), with a 25 mm thick base and 50 mm tall cylindrical protrusions. The total length of the tiled section was 4.55 m and the 8 m working section of the flume was bounded by flow straighteners up and downstream that also acted as screens to keep the fish within the area. Downstream of the tiles a 1 m long area was used as an acclimation zone for the sticklebacks before they were released at the start of the

experiment and upstream of the tiles a portion of the flume was used to collect sticklebacks that swam upstream. The flow conditions were kept constant with a flow depth (H) of 0.155 m, a bulk velocity (U) of 0.35 ms^{-1} and a Reynolds number (Re) of 40,931 based on the hydraulic radius (measured along the flume at 1 m intervals with a vernier scale and PIV). These were chosen to represent challenging conditions for the sticklebacks (Blake et al., 2005; Tudorache et al., 2007) but still within their range of burst swimming capabilities. The relative submergence (H/h) of the tiles was 2.07 under these flow conditions.
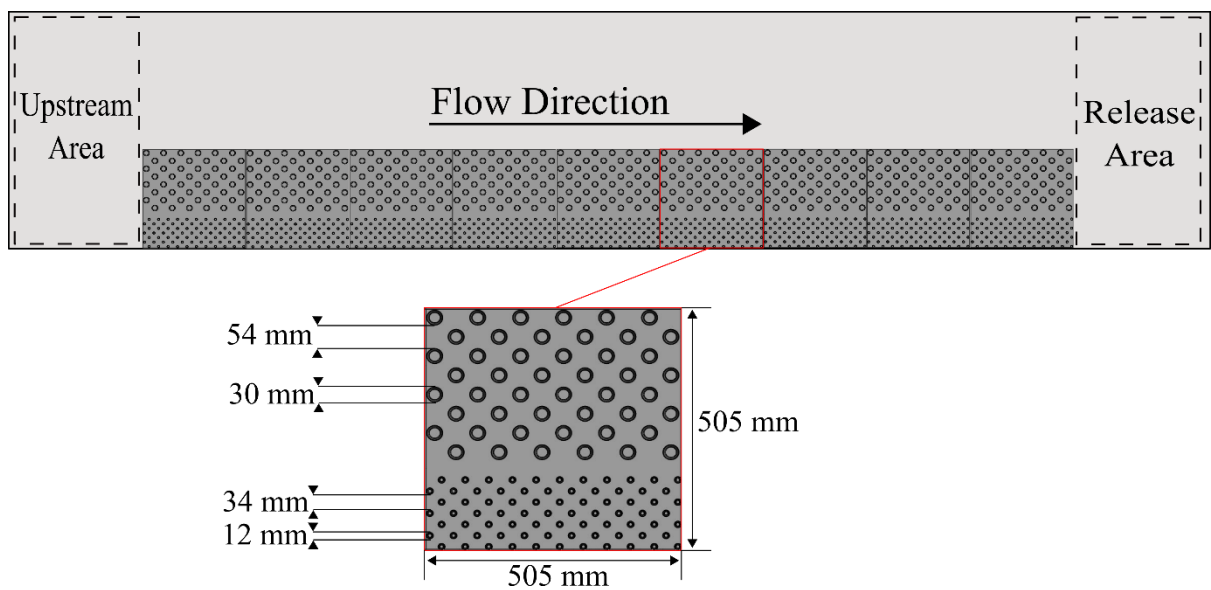
Figure 5.1. Topview of the flume used for the experiment with the tiles mounted along one side and topview of a magnified tile with dimensions of the protrusions and the spacing between them shown. The protrusion spacing given in the diagram is equal in both streamwise and spanwise directions. The large protrusions have a diameter of 30 mm at the base and the small protrusions have a diameter of 12 mm at the base.

5.2.3 Hydrodynamics of the Tiles

The tiles reduced flow velocity within the protrusions and in the surrounding flow. Data acquired by Particle Image Velocimetry (PIV) revealed two distinct layers of flow; the protrusion layer and the unobstructed flow layer, where these two layers meet there is a mixing layer and the Reynolds Shear Stress is at a peak. This creates potential for a Kelvin-Helmholtz (KH) instability (H. Nepf & Ghisalberti, 2008) with vortices at the scale of the

protrusion heights as often seen in canopy and vegetated flows (H. Nepf & Ghisalberti, 2008; H. M. Nepf, 2012). In the case of the tiles, the KH vortices are not fully formed, instead creating periodical vertical and horizontal fluctuations. Protrusion scale (or stem scale) vortices can also be shed by individual protrusions. Both the individual and combined effect of these periodical fluctuations have the potential to create unstable swimming conditions for fish but overall the reduced flow velocities generated by the tiles are a benefit to eels trying to swim upstream.
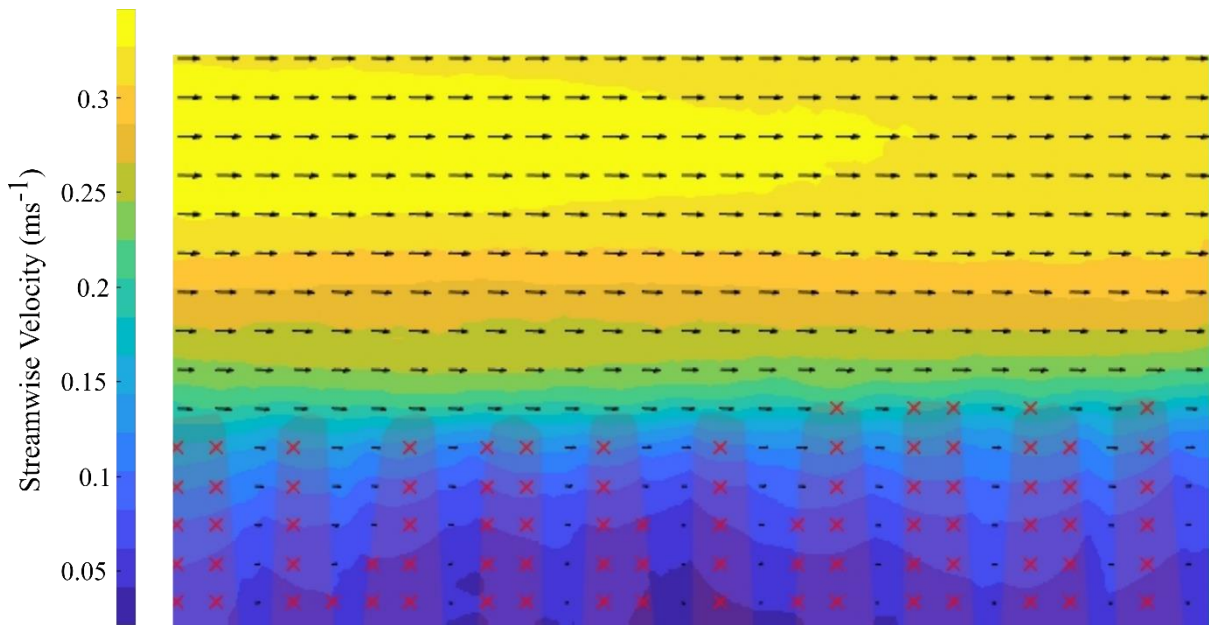
Figure 5.2. Side view of the time-averaged streamwise flow velocity within the small protrusions, the arrows indicate the direction of flow. The shaded areas with red crosses represent the masked area occupied by the protrusions.

5.2.4 Experimental Design

Four treatments were tested in this experiment (Table 5.1): a single fish with tiles (treatment T1), a single fish without the tiles (treatment C1), a shoal of 3 fish with the tiles (treatment T3) and a shoal of 3 fish without the tiles (treatment C3). The codes for the treatments represent the presence of the tiles (T = tiles, C = control) and the number of fish in the flume (1 = single fish, 3 = shoal of 3 fish), a total of 30 repeats were performed for each treatment and each fish was only used once. Treatments C1 and C3 in this case served as controls. For all treatments the procedure was as follows. Before fish were released into the flume they were measured for total length, and visually checked for any abnormalities. Each fish or shoal was acclimated in flume water for a minimum of 1 hour before the start of the

experiment, the flowrate was then increased slowly from ~ 0 ms^{-1} over 3 minutes to the experimental condition and the fish were allowed to acclimate for a further 2 minutes at the downstream end of the working section ahead of being released into the test section. The short acclimation time was necessary to avoid exhausting the sticklebacks before the test began. The fish or shoal was then released and allowed to swim freely in the test section for 10 minutes then removed from the flume and returned to the holding tank. The fish were only removed before 10 minutes had elapsed if they passed upstream or if they became impinged against the downstream flow straightener. Impingement was defined as the fish lying flat against the straightener for 60 seconds without successfully moving from this position. If the fish were unable to move even when the back of the straightener was tapped the fish was considered impinged. Gently tapping the back of the flow straightener was used as a method of scaring the fish into moving away and was selected rather than making physical contact with the fish itself to avoid any potential injuries to the fish. When impinged, the fish showed signs of distress such as fast gasping and when removed from the flume, they were not able to react to the net or resist being lifted out of the flume, further demonstrating their exhaustion. This definition of impingement was used due to the lack of a standardised measure for this metric. In the event of impingement, the fish was removed and the experiment terminated before the full 10 minutes. The impinged fish was then checked visually for any external injury, measured and placed back in the holding tank. The experiments were carried out in the hours of daylight (between 09:00 and 17:00) with blinds used to block out natural light and artificial light used throughout to eliminate light intensity as a variable factor. Sticklebacks can demonstrate both diurnal and nocturnal behaviours but in this experiment all data were collected during day time with constant light intensity (552 Lx on average).

5.2.5 Data recording

JWatcher (Blumstein et al., 2000; Blumstein & Daniel, 2007) was used to record fish behaviour live by direct observation by two observers. Behaviour and modifiers were defined such that the fish could be tracked by logging the position of the fish within the flume by defining five main areas: within the small protrusions, within the large protrusions, on the side of the tile (at the interface with the free stream region, 100 mm wide), above the tile and in the open channel region. Modifiers from 1 to 9 were applied to these areas to indicate which tile a behaviour was associated with. A different set of keys was specified for the same behaviour listed above corresponding to number of fish in a shoal. Other

behaviours that were logged were successful passage upstream, resting, impingement and spills. The fish was deemed to be resting if it was stationary and positioned facing the flow and clearly in control of its position whereas if the fish lay flat against the flow straightener despite efforts to move it was recorded as impinged. A 'spill' was defined as a temporary destabilisation and loss of control by a fish while swimming (Tritico & Cotel, 2010). To accurately record fish movements, two people observed and monitored the fish to ensure the robustness of the behaviour scoring, the same two observers conducted all the trials. In the case of the shoals, a randomly selected focal fish was chosen before the fish were released after acclimation and only the behaviour of this fish was monitored in terms of position of the fish within the flume and number of shoalmates when it was shoaling (which included the focal fish). Fish were considered to be shoaling when within a maximum of five fish lengths of each other (Tien et al., 2004). In treatments with three fish, only the focal fish was recorded and all metrics associated with these treatments only apply to this fish.

Table 5.2. The behaviours and metrics logged for the sticklebacks and their respective definitions.

Metric	Definition
Pass	A fish was deemed to have passed when the entire body had passed upstream of the ninth tile.
Time to pass	The time elapsed from the start of the test to when a fish had passed upstream.
Area	Described the position of the fish transversally to the channel: small protrusions, large protrusions, tile side, above the tile, or open channel, as well as the streamwise position recorded as the number of tile lengths from the downstream end.
Resting time	The amount of time the fish spent resting, stationary and positioned facing the flow and clearly in control of its position.
Impingement	If the fish lay flat against the flow straightener despite efforts to move it was recorded as impinged.
Spill	A clearly visible destabilisation and subsequent recovery in the fish's swimming.
Shoaling time	The time spent within 5 body lengths of other fish

5.2.6 Data Analysis

The data were analysed in RStudio version 4.2.2 (R Core Team, 2022). The data were first inspected with histograms and a Shapiro-Wilk test to examine the distribution of the data. Generalised linear models (GLMs) were used to fit the data using the MASS package (Venables & Ripley, 2002). Different models were considered based on the data distribution, the residual distributions and AIC values were then inspected and the best model chosen. An Inverse Gaussian GLM with $1/mu^2$ link was used for total length comparisons across treatments and shoalmates, maximum progress (furthest upstream position reached by the fish) and length, time to pass with treatment and length, time shoaling with treatment, and time above with treatment. For time in a shoal of two fish and treatment, and time in a shoal of three fish and treatment an Inverse Gaussian GLM with identity link was used. A Binomial GLM with probit link was used to model the pass against treatment data, while a Negative Binomial GLM was used to analyse spill against treatment (log link), to compare the spill count with passes (log link), to model number of spills and total length (sqrt link), and the spills by area (log link). Gaussian GLMs were used in the case of total length and passes (sqrt link), time on the tile side with total length and treatment (identity link), and proportion of time spent in each area in treatments T1 and T3 (identity link). A Gamma GLM was used to model the maximum progress with treatment (identity link), time resting with treatment (identity link), time in the small and large protrusions with treatment and total length (inverse link), time in the open channel section with treatment and total length (inverse link), and time spent alone with treatment (identity link). A Zero Inflation model (ZINB) with a logit link was used for total time impinged against treatment and length using the pscl package (Zeileis et al., 2008). When modelling total time, a transformation of + 0.001 was used to avoid zero values. The confidence interval used in all cases was $p = 0.05$.

5.2.7 Animal Ethics

All work was approved by the Cardiff University Animal Ethics Committee and conducted under UK Home Office licence PP8167141, and permission to collect fish was obtained from St Fagans National Museum of History.

5.3 Results

5.3.1 Passage and Swimming Performance

Overall, passage within the experimental time was increased by shoaling more than it was by the presence of tiles although both shoaling and tiles produced more passes. The number of successful upstream passes was 26.7% more in T3 compared to C1, a significantly higher pass rate (GLM, p = 0.02) with 40% of fish passing compared to 13.3%. Treatment T3 (40%) had statistically the same passage success of T1 (20%) and C3 (30%), (GLM, p = 0.09 and p = 0.59 respectively). There was a significant correlation between passage success and fish length (GLM, p < 0.001); larger fish were more likely to pass upstream than smaller fish, likely relating to their stronger swimming ability. Time to pass (time taken from the beginning of the experiment to the successful passage of the focal fish) did not vary between treatments, and there was no link between fish length and time to pass (GLM, p = 0.19).

The maximum distance upstream of the release area was calculated for every fish based on the tile number reached and provides a metric to evaluate performance that is less discretised than passage (Figure 5.3). The maximum distance reached for the control treatment with a single fish (C1) was lower than C3 and T3 (GLM, p < 0.03) but not lower than T1 (GLM, p = 0.12). Larger fish were more likely to progress further than smaller fish (GLM, p = 0.004) further indicating that stickleback swimming performance increases with size.

Spills occur when a fish experiences a destabilisation while swimming, this is distinct from a change of direction by being clearly involuntary and often occurring while station holding. In the control treatments, a negligible number of spills was recorded when compared to the tile conditions where 190 spills were recorded overall, with T1 and T3 significantly different to control treatments (GLM, p < 0.0002) but not significantly different from each other. Fish length was correlated with number of spills indicating that smaller fish were more likely to spill (GLM, p = 0.009), since spilling is often related to turbulence this correlation is probably affected by turbulent parameters in a particular area. However, the more time a fish spent swimming, the more likely it was to spill (GLM, p<0.0001), as more time spent swimming increases the opportunities to spill. This might also be the reason that spill number was negatively correlated with passage success (GLM, p = 0.03). Most spills occurred within the large protrusion areas of the tiles compared to all other areas of the flume (GLM, p < 0.006).

The time spent resting was highest in the C1 and C3 treatments, and least in T3 (GLM, $p < 0.05$), whilst T1 was not significantly different to any other treatment. In the tiled treatments, resting did not only occur against the downstream flow straightener, but also within the small protrusions as the spacing allowed the fish to rest their body on consecutive protrusions or between protrusions and the sidewall without the need to swim. Despite increased resting opportunities the fish rested less with the tiles compared to the controls. The time spent impinged was the lowest in treatments T1 and T3, specifically, less time was spent impinged in T1 than C1 (ZINB, $p = 0.002$) and less time was spent impinged in T3 than C1 and C3 (ZINB, $p < 0.02$). There was no significant correlation between fish length and time spent resting or being impinged.

In the control conditions, the only area available for the fish was the open channel so this was not analysed in terms of where fish spent most time by treatment. The fish in the control conditions did swim primarily near the walls where the flow is the slowest (around 0.2 ms^{-1}, equivalent to 57% of the bulk velocity). In the tile conditions, the fish did not spend significantly different amounts of time above the tiles, on the side of the tiles, in the large protrusions, in the small protrusions or in the open channel when comparing T1 and T3, showing that shoaling did not have an impact on area selection. Larger fish, however, were less likely to spend time in the small protrusions than smaller fish (GLM, $p = 0.006$).

In treatment T1, the sticklebacks spent more time in and around the tiles than they did in the open channel (GLM, $p < 0.0001$). More specifically, more time was spent in the small protrusions than in the open channel, tile side and above tiles areas (GLM, $p < 0.002$) but not significantly different than in the large protrusions (GLM, $p > 0.8$). More time was spent amongst the large protrusions compared to any other area with the exception of the small protrusions (GLM, $p < 0.004$). The areas above the tiles and on the side of the tiles were used more than the open channel when summed (GLM $p = 0.02$) but not significantly if considered individually (GLM, $p > 0.05$). Similar results can be seen in treatment T3, the fish spent more time cumulatively in and around the tiles compared to the open channel (GLM, $p < 0.0001$). The time spent in the small and large protrusions individually was greater than for the open channel for both (GLM, $p < 0.0002$) but the tile side and above tiles areas did not have a significantly different amount of time to the open channel (GLM, $p > 0.5$). The time spent in the small protrusions was also significantly more than the time spent in the above tile and tile side areas (GLM, $p < 0.002$) but not different compared to

the large protrusions (GLM, p = 0.87). More time was also spent in the large protrusions than in the above tile and tile side areas (GLM, p < 0.001) but there was no difference in time spent between the above tile and side tile areas (GLM, p = 0.2).

5.3.2 Shoaling behaviour

Overall, there was no significant difference in the total time spent shoaling between the control C3 (32% of time) and tile T3 conditions (21% of time; GLM, p = 0.3), there was also no correlation with fish length (GLM, p = 0.42). There were no differences in the time spent in shoals of 2 fish or shoals of 3 fish between the two shoaling treatments (GLM, p > 0.18). In treatment T3, the focal fish spent significantly more time alone (not shoaling) than in shoals of 2 or 3 fish (GLM, p < 0.0001), and significantly more time in a shoal of 2 compared to shoal of 3 fish (GLM, p = 0.02). In treatment C3, the fish spent less time shoaling than either in shoals of 2 or 3 fish (GLM, p < 0.0001), but there was no significant difference between the time spent in shoals of 2 or 3 fish (GLM, p = 0.18). For treatment T3, we also analysed shoaling time per area; fish shoaled most in the area with small protrusions, this area was significantly different to all other areas (GLM, p < 0.004) except for the large protrusion area (GLM, p = 0.09).
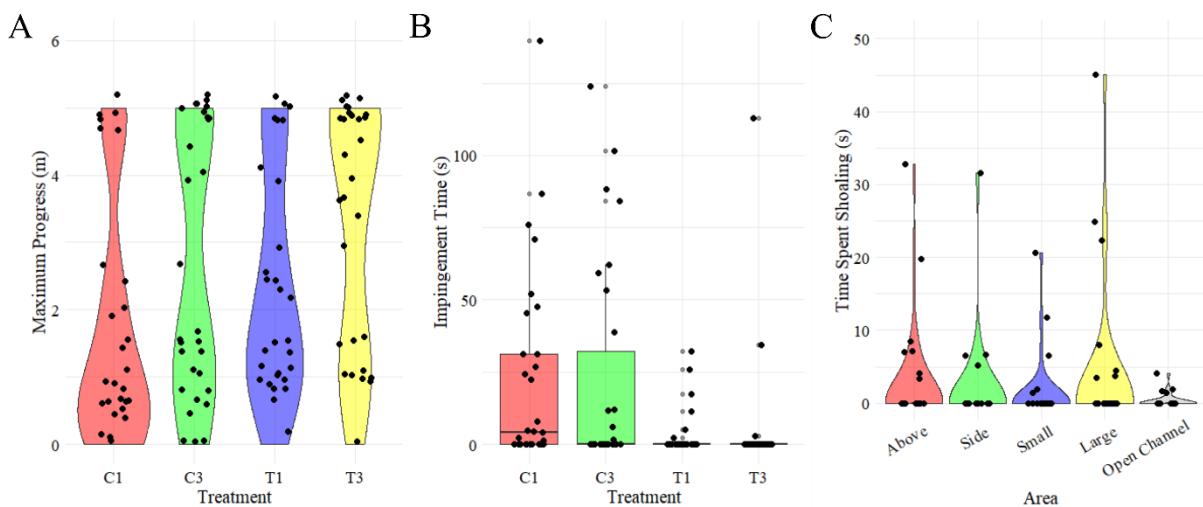
Figure 5.3. (A) Maximum distance from the downstream end of the flume reached by the focal fish, past five metres a fish was considered to have passed upstream as the tiles ended there. (B) Total impingement time data for each fish. Boxes represent interquartile range and whiskers represent the 95% range. (C) The amount of time spent in the company of at least one other fish by area. This is exclusively for the shoaling conditions with the tiles.

117

5.4 Discussion

The passage success of three spined sticklebacks was positively affected by the presence of shoalmates, sticklebacks achieved the highest number of upstream passes when shoaling and in the presence of tiles. Behavioural data suggest that the effects of the tiles may be greater than is evident from the passage data.

The sticklebacks impinged less with the tiles which may explain why the tiles did not appear to have a greater positive impact on passage. If a fish was impinged during this experiment after attempting to swim, it indicated the fish was unable to carry on swimming and therefore exhausted; in the control conditions most fish either passed or impinged within the 10 minute experimental period. In contrast, with the tiles fish commonly spent the entire time in the tiles and were not exhausted by the end of the experiment. The tiles also allowed the fish to rest among the small protrusions at any distance from the downstream end (therefore conserving any progress made at the time of resting) so given a long timeframe, it is likely that the sticklebacks would be able to eventually pass upstream. Overall, this suggests that the current study underestimates the potential for stickleback passage using the tiles while representing the passage under control conditions fairly, similar to findings by previous studies on the tiles (Chapter 4). Migratory morphs of this species with higher swimming capacities (Tudorache et al, 2007), may have increased and faster passage. The ability for fish to rest anywhere on the tiles not only allows them to maintain progress already made without being swept downstream but it also means that the resting fish will be more evenly distributed, decreasing the likelihood of many fish resting in one place, thus creating a focal predation opportunity (Jepsen et al., 2010). The increased ability to rest within the tiles and the decrease in impingement also point to a probable decrease in energy expenditure, increasing the chances for the fish to be productive once they have passed. Sticklebacks are naturally found in highly vegetated areas with slow flows and many refugia (Arai et al., 2020; NatureServe, 2019), a bare culvert provides none of these and is therefore much less attractive to a stickleback so not only are the fish less likely to succeed in passing a velocity barrier, they might also not attempt to do so in the first place. The tiles provide cover, resting areas and refugia so the sticklebacks are more likely to use them and pass upstream, but this is unlikely to create new permanent habitat for them unless the unmaintained tiles cause sedimentation and there is food availability. In the current study, the sticklebacks were released directly into the flume and they had no choice regarding the terrain so the comparative performance of the tiles is potentially further underestimated here.

The tiles also have the potential to help sticklebacks by modifying the flow dynamics below the protrusions and around the tiles. Clearly flow reduction is advantageous and here the tiles work well in two ways; they accommodate areas where the fish can station hold and rest and at the same time provide areas of slightly faster (but still reduced) flow for the sticklebacks to progress upstream. The large scale turbulence recorded above and on the side of the tiles did not seem to affect the stability of stickleback swimming, evidenced by the low number of spills in these areas. This is probably due to the turbulent lengthscale being too large and rarefied to affect the fish. Fish can be destabilised by vortices in the range of 0.75 or larger body lengths (Muhawenimana et al., 2019; Tritico & Cotel, 2010) and the large scale turbulence of the current study falls outside these parameters. However, the vortices shed by the large protrusions are within range for spills to occur. Most spills did occur within the large protrusions as the sticklebacks often held station behind a protrusion and the chance of spilling decreased with increasing fish size. This is a potential drawback of the tiles as increased spilling produced a decreased likelihood of passage but this may be a result of the fact that fish that passed quickly spent less time in the tiles and therefore had reduced chances of spilling. The fish still showed the ability to make progress in the large protrusions despite the destabilisations but more commonly would use this area to hold station and then move to the side of the tile or above the tile to swim further upstream. This contrasts with the control conditions where the fish rarely swam for the 10 minutes of the experiment, either passing upstream before that or in most cases, impinging on the flow straightener. This indicates that the flow conditions were on the limit of the swimming performance of these fish. Despite the flume having the potential to constrain the sticklebacks and forcing them closer to each other so that they may be considered to be shoaling, the flume was wide compared to the fish size and the shoaling statistics show that much of the time the sticklebacks did not shoal.

Shoaling had a significant effect on fish behaviour and sticklebacks were more likely to pass if they had shoalmates. There are multiple potential explanations for why the presence of two shoalmates helped performance; firstly, sticklebacks are a naturally shoaling fish and this behaviour is associated with reduced energy expenditure (Johansen et al., 2010), isolated sticklebacks lose this advantage and may potentially experience stress as a result of not being in a shoal. In the wild, stickleback shoals are usually larger (Barber & Ruxton, 2000; Mehlis et al., 2015) than used in the current experiment so we would expect the effects observed here with just three fish per shoal to be even more marked. Sticklebacks can tell

the difference between shoals of different sizes and always choose the larger group (Mehlis et al., 2015). Shoaling provides more social interactions (Cushing & Jones, 1968) reduces predation risk and increases foraging opportunities (Mayer, 2010). When subjected to flow, however, fish shoal more closely (de Bie et al., 2020) and when migrating shoal sizes are at their largest (Mayer, 2010). A combination of these mechanisms is the likely cause of the increased success of the stickleback shoals in this experiment but the hydrodynamic benefit is the most obvious and direct explanation in this case. It must also be considered that the sticklebacks did not shoal all the time they were in the flume and spent more time alone. This may be explained by several factors. Firstly, the flow conditions were not suited to shoaling as in the control condition bulk velocity was at the limit of the stickleback capability which would eventually separate fish with different swimming abilities. With the tiles there was more turbulence to destabilise the fish, making coordinated swimming harder as constant position adjustments can increase energy expenditure (Johansen et al., 2010). The spacing of the protrusions of the tiles also made shoaling harder as fish could not easily fit close to each other and may have also lost sight of each other among the tiles. This suggests that although there may be a hydrodynamic benefit to shoaling, the presence of other shoalmates is likely affecting the motivation of the sticklebacks in other ways that increase their likelihood of successfully passing upstream. The sticklebacks were wild caught and despite being visually checked for disease the fish may have had cryptic infections. This is relevant since infection can cause decreased swimming performance (Stewart et al., 2018) and reduced shoaling (Rahn et al., 2015; Ward et al., 2005). The degree to which the sticklebacks in this study were familiar to each other is unclear, they were caught in the same location and housed in the same tank but the shoals were not given time alone to familiarise and this can impact shoaling (Barber & Ruxton, 2000). In considering all these factors, it is still evident from this study that shoaling aided passage; the mechanism is uncertain but likely a combination of the hydrodynamic and social benefits.

For the tiles to have the desired effect of reconnecting fish populations and habitats, they need to benefit multiple species and different sizes of fish. These tiles can be effective for eels (Chapter 4) and potentially sticklebacks, two species with diverse morphologies, swimming dynamics, and passage requirements, indicating that they have the potential to help more species, especially fish small enough to fit within the protrusions or that can exploit the low velocities surrounding the tiles. The tiles also have the advantage of being cheap to purchase, easy to install and importantly, do not affect the whole channel. The tiles

need only cover part of the channel near the bank and do not affect the rest of the channel, leaving it to flow freely and allow high performance swimmers like salmonids that may not require the tiles to continue their journey undisturbed.

5.5 Conclusion

Eel tiles show promise as passage solutions for three-spined sticklebacks by providing decreased flow velocities, refugia and resting opportunities. The presence of other sticklebacks in the flume was the factor with the largest effect on passage however harsh flow conditions can break up shoals. By being effective for multiple species, the tiles have the potential to reconnect habitats at high velocity barriers and by modifying the flow around them potentially help other species pass too. This chapter built on chapters 3 and 4 by introducing shoaling as a factor and confirmed some of the benefits of and behavioural modifications produced by shoaling whilst evaluating eel tiles as a passage solution with potential to help non-target species meeting objectives 1, 2, and 3.

Chapter 6. Shoaling dynamics of the Three-Spined Stickleback (*Gasterosteus aculeatus*)

Conceptualisation and methodology by Prof. Jo Cable, Prof. Catherine Wilson, and Guglielmo Sonnino Sorisio. Data collection by Guglielmo Sonnino Sorisio. Data processing by Guglielmo Sonnino Sorisio and Joseph Johnson. Analysis, visualisation, and writing by Guglielmo Sonnino Sorisio and editing by all of the above.

Summary

The energetic and hydrodynamic advantages of fish swimming in shoals are an established but not fully understood phenomenon, particularly for labriform fish that swim primarily with their pectoral fins. The three-spined stickleback is a common freshwater fish in the global north and exists in both diadromous and resident populations. Sticklebacks are well known for their shoaling abilities but their shoaling dynamics in moving flow have not been studied. Shoals and individual sticklebacks were allowed to swim in an experimental open channel recirculating flume under four increasing bulk velocities. The trials were filmed and shoaling behaviour and kinematics analysed for groups of 1 to 5 fish to evaluate behaviour and swimming effort. Shoaling significantly reduced the fin-beat frequency of the sticklebacks by between 24.4% and 34%, which was significantly enhanced with increasing flow velocity and shoal size. The fin beat was also less powerful for fish swimming in shoals, potentially providing further energy savings. There were no fixed patterns of shoaling and fish in shoals were often disorganised and frequently changed positions. The leading fish in the shoal displayed almost the same reduction in swimming effort as the following fish. Shoaling reduced swimming effort but the exact hydrodynamic mechanisms through which this occurs are still unclear.

6.1 Introduction

Shoaling is a key behavioural aspect of most fresh and saltwater fish species and can serve a multitude of purposes depending on species, environmental factors, and pressures faced by the population (Cushing and Jones, 1968; Mayer, 2010; Ligman et al., 2024). The primary functions of shoaling are thought to be varied. Predator avoidance (Cushing and Jones, 1968; Mayer 2010), in response to predation from birds, shoal sizes and cohesiveness increases

(Tien et al., 2004; Seppälä et al., 2008; Mayer, 2010), decreasing predation (Enstipp et al., 2007). Increased foraging success (Cushing and Jones, 1968; Larsson, 2012), social interaction, and mating (Cushing and Jones, 1968; Barber and Ruxton, 2000) are also primary drivers of shoaling. When fish encounter long swimming distances, migrations, or flowing water however, it becomes necessary to swim expending the least amount of energy possible, and shoaling allows fish to draw hydrodynamic benefit from neighbouring fish (Johansen et al., 2010; Ligman et al., 2024; Wei et al., 2023; Weihs, 1973; Zhang & Lauder, 2024). In a changing environment faced with disrupted migrations and habitat fragmentation (Belletti et al., 2020; Jones et al., 2019) through which efforts are made to improve connectivity by introducing fish passage facilities, knowledge of fish swimming dynamics is essential. Shoaling is a major modifier of swimming behaviour and capabilities (Weihs, 1973; Barber and Ruxton, 2000; Tien et al., 2004; Mayer, 2010; Ardekani et al., 2013; Ligman et al., 2024) and therefore needs to be understood for a wide range of species and situations.

The hydrodynamic advantages of shoaling are well established. A benefit can be gained from a single shoalmate (Thandiackal and Lauder, 2023) or from multiple shoaling fish (Johansen et al., 2010; Ligman et al., 2024). Estimates have shown that shoaling fish can swim 20% faster than an individual using the same amount of energy for fish swimming in a rectangular school (Daghooghi and Borazjani, 2015). Shoaling in Giant danio (*Devario aequipinnatus*) lowers the cost of transport by up to 53% (Zhang & Lauder, 2024), and in Bluegill (*Lepomis macrochirus*) lowers the metabolic rate (Currier et al., 2021). In Grey mullet (*Mugil cephalus*) every shoal member, including the leader, energetically benefits from shoaling, with the followers gaining the most (Marras et al., 2015). Energetic savings were greatest at low speeds for the Grey mullet (Marras et al., 2015), and similar energy savings have been found in striped surfperch *(Embiotoca lateralis*) fish behind the leader of the shoal (Johansen et al., 2010). Energetic advantages occur both in flowing water (Marras et al., 2015) but also in open water with no flow (Ligman et al., 2024). The mechanisms through which energetic gains are made for small and large shoals have been investigated numerically and experimentally, but hypotheses differ over the specific mechanism or range of mechanisms for fish primarily propelling themselves with oscillatory motion of the body and caudal fin. The most common explanation is that fish exploit the vortices shed by fish in front by utilising the Karman or reverse Karman street and adapting their swimming gait to propel themselves forwards (Weihs, 1973; Liao et al., 2003; Harvey et al., 2022; Ren et al., 2023).

Diamond shaped shoals with staggered fish allow the vortex street to be exploited in a shoal as well as reducing drag (Deng and Shao 2006) but other studies have found that wakes are too disorganised (Daghooghi and Borazjani, 2015; Wei et al., 2023) and fish rarely swim in exactly the same depth in the water column (Partridge and Pitcher, 1979), casting doubts over the vortex hypothesis. Another potential mechanism for the hydrodynamic benefits of shoaling is the channelling effect (Weihs, 1973; Daghooghi and Borazjani, 2015) driven by a decrease in drag (and therefore thrust required) due to fish swimming at close distance. Information transfer is also an important aspect of shoaling for some species like the red nose tetra fish, where synchronisation of shoaling pairs creates beneficial shoaling conditions (Ashraf et al, 2016).

The Three-spined stickleback (*Gasterosteus aculeatus*), however, is known to be a labriform swimmer, using the pectoral fins for thrust generation, unlike most other fish for which shoaling has been studied. The three-spined stickleback is found in coastal and freshwater of the global north (NatureServe, 2019). They can exist in anadromous and river resident populations for which morphologies differ (Blake et al., 2005; Dalziel et al., 2012; Reyes and Baker, 2016). Sticklebacks prefer to live in densely vegetated aquatic environments away from fast flows (Gagnon et al., 2019; Arai et al., 2020) and are well known to live in large shoals (Mehlis et al., 2015; NatureServe, 2019). The shoaling behaviour and global distribution of sticklebacks have led to their extensive use in studies on evolution and adaptation (Scharsack et al., 2012), as well as research on the effects of external factors on shoaling (Stewart et al., 2018) and their potential use as a sentinel species (Pottinger et al., 2002). Sticklebacks prefer to shoal with familiar fish (Barber and Ruxton, 2000) and with uninfected fish (Rahn et al., 2015) but will generally shoal in as large a shoal as possible (Mehlis et al., 2015).

Swimming endurance and performance is generally higher for migratory populations (Tudorache et al., 2007) with critical swimming speed of 8.5 BL/s (body lengths per second) compared to 7 BL/s (Tudorache et al., 2007; Dalziel et al., 2012; Reyes and Baker, 2016) and anadromous sticklebacks fatiguing significantly later at 5 BL/s but having lower maximum swimming speeds than resident fish with a difference of 0.23 m/s (Taylor and McPhail, 1986). Parasitic infections, however, reduce swimming performance (Stewart et al., 2018) as well as external factors like temperature (Clough et al., 2004).

Labriform propulsion is characterised by the usage of the pectoral fin, rather than the more commonly used caudal fin. But even within labriform fish there are several different ways to engage the pectoral fins for propulsion. An up-and-down motion of a flexible fin oriented with the largest surface facing vertically generates lift based propulsion due to the structural flexibility of the fin (Shoele and Zhu, 2009) while a back and forth rowing motion is a drag based model of generating thrust (Blake, 1981). In each case, the flexibility of the fin is fundamental in generating thrust as even in the drag based rowing fin beat, the recovery stroke during with the pectoral fin is brought upstream in preparation for the next power stroke requires the flexible fin to bend to prevent the generation of backwards thrust (Shoele and Zhu, 2010). Each beat of the pectoral fin can produce different types of wake depending on morphology and activation patterns. Surfperch produce two distinct ventrally linked vortex rings at all swimming speeds but with the vortex rings being oriented more directly downstream at higher velocities (Drucker and Lauder, 2000). Bluegill sunfish, however, only produce one vortex ring at low speeds and only produce two at higher swimming speeds but notably, Surfperch have twice the maximum swimming speed as Bluegill sunfish (Drucker and Lauder, 2000). Few studies have considered the shoaling dynamics of any labriform fish but Johansen et al. (2010) found that the trailing members of a shoal of Striped surfperch had a 14.9% reduction in fin-beat frequency (FBF) and 25.6% reduction in oxygen consumption compared to the shoal leader.

Labriform shoaling remains a knowledge gap, particularly considering the large differences in how the pectoral fins are positioned, shaped, and used in labriform fish species. The three-spined stickleback is an extensively studied fish and is known for its shoaling abilities but the shoaling of this labriform fish in the presence of flow has not been studied. Knowledge of the sticklebacks shoaling dynamics could not only enrich the body of knowledge on how hydrodynamic benefit is produced by shoaling but also improve the ability to adequately design passage solutions for weak swimmers such as sticklebacks. This study seeks to estimate the reduction in cost of transport (if any) brought by the presence of shoalmates compared to an individual fish. The hypotheses tested here are that shoaling in sticklebacks (as labriform fish) reduces swimming effort, that shoal size can increase this effect, that fish leading the shoal also benefit from shoaling, and that the labriform gait could me modified by the presence of shoalmates. The kinematics of stickleback swimming, alone and in a shoal are also examined to find the underlying mechanics of stickleback swimming. To achieve this, three-spined sticklebacks were allowed to swim in a recirculating open channel

flume alone, or in a shoal of 5 fish at 4 different bulk velocities for which the fish remained primarily labriform.

6.2 Methods

6.2.1 Fish origin and maintenance

Three-spined sticklebacks (*Gasterosteus aculeatus,* N=150) were collected with hand nets from St Fagans ponds (pond water at 14°C), Cardiff, UK (Grid Reference: 51.487426, -3.270094) on the 13/03/2022 and transported to Cardiff School of Biosciences. Upon arrival, the fish were measured for standard length with calipers sorted into 20 size-matched shoals of 5 fish each. Each shoal was individually housed in a 300 mm long, 150 mm wide and 150 mm tall tank within a rack system, and the control fish were housed in the same tanks but not in shoals. All fish were kept at 16°C on a 12 h: 12 h light:dark cycle in dechlorinated water and fed thawed bloodworm daily, each tank was water changed once every 48 h. After an initial 24 h of acclimation, a subsample of 10 sticklebacks was anaesthetised with MS-222 and screened for external parasites with a microscope. The screening revealed that all fish were infected with an unspecified *Gyrodactylus* species and all the fish were therefore treated with two rounds or Praziquantel to remove these infections. After the treatment, sticklebacks were re-screened to confirm all the fish had successfully cleared their infections. On completion of the 14 days of acclimation, the trials were initiated. For testing, between 10 and 25 fish were transported to the School of Engineering and kept in temporary tanks with dechlorinated water. Every stickleback was tested in all four experimental flow conditions but always given at least 48 hour recovery period between tests. Tests were performed in a random order. After the conclusion of the flume trials, all the fish were measured for standard length, total length, and mass and their pectoral and caudal fins were measured at their base, their trailing edge and their length using calipers (±0.1 mm) for detailed measurement averages, see Table 6.1.

Table 6.1. Measurements of the sticklebacks used in this study. The measurements of the fish are given as the mean±SE and the sample size is given in the column to the right of the values. Some fish are missing from the measurements due to having damaged fins in the control (single fish) and in shoals. Fin area is calculated with the assumption that the fin is trapezium shaped.

Variable	Control Fish	Control Fish (N)	Shoal Fish	Shoal Fish (N)
Standard Length (mm)	38.6±0.9	20	38.6±0.6	95
Total Length (mm)	42.5±2.2	20	45.3±0.7	95
Mass (g)	0.836±0.052	20	0.910±0.044	95
Pectoral Fin Base (mm)	2.9±0.1	18	2.9±0.0	95
Pectoral Fin Edge (mm)	7.4±0.3	18	7.0±0.2	95
Pectoral Fin Length (mm)	5.9±0.1	18	5.7±0.1	95
Pectoral Fin Area (mm^2)	30.7±1.5	18	29.3±1.2	95
Caudal Fin Base (mm)	2.8±0.1	19	3.0±0.1	95
Caudal Fin Edge (mm)	9.3±0.5	19	9.5±0.2	95
Caudal Fin Length (mm)	5.4±0.2	19	5.2±0.1	95
Caudal Fin Area (mm^2)	32.4±1.8	19	33.6±1.3	95
Caudal Peduncle (mm)	1.6±0.1	19	1.5±0.0	95

6.2.2 Experimental setup and procedure

A recirculating flume in the hydraulics laboratory at the Cardiff School of Engineering was used in this experiment. This flume is 10 m long, 0.3 m wide, and 0.3 m deep with a 1/1000 bed slope. The working section started 6 m from the upstream end of the flume and was 0.6 m long, 0.3 m wide and 0.23 m deep. It was bounded by a flow straightener upstream and a flow straightener covered by plastic mesh downstream to prevent the fish from coming into contact with the sharp flow straightener which might cause abrasions if the fish become impinged on it. The flume water was maintained at 16 ± 1 °C with a D-D Aquarium Solution DC 2200 cooler and was dechlorinated with Prime Dechlorinator. On the bed of the working section a white PVC sheet was placed to increase the contrast of the fish being filmed from above. The flume was lit by two neutral white lights positioned either side of the flume and illuminated the fish through the glass walls of the flume as overhead lighting which was maintained constant throughout the duration of the experiment. The working section was covered by a plexiglass sheet to avoid image distortion, the plexiglass was supported from above to minimise its impact on the flow. The experiments were recorded from above with

a Baumer VLXT-50M.I camera with Kowa LM8JC10M 8.5cm lens which recorded the entire length of the experiment at 80 frames per second (fps) to analyse behaviour and track each fish's trajectory. A subsample of experiments was also recorded from the side through the glass flume wall by the same camera setup. All videos were recorded through Streampix software and stored in an external hard drive.

The experimental flow conditions were established using a pointer gauge with a vernier scale and fine-tuned by changing the flowrate and downstream tailgate weir until there was constant flow depth along the flume's length. For all conditions, flow depth was kept constant at 0.23 m and the bulk velocities chosen were 0.1, 0.15, 0.19, and 0.23 ms^{-1} to represent a full range of moving flow conditions for which the sticklebacks did not engage their caudal fin for propulsion. All treatments are shown in Table 6.2.

Table 6.2. The treatments and flow conditions tested in this study. The treatments are named such that C represents the control conditions with a single fish and S means shoal (of 5 fish). The number following the letter in the treatment names represents the bulk velocity in ms^{-1}. For each treatment 20 repeats were performed using the same fish between each treatment. The bulk velocity was varied whilst the flow depth was kept constant by adjusting flowrate and the weir at the downstream end of the flume.

Treatment	Number of Fish	Flowrate, Q (Ls^{-1})	Bulk Velocity, U (ms^{-1})	Flow depth, H (m)	Flume Re (-)
C-0.1	1	6.9	0.10	0.23	8620
S-0.1	5	6.9	0.10	0.23	8620
C-0.15	1	10.3	0.15	0.23	12,929
S-0.15	5	10.3	0.15	0.23	12,929
C-0.19	1	13	0.19	0.23	16,377
S-0.19	5	13	0.19	0.23	16,377
C-0.23	1	17	0.23	0.23	21,549
S-0.23	5	17	0.23	0.23	21,549

Fish were placed in the flume at the downstream end and allowed to acclimate for 10 minutes, the first 2.5 minutes at a bulk velocity of 0.1 ms^{-1}, the following 2.5 minutes at 0.15 ms^{-1} and final 5 minutes at the test bulk velocity before the experimental period of 10 minutes where the fish are recorded. In the cases of treatments with bulk velocities of 0.1 and 0.15 ms^{-1}, the bulk velocity was not increased during the acclimation after the test velocity was reached. On completion of the 10 minute acclimation, the recording was

started. After the tests the sticklebacks were removed and visually inspected for any external lesions. The treatment order was randomised for each individual and shoal.

6.2.3 Hydrodynamics

To quantify the flow velocity in the test section, Particle Image Velocimetry (PIV) was carried out. A Baumer VLXT-50M.I with a Kowa LM8JC10M 8.5cm lens was mounted perpendicular to a thin laser sheet 400 mm wide generated by a Polytec BVS – II Wotan Flash stroboscope at 15% intensity triggered through a STEMMER IMAGING CVX Triggerbox by a Rigol 1032Z wave generator that also triggered the camera to record at 120 Hz. The flow was seeded with AXALTA Talisman 30 White 110 particles. The images were analysed in PIVlab 3.02 in Matlab R2024a (Thielicke and Stamhuis 2010; Thielicke and Sonntag 2021; The MathWorks Inc. 2024). The flow velocity varied from the bed to the water surface and from the wall to the centre of the channel as shown for each treatment in Figure 6.1.
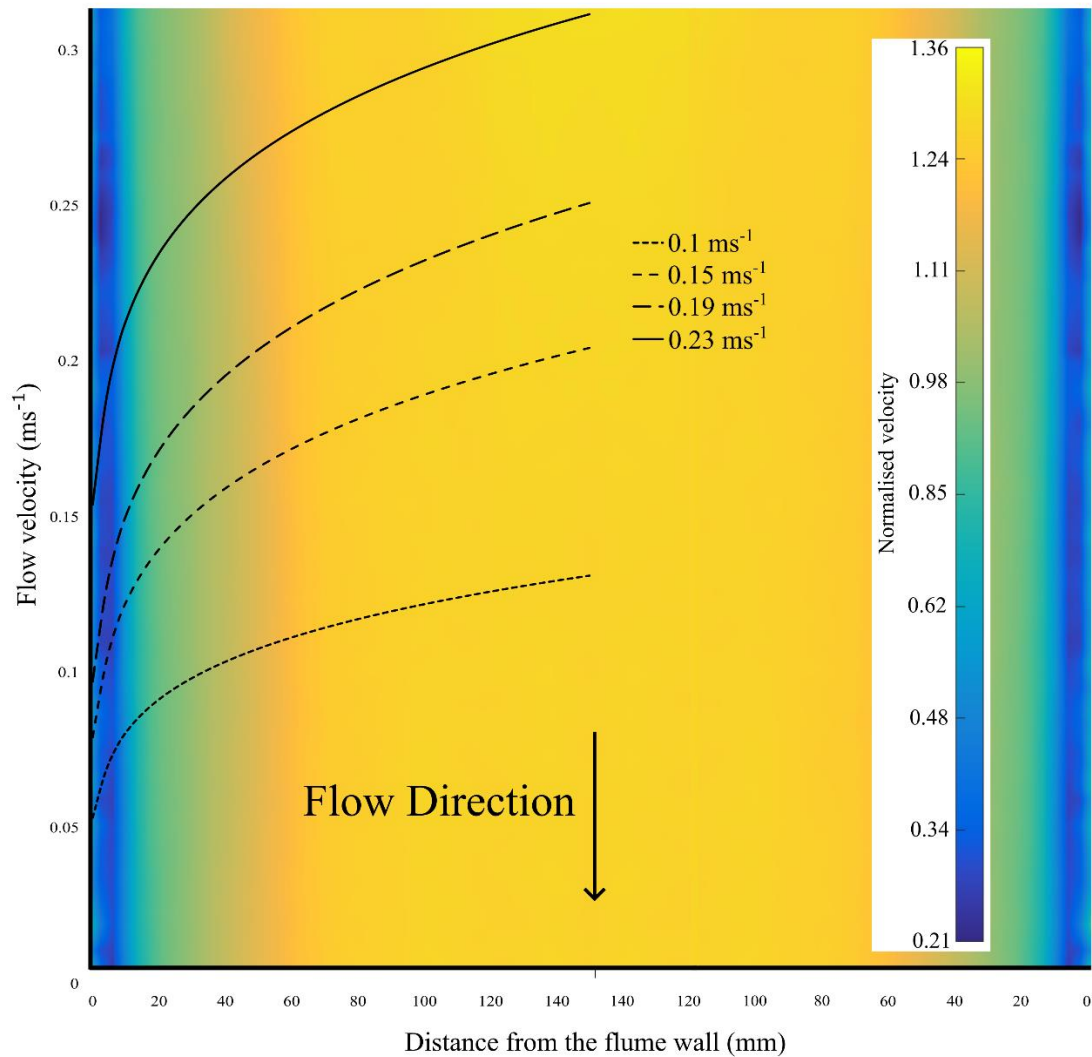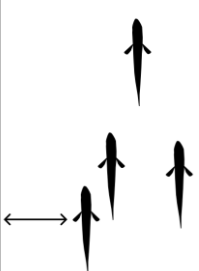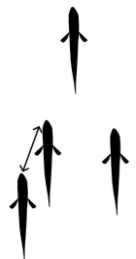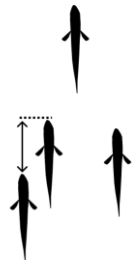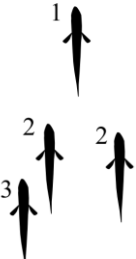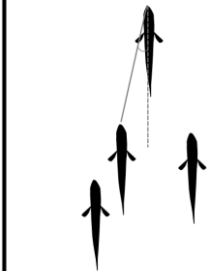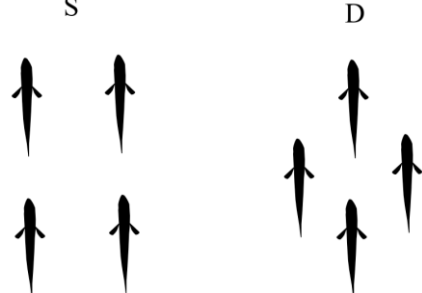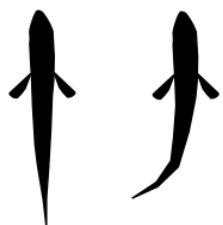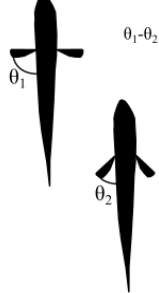
Figure 6.1. Particle Image Velocimetry plot of the top view hydrodynamics of the flow in the flume. The colour plot depicts the variation of the velocity at mid flow depth throughout the flume. Each velocity profile plotted on the left hand side represents the velocity profile for each flow condition tested and is denominated in the key with the bulk velocity of the condition.

6.2.4 Analysis

From all video footage of the trials, videos were extracted where the fish swam constantly and held station against the flow. For the shoaling treatments, videos were extracted of the fish shoaling as shoals of 2, 3, 4, and 5 fish for each shoal. For all clips of fish swimming, several values were extracted listed in Table 6.3 using Kinovea (Charmant 2022). The results were tabulated and for each case the flow velocity experienced by the fish was calculated by finding the flow velocity at the same distance to the wall as the fish from the PIV data.

Table 6.3. Variables calculated with the kinematic analysis with descriptions and schematics. For all parameters where shoaling was analysed, an NA was recorded for the control fish.

Variable	Description	Diagram
Distance from the wall	Distance of individual fish from the nearest flume wall (m).	
Distance to leader	Distance of individual fish from the shoal leader (m). The leader was noted as NA.	
Nearest neighbour distance (NND)	Distance of each fish from its nearest neighbour (m).	
Distance to fish in front	Distance of each fish to the fish directly in front (m). The leader was noted as NA.	
Position in shoal	The row each fish occupied within the shoal. A fish was considered behind another when the tip of the head was behind the pectoral fins of another fish (-).	

Angle to fish in front	The angle of a fish from the fish in front (°). The leader was noted as NA.	
Formation	The arrangement of the fish in a shoal simplified as either square (fish directly behind one another) or diamond (fish are staggered). (-)	
Caudal fin engagement	For each fish a binary response was recorded regarding the use of the caudal fin to correct trajectory or for propulsion. (-)	
Fin-beat frequency (FBF)	The frequency with which the fish beat the pectoral fins (Hz).	
Fin-beat cycle analysis	The angular position of the pectoral fins was tracked throughout the power and recovery strokes and angular acceleration calculated from these angles.	
Fin-beat phase synchronisation	The phase difference between fin-beats of shoalmates (°).	

The statistical analyses were performed in Rstudio with R Version 4.2.2 (R Core Team, 2022). As the same fish and shoals were used more than once, pseudo-replication was accounted for by using generalised linear mixed models (GLMMs) and inserting the fish or shoal ID as a random effect. The lme4, nlme, and lmertest packages were used to perform Gaussian and Gamma GLMMs (Bates et al., 2015; Kuznetsova et al., 2017; Pinheiro et al., 2020). Different GLMMs were considered for each set of variables and compared by the residual distributions. Time and order of the tests was included in most models to account for different experimental days and times. For all tested combinations, the Gaussian GLMMs had the best residual distributions and were therefore selected. To perform hierarchical cluster analysis with Euclidian distance on the shoaling data hclust package was used and for principal component analysis the prcomp package was utilised. The ggplot2 package was used to visualise the data (Wilkinson, 2011).

6.2.5 Animal ethics statement

All work was approved by the Cardiff University Animal Ethics Committee and conducted under UK Home Office licence PP8167141.

6.3 Results

6.3.1 Stickleback swimming characteristics

All sticklebacks primarily swam in the labriform mode, using only their pectoral fins for propulsion and occasionally engaging their caudal fin to perform corrections. The two main phases of the labriform fin beat are characterised as the power stroke, where the thrust is generated by moving the pectoral fin backwards, and the recovery stroke, where the pectoral fin is first re-oriented to show a smaller area to the flow (and therefore avoid generating thrust against the direction of motion) before being brought forwards ready for a new power stroke, these steps are outlined in Figure 6.2. Both pectoral fins are synchronized, with no phase difference and activated simultaneously.
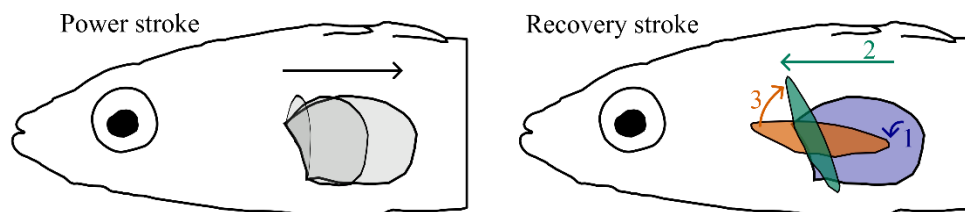
Figure 6.2. Side view diagram showing the power and recovery stroke in a three-spined stickleback that make up one complete fin beat. In the power stroke, the fin is brought back

from an angle around 90 degrees from the body to being in contact and aligned with the body. In the recovery stroke, the pectoral fin is first turned sideways (step 1), then brought forward (step 2), and finally brought upright (step 3).

The fish also adapted the position of their dorsal, anal, and caudal fins. Two main modes are outlined in Figure 6.3. Figure 6.3A shows the dorsal, anal, and caudal fins fully open and this posture was used whenever maneuvering or making corrections. However, when swimming steadily without the need to make corrections, the sticklebacks assumed the position in Figure 6.3B, where the dorsal, anal, and caudal fins are kept closed and remain unused during these phases of swimming. The caudal fin was also kept slightly raised upwards in this low-drag swimming configuration.
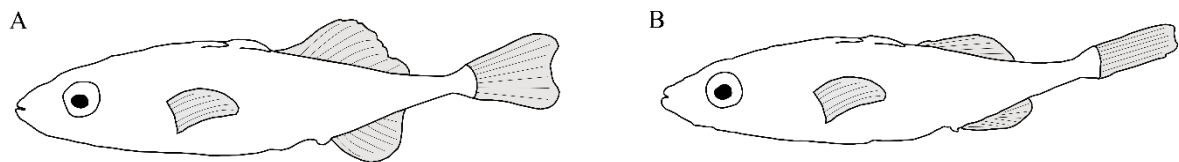
Figure 6.3. Side view diagrams showing a three-spined stickleback in two different swimming configurations. Both are line diagrams overlayed directly from side view images from the swimming tests. In A, the dorsal, anal, and caudal fin are kept fully open and in B these fins are closed and the caudal fin is tilted upwards and this position was typically adopted when swimming steadily.

The sticklebacks generally preferred to swim near the wall where the velocities were lowest for all flow conditions as shown in Figure 6.4. With increasing discharge, the fish increasingly swam near the wall (plots on the right in Figure 6.4) to avoid high velocities present at higher discharges. Interestingly, for all histograms one of the less frequented areas occurs not at the flume centre but at around 100 mm from the flume wall. During the tests, the fish varied widely in the occupation of the water column.
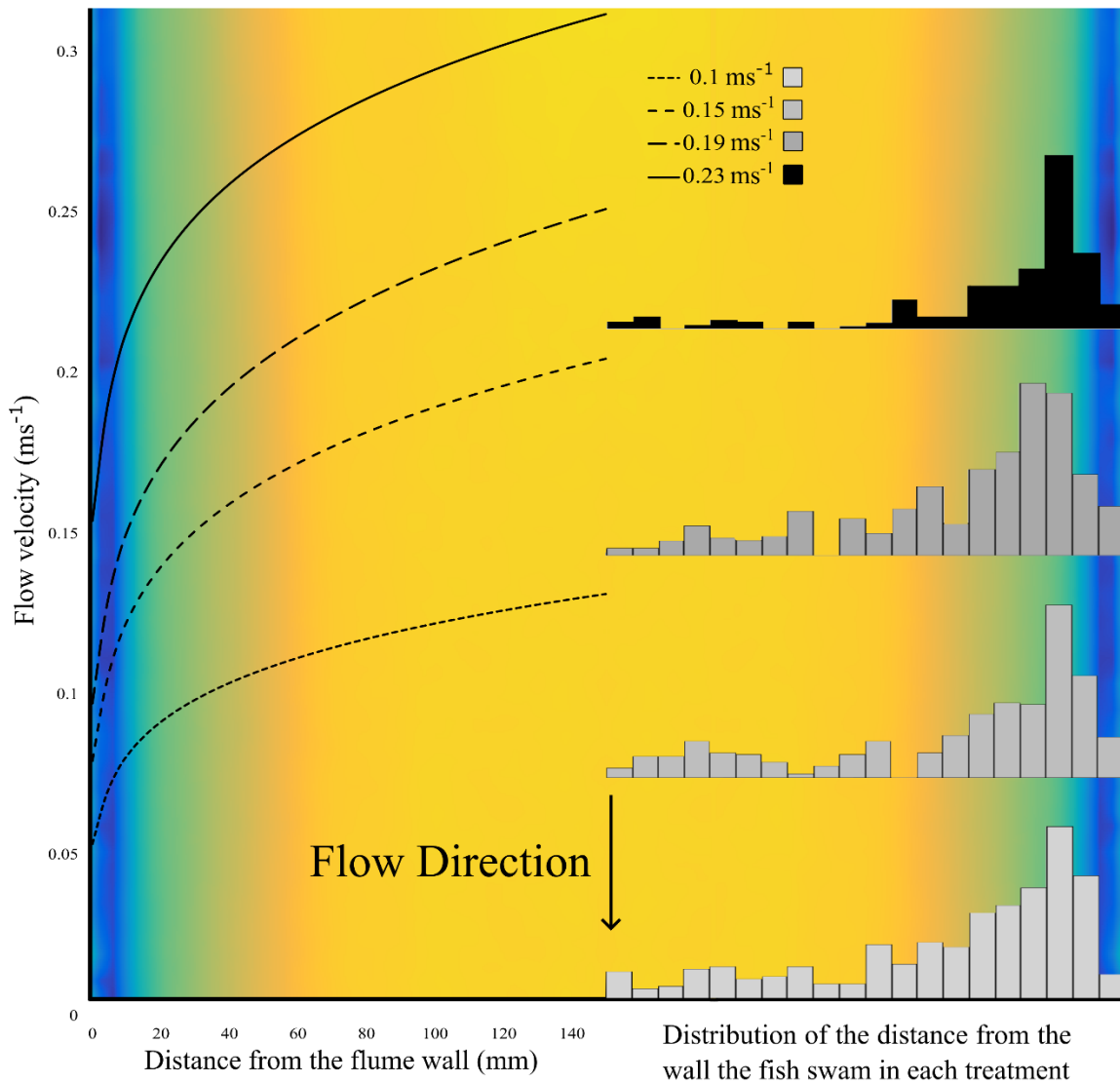
Figure 6.4. On the left, flow velocity distributions for all flow conditions at mid flow depth. On the right, scaled distribution of where fish chose to swim (time spent) for each flow condition from the middle of the channel to the wall. Treatments of individuals and shoals are combined by flow condition for the histogram data. The distance from the wall for all fish was calculated to the nearest wall and the data from both sides combined. The velocity distributions on the left were used to find the flow velocity each stickleback was swimming.

6.3.2 Shoaling parameters

The sticklebacks overwhelmingly shoaled in a staggered (or diamond) formation, although this tendency decreased with increasing flow velocity where a square formation was more widely adopted but never the predominant formation (Figure 6.5B; GLMM, p=0.002). However, the fish rarely shoaled in a perfect square or diamond, rather the positioning was dynamic, and varied throughout each trial. The mean nearest neighbour distance was 38 mm

(or around one body length) and did not vary significantly between treatments or flow velocity (GLMM, p>0.81). The distance to the fish in front similarly, did not vary significantly with velocity (GLMM, p=0.29). Similar to the shoaling formation being dynamic, the number of fish in a shoal varied throughout the trials. The use of the caudal fin increased with flow velocity as fish made more corrections and occasionally used the caudal fin for propulsion in short bursts (GLMM, p=2e-16). When shoaling however, there was a significant increase in caudal fin engagement over the single fish controls in all flow conditions (Figure 6.5A; GLMM, p<0.0019). The caudal fin engagement was also significantly higher for fish shoaling in a square formation (GLMM, p=0.008), potentially linked to the higher usage of the square formation at higher streamwise velocities.
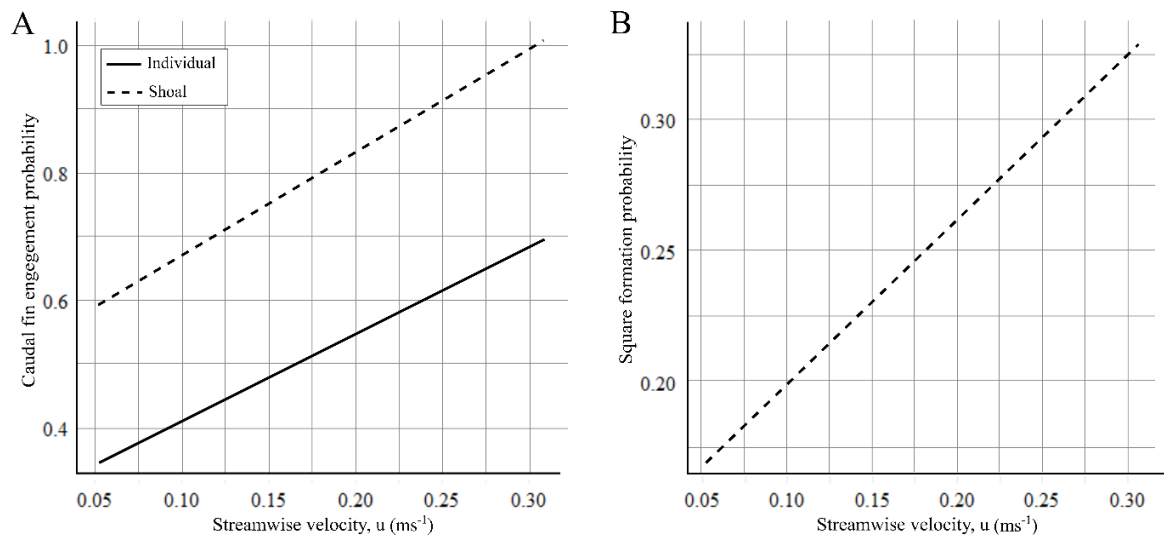
Figure 6.5. Plots describing: A – Caudal fin engagement variation with streamwise velocity magnitude. At the highest flow velocities the probability approaches 1 for shoals and individual fish. B – The probability of the fish shoaling in a square formation over a staggered (or diamond) formation. The staggered formation was always used more often than the square over all treatments and flow velocities but the square formation was used more frequently at higher velocities.

None of the shoaling parameters tested correlated significantly with fish length, mass, or fin size. The shoals were size matched so all shoalmates had the same standard length, and the mass and fin size also did not vary within shoals due to these measurements all being highly significantly linked to each other (GLMM, p=2e-16). A full set of detailed fish length, mass and fin size measurements is available in the supplementary materials. The cluster analysis and a principal component analysis revealed that the clusters produced still had very high

overlap between each other and the Euclidean distances between data points did not reveal any obvious clusters of different shoaling modes. This suggests that shoaling positions and formations are not fixed and that there are no well-defined shoaling strategies across the set of independent variables tested.

6.3.3 Fin-beat frequency

Fin-beat frequency (hereafter FBF) was significantly higher for fish swimming alone than for fish swimming with any other fish (GLMM, p=1e-14). A comparison of FBF values of treatments with the same flow conditions also revealed in all cases that FBF was higher in the control (individual fish) conditions (Figure 6.6A; GLMM, p<2.3e-9). The number of fish in a shoal also affects FBF, with larger shoals having overall lower average values of FBF (GLMM, p=6.6e-6), Figure 6.6D shows this relationship and also shows that the FBF does not decrease as the shoal gets larger than 4 fish as the relationship plateaus. Overall, all members of the shoal have a lower FBF than individual fish but Figure 6.6B shows that for bulk velocities of 0.1 and 0.15 ms^{-1}, the followers have a significantly lower FBF than the leaders (GLMM, p<0.025). Flow conditions with bulk velocity 0.19 and 0.23 ms^{-1} however, have the same FBF between leaders and followers (GLMM, p>0.11). Percentage reductions in FBF are available in Table 6.4, and shows further evidence of how FBF reduction increases with increasing bulk velocity so there is greater benefit at higher flows. Among followers, there was no difference in FBF.

Table 6.4. Relative percentage reductions in FBF between individuals, leaders, and followers for each treatment. *The only non-significant differences are between the leader and followers in the two treatments with the highest bulk velocities.

Bulk velocity, U (ms^{-1})	FBF reduction between individual and shoal (%)	FBF reduction between individual and shoal leader (%)	FBF reduction between shoal leader and followers (%)
0.1	24.4	17.4	10.1
0.15	25.7	24.3	2.0
0.19	29.8	29.1	*1.0
0.23	34.0	37.8	*-5.6

The nearest neighbour distance did not affect FBF (GLMM, p=0.48) but the distance to the fish in front of the fish whose FBF was recorded was significantly linked to lower FBF for lower distances to the fish in front (GLMM, p=0.039; Figure 6.6C). Across treatments, the

average FBF values did not vary between the highest three bulk velocities but flow conditions with 0.1 ms^{-1} bulk velocity had a significantly lower FBF (GLMM, p=0.0003). There was no difference in FBF between the square or diamond shoaling formation (GLMM, p=0.96), but there were higher FBF values associated with decreased caudal fin engagement (GLMM, p=0.001), possibly related to higher caudal fin usage in shoals.
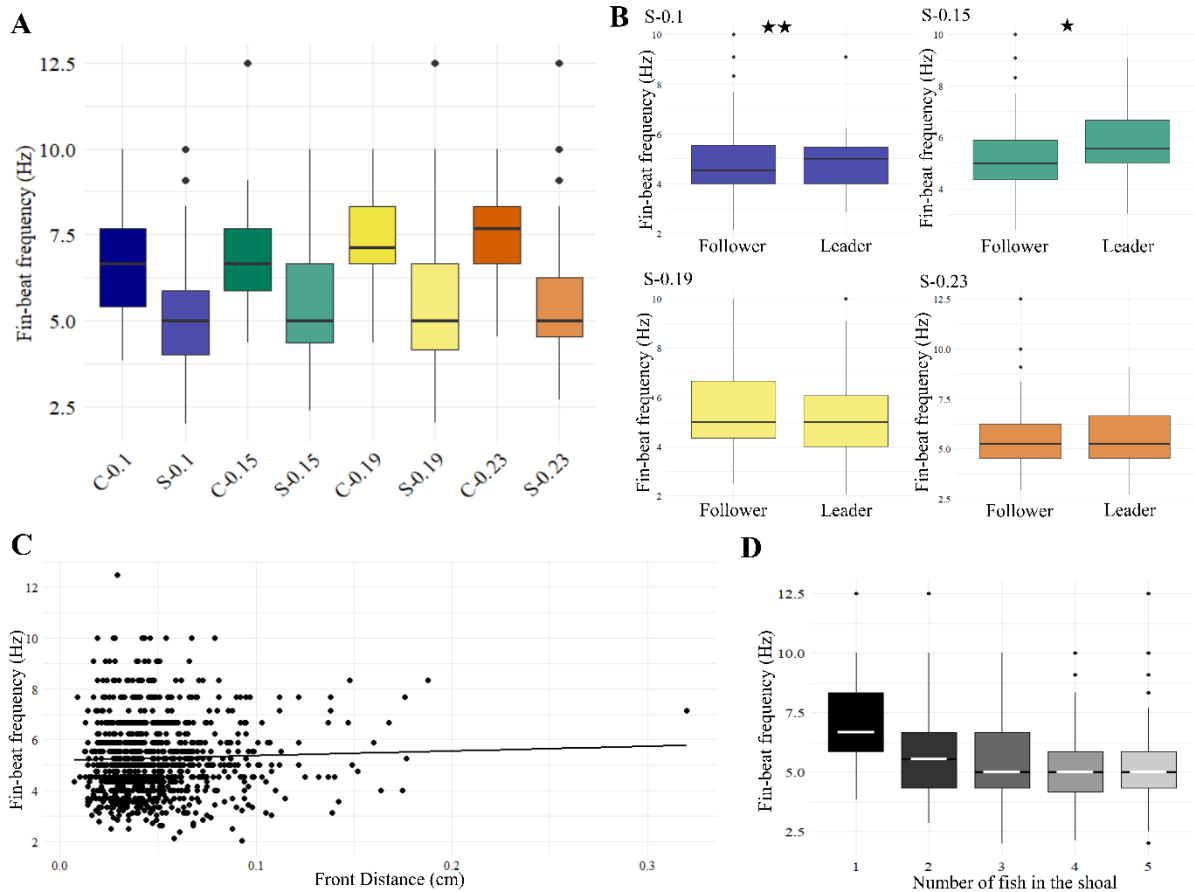
Figure 6.6. A – Boxplots of the fin-beat frequency (FBF) in each treatment. Each flow condition is represented by a colour and shoaling treatments are represented by a lighter shade of the colour assigned to the flow condition. Outliers are shown as black dots and the boxplots show the median, interquartile range and 95th percentile of the data. B – Each of the four plots corresponds to the flow condition indicated at the top left of each plot. Each plot shows the FBF difference between the shoal leader and the followers. The colours of each of the plots also match the treatment from plot A. Stars at the top of each plot indicate significant differences between the leader and the followers. Data for the followers is combined. C – FBF variation with distance between the fish for which FBF was recorded and the fish in front of it in the shoal. FBF increases with increasing distance from the fish in front. D – The average FBF in a shoal (or individual fish) by the number of fish shoaling.

The fin beats of fish shoaling together did not display any sign of synchronisation or patterns of phase differences, regardless of flow velocity, shoal formation, or number of members. Within each examined shoaling event, the phase difference varied widely within every few fin beats and deeper analysis did not reveal any pattern of synchronisation.

6.3.4 Angular acceleration of the pectoral fin

The analysis of the pectoral fin angular velocity shows the power stroke (rising limb) and the recovery stroke (falling limb) characteristics of the beat in each treatment. When the bulk velocity was 0.1 ms^{-1} (Figure 6.7A), the shoaling fish and the individual had very similar fin beat characteristics and angular acceleration magnitude. This may be due to the reduced flow velocity in this treatment but Figures 6B, C, and D reveal that at higher flow velocities, the fin beat of individual fish is shorter, and with a peak value of angular acceleration more than double the one of the shoaling fish. The angular acceleration of shoaling fish does not fluctuate greatly between flow conditions, and remains similar throughout the range of flow velocities. The fin beat of the individual fish in plots B, C and D are also extremely similar despite the change in discharge.
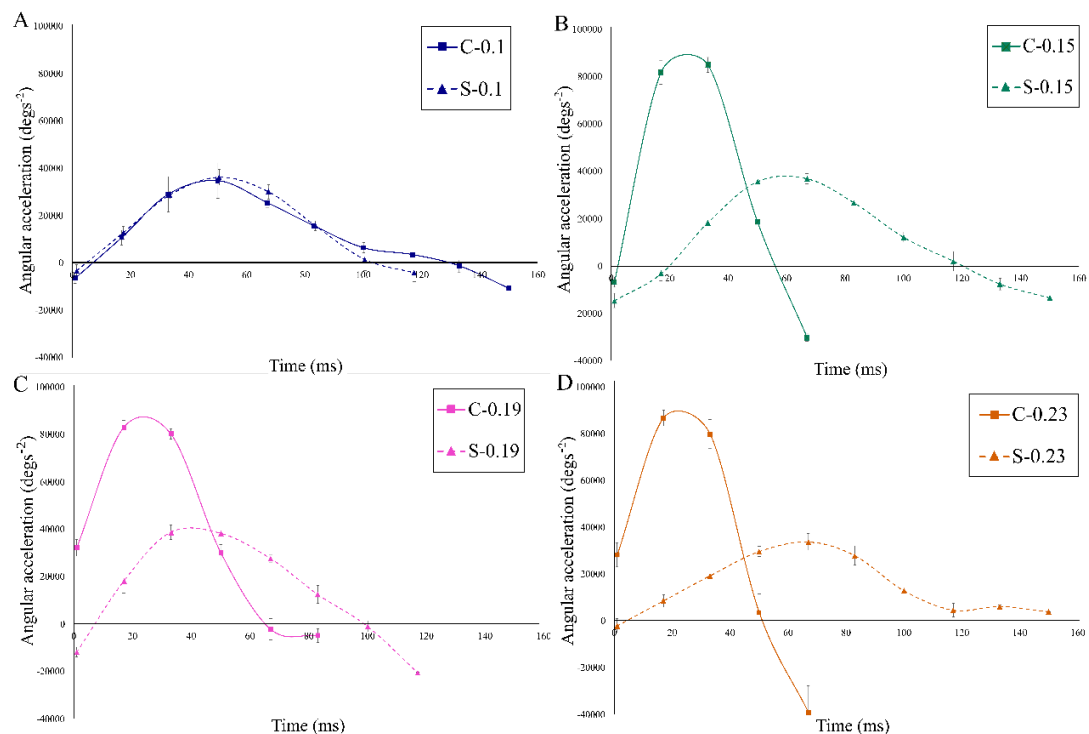
Figure 6.7. Angular acceleration plots of the pectoral fin for individual fish (C) and shoaling fish (S) for each flow condition where bulk velocity is specified in the legend of each

subfigure. Dashed lines represent shoaling fish and solid lines represent individual fish. Each line is a mean average of multiple fin beats and the whiskers on each data point represent the standard error. The rising limb of each plot represents the power stroke and the falling limb is the recovery stroke.

6.4 Discussion

Fin-beat frequency (FBF) decreased between 24.4% and 34% for shoaling fish compared to individuals, confirming that shoaling brings hydrodynamic benefits to sticklebacks that increases with swimming speed. Interestingly, the shoal leaders had almost as much and sometimes the same FBF reduction as the followers. This has been found in other studies where all positions showed reduced swimming effort but for Grey mullet the energetic advantage was greatest at low speeds (Marras et al., 2015) contrary to the current findings. Here, the followers had a lower FBF than the leaders for the flow conditions with 0.1 and 0.15 ms^{-1} bulk velocity (as shown in Table 6.4) an advantage which steadily decreased at higher speeds despite an overall greater FBF reduction. This may be explained by the swimming becoming less stable behind other fish at high speeds, especially considering the low swimming capabilities of river resident sticklebacks (Taylor and McPhail, 1986; Tudorache et al., 2007; Reyes and Baker, 2016). The wake of the leaders at high flow velocities may create turbulent structures that require the followers to make more frequent corrections. This is consistent with the increased usage of the caudal fin (Figure 6.5A) found in shoaling fish and increasing with speed as this fin is often used to make corrections when not closed (Figure 6.3B). The increased caudal fin engagement for shoaling fish over all tested speeds also points to the fish needing to make more frequent corrections when shoaling either due to the wake of the fish in front or to maintain shoal cohesion as fish will exist in an attraction zone to other fish when too far away from the nearest shoalmate or a repulsion zone if too close (Tien et al., 2004) and they must therefore keep within these boundaries as the shoal dynamically changes. The mechanism by which the leader has a greatly reduced FBF compared to an individual fish is unclear, other studies on labriform shoaling have not found this same reduction, finding instead the leader to have an increased FBF compared to an individual fish (Johansen et al., 2010). In studies where the leader has been found to have a reduced swimming effort, the pressure mechanism was attributed with aiding the leading fish (Ren et al., 2023). This effect, however, has not been found to be

large enough in magnitude to explain a maximum FBF reduction for the leaders of 37.8%, so there may be other mechanisms, hydrodynamic or social, that contribute to the reduced swimming effort of the leader and potentially the followers.

The FBF reduction was higher for larger shoals but reached a stable point at a shoal size of 4 fish beyond which more shoalmates did not reduce the average FBF of the shoal. There was no link between nearest neighbour distance and FBF showing how, unlike carangiform swimmers, there may be no advantage of shoaling in a square formation (de Bie et al., 2020; Ren et al., 2023) for labriform fish. There, however, was a significant relationship between FBF and the distance to the fish in front of the measured fish, indicating that some of the hydrodynamic benefit comes from the wake of the fish in front and that the stronger the wake (closer to the fish), the greater the advantage. The wake of the fish in front will produce vortex streets from the beats of the pectoral fins either side of the fish but also reduced velocities immediately behind the fish that reduce the pressure on the head of the following fish (Thandiackal and Lauder, 2023) and drag. The pressure on the head of the follower fish, however, is still higher than the surrounding flow because of the stagnation effect, although this is highly dependent of follower position and stagnation pressure. Since follower fish were often at least partially alongside the leader (the tip of the head was ahead of leader's caudal fin), the increased pressure downstream of the leader's pectoral fin beat may explain some of the benefit gained by the leader. The vortex theory is commonly used to explain energetic benefit of shoaling carangiform fish (Weihs, 1973; Liao et al., 2003; Harvey et al., 2022; Ren et al., 2023) despite not having yet been quantified between two live shoaling fish. Evidence from other studies has found that almost any shoaling formation can produce energetic benefits (Hemelrijk et al., 2015) by using the drag wake and that fish in any position can reduce swimming costs (Marras et al., 2015). Furthermore, vortices shed by fish may not be discrete or organized enough to allow reverse Karman gaiting (Daghooghi and Borazjani, 2015). These findings, combined with the variable wake of labriform fish (Drucker and Lauder, 2000) and the size of the vortices shed by the pectoral fins compared to the lengthscale of vortex that fish interact the most with (Liao et al., 2003; Muhawenimana et al., 2019), make the vortex theory an unlikely explanation for the reduction in FBF seen in sticklebacks. No distinct pattern of phase synchronisation of the fin beats was observed and the sticklebacks do not seem to use or avoid the vortices shed by the fish in front to maximise their efficiency.

Johansen et al. (2010) found a reduction in FBF for shoaling labriform fish and an even greater reduction in oxygen consumption. The findings in the present study indicate that part of the swimming cost reduction comes from a reduced FBF for shoaling fish but not exclusively from this mechanism as some may come from the angular velocity reduction, potentially explaining the higher oxygen reduction found in other studies (Johansen et al., 2010). The angular acceleration of the pectoral fin shows two main modes of actuation of this fin, the angle that the fin is opened to remain constant but when shoaling and swimming at low speeds (Figure 6.7) the pectoral fin experiences lower angular acceleration over a wider period of time compared to the individual fish at higher flow speeds where the peak angular acceleration is more than twice as large and the beat is executed over a shorter period. The pectoral fin therefore beats harder at higher speeds but the period of the angular acceleration curve does not relate completely to the FBF indicating that there are pauses between beats where the pectoral fins are kept against the fish's body so increased swimming effort by a stickleback comprises both a higher FBF and a more powerful fin beat. The more powerful stroke may also explain why the FBF did not increase linearly like it does for Striped surfperch (Drucker and Lauder, 2000).

There was no clearly organised prevalent shoaling formation identified in this study but overall the diamond formation was more common than the square formation, but both were used. A rectangular shoal can increase the sheltering effect (Daghooghi and Borazjani, 2015) and this may explain why it was used more frequently at higher flow velocities, whilst diamond shoals have also been found to reduce drag (Deng and Shao, 2006). Overall, however, the dynamic nature of the stickleback shoals makes it difficult to determine which is the prevalent mechanism. The sticklebacks move their pectoral fins to reduce the thrust against the direction of motion produced in the recovery stroke by re-orienting the fin to face the smallest surface area possible to the flow and then doing the reverse on the power stroke to generate maximum thrust. The sticklebacks thus swim primarily with drag based locomotion. The most likely explanation for the reduction in swimming cost is therefore a drag reduction effect caused by the drag wake of fish in front that allow the sticklebacks to row their pectoral fins in the drag based thrust production. Sticklebacks also save energy by increasingly swimming closer to the flume wall with higher bulk velocities, which is also consistent with their choice of habitat as river resident sticklebacks (Gagnon et al., 2019).

The hydrodynamic and kinematic factors that contribute to the reduced swimming cost found in this study have been evaluated but shoaling is a highly social behaviour and even though an experimental flume removes factors such as predation, foraging, and mating (Cushing & Jones, 1968; Larsson, 2012), there will always be a level of social interaction between the fish. The social aspect of shoaling in moving water needs to be better studied to understand if any energy savings occur as a direct result of it; in particular, more work is required to explain the large FBF reduction the leader experiences.

6.5 Conclusion

For labriform swimmers shoaling brought a large reduction in fin-beat frequency (FBF) compared to a fish swimming alone with the reduction increasing with shoal size but stabilizing at four fish. The FBF reduction was greatest at higher swimming speeds. The shoal leader experienced a slightly lower FBF than the followers at low flow velocities and an equal FBF reduction as the followers in the treatments at higher bulk velocities. Shoaling fish changed positions dynamically and shoaling patterns were not stable. Shoaling fish did not synchronise their fin beats in any way making it likely that the mechanism of FBF reduction in shoals was due to the reduced drag behind other fish and the channeling effect rather fish benefiting from using a vortex or vortex street. The sticklebacks reduced swimming effort in shoals by reducing FBF and also by delivering a less powerful fin beat when swimming in shoals, in contrast to individual fish swimming where they needed to reach double the amount of angular acceleration with their pectoral fin compared to a shoal. Sticklebacks closed their dorsal, anal, and caudal fins when swimming steadily to reduce drag but in shoals the caudal fin was used more often to make corrections, indicating that swimming in groups may be a less stable but still beneficial system for swimming. In this chapter the benefits of shoaling were explored in the absence of complex flow dynamics and linked some key kinematic parameters in response to shoalmates meeting thesis objectives 1 and 2.

Chapter 7. Rainbow trout behaviour in the presence of single and twin Vertical Axis Turbines (VATs)

Conceptualisation and methodology was by Prof. Jo Cable, Prof. Catherine Wilson, Dr. Stephanie Müller, Dr. Pablo Ouro, Dr. Valentine Muhawenimana, and Guglielmo Sonnino Sorisio. Data collection by Guglielmo Sonnino Sorisio and Dr. Stephanie Müller. Analysis, visualisation, and writing by Guglielmo Sonnino Sorisio and editing by all of the above.

Summary

Hydrokinetic turbines are an emerging technology to supply reliable and renewable energy by exploiting river flow. They are a potential alternative to current hydropower schemes that impound rivers, cause habitat fragmentation and fish mortality. However, limited information is available about fish behaviour in the vicinity of these devices and the effects of shoaling have not yet been evaluated. In this study, juvenile rainbow trout (*Oncorhynchus mykiss*) were allowed to swim in an laboratory flume with five turbine configurations of single and paired turbines, either individually or as a shoal of three fish. In a relatively wide channel, the turbines did not significantly reduce fish passage when rotating. Fish were significantly more likely to swim in the turbine wake and upstream of the turbine (known as bow wake) when there were two turbines because of the larger area of low velocity in their wake. Fish approached the turbines significantly more often in shoals than as individuals and were overall bolder in shoals.

7.1 Introduction

Reliable power supply is essential to modern society, and affordable and clean energy is one of the UN sustainably goals (UNEP, 2023). Most large cities and settlements have access to national energy grid networks and power plants that deliver a stable power supply to homes and industry through a mixture of fossil, nuclear, and renewable energy. Remote communities, however, still struggle with reliable power supply and may depend on renewable resources that may not be predictable. The UN aims for a reduction in fossil fuel usage (UNEP, 2023), favouring an increase in renewable and low carbon resources, ideally using resources that do not damage the natural environment.

Freshwater watercourses are a valuable store of energy which has a long history of being exploited by humans. The most common form of energy extraction from rivers in modern times is by impounding large volumes of water with a dam and forcing it through turbines to generate power. Such hydropower plants (HPP) generate 14.3% of the world's electricity, but their contribution varies widely by country and region, ranging from 0% to 100% (Ritchie and Rosado, 2020; Energy Institute, 2024). HPPs are considered a low carbon energy source but they still have a negative effect on the rivers, causing fragmentation, preventing and/or delaying fish migration, disrupting natural sediment transport characteristics, and causing fish mortalities (Piper et al., 2018b; Pracheil et al., 2016). Over 3000 new HPPs are planned (van Treeck et al., 2021), particularly in relatively untapped rivers such as the Amazon, Congo, and Mekong (Winemiller et al., 2016), home to a third of freshwater species, some found nowhere else. HPP installations without any technical or natural fish passage solution, however, can cause up to 100% mortality in freshwater fish (Dainys et al., 2018b) and block the migration of others (Piper et al., 2018b), with small dams having the largest ecological impact relative to capacity (Couto et al., 2021; van Treeck et al., 2021).

For communities not connected to the wider grid and in need a reliable source of power, hydrokinetic turbines are emerging as an alternative and less environmentally-damaging solution to hydropower plants, with more than one hundred permits issued in the Mississippi River alone (Schweizer et al., 2011). Hydrokinetic turbines use the flow velocity of rivers to generate power. They do not impound rivers or form a barrier that stretches the entire width of the river (Chaudhari et al., 2021). Hydrokinetic turbines are also easier and cheaper to install than HPPs with potentially fewer environmental drawbacks and predictable power delivery (Badrul Salleh et al., 2019; Chaudhari et al., 2021), making them ideal for use in remote regions (Badrul Salleh et al., 2019; Couto et al., 2021).

Although hydrokinetic turbines potentially have less impact on river's hydrodynamics and morphology (Musa et al., 2018), they still block part of the watercourse, and therefore we must seek to understand how they alter the flow fields and associated habitats before this technology is widely adopted. Vertical Axis Turbines (henceforth referred to as VATs) are a prominent design for hydrokinetic turbines (Bender et al., 2023; Ouro et al., 2019). They can generate energy from flows with velocities below 1.5 m/s (Lundin et al., 2016), and have little effect on the flow when stationary, making them suitable for a wide range of rivers.

The effect of full scale turbines on the flow when rotating have also been studied, a deployed turbine in Alaska, for example, created an induction zone upstream where there was a velocity decrease and increased turbulence compared to the surrounding flow (Guerra and Thomson, 2019). Downstream of the same turbine, the near wake had a fast recovery turning into a low energy far wake (Guerra and Thomson, 2019). Numerical and experimental studies of VATs have investigated the wake behind a varied range of turbine configurations; a single turbine featured a small stagnation point upstream of the turbine (Ouro and Stoesser, 2017; Posa, 2019; Posa, 2020) with a downstream wake that expanded laterally demarcated by high levels of vorticity and low velocity, which started to converge at two and a half turbine diameters (2.5D) downstream with vortices reaching a maximum extension of 0.85D (Ouro and Stoesser, 2017). The wake can be split into three main regions: the near wake extending 2D from the turbine featuring low momentum and bounded by high energy vortices, a transition region between 2D and 5D downstream of the turbine where there is momentum recovery but still maintains a high level of turbulence and where the wake expands vertically, and the far wake beyond 5D where the velocity is recovered to 95% with some minor fluctuations (Ouro et al., 2019). Using twin VATs (TVAT) can potentially generate more energy where the channel is wide enough, but there are possible interactions between the wakes of the two turbines, depending on which directions they spin relative to each other. When they are rotating in the same direction (co-rotating), there is a reduced velocity in the wake compared to a single turbine and there is the largest lateral expansion of the wake, whereas counter-rotating turbines will have the fastest wake velocities and momentum recovery by 5D if counter-rotating forwards (see Figure 7.2) or a wake with a large vertical extension if counter-rotating backwards (Müller et al., 2021).

The limited knowledge of fish behaviour around hydrokinetic turbines is based on laboratory flumes, river, and tidal turbine studies. In flume trials and rivers, salmon and rainbow trout avoided the turbine when operational, but passage remained unaffected (Bender et al., 2023; Amaral et al., 2011, 2015; Berry et al., 2019; Müller et al., 2023; Yoshida et al., 2022). In tidal channels, a 35% decrease in turbine interactions was observed when the turbine was operational (Viehman and Zydlewski, 2014). Other field studies, however, reported attraction to the turbines and increased presence of fish in the wake (Viehman and Zydlewski, 2014; Fraser et al., 2018) and a 378% increase in shoaling behaviour (Fraser et al. 2018). Such aggregations can create predation hotspots (Lieber et al., 2019). Mostly, fish prefer to pass to the side (Müller et al., 2023; Sonnino Sorisio et al., 2023; Zhang et al.,

146

2017) or above the turbine when spatially constrained (Castro-Santos and Haro, 2013). In a narrow flume (Müller et al., 2023) or in a tidal channel (Hammar et al., 2013), turbine presence did produce a movement barrier for rainbow trout. Survival rates for turbine exposure are generally reported as being above 95% (Amaral et al., 2011, 2015; Berry et al., 2019; Romero-Gomez & Richmond, 2014; Sonnino Sorisio et al., 2023) but blade strike risks can vary widely in laboratory and numerical studies from 0-1.3% (Zhang et al., 2017; Yoshida et al., 2020) to 6-68.9% (Romero-Gomez and Richmond, 2014; Peraza and Horne, 2023). Injury rates from turbines also vary, with maximum values reaching 20% with bruising and descaling being the most common form of injury (Amaral et al., 2015). While the turbine sound does not appear to impact fish responses, visual cues and turbine visibility do affect behaviour (Viehman and Zydlewski, 2014; Yoshida et al., 2020; Sonnino Sorisio et al., 2023).

Few studies have analysed the effects of fish shoaling near a hydrokinetic turbine (Viehman and Zydlewski, 2014; Fraser et al., 2018), even though most fish species shoal during their life. Hence, this effect should be considered when evaluating fish behavioural responses to hydrokinetic turbines. The primary drivers of fish shoaling are well understood to be predation avoidance (Cushing and Jones, 1968; Enstipp et al., 2007; Seppälä et al., 2008; Mayer, 2010; Larsson, 2012), foraging (Mayer, 2010), social interactions (Cushing and Jones, 1968), and hydrodynamic benefits (Weihs, 1973; Ligman et al., 2024). However, the interplay between these factors is debatable (Cushing and Jones, 1968; Weihs, 1973; Larsson, 2012) and this balance will shift according to context. With regard to hydrokinetic turbines and moving flow, shoaling might bring a primarily hydrodynamic benefit (Weihs, 1973; Ligman et al., 2024). Fish can reduce their energy expenditure by up to 53% in shoaling Giant danio (Zhang and Lauder, 2024). Experimental studies (Currier et al., 2021; de Bie et al., 2020; Johansen et al., 2010; Marras et al., 2015), a fish and a flapping foil (Harvey et al., 2022; Thandiackal and Lauder, 2023), and numerical studies (Deng and Shao, 2006; Ren et al., 2023) have also found energetic benefits of shoaling, but the driving mechanism of the energy reduction of shoaling is unclear. The leading fish in a shoal can also benefit from shoaling (Chapter 6) due to the pressure difference generated by the fish behind (Ren et al., 2023). A more common explanation for the hydrodynamic benefits, however, is that following fish can exploit the lower drag and the reverse Karman street vortices in the wake of the leading fish. They achieve this by swimming directly behind the fish in front (Thandiackal & Lauder, 2023; Wei et al., 2023) or in a staggered or diamond

formation (Weihs, 1973; Deng and Shao, 2006). Fish in a shoal could occupy any position and gain energetic benefits. As positioning is dynamic, this has led to arguments against the theory of the vortex street (Partridge and Pitcher, 1979; Marras et al., 2015). There are studies, however, that have not found any metabolic difference caused by shoaling in rainbow trout (Currier et al., 2021), demonstrating that the principles discussed may not be universally transferable between species and flow conditions. Other factors affecting shoaling are the familiarity and geographic origin of the fish with its shoal mates (Olsén et al., 2004; Ralph et al., 2012), infection status (Barber & Ruxton, 2000; Seppälä et al., 2008; Ward et al., 2005), and presence of predators (Seppälä et al., 2008).

Rainbow trout are often used as a model for shoaling studies (Currier et al., 2021) and studies involving turbines (Müller et al., 2023) as well as being present in their native range in areas where many permits for hydrokinetic devices exist. There is still a knowledge gap concerning turbine configuration and shoaling in the context of hydrokinetic turbines that needs to be filled before these devices can be implemented in fragile ecosystems. This study examines the behaviour of juvenile rainbow trout (*Oncorhynchus mykiss*) in the presence of five different configurations of single or twin VATs, and compares a single fish with a shoal of three fish. The aim was to test the effect of the presence of shoalmates on behaviour around hydrokinetic turbines (as already seen in chapters 5 and 6), and to evaluate the effect of the wake of a stationary, single, and pair of turbines and the associated hydrodynamic effects. The introduction of an actively moving turbine adds a layer of complexity building on the shoaling evaluations in the previous two chapters as well as testing a potential emerging threat to fish migrations.

7.2 Methods

7.2.1 Fish origin and maintenance

Fish trials were performed between 29th March and 7th April 2021 from 8:00 to 17:00 for individual fish and between 22nd March and 30th April 2021 from 8:00 to 17:00 for shoaling fish. The fish used in these trials were female triploid Rainbow trout (*Oncorhynchus mykiss*, N = 80) purchased from Bibury Trout Farm, UK. Trout total length was 67.5±10.7 mm. Before the experiment, they were housed in a Recirculating Aquaculture System (RAS) in tanks of 60-80 L at a density of 40 fish per tank in Cardiff School of Biosciences on a 12h:12h light:dark cycle at 15±1°C in water being constantly filtered by the RAS. They were fed daily with trout pellets in the morning. Shortly before the start of the flume trials, the

trout were transported to a holding tank in Cardiff School of Engineering where they were separated into size-matched shoals, isolated in plastic mesh cylinders within a larger holding tank of 500 L. The trout were maintained in dechlorinated water (Tetra AquaSafe Seachem Prime Concentrated Conditioner), aerated with multiple air pumps, cooled to $13\pm1°C$ by a D-D Aquarium Solution DC 750 chiller, and filtered by an external canister filter (Aquamanta EXF 600). Water quality was checked weekly with a water quality test kit (Nutrafin). The trout were kept on a 14h:10h light:dark cycle to allow all experimentation to be conducted during daylight hours and fed trout pellets every morning. The tank was provided with plastic tubes and other refugia. The shoals were acclimated for two weeks in this setup before any testing occurred to allow fish to familiarise with their shoal. The shoaling trials were carried out in three batches over the course of two months. After the end of the trials, the fish were transferred back to the RAS at Cardiff School of Biosciences. In the case of the single fish treatment, the 20 trout were housed in the 500 L tank with no plastic mesh sub-dividers but otherwise kept in the same way as the shoals. When the single trout had completed the experiment, they were transferred directly back to the School of Biosciences.

7.2.2 Experimental setup

A recirculating open channel flume (10 m long, 1.2 m wide, and 0.3 m high with a 1/1000 bed slope) at Cardiff School of Engineering was used in this study. The working section of the flume was bounded up and downstream by honeycomb flow straighteners and on the flume walls by glass. The flume bed in the working section was a white PVC sheet and the water surface was covered by a transparent acrylic sheet. The upstream end of the working section was located 4.4 m from the upstream end of the flume and measured 1.2 m long and 1.2 m wide with a flow depth of 0.23 m. Vertical Axis Turbines (VATs) at a scale of 18:100 were constructed with a diameter and height of 0.12 m, with three blades of 0.03 m chord length and a NACA0015 profile. With a single VAT, it was positioned at the centre of the working area, at (x = 60 cm, y = 60 cm) in Figure 7.1, whereas when a second turbine was present it was inserted at (x = 42 cm, y = 60 cm) in Figure 7.1, a spacing of 1.5 turbine diameters. Each blade was mounted to a central shaft by two 3 mm diameter struts and was laser sintered from white PA2200. The central shaft was mounted in a bearing embedded in the flume bed and held the bottom of the blades 20 mm from the bed. The upper end of the shaft was connected to an encoder and a DC motor (Kübler, 5-30VDC, 100 mA and Nider

DMN37K50G18A, DC 12 V respectively) which was held by a beam resting on the sides of the flume. The turbine operated at a fixed rotational speed of 59 rpm, combined with a bulk velocity of 0.19 ms^{-1} (Q = 53 Ls^{-1}), this gave the optimum tip speed ratio of 1.9 (S. Müller, Muhawenimana, et al., 2021; Ouro et al., 2019). The working area was illuminated from both sides by a total of four spotlights (Neewer Bi-Colour LED) and recorded at 55 frames per second (fps) from an overhead camera (Baumer VLXT-50M.I). The water in the flume was dechlorinated using Prime Dechlorinator and cooled to 14±1°C by a D-D Aquarium Solution, DC2200.
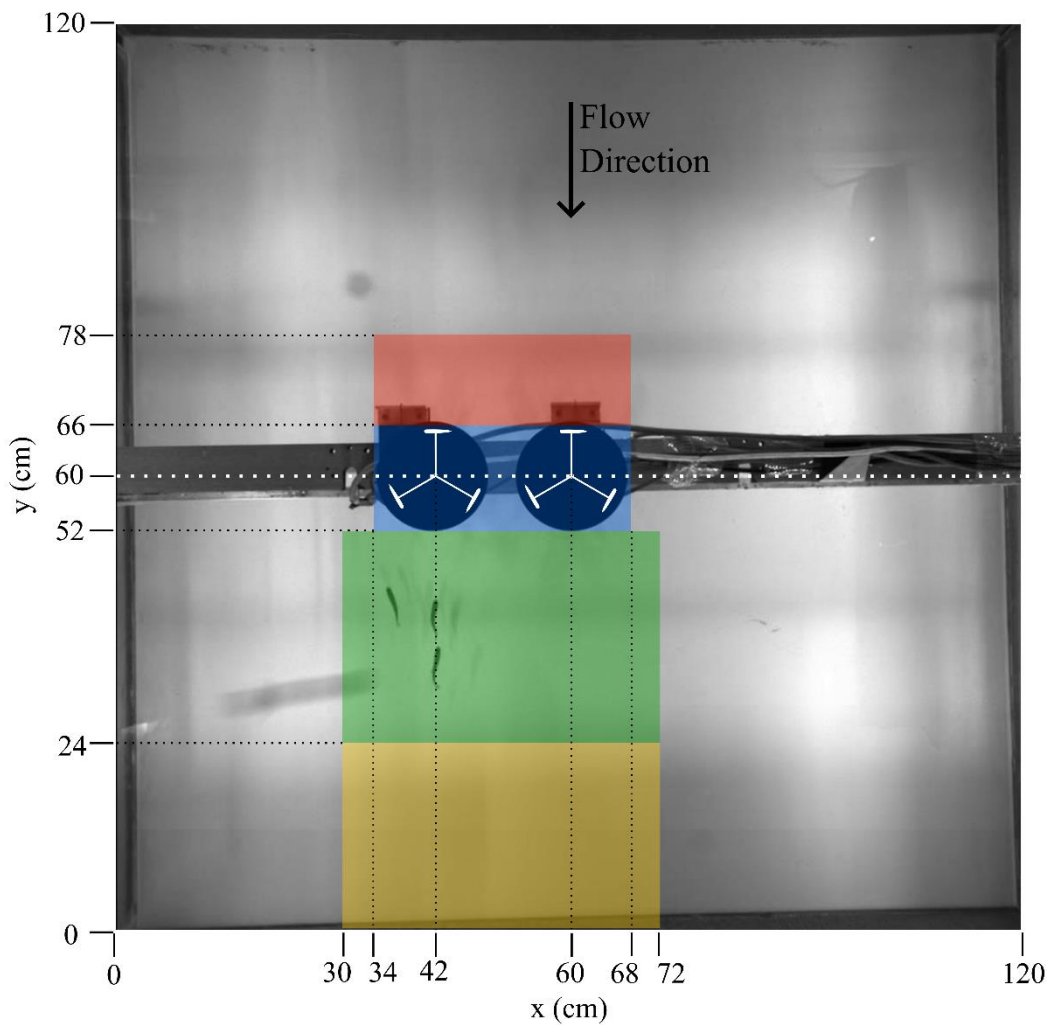
Figure 7.1. Schematic of the working area with all measurements in cm and the water flowing from top to bottom with the lateral direction defined as the x axis and the streamwise direction as the y axis. The two turbines are both depicted as rotating counter-clockwise (TVATCO-3 treatment, in Table 7.1). The single turbine tests were conducted with a turbine positioned on the flume centreline and the turbine centred at (y = 42 cm, x = 60 cm) was

removed. The coloured areas represent the areas defined in Table 7.2, where yellow = far wake, green = near wake, blue = turbine, and red = bow wake.

7.2.3 Experimental procedure

For shoaling treatments, n = 19 groups of three fish and for the single fish treatment n = 16 individual fish were included in the analysis. Each shoal (or single fish) was transferred from the holding tank to the flume in a bucket of water and released at the downstream end of the experimental area. The fish were then allowed to acclimate for a total of 20 minutes. The first 5 minutes at a reduced flowrate of 24.5 Ls^{-1} and corresponding turbine rotation of 7 rpm, the following 5 minutes at 37 Ls^{-1} and 30 rpm, and the final 10 minutes at the nominal flowrate of 53 ls^{-1} and 59 RPM. At the end of the acclimation period, the fish were removed from the working area into a bucket whilst the perspex sheet was placed above the area so they could be re-inserted downstream of the turbines following (Müller et al, 2023). The recording was started with a 10 minute 30 second timer, with the first 30 seconds used to place the trout at the downstream end of the experimental area and to start the experiment (these initial 30 seconds were discarded from the analysis). There were no visible startling behaviours noted upon reintroduction. After the 10 minute experiment expired, the trout were removed from the flume and transferred back to their holding tank. In the case of the single fish, the fish length and weight were measured with a calliper and a scale and then immediately transferred to a tank. The single fish only took part in one treatment, namely a single fish with a single turbine (SVAT-1, Table 7.1), with more information on the single fish treatment (SVAT-1) available in Müller et al. (2023) where the results of this treatment were used to investigate the impact of flume width on fish swimming behaviour. In contrast, the shoals of three fish took part in all treatments (Table 7.1), with each shoal only taking part in one treatment per day, completing all five different treatments over five consecutive days. The treatment order was randomised for the shoals to remove any temporal, learned behaviour, or tiredness bias.
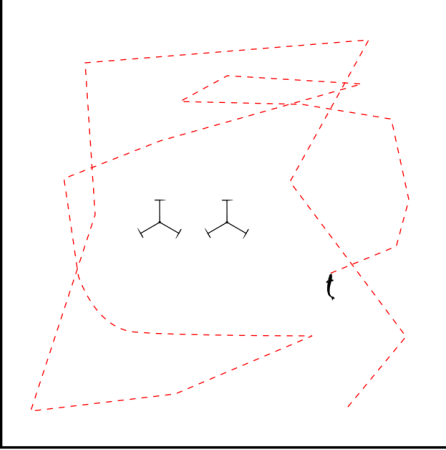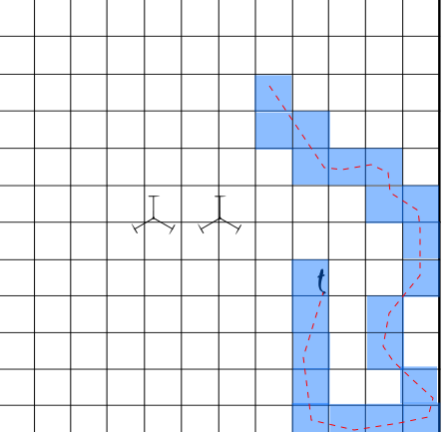
Table 7.1. Details of the treatments investigated in the study, where in the treatment names C = Control, SVAT = Single VAT, TVAT = Twin VAT, CO = Co-Rotating, CRB = Counter-Rotating Backwards, CRF = Counter-Rotating Forwards, and the number denotes the number of fish. In the rotation direction column, where two turbines are present, their relative rotational directions are described from left to right looking upstream (Figure 7.1). For shoaling treatments n = 19 shoals (used for every treatment except for SVAT-1) and for the single fish treatment n = 16 (used only once in SVAT-1).
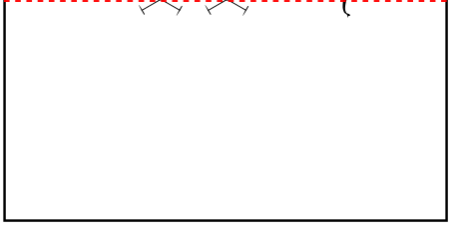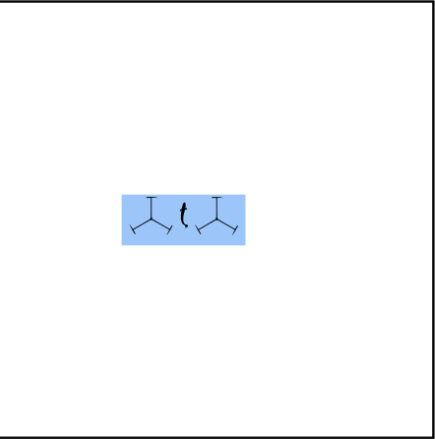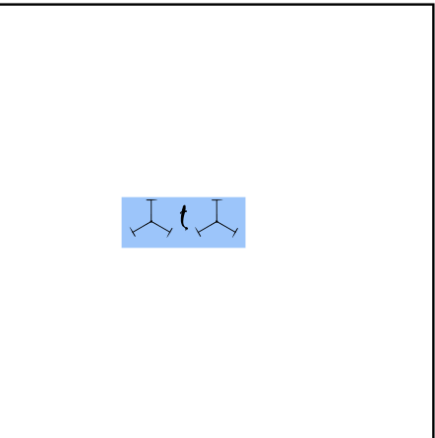
Treatment	No of Fish	No of Turbines	Rotation direction	Turbine Rotational speed (rpm)	Flowrate (Ls^{-1})	Bulk Velocity (ms^{-1})	Flow Depth (m)
C-3	3	1	Stationary	0	53	0.19	0.23
SVAT-1	1	1	Counter-Clockwise	59	53	0.19	0.23
SVAT-3	3	1	Counter-Clockwise	59	53	0.19	0.23
TVATCO-3	3	2	Counter-Clockwise	59	53	0.19	0.23
TVATCRB-3	3	2	Clockwise and Counter-Clockwise Backwards	59	53	0.19	0.23
TVATCRF-3	3	2	Counter-Clockwise Forwards and Clockwise	59	53	0.19	0.23
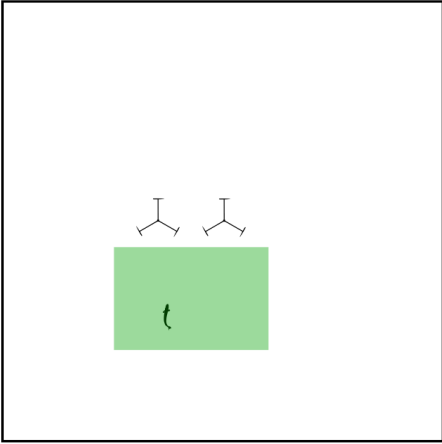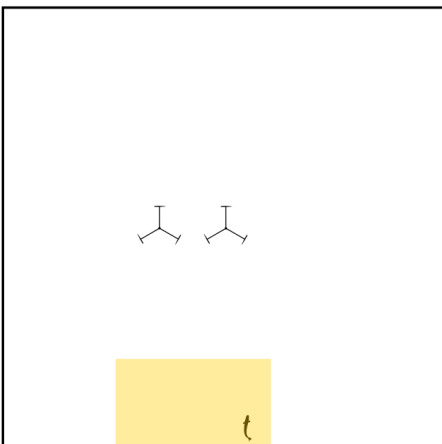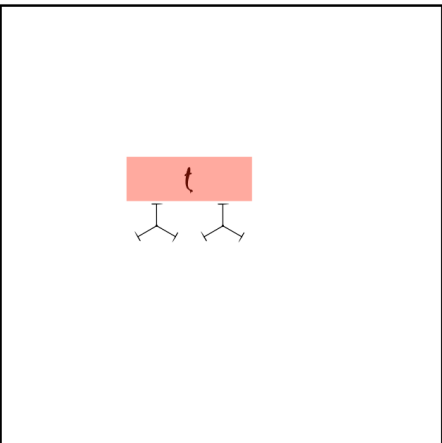
7.2.4 Data Analysis
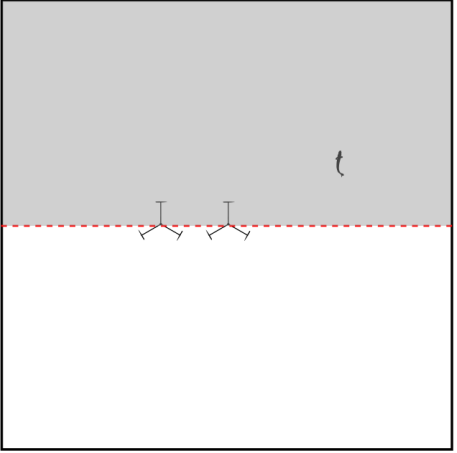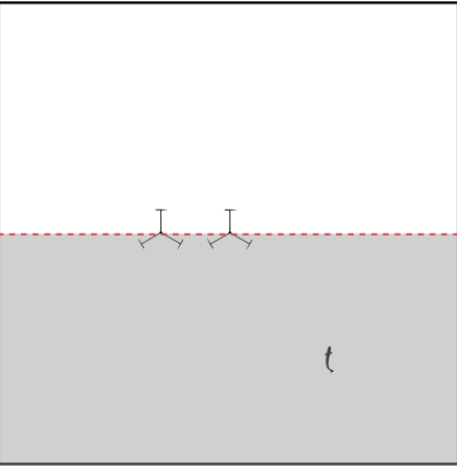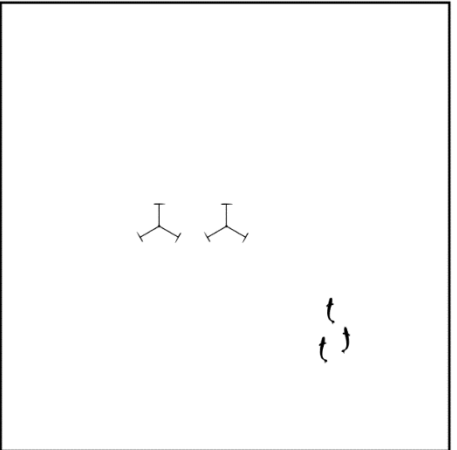
The video recordings of the fish were processed removing the initial 30 s using Matlab R2024a (The MathWorks Inc. 2024), and then they were then analysed in TRex (Walter and Couzin 2020) with which the positions and midline points of all fish for each frame were inspected, corrected where necessary, and exported as Matlab files. The data for each fish were then analysed in Matlab to obtain the parameters shown in Table 7.2, some of which are based on a grid defined with the origin at the left corner of the downstream end of the working area, also shown in Figure 7.1.
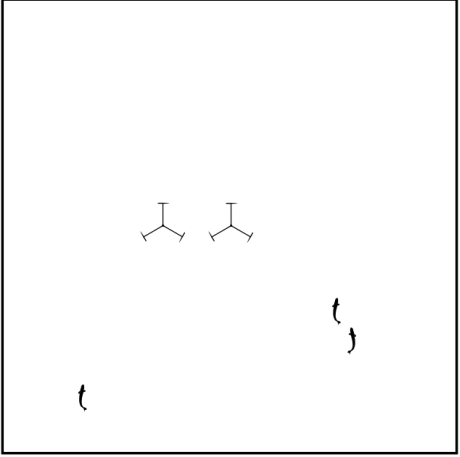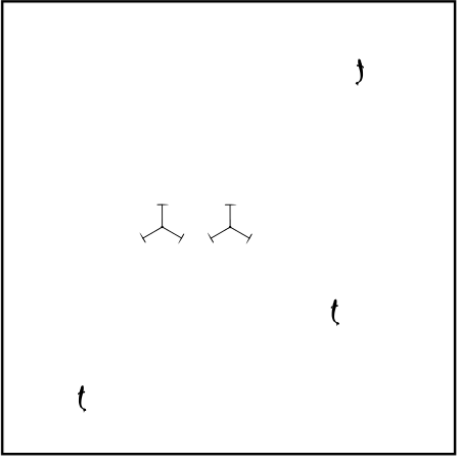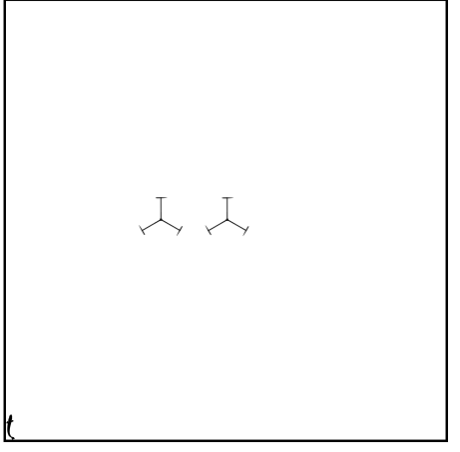
Table 7.2. The variables calculated from the tracking and posture data of rainbow trout in the current study. The x and y values (given in cm) in the description are in reference to the coordinates shown in Figure 7.1. Areas are also defined in Figure 7.1.
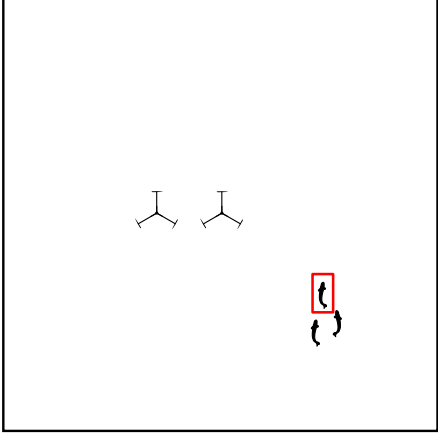
Variable	Description	Diagram
Distance (m)	Total distance travelled by each fish, calculated by summing the distance between each frame over the 10 minutes of the trial.	
Proportion explored (-)	The 14,400 cm^2 working area was split into 100 cm^2 squares and the number of squares entered by each fish counted and expressed as a proportion of the total number of squares.	

Cross count (-)	Number of times each fish passed upstream or downstream of the turbines ($y = 60$ cm).	
Turbine count (-)	Number of times each fish entered the turbine rotor region, defined as ($52 < x > 68$ cm, $52 < y > 66$ cm) when one turbine was present and as ($34 < x > 68$ cm, $52 < y > 66$ cm) for two turbine configurations.	
Turbine time (s)	Time spent in the turbine area (defined above).	

Near wake time (s)	Time spent by each fish in the near wake ($30 < x > 72$ cm, $24 < y > 52$ cm).	
Far wake time (s)	Time spent by each fish in the far wake ($30 < x > 72$ cm, $0 < y > 24$ cm).	
Bow wake time (s)	Time spent by each fish in the bow wake (directly in front of the turbine) ($34 < x > 68$ cm, $66 < y > 78$ cm).	

Time upstream (s)	Time spent by each fish upstream of the turbine ($60 < y > 120$ cm).	
Time downstream (s)	Time spent by each fish downstream of the turbine ($0 < y > 60$ cm).	
Time in 3 fish (-)	The amount of time for which all three fish were within three fish lengths of each other (based on the average total fish length of that shoal) expressed as a proportion of the total time. This analysis was also repeated for each of the areas defined above by only considering time in that area.	

Time in 2 fish (-)	The amount of time for which two fish were within three fish lengths of each another (based on the average total fish length of that shoal) expressed as a proportion of the total time. This analysis was also repeated for each of the areas defined above by only considering time in that area.	
Time alone (-)	The amount of time for which all fish were more than three fish lengths away from one another (based on the average total fish length of that shoal) expressed as a proportion of the total time. This analysis was also repeated for each of the areas defined above by only considering time in that area.	
Time resting (s)	Number of frames during which the swimming speed and tailbeat frequency of the fish was approximately zero.	

Dominance (-)	The proportion of time during shoaling for which each fish was upstream of its shoalmates was calculated for each fish and the second highest proportion was subtracted from the highest proportion.	
Tailbeat frequency (TBF) (Hz)	The tail movement was extracted from the posture tracking and a fast Fourier transform performed on the signal. The dominant frequency was extracted for every second of data. This method was validated against human analysed swimming clips. This analysis was also repeated for each of the areas defined above by only considering frames in that area.	

7.2.5 Statistical Analysis

The statistical analysis for this study was performed in RStudio (R Version 4.2.2) (R Core Team, 2022). The data was imported into R and checked for normality. Due to the repeated use of the same shoals, Generalised Linear Mixed Models (GLMM) were utilised to account for pseudo-replication by including shoal ID as a random effect. To perform the GLMMs the lme4, nlme, and lmertest packages were used (Bates et al., 2015; Kuznetsova et al., 2017; Pinheiro et al., 2020). The study was performed in batches, so batch effects were first inspected to verify that there were no statistical differences between batches for all response variables (GLMM, $p > 0.44$). The data was normally distributed so a Gaussian GLMM produced the best residual distributions compared to other GLMMs tested. Count data was analysed using a poisson GLMM which outperformed negative binomial and other GLMMs. To further analyse TBF, Matlab was used to perform a Probability Density Function (PDF) for TBF in different areas of the working section. In all cases the p value use to determine significance was 0.05, where multiple relationships are reported on (for instance the relationship of all treatments compared to control), the upper bound of the p value for significant results is given.

7.2.6 Hydrodynamics

A previous experimental study by Müller et al. (2021) fully characterised the three dimensional wake shape from Acoustic Doppler Velocimetry data for the turbine configurations tested. Data was available for the following distances downstream of the turbines: 1D, 1.5D, 2D, 3D, 4D, and 5D where D is the turbine diameter equal to 12 cm. Figure 7.2 provides contours of time-averaged streamwise velocity for flow depth z = 100 mm. The slowest velocities in the wake are generated in the downstream region corresponding to the upstream motion of the blades. The TVATCRB setup generated the wake with the smallest horizontal footprint while the velocity deficit is largest for the TVATCO (Müller et al., 2021). The highest turbulence intensity across the wake is from the TVATCRB (Müller et al., 2021).
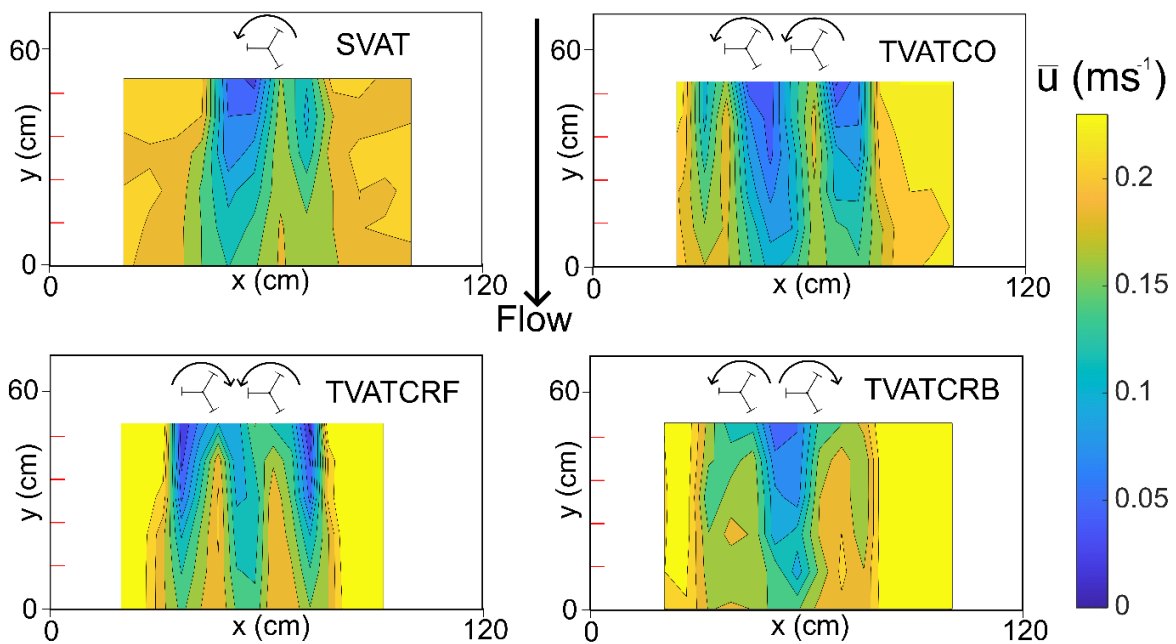
Figure 7.2. Contour plots of time-averaged streamwise velocity taken at mid turbine depth for all turbine configurations. The coordinate system on each plot aligns with that of Figure 7.1. Acoustic Doppler Velocimetry was used to collect this data by Müller et al. (2021). The turbine spacing was 1.5 turbine diameters and longitudinal extent of the wake is shown downstream of the turbines up to the flow straightener at y = 0 cm (5 turbine diameters, Figure 7.1).

7.2.7 Animal ethics statement

All work was approved by Cardiff University Animal Ethics Committee and linked to UK Home Office PP816714.

7.3 Results

7.3.1 Distance, exploration and passage

Fish swam the largest distance in the control conditions (C-3) with a mean of 4.5 m (C-3, Figure 7.3A), and significantly less in treatments SVAT-1, TVATCO-3, and TVATCRF-3 within the working section of the flume in comparison with C-3 (GLMM, $p<0.02$). This is reflected in the proportion of the total working area explored by each fish (Figure 7.3B), where the fish in C-3 on average explored significantly more of the working area than the fish in TVATCO-3, TVATCRF-3, and SVAT-1 which was significantly lower than all other treatments too (GLMM, $p<0.017$). The decreased distance and exploration did not, however, affect passage success past the turbines, all treatments statistically having the same passage as control with the exception of TVATCO-3 which had significantly more (GLMM, $p=0.001$) as shown in Figure 7.3C. Figure 7.3D shows fish entering the turbine area, compared to control; SVAT-1 had significantly fewer interactions with the turbine (GLMM, $p=0.002$) whereas SVAT-3 had more (GLMM, $p=5e-6$), TVATCRB-3 and TVATCRF-3 had significantly more than C-3, SVAT-1 and SVAT-3 (GLMM, $p=2e-16$), and TVATCO-3 had the most out of all treatments (GLMM, $p=2e-26$). This finding is consistent with the amount of time spent very close to the turbines (blue rectangle in Figure 7.1), with fish in TVATCO-3 and TVATCRF-3 spending significantly more time there (GLMM, $p<0.03$). It is also shows the same trend in the results from the relationship between treatment and distance to the turbines (Figure 7.3E), where fish in SVAT-1 stayed significantly further away from the turbine than all other treatments (GLMM, $p<0.005$), and the three treatments with twin turbines staying significantly closer than control (GLMM, $p<0.008$).
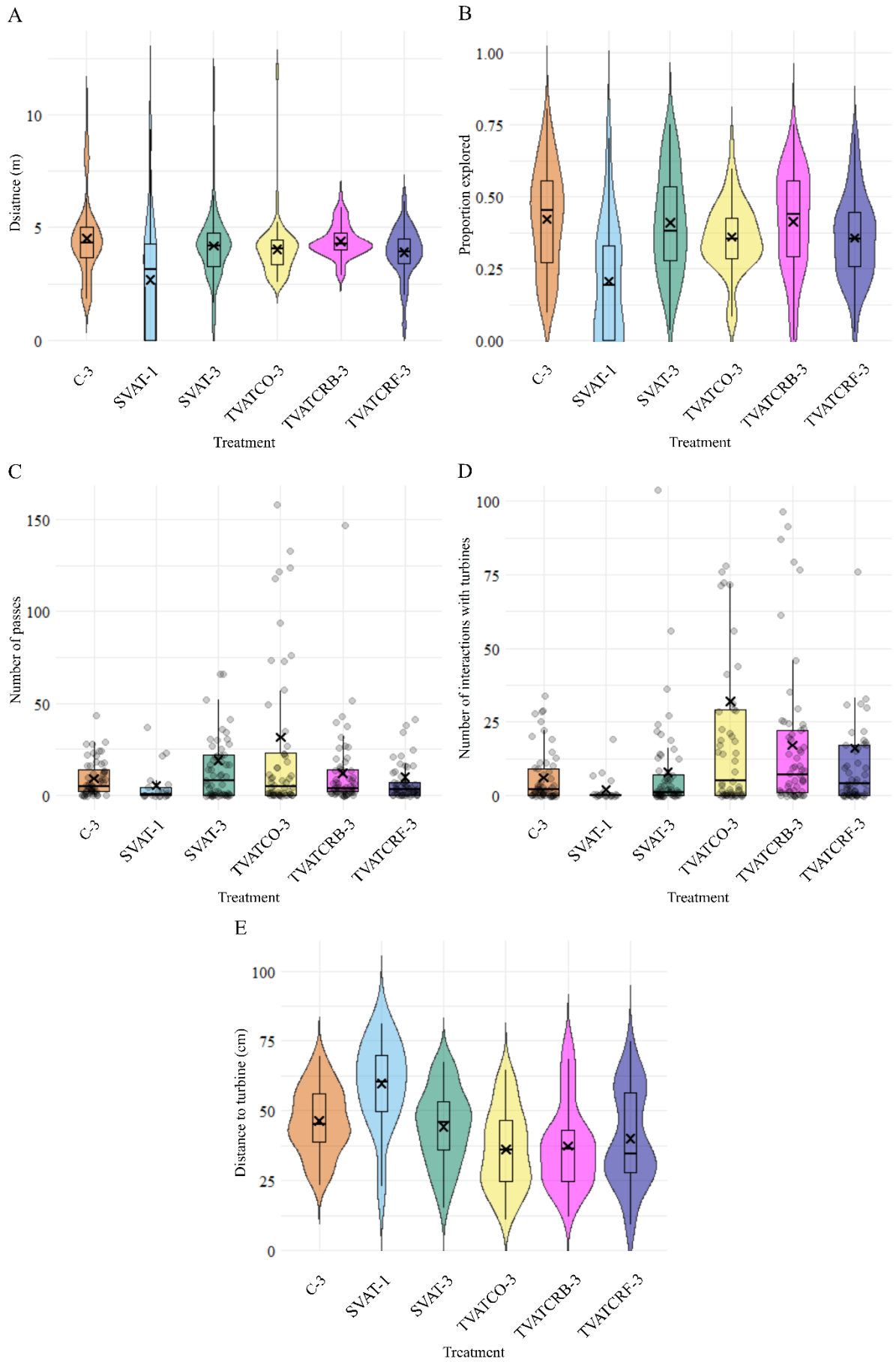
Figure 7.3. Violin and Boxplots describing: A) distance swam by fish in each treatment; B) The proportion of the working area explored by fish in each treatment; C) The number of times each fish passes from downstream to upstream or from upstream to downstream of the turbines by treatment; D) Number of times fish had any interaction with either turbine in every treatment; E) The average distance between fish and the nearest turbine throughout the trial by treatment. In all cases, the boxplots show median, interquartile range, and 95th percentile and the cross marks the mean.

7.3.2 Time in the working area

Fish in all treatments spent approximately 25% of time upstream and 75% downstream of the turbines (GLMM, p>0.12). Part of the downstream time was spent resting on the flow straightener, where fish in SVAT-1 spent significantly more time resting (GLMM, p=0.007) and fish in TVATCRB-3 spent significantly less time resting (GLMM, p=0.003) compared to control (C-3). Time spent in the near wake (Figure 7.3E) was highest in the three treatments with paired turbines (GLMM, p<0.005) with a mean value of 123 s which is 20.5 % of the experiment's duration, while with the rest of the treatments being statistically the same as control (Figure 7.4A). Time in the far wake, however, did not vary across treatments with the exception of TVATCRF-3 where it was 45.8% lower than control (GLMM, p=0.044). Time in the bow wake (Figure 7.4B) was the statistically the same for all treatments but TVATCO-3 in which the fish spent more time there, around 20 s on average (GLMM, p=0.0015).
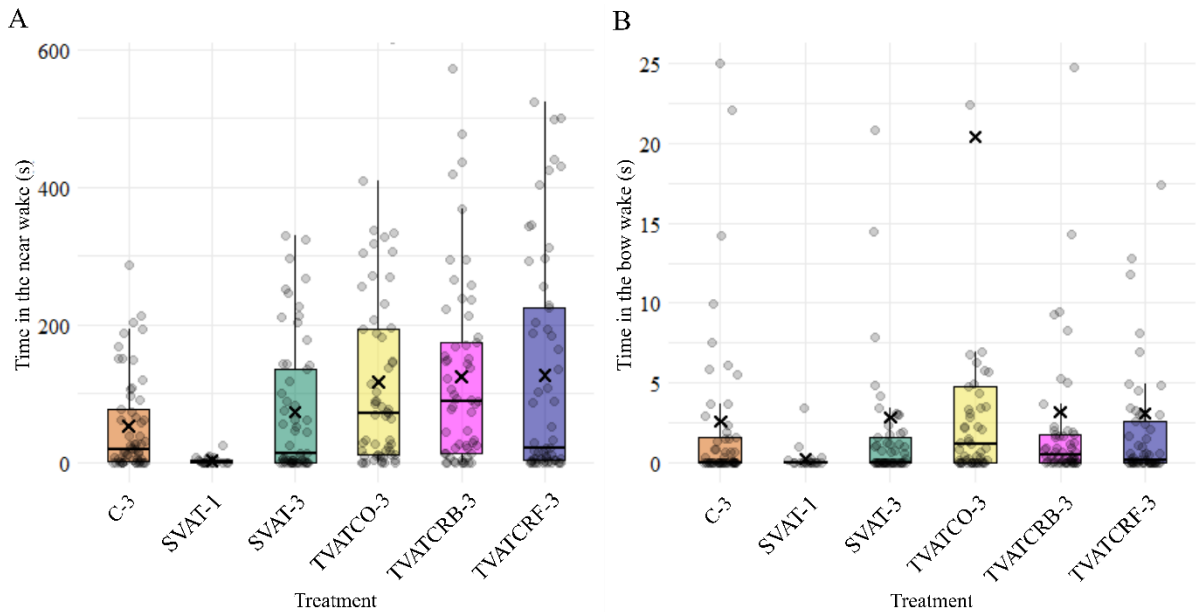
Figure 7.4. A) Time spent by fish in the near wake region (green box in Figure 7.1) by treatment; B) Total time spent per fish in the bow wake (red box in Figure 7.1) by treatment; In all cases, the boxplots show median, interquartile range, and 95th percentile and the cross marks the mean.

7.3.3 Tailbeat frequency

Overall tailbeat frequency (TBF) was 14.6% higher in C-3 than SVAT-1, SVAT-3, TVATCO-3, and TVATCRF-3 (GLMM, $p<0.02$) throughout all swimming areas. In the far wake (Figure 7.5A), the trend is consistent with the overall pattern, with all treatments having a lower TBF than control (GLMM, $p<0.012$). In the near wake, however, TBF was only significantly lower than control in treatments with paired turbines (GLMM, $p<0.002$), shown in Figure 7.5B whereas in the bow wake (Figure 7.5C), there was no statistical difference between any treatment in TBF (GLMM, $p>0.08$). When in a shoal of three fish (Figure 7.5D), the combined TBF values for all shoaling fish were lower on average by 21% in all three treatments with paired turbines (GLMM, $p<0.005$) while this was 4.1 Hz in the control (C-3) and single turbine cases (SVAT-1 and SVAT-3). When shoaling as a pair (Figure 7.5E), fish swimming together had a lower TBF only in TVATCO-3 and TVATCRF-3, all other treatments being the same as control. When swimming alone, however, all treatments but TVATCRB-3 had a lower TBF than the control (GLMM, $p<0.02$), as shown in Figure 7.5F.
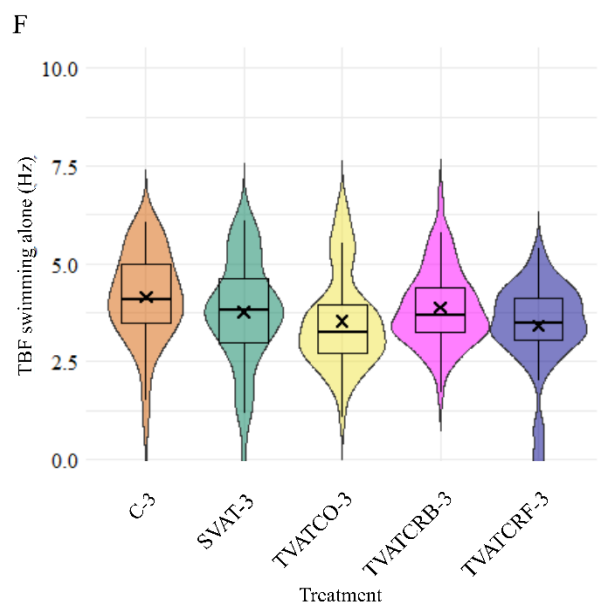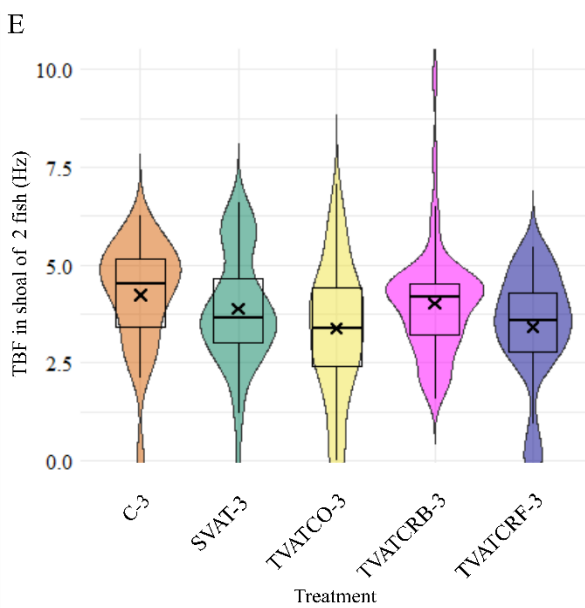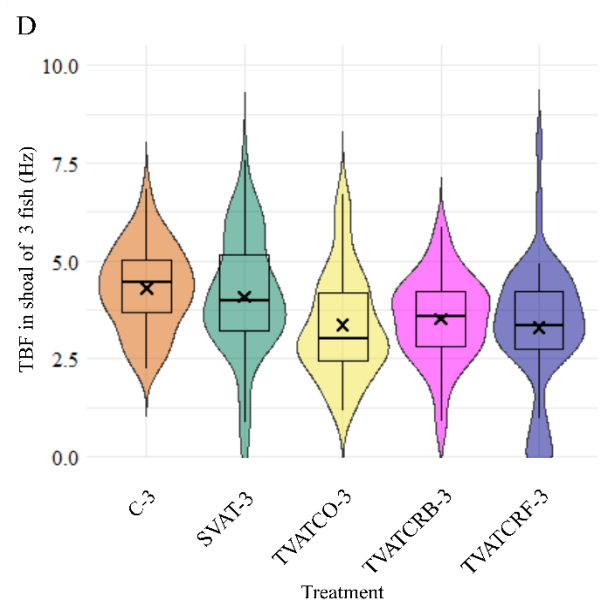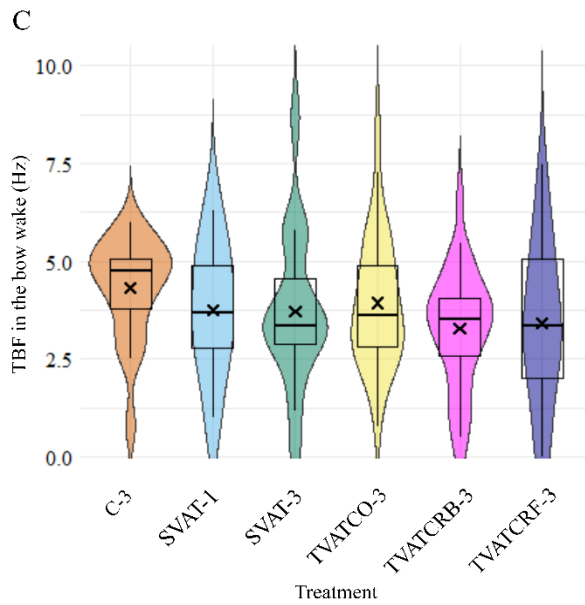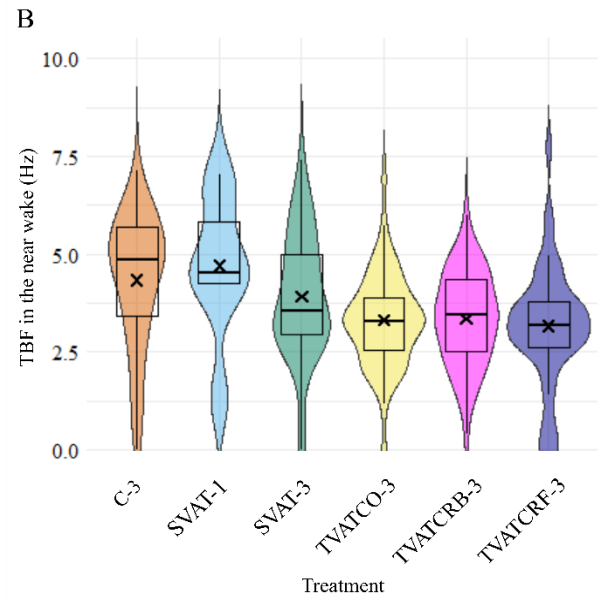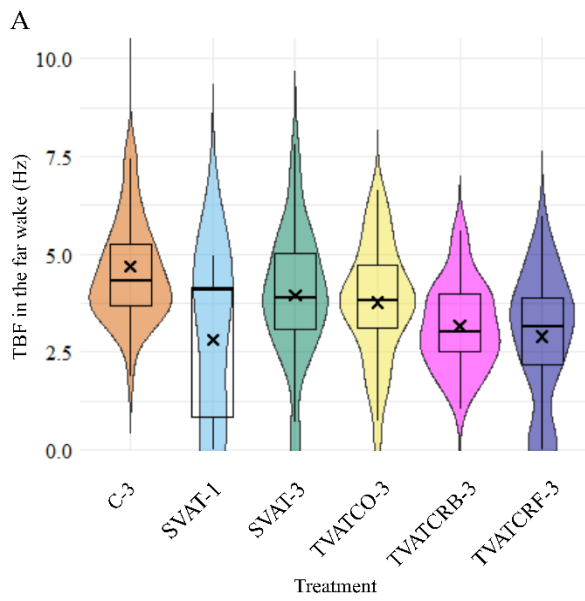
Figure 7.5. Plots of average tailbeat frequency (TBF) for each fish for several swimming areas and shoal configurations. A) Far wake (yellow box in Figure 7.1) for each treatment. B) Near wake (green box in Figure 7.1) for each treatment. C) Bow wake (red box in Figure 7.1) for each treatment. D) When swimming in a shoal of three fish for each treatment. E) For the fish swimming in a shoal of 2 fish (disregarding the fish swimming alone) for each treatment. F) When swimming alone. In all cases, the boxplots show median, interquartile range, and 95th percentile and the cross marks the mean.

7.3.4 Shoaling behaviour

While shoaling, the proportion of time that an individual led was split equally between the three fish the longer they shoaled, with an individual only appearing dominant if the shoaling duration was short (GLMM, p=0.005) and there was no difference in dominance of an individual between treatments (Figure 7.6A; GLMM, p>0.11). The proportion of time that fish spent shoaling was not related to treatment, distance, proportion of the swimming area explored, time spent within the turbine region, or time spent anywhere within the working area (GLMM, p>0.07). Shoaling, however, was associated with a reduced TBF in the bow wake (Figure 7.6B; GLMM, p=0.007) but not in the near and far wake (GLMM, p>0.62). Shoaling fish also spent less time resting, as shown in Figure 7.6C (GLMM, p=0.004), and were more likely to interact with the turbine (GLMM, p=2.4e-14).
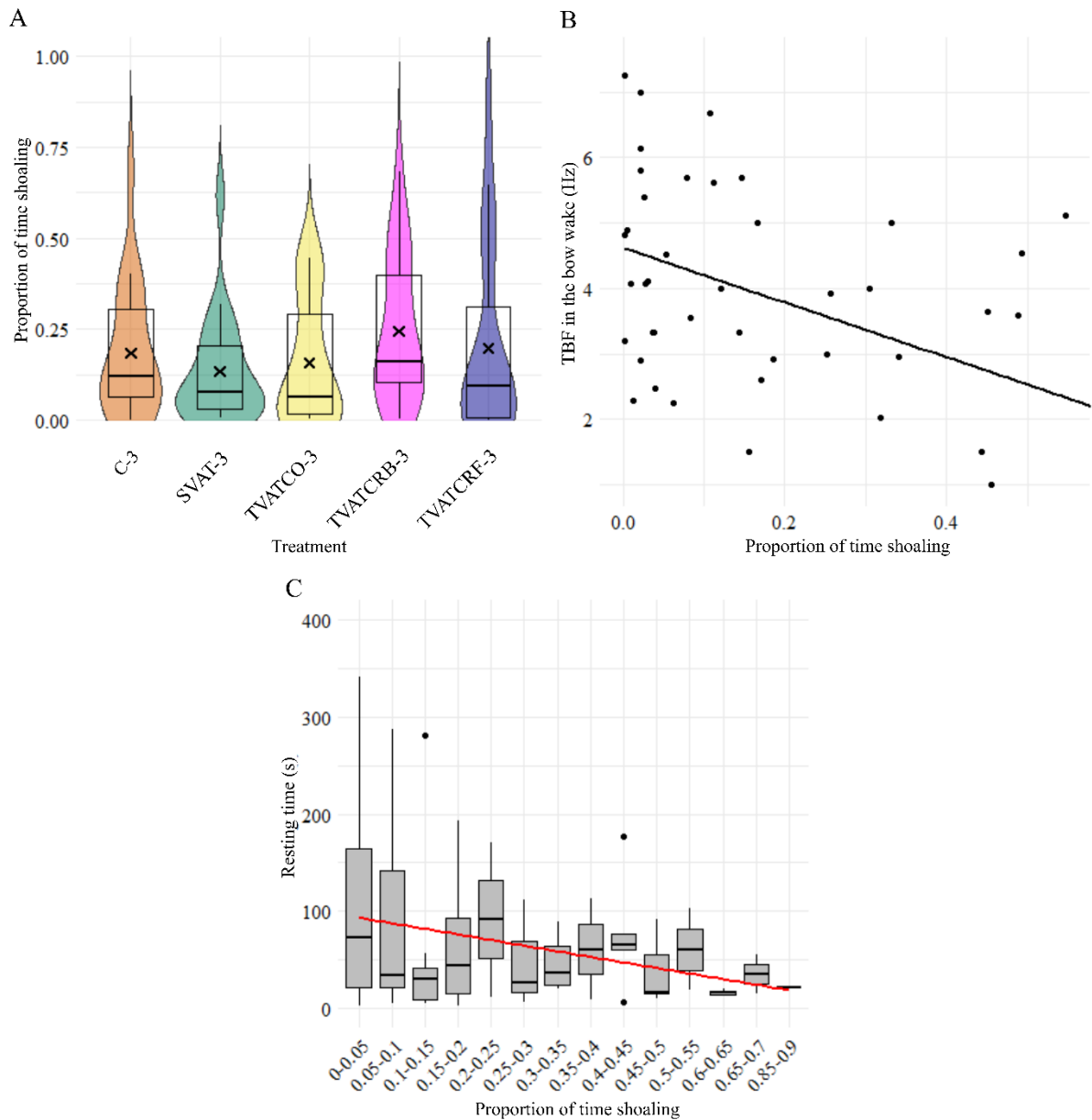
Figure 7.6. A) The proportion of time spent shoaling (combined data for a shoal of three and a shoal of two) per treatment with treatment SVAT-1 excluded. B) Inverse correlation (GLMM, p=0.007, R^2=0.15) between the proportion of time spent shoaling and the tailbeat frequency (TBF) value in the bow wake C) Negative correlation between the time spent resting on the downstream flow straightener and the proportion of time spent shoaling.

7.3.5 Individual and shoal behaviour comparison

Individual fish swam significantly shorter distances than shoaling fish with the same turbine configuration (Figure 7.3A; GLMM, p=0.02) and explored less of the working area (GLMM, p=5.6e-6) but this did not translate to a reduced passage rate. Resting time was

166

increased by an average of 181 s in SVAT-1 compared to SVAT-3 (GLMM, p=0.003), with very few turbine interactions (GLMM, p=0.002) and less time spent near the turbine (GLMM, p<0.04). Despite the presence of shoalmates in SVAT-3, fish in SVAT-1 had the same TBF values in all areas (GLMM, p>0.12).

7.4 Discussion

The turbines, for all tested configurations, did not limit fish passage in a flume where the turbines blocked 25% of the lateral space. This supports findings from laboratory and field studies evaluating Hydrokinetic turbine passage (Amaral et al., 2015; Bender et al., 2023; Berry et al., 2019; Müller et al., 2023; Yoshida et al., 2022). Narrow channels, however, can constrict movement (Hammar et al., 2013; Müller et al., 2023) but in the relatively wide channel where neither turbine nor their wakes reach the sides, fish were able to use the wide corridors with no turbines to pass up and downstream. The passage data is further supported by the lack of differences in time spent upstream and downstream of the turbines across treatments. This is despite the decrease in distance covered and proportion of the area explored caused by presence of rotating turbines, but this may be explained by fish choosing to spend more time holding station in the turbine wake. The treatments for which distance covered was lower than the control (single fish, and shoals with co-rotating turbines and forward counter-rotating turbines) were the same in which either the amount of time spent resting was higher (SVAT-1) or the amount of time entraining in the near wake and the bow wake was higher (TVATCO-3 and TVATCRF-3). TVATCO-3 was also the only treatment to have significantly higher passage rates than C-3 but still had lower distance and exploration, this may be explained by the increased time spent in the bow wake in which fish may have crossed the passage line briefly between the turbines. This is apart from TVATCRB-3 in which fish spent time in the near wake on a similar level as TVATCRF-3 but did not swim significantly shorter distances compared to C-3. The proportion of the area explored followed the trend of distance travelled and may be explained similarly by the fish finding hydrodynamic benefit generated by the turbine wake, which is absent when the turbine is stationary (Lundin et al., 2016). Finding favourable hydrodynamic conditions may then lead to a reduced need to explore areas with higher flow velocity. This conclusion can be supported by lower tailbeat frequency (TBF) values for treatments with paired turbines that produce a larger wake region and from previous studies where rainbow trout entrained behind moving foils and cylinders (Przybilla et al., 2010; Harvey et al., 2022; Thandiackal

and Lauder, 2023). The current findings also agree with existing literature (Amaral et al., 2011, 2015; Berry et al., 2019; Müller et al., 2023; Romero-Gomez & Richmond, 2014; Sonnino Sorisio et al., 2023) regarding 100% survival and no visible injuries after the trials. Although the turbine used in our study was a scaled version of a VAT and is therefore not representative of a full-scale turbine in terms of injury and mortality, the findings remain encouraging and support a field study with similar rpm ranges (Hammar et al., 2013).

The most widely observed response to turbines is avoidance (Amaral et al., 2011; Müller et al., 2023; Yoshida et al., 2022), and this was also seen in our individual fish treatment (SVAT-1), where the distance to the turbine was significantly higher and turbine interactions significantly lower than control. When shoaling, however, the trout had increased turbine interactions and spent more time closer to the turbines showing bolder behaviour as they made wider use of the near wake and bow wake, particularly for co-rotating turbines. Despite a higher count of interactions with turbines for all shoaling treatments, only fish in TVATCO-3 and TVATCRF-3 spent more time in the area very close to the turbines, suggesting either that the flow within and between the turbines was too turbulent in other treatments, or that the turbine was still perceived as dangerous by the fish and that it may not have been visible to them until very close (Sonnino Sorisio et al., 2023). Another explanation is that more time spent in the bow wake led to crossing the boundary into the upstream turbine region and spending time upstream of the turbines leading to a higher amount of time spent in the turbine area. The individual fish in SVAT-1 spent more time resting than all shoaling treatments, a behaviour also noted in our previous studies (Müller et al., 2023; Sonnino Sorisio et al., 2023) but which is not entirely explained by the hydrodynamics as the flow velocities were not considered to be particularly high for trout of this size and the shoals did not seem to create a hydrodynamic advantage. This suggests that increased resting time may be socially driven by the absence of shoalmates as revealed by the analysis of the resting time compared to the proportion of time spent shoaling (Figure 7.6C). The far wake usage by the fish did not change with treatment (except for TVATCRF-3 that had less time there) so the fish did not make use of the far wake of the rotating turbines. The velocity in the wake of a single VAT is 95% recovered by 5D (five turbine diameters) downstream of the turbine (Ouro et al., 2019) and with the TVATCRF turbine configuration, momentum recovery has occurred by 5D (Müller et al., 2021). This indicates that the potential benefits of a turbine wake like lower velocities have degraded by the downstream end of the working area, especially for TVATCRF-3, whereas TVATCO-3 was the only treatment to have a mean

value of time in the far wake above C-3 (although not significantly). This also matches well with the observed hydrodynamics which found the TVATCO configuration to have the lowest wake velocities (Müller et al., 2021). In the upstream end of the far wake region, however, there were reduced TBF values for treatments with twin turbines, showing that velocity reductions could still be exploited in what Müller et al. (2021) termed the transition zone.

Time spent in the bow wake was very consistent across treatments (t values from GLMM below 0.5) with the exception of TVATCO-3 in which significantly more time was spent there. With the TVATCO turbine setup, there is a velocity reduction at the stagnation point of the turbines which is consistent across the front of both turbines, potentially providing a more stable swimming environment for the fish than the TVATCRF, TVATCRB, and SVAT layouts (Posa, 2019). The SVAT setup has reduced velocities upstream of the turbine but to a lesser magnitude and physical extent than twin turbines, TVATCRF has a stronger velocity reduction but the velocity gradient is larger and the reduction more localised whereas TVATCRB has a lower velocity reduction and flow accelerating between the two turbines driven by the turbine rotation (Posa, 2019). The TBF on the bow wake was only reduced while the trout were shoaling, potentially indicating that it was still an unstable area to swim in for single fish since TBF was not overall lowered in the bow wake. A probability density function analysis of the midline data did not, however, reveal any obvious destabilisations of the fish swimming in the bow wake. Some shoaling studies suggest that one mechanism of information transfer and hydrodynamic benefit of shoaling is the pressure difference and lower velocity directly in front of fish behind the leader (Ren et al., 2023). These hydrodynamic conditions are partially replicated by the turbine stagnation points, so there is a possibility that fish were in effect 'shoaling' with the turbines as the VATs had diameters in the same order of magnitude as the fish (the ratio of mean fish size to turbine diameter is 0.56) and turbine rotors were spaced relatively close to each other. Similarly, time spent in the near wake was higher for all treatments with paired turbines as they produced a larger velocity reduction in the near wake compared to a single turbine (Müller et al., 2021). Tailbeat frequency data matches the trend of time spent in the near wake with TBF in the near wake being significantly lower in treatments with paired turbines. This is most likely due to the reduced velocities but could also be due to the vortices shed by the turbine blades which match the TBF of the fish (59 rpm with three blades leads to 2.95 Hz and the TBF was around 3.4 Hz) and fish have been shown to use vortex streets to reduce energy

consumption (Liao et al., 2003; Harvey et al., 2022). The vortices behind the turbines, however, are likely unsuitably placed for fish to draw a hydrodynamic gain from them so velocity reduction is the most likely explanation for the lower TBF values.

Overall, TBF was not affected by shoaling and most reductions in tailbeat frequency were associated with the turbine wake region indicating that shoaling in this study did obviously advantage to the fish contrary to previous findings reporting shoaling reducing swimming effort (Deng and Shao, 2006; Johansen et al., 2010; Marras et al., 2015; Zhang and Lauder, 2024) but in line with a previous study where not metabolic benefit was found in rainbow trout shoaling (Currier et al., 2021). An analysis of TBF by treatment filtered by shoal size also did not find differences. It is possible that a shoal of three fish was not of sufficient size to bring energetic benefits but there is evidence to show that it did affect behaviour by increasing turbine interactions and decreasing resting time. Hence, shoaling does not have an exclusively hydrodynamic role but that there are social benefits to being close to other fish.

The longer a fish shoaled, the more equally distributed the role of leader was among the shoalmates. This offers insight into the shoaling dynamics of the trout, in very short durations of shoaling there was insufficient time for fish to take their turn as leader but for longer durations, the fish were able to share this role equally, independent of treatment or location within the working area.

The ecological considerations arising from this study are overall positive. Passage remains unaffected with one or two turbines in a relatively wide channel and the probability of strike, mortality and injury are very low. There is also evidence to suggest that turbine wakes may reduce energy expenditure as fish were more likely to hold station in these areas but this may potentially lead to increased predation hotspots (Lieber et al., 2019). With passage and survival rates far exceeding those of most hydropower plants, hydrokinetic turbines could score better on evaluation techniques such as EFHI (van Treeck et al., 2021) which can be used as management tools by regulators to evaluate environmental impact. These results also highlight the difference between the behaviour of a shoal and an individual fish. Shoaling is often overlooked in flume studies assessing fish movement and behaviour but this study has shown marked differences in behaviour while shoaling thus studies with a single fish only reveal part of the picture. Shoaling is common is many species of fresh and saltwater fish and should therefore be considered more widely in future studies.

7.5 Conclusion

An experimental study of single and twin hydrokinetic turbines show that these devices nor limit upstream or downstream passage of rainbow trout neither cause any mortality or visible injury to the fish. Paired turbines led to increased engagement by shoals of trout that used the bow wake and the near wake to potentially reduce energy consumption over a single turbine because of the larger wake area and lower velocities in the wakes. Tailbeat frequency was reduced by low velocity areas in the turbine wakes but was for the most part unaffected by shoaling. Fish swimming as individuals displayed increased resting times and fewer approaches to the turbine whilst shoals were bolder and more likely to exploit the potential hydrodynamic benefits of the turbine wakes. This chapter completed the investigation into shoaling at different levels of flow complexity, completing objective 1 and combined behaviour and kinematics in response to the turbine hydrodynamics to produce as assessment of hydrokinetic turbines meeting objectives 2 and 6.

Chapter 8. Colour as a behavioural guide for fish near hydrokinetic turbines

Conceptualisation and methodology was by Prof. Jo Cable, Prof. Catherine Wilson, Dr. Stephanie Müller, Dr. Pablo Ouro, and Guglielmo Sonnino Sorisio. Data collection by Guglielmo Sonnino Sorisio and Dr. Stephanie Müller. Analysis, visualisation, and writing by Guglielmo Sonnino Sorisio and editing by all of the above.

Summary

Hydropower is a traditional and widespread form of renewable energy and vertical axis turbines are an emerging technology suitable for low to medium velocity water bodies such as rivers. Such devices can provide renewable power to remote communities but may also contribute to fragmenting already poorly connected riverine habitats and the impact could be particularly pronounced for migratory diadromous aquatic species such as salmonids by limiting their ability to pass the turbines. Optimising the design of such turbines is therefore essential to mitigate their impact on aquatic fauna. One easily altered property that does not impact turbine performance is blade colour. Here, juvenile rainbow trout (*Oncorhynchus mykiss*) free swimming within a flume were monitored in the presence of a vertical axis turbine that was either stationary or rotating, and coloured white or orange. The orange colour of the turbine significantly affected behaviour by increasing turbine avoidance and decreasing the number of potentially harmful interactions with the turbine when it was rotating, whilst not significantly affecting passage or mobility of the trout compared to the white turbine. Visibility is therefore a potentially useful tool in mitigating the environmental impact of hydrokinetic turbines.

8.1. Introduction

Renewable energy is becoming more widespread both in number and type of installation to meet global targets (UNEP, 2023). Taking the European Union directives as an example, current targets from the 2018 recast directive are 32% share of renewables by 2030 but current proposals under REPower EU aim to increase this to at least 45%, a large increase from the 2020s 22% renewable energy share (DG ENER, 2022; Eurostat, 2022).

172

Hydropower is an established technology of renewable energy but a major drawback of large hydropower schemes that span the width of the river is that they fragment the river course, separating habitats and migration pathways of diadromous fish species that move between the sea and freshwater (Belletti et al., 2020; Duarte et al., 2020). Upstream migrating fish are often delayed or prevented from travelling upstream of large dams even when passage is provided (Lundqvist et al., 2008) and downstream migrating fish may encounter extremely high mortality rates, injuries, or delays (Algera et al., 2020). Dams also impound water and prevent sediment transport in rivers (El Aoula et al., 2021; Kondolf, 1997), which can be detrimental to habitats downstream.

An emerging form of renewable energy schemes that partially mitigates the problem of fish passage is the hydrokinetic turbine. Vertical axis turbines (VAT) are particularly suitable to riverine applications, these devices do not require large alterations to the flow of the river, do not impound water and do not block the entire width of the river. Therefore, as an alternative means of producing renewable energy, they may have a reduced effect on fish migration and allow the river to remain, at least partially, connected. VATs are a suitable solution to produce power in remote communities out of reach of the main grid because of their low cost, ease of installation and wide range of operating conditions (Vermaak et al., 2014). VATs have been deployed in remote areas all over the globe and across all continents and applied to a diverse range of water bodies, from irrigation channels to large river systems (Badrul Salleh et al., 2019; Ramadan et al., 2021; Sheikh et al., 2021; Sornes, 2010). Little is known, however, about their impact on fish movement and welfare, posing the question whether VATs present a migration barrier. Like other salmonids, rainbow trout (*Oncorhynchus mykiss*) are important to wild fisheries and angling communities, having a global monetary value of up to €500 million annually (Myrvold et al., 2019) , in addition to high conservational value in their native ranges. Most salmonids are anadromous, they migrate from freshwater to the sea as juveniles (known as smolts) and return to freshwater as adults. These migrations are essential for completing their life cycle but are often disturbed by anthropogenic barriers such as hydropower schemes. Rainbow trout, having a high trophic role, have highly developed eyesight, relying on it to navigate through turbulent flows, for hunting, and are able to perceive ultraviolet and polarized light (Hawryshyn et al., 1989; Hawryshyn & Hárosi, 1994; Liao, 2006; Parkyn & Hawryshyn, 2000; Spurgeon et al., 2015). The auditory capabilities of trout are of importance when a device might also generate sound, although, rainbow trout do not appear to be sensitive to sounds produced by

hydrokinetic turbines (Popper & Hastings, 2009; Schramm et al., 2017). There is not enough data on the effect of VATs on fish passage and potential blade strike risk, but we know VATs influence the flow by creating areas of low velocity flow in their wake with high turbulent intensity and kinetic energy (Müller et al., 2021; Ouro et al., 2019). In an *in situ* study where the VAT was small in comparison to the river width, brown trout (*Salmo trutta*) avoided the turbine at all times while Atlantic salmon (*Salmo salar*) only avoided it when rotating (Bender et al., 2023). In marine settings and in lab experiments, fish displayed reduced movement around VATs (Castro-Santos & Haro, 2013; Hammar et al., 2013). Encouragingly, studies have found that no juvenile Atlantic salmon nor brown trout contacted a VAT under experimental conditions and that time spent in the vicinity of the turbine did not lead to increased mortality or injury in Atlantic salmon and American shad (Berry et al., 2019). However, the different species behave differently, salmon are generally bolder than brown trout and shad. With increasing flow velocity salmon and trout passed through the turbine more often (Berry et al., 2019). Fish species is therefore a factor that affects passage, but turbine placement and the blockage of the turbine can also affect how the fish interact with the turbines (Müller et al., 2023).

Rainbow trout are native to freshwater catchments connected to the Pacific Ocean from North America and Northern Russia to Mexico (Wild Trout Trust, 2020) but they have been introduced to many other countries where VATs are likely to be installed to support renewable energy production. Therefore, rainbow trout have been chosen as a model species to assess the impact of such devices. Instream VATs can limit rainbow trout movement as measured in a laboratory flume (Müller et al., 2023) but changing features of their design might help to reduce their environmental impact. One of the simplest alterations to wind turbines, which are typically white, is to colour one of the blades black, reducing the number of bird fatalities by 70% (May et al., 2020), indicating visibility could be key to preventing high strike rates. In the presence of a natural flood barrier, colour significantly affected fish passage with orange leading to increased passage compared to the natural wood colour of the barrier (Müller et al., 2021). Colour has also been used in the form of strobes to deter fish, as well as being used as a guidance technique (Elvidge et al., 2018; Ford et al., 2018, 2019; Jesus et al., 2019; Johnson et al., 2005). The strobes most often cause negative phototaxis (movement away from light) and the effectiveness of this solution can change with either strobe rate or colour of the light emitted (Johnson et al., 2005). Turbine visibility has been identified as a knowledge gap (Schweizer et al., 2011), consequently, colour might

be a non-invasive and inexpensive solution to mitigate potential negative impacts of turbines on multiple species, which serves as the motivation for this study.

In this study, we assess whether turbine colour can affect fish passage and reduce collision risk by evaluating the effect of VAT blade colour on the behavioural response of rainbow trout. Passage statistics, spatial and hydrodynamic preferences and the reactions of the fish were assessed in an open-channel flume with two differently coloured turbines (a white and an orange) with either rotating or stationary blades under the same bulk velocity and flow conditions.

8.2. Methods

8.2.1 Animal source, maintenance, and experimental set-up

Rainbow trout (*Oncorhynchus mykiss*) (N = 80) sourced from Bibury Trout Farm, Gloucestershire, (UK) were transported to and maintained in the Aquatics laboratory of Cardiff School of Biosciences in a Recirculating Aquaculture System (RAS). Trout were fed daily with Skretting pellets. Shortly before the experiment, the trout were moved to a circular tank (diameter = 1.3 m, height = 0.6 m) filled with dechlorinated water at 13.5 ± 0.5 °C with a 10h:14h light:dark cycle. Water from the main tank was filtered (Aquamanta, EFX 600 External Canister Filter), cooled (D-D Aquarium Solution, DC 750) and then pumped into a sump tank before being pumped back into the main tank. The tank was covered with a net to prevent trout from jumping out while still allowing light into the tank. Aeration was provided by air pumps and tank enrichment consisted of stones, pipe sections and ceramic pots. The trout were kept in this tank at a density of 2 litres per fish for at least one week prior to the flume experiments. There was no significant difference between treatments in fish standard length, total length, and mass (GLM, $p > 0.05$), the average values for these measurements are given in Table 8.1.

Table 8.1. Average lengths (and standard deviation) of the fish used in all four treatment groups, with 20 fish tested per treatment.

Treatment Name	Standard Length (mm)	Total Length (mm)	Mass (g)
White Rotating (WR)	56.2 ± 5.2	65.7 ± 5.7	2.9 ± 0.7
White Stationary (WS)	57.0 ± 5.5	67.9 ± 7.6	3.4 ± 0.9
Orange Rotating (OR)	56.1 ± 5.8	67.4 ± 6.3	2.8 ± 0.9
Orange Stationary (OS)	56.3 ± 7.3	66.8 ± 7.5	2.9 ± 1.0

The open channel recirculating flume located at Cardiff School of Engineering (UK) used for this study was 10 m long, 0.3 m wide and 0.3 m tall with a fixed 1/1000 bed slope and glass side walls. The 1.2 m long working section was located at 4.8 m to 6 m from the upstream inlet of the flume, bounded by aluminium honeycomb flow straighteners (metallic grey). At the water surface a perspex sheet was used to enhance the view from above. The vertical axis turbine, illustrated in Figure 8.1, was mounted on the center line of the working section. The flume bed was made from white plastic. The flume was filled with dechlorinated water and the temperature controlled (D-D Aquarium Solution, DC 2200) and maintained at 15 ± 2 °C. After the experiments, the trout were transferred to a secondary holding tank with similar environmental conditions adjacent to the flume. At the end of the experimental day, the trout were transported back to the Aquatics lab and not re-used.

The turbine used in this experiment was a vertical axis turbine (Figure 8.1) with a diameter and height of 120 mm, representing an 18:100 scale resolution. The turbine comprised of a 6 mm diameter central shaft to which three blades were mounted (S. Müller, Muhawenimana, et al., 2021). Each blade had a NACA0015 profile and chord length of 30 mm, and was mounted to the shaft using two 3 mm diameter struts. The blades were additively manufactured using laser sintering with PA2200 nylon. The central shaft and the struts were stainless steel, which held the bottom of the blades 20 mm above the flume bed. The geometric scale of the turbine diameter in relation to the mean standard fish length was approximately 1:2.15.
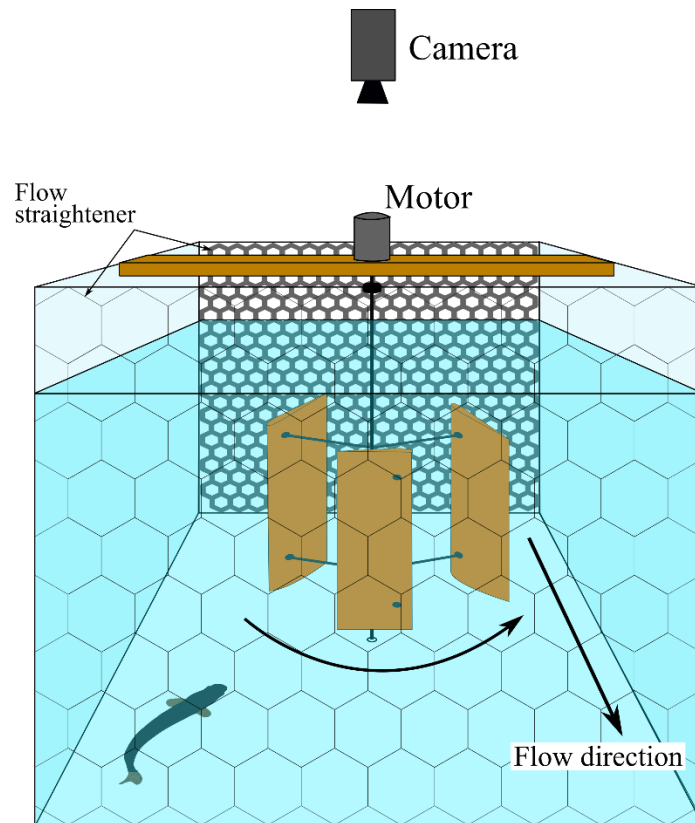
Figure 8.1. Experimental setup of the working area through the flume cross-section, looking in the upstream direction. The motor that drives the vertical axis turbine (VAT) is mounted on a support structure that holds the turbine vertically and the bottom of the turbine shaft is inserted into a bearing on the flume bed. The sides of the area are bounded by glass walls, and the upstream and downstream ends bounded by flow straighteners. The camera is mounted above the flume to record fish behaviour.

The bottom end of the turbine's central shaft is inserted into a bearing in the flume bed to allow it to rotate freely while the upper end was connected to the motor and encoder which were mounted on a plastic beam, spanning the width of the flume to hold the turbine in place. The turbine was located centrally within the working section, 0.6 m from each flow straightener and 0.15 m from each sidewall. The colour of the blades when manufactured was white and this represented our control treatments. For two of our four treatments, the blades were painted orange with custom orange paint mixed to be equivalent to 610 nm, this was chosen to match a range of red colours that affected fish behaviour in previous studies. The water-resistant paint was applied in two coats, it was left to dry completely before being mounted onto the turbine body, and it did not degrade over the test period.

The working area of the flume was lit by four neutral white lights with average illuminance of this area being 1858 lx (measured with a Testo 540 Pocket Light Meter at 10 locations across the working area and spatially averaged). The fish behavioural trials were recorded by two cameras, a Baumer camera (Baumer VLXT-50M.I) mounted above the flume recording at 80 frames per second (fps) in greyscale, and a GoPro Hero 5 camera on the side of the flume recording through the glass wall at 25 fps in colour.

8.2.2 Experimental design

Flow depth and bulk velocity were kept constant over all treatments and along the length of the flume, the flowrate (Q) was 13 L/s and the flow depth (h) was adjusted to be 0.23 m by the weir at the downstream end of the flume, producing a bulk velocity ($\bar{U}$) of 0.19 m/s. These conditions correspond to a flow Reynolds number based on the hydraulic radius of the flume (R) $Re = \frac{\rho \bar{U} R}{\mu}$ of 13,184 where ρ is the fluid's density, μ is the dynamic viscosity and $\bar{U}$ is bulk velocity. Four treatment conditions were tested: WS, WR, OS and OR, where W = white blades, O = orange blades, S = stationary turbine and R = rotating turbine, outlined in Table 8.2. When the turbine was rotating, the rotational speed (ω) was set to 59 rotations per minute (RPM). For each of the four experimental treatments, N = 20 fish were used per treatment with a total of 80 fish used. The bulk velocity was chosen to be in the range of the sustained swimming speed for the fish to avoid fish becoming exhausted which would affect the results (Wilson & Wood, 1992).

Table 8.2. Treatment details and flow conditions. Flowrate (Q) and flow depth (h) were kept constant whilst the turbine speed (ω) and the turbine colour varied. For all treatments, N = 20.

Treatment Name	$\bar{U}$ (ms^{-1})	h (m)	Q (Ls^{-1})	ω (rpm)	Turbine Colour
White Rotating (WR)	0.19	0.23	13	0	White
White Stationary (WS)	0.19	0.23	13	59	White
Orange Rotating (OR)	0.19	0.23	13	0	Orange
Orange Stationary (OS)	0.19	0.23	13	59	Orange

The fish were allowed to acclimate to flume conditions for 20 minutes prior to 10 minutes of behavioural recording. During acclimation, flow velocity was increased in three steps and

if the turbine was rotating then its speed was also increased in three steps. Before each fish were released into the working area by net, the flowrate was adjusted to 6 L/s and the turbine to 7 RPM. After 5 minutes, the flowrate was increased to 9 L/s and the turbine to 30 RPM, after a further 5 minutes the flowrate was increased again to 13 L/s and the turbine to 59 RPM. To complete acclimation, each fish was left for a further 10 minutes before it was removed from the flume and placed in a temporary tank producing a total acclimation time of 20 minutes per fish followed by the test. The working area was then covered with a 10 mm thick plexiglass sheet to avoid reflections of the water surface when the image was captured by the camera above the flume. The camera was set to record for 10 minutes and 30 seconds, with the first 30 seconds accounting for the time in which the trout were re-released at the downstream end of the working area. On completion of the flume trial, the plexiglass sheet was removed, the trout re-captured and the standard length, total length and mass measured with vernier calipers and scales. The total time each trout was in the flume for was therefore 30 minutes and 30 seconds; 20 minutes of acclimation and 10.5 minutes of test.

8.2.3 Data analysis

To analyse the behaviour of the trout under the four different treatments, video recordings were analysed using JWatcher software v1.0 (Blumstein et al., 2000; Blumstein & Daniel, 2007). This software allows the user to specify behaviours and assign keys to them so that when a particular behaviour starts and the associated key is pressed, the software will record the time ($\pm$ 1 ms) and duration of this behaviour. Duration was calculated by recording the amount of time elapsed until the next key was pressed as behaviours (Table 8.3) are assumed to be mutually exclusive unless specified otherwise. Modifiers can be added to the behaviours and each modifier is also assigned a key; for this study, adding modifiers allowed further differentiation between swim forward, swim backward, station holding, and passing behaviours. The working area was split into 12 sections as shown in Figure 8.2 and each section was assigned a corresponding key to work as a modifier for these four behaviours. JWatcher includes an analysis function which processes the raw behavioural data and presents a summary for each behaviour and modifier for both the total time the fish spent in each behaviour and the number of total times the behaviour was observed.

179

Table 8.3. Behaviours and their descriptors used to analyse the video data at a reduced framerate of 40 fps. Further clarification of the modifiers is given in bold, see Figure 8.2.

Behaviour	Description
Swim Forwards	The fish swims forward more than one fish length while facing upstream (positive rheotaxis); **subject to modifiers in Figure 8.2.**
Swim Backwards	The fish swims, either facing upstream (drifting) or downstream (negative rheotaxis), more than one fish length in the downstream direction; **subject to modifiers in Figure 8.2.**
Station Holding	The fish swims steadily and remains in the same place± 2 BL; **subject to modifiers in Figure 8.2.**
Rest	The fish does not swim and rests either against the downstream flow straightener, wall or on the flume bed.
Approach	The fish swims directly upstream towards the turbine and reaches within one turbine diameter of the turbine.
Entrain	The fish swims in the near wake of the turbine (within 2 turbine diameters) and holds station in the near wake.
Pass	The fish passes by or through the turbine and moves from either the upstream area into the downstream area or from the downstream area into the upstream area. **Modifiers Y and D were used to differentiate between up and downstream passes.**
Rejection	The fish approaches the turbine or attempts to pass by but sharply turns and quickly swims away.
Far Wake Swimming	The fish swims in the wake of the turbine and holds station more than 2 turbine diameters downstream of the turbine.
Front	The fish swims within 1 turbine diameter upstream of the turbine and holds station facing upstream, also known as bow-waking.
Hit or Strike	The fish makes physical contact with the turbine blade.
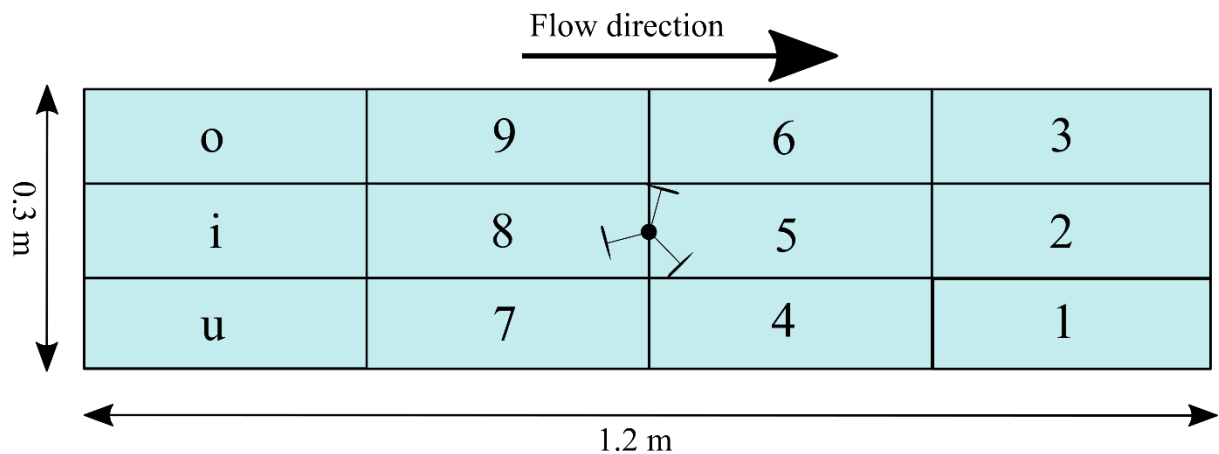
Figure 8.2. The working area represented as smaller subsections and the keyboard codes used to pair the location of behaviours (Table 8.3) with location within the working area. The letters U, I and O were used to denominate the furthest upstream zones. Turbine not to scale.

Reliability testing was carried out for JWatcher to assess scoring accuracy. Three videos were randomly sampled from the dataset and analysed twice, one week apart. The reliability test function was used to estimate accuracy which was evaluated to be 94.3% (mean average of the accuracy for three videos). The main sources of error came from differences in key order and timing when the fish moved quickly. These differences had a negligible overall impact on the video analysis. Time spent resting was not included in the analysis of time spent in each section of the flume as the only place the fish could rest was against the downstream straightener or on the flume bed immediately upstream of it. This would lead to the downstream sections of the working area appearing to be more preferable than in reality.

Further analysis to track the path of each fish was conducted with Animal Tracker (Gulyás et al., 2016) in ImageJ. For this application the video recordings of the fish were converted to 4 fps videos using Matlab (2022a) to minimise computational effort whilst still obtaining precise tracking data. The tracking area was designed with the *Zone Designer* module in the program. The selected area included the entire flume section available to the fish and excluded the turbine and its supports as well as everything outside the flume. This *Zone* file was saved and used for all fish and treatments. The *Tracker* module was then used to filter out all objects that were stationary for the duration of the video with the background

subtractor. A gaussian blur filter was added to reduce the likelihood of small particles in the flow being picked up by the tracker. A threshold was established for each video separately to maximise the visibility of the fish whilst minimizing any noise or other source of movement in the video. Post-processing filters to exclude objects too big or too small and to erode and dilate the image were applied to further isolate the fish and improve the tracking. Tracking began after the 30 seconds allowed for the fish to be released into the flume. After tracking, the results were first checked to ensure the fish had been followed accurately and then saved. The tracking was then verified and repeated if necessary. This was used to calculate paths, distances, and velocities of the fish.

8.2.4 Statistical analysis

All data was statistically analysed with R version 4.2.2 (R Core Team, 2022). The data was first inspected for normality of the data and checked with a Shapiro-Wilk test. The data was subsequently modelled with a Generalised Linear Model (GLM) using the MASS package (Venables & Ripley, 2002), the residuals and overdispersion were then inspected and a Box Cox transformation used when necessary. The GLM used was determined by inspecting the AIC value along with residual distributions. A gaussian GLM with identity link function was used to analyse fish length, mass, total distance swam and differences in time spent in a zone or grouping of zones across treatments. Binomial GLMs were used to analyse how many fish were hit by the turbine (probit link) and how many fish passed by the turbine (cauchit link) Where the data was zero inflated, a Zero-Inflated Negative Binomial (ZINB) or a Zero-Inflated Poisson (ZIP) model was used with the pscl package (Zeileis et al., 2008). ZINB models with a logit link function were used to analyse number of passes, rejection, entrain, upstream and comparison of time spent in different zones within the same treatment. A ZIP model with logit link was used for the approach data. For all tests the level of significance used was $p < 0.05$.

8.2.5 Animal Ethics

All work was approved by the Cardiff University Animal Ethics Committee and conducted under UK Home Office licence PP8167141.

8.3. Results

8.3.1 General behaviour and spatial distribution

Fish approached the turbine significantly more in the white rotating (WR) treatment compared with both orange rotating (OR) and orange stationary (OS) (ZINB, $p < 0.02$, Figure 8.3D) treatments. Under the white stationary (WS) treatment there were fewer approaches than WR but not significantly (ZINB, $p = 0.1$).

Fish sharply rejected the turbine significantly more under the WR treatment (GLM, $p = 0.0002$, Figure 8.3C), with this behaviour never occurring with the stationary conditions regardless of colour and only to a lesser extent in OR. Physical contact with the turbine was most common in the WR treatment, with five strikes observed compared to one strike for OR and OS and no strikes in treatment WS. The number of strikes was not significant between any treatment (GLM, $p = 0.9$), and the fish experienced no apparent visible damage.

The entrain and bow-waking behaviours, where the fish swam immediately downstream (in the near wake) and immediately upstream of the turbine respectively, were observed most in the WR treatment (Figure 8.3E-F). Each time a fish would present these behaviours it was counted as one occurrence. Fish entrained significantly more often in WR than OS (GLM, $p < 0.01$) but not for the other two treatments, although both WS and OR had 21 and 25 fewer occurrences, respectively.

Swimming directly upstream of the turbine was also most frequently observed in WR (Figure 8.3E), with a significant difference between treatment WR and both stationary turbine treatments (GLM, $p < 0.05$). Interestingly, OR was also higher than OS (GLM, $p < 0.0005$). This result indicates potential hydrodynamic benefits as the turbine would not be in sight of the fish swimming immediately upstream of the turbine with the turbine directly behind them which means that visual impacts can be reduced in this case.
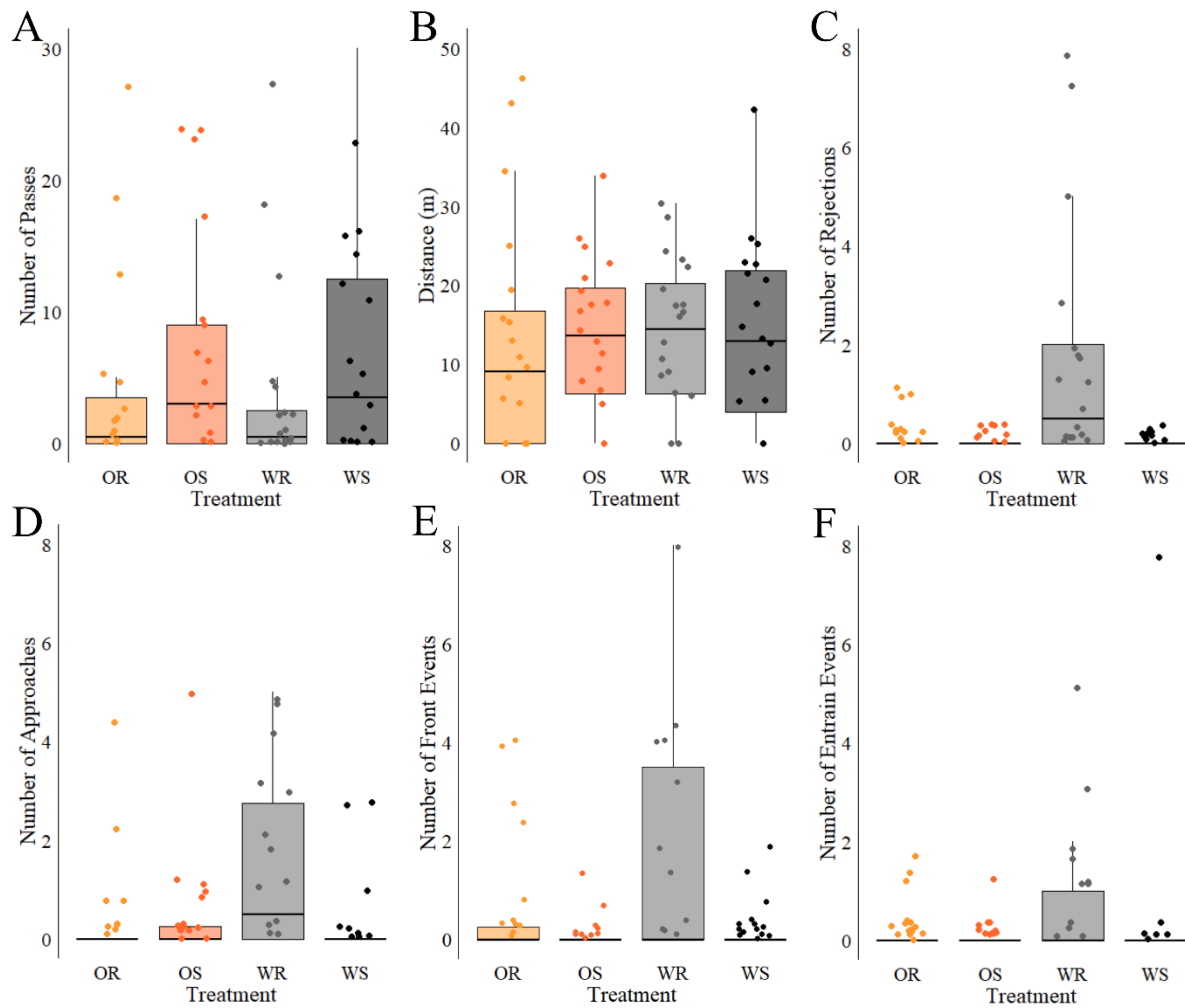
Figure 8.3. A panel of boxplots of the main behavioural and spatial results, the boxes show interquartile range and the whiskers represent 95% range of the data. OR = Orange Rotating, OS = Orange Stationary, WR = White Rotating, WS = White Stationary. The plots in this figure show different metrics by treatment, each plot is labelled A-F: A = Passes, B = distance swam, C = number of rejections, D = number of approaches, E = number of bow-waking occurrences, F = number of occurrences of entrainment behind the turbine.

The number of fish passing the turbine at least once was highest in the stationary treatments, with 12 and 14 fish passing for the white (WS) and orange (OS) configurations respectively (Figure 8.3A). In the rotating turbine treatments (WR and OR), only 10 fish passed the turbine at least once but there was overall no significant difference between number of fish to pass upstream of the turbine between any two treatments (GLM, $p > 0.2$). Similarly, the number of passes per fish was highest for WS (9.4 mean passes) and OS (8.4 mean passes) whereas OR and WR had 6 and 4.7 mean passes respectively although no significant difference was found between treatments (ZINB, $p > 0.3$).
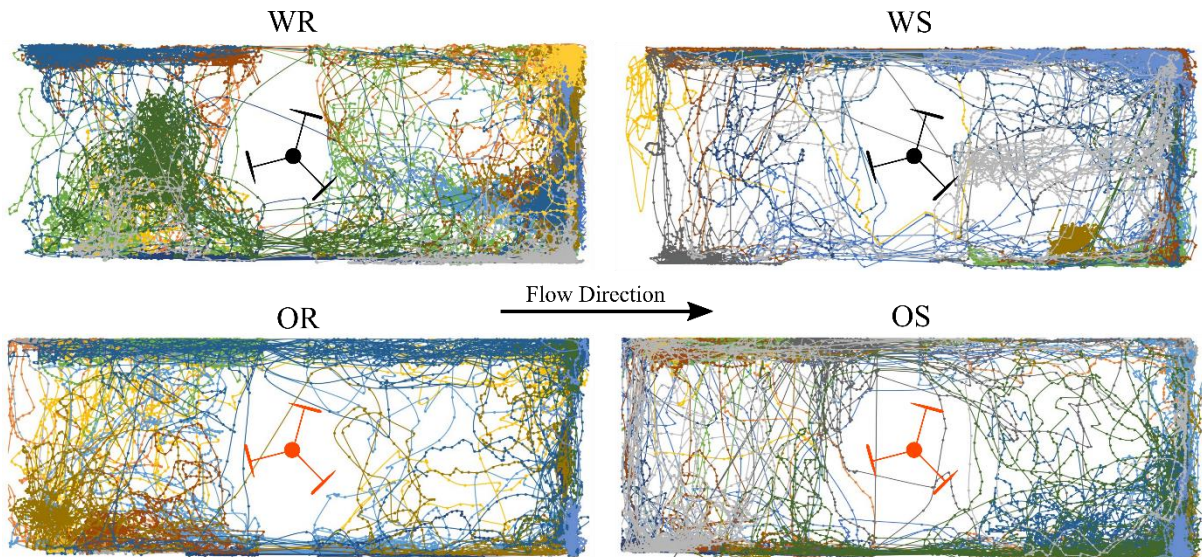
Figure 8.4. Tracked paths of each individual fish in each treatment computed with Animal Tracker. Each fish's path in each treatment is represented by a different colour and each dot on the tracked line represents each tracking frame (every 0.25 s) for this fish. The paths in the area near the turbine are interpolated since the support structure of the turbine obscured this region. The turbine is not to scale in its internal proportions. Flow from left to right. OR = Orange Rotating, OS = Orange Stationary, WR = White Rotating, WS = White Stationary.

The trajectories of fish plotted in Figure 8.4 revealed that some individuals had spatial preference for one side of the flume or a specific area (e.g. the downstream right hand side next to the wall) while others explored the entire area, highlighting how individual fish behaviour with treatment. For all treatments, there are fewer trajectories within 2 fish lengths of the turbine, which indicates avoidance behaviour. In treatments OS and OR in particular, fewer fish went near the turbine (Figure 8.5) and did not repeatedly approach the turbine when compared to treatments WS and WR. This shows that turbine rotation is not solely responsible for fish not approaching the turbine. The lack of trajectories also shows that the fish did not often swim directly in the wake of the turbine did not spend time in areas that would allow them to exploit any hydrodynamic benefits such as the lower velocities. This is further evidenced by the comparatively small proportion of time spent directly in the turbine wake as shown in Figure 8.5. The trajectory results also highlight how individual fish behaviour varies within a treatment.

The total distance travelled by fish in the different treatments do not vary significantly (GLM, $p > 0.8$; Figure 8.3B). Fish that did not rest for prolonged periods of time against the

downstream flow straightener covered around 15 m on average throughout the 10 minute experiment.

8.3.2 Temporal distribution

For the analysis of the time spent in each zone of the test section, the zones are referred to by their code specified in Figure 8.1 for simplicity, are presented in Figure 8.5 along with the temporal distribution. Fish spent significantly more time in the near wake of the turbine (zone 5) in WR than in OR (GLM, $p < 0.05$) and more time in zone 6 in WS than all other treatments (GLM, $p < 0.05$). There was no other significant difference between time spent in other individual zones and between different treatments. The combined time spent in zones 4, 5 and 6 (zones immediately downstream of turbine), however, was significantly more in WS than OR and OS (GLM, $p < 0.05$). Overall, in each treatment the least amount of time was spent in the immediate vicinity of the turbine, particularly zone 5 was avoided compared to other zones (GLM, $p < 0.05$). Zones 1, 2 and 3 (furthest downstream area) were generally used the most but that did not necessarily indicate that more time was spent downstream of the turbine. The areas in the immediate vicinity of the turbine were avoided the most but zones o, i and u (furthest upstream area) were used by the fish but not as much as zone 1, 2 and 3. In treatments OR and OS, combined time spent upstream of the turbine was approximately equal to that spent downstream of the turbine, whereas for WR and WS more time was spent downstream. There was no significant difference in side preference of the fish between treatments, indicating that the asymmetrical wake of the turbine did not cause the fish to prefer one side to the other.
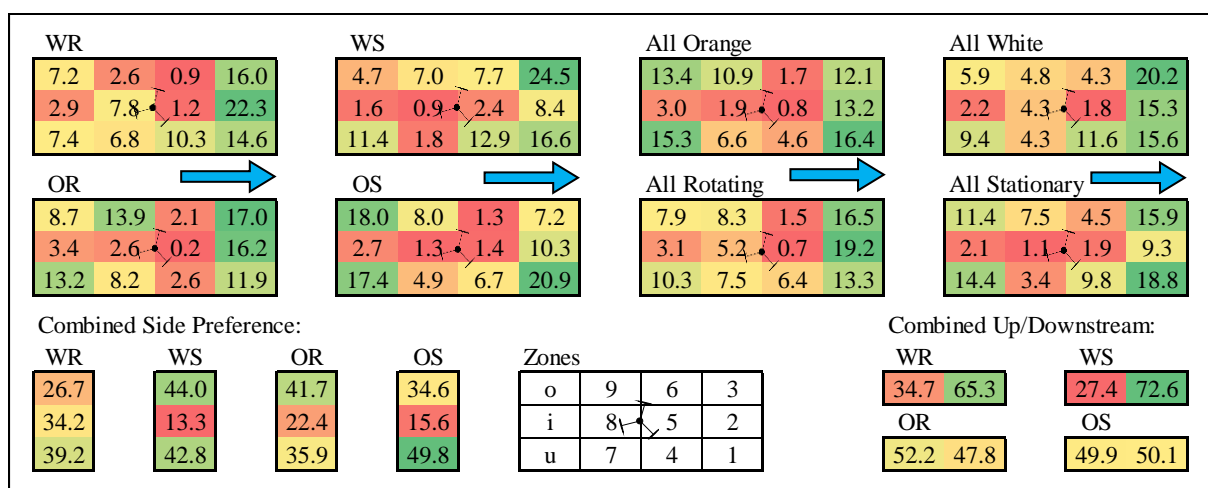
Figure 8.5. Average percentage of time spent by fish in each zone of the working area. The blue arrows indicate the flow direction, each panel within the figure represents a single

treatment or a combination of treatments or zones. The cells within the panels represent a single zone of the working area and are coloured by time spent on a sliding scale from the most time (green) to the least (red). OR = Orange Rotating, OS = Orange Stationary, WR = White Rotating, WS = White Stationary.

8.4. Discussion

The current study indicates that rainbow trout in the presence of an orange turbine spent less time in the vicinity of the turbine and experienced decreased interactions with it compared to fish encountering a white turbine. Turbine colour did not impact trout passage or general mobility such as distance covered. There was an adverse effect on temporal distribution and behaviour of the trout in the presence of white rotating (WR) turbine; fish in this treatment were most prone to dangerous interactions with the turbine. The orange turbine decreased the risk of fish colliding with the rotating turbine, coming close to it or spending time near it (zones 4, 5 and 6). This is desirable since it does not further fragment their habitat, and connectivity is unchanged but with a decreased chance of the trout being affected by the turbine, even in a channel where the turbine occupies a significant proportion of available space, which can be the case in a river setting.

There are two possible explanations for the observed change in fish behaviour in the presence of differently coloured turbines. Firstly, fish can react differently to specific colours and they may be displaying avoidance behaviour when encountering specific colours. Rainbow trout do react to colour in diverse ways; in particular, the red spectrum negatively affects growth (Heydarnejad et al., 2013; Luchiari & Pirhonen, 2008) and elevates stress levels (Heydarnejad et al., 2013). Furthermore, an orange coloured leaky barrier increased trout passage (Müller et al., 2021) and strobes of different colours (including red and orange) are an effective guidance tool for white sturgeon (*Acipenser transmontanus*), walleye (*Sander vitreus*) and European eels (*Anguilla anguilla*) (Elvidge et al., 2018; Ford et al., 2018, 2019). The other explanation for the change in behaviour is simply that the orange turbine is more visible than the white turbine to the trout, either due to the wavelength of the colour or because the orange turbine presented a greater contrast against the background in the flume. The latter seems less likely because the light levels in all treatments were high such that everything in the flume should have been visible to the fish. Despite the uncertainty of the underlying mechanism for the increased visibility of the turbine, higher visibility would allow the trout to detect the turbine at a greater distance, thereby encouraging

avoidance movements. The increased visibility explanation is supported by the findings from a wind turbine study where less turbine related fatalities in birds occurred when one of the turbine blades was painted black (May et al., 2020). The idea that visibility is the main factor influencing fish behaviour is also supported by our current results under the stationary turbine treatments. Here, colour did not cause significantly different results and the overall fish behaviour was similar (Figure 8.3). This implies that the stationary turbine was easily visible to the trout as they did not often display evasive behaviour such as rejections upon encountering the stationary turbine. This suggests that the trout were not dissuaded by the turbine when it was not moving, a similar finding to that of Bender et al. (2023) with Atlantic salmon interactions with a VAT. When the white turbine was rotating, the fish swam towards it and rejected it more often. An explanation for this is that they were not directly approaching the turbine because of being attracted to it, instead, the fish were swimming in the middle of the flume and only detected the turbine when close to it which led more frequently to the fish rejecting or colliding with the turbine. Increased rejections and time spent near the turbine may not only result in increased blade contacts, but also implies a waste of energy. When the orange turbine was rotating (OR), the data suggests it was more visible and the trout were able to avoid the turbine as they could detect its position in the flume and swim around it without being surprised and taking sudden evasive action. Importantly, the 'approach behaviour' cannot be assumed to indicate fish attraction to the turbine. As the turbine occupies 40% of the cross-sectional area of the flume, random swimming may explain proximity to the turbine.

The hydrodynamics produced by turbines and how fish react to them should be explored in future studies to explain the observed differences between rotating and stationary conditions. When the turbine is rotating it produces a region of lower velocity immediately downstream of the turbine, with this region also being highly turbulent compared to the rest of the flume (Ouro et al., 2019; Ouro & Stoesser, 2017). A wake is also generated behind the stationary turbine, although smaller in comparison to the rotating turbine's wake. There is also a small region of reduced flow velocity immediately upstream of the turbine (bow wake) but this area was not often used by the fish (Figure 8.5). The trout did not spend significantly more time in the wake of the turbine compared to other areas in any of the treatments and it is unclear to what extent the turbulence and/or reduced flow velocity in the wake affected fish motion and behaviour. A potential consequence of the turbine wake, however, is that in confined channels such as this where the velocity on either side of the turbine is increased,

turbines can affect passage and fish avoid the turbine wake (Müller et al., 2023). That means that in the current experiment the fish were more likely to interact with the turbine considering its size relative to flume width. When discussing the role that vision has in sensing a turbine, the ability of the fish to sense hydrodynamic parameters is also a factor to be considered. Fish predominantly detect flow characteristics using their lateral line organs which detect pressure changes and velocity gradients in the surrounding flow through the mechanosensory hair cells on the neuromasts (Cartner et al., 2019; Coombs et al., 1989). When reacting to any flow field, a combination of vision and lateral line sensors are responsible for fish behaviour and kinematics (Liao, 2006). This may explain the differences in behaviour between stationary and rotating treatments in the current study. However, in line with our previous study (Müller et al., 2023), the turbine wake did not seem to significantly affect fish behaviour in any of the treatments and the behavioural differences observed between treatment WR and the stationary treatments (WS and OS) were also observed when comparing OR and WR. This suggests that the colour change and not the hydrodynamics were responsible for the differences in this experiment.

A further confounding factor when considering field applications is the effect of turbidity since river water is rarely as clear as that used in this experiment. In turbid conditions there would be reduced visibility of the turbine in general and as evidenced by the results of this experiment, the trout used sight when interacting with the turbine. More studies are needed to address the role of turbidity and of light colour, type, and intensity on fish behaviour around turbines. In addition, a factor not considered in this study, but one important to investigate, was latency to pass the turbine. This metric would have been of limited use here considering the relatively short duration of the experiment but in natural conditions the fish may need to navigate multiple barriers so multiple delays could be compounded to negatively affect the fish, as barriers are pervasive in many rivers (Belletti et al., 2020; Fuller et al., 2015). Lastly, it is important to note that this study is species-specific, rainbow trout have well-developed vision and have known sensitivity to the specific colour used in this study and it is therefore necessary to evaluate other species independently before colour is adopted as a solution.

8.5. Conclusion

In summary, this experiment supports the argument that turbine colour increases visibility and in turn, reduces the threat they pose to aquatic wildlife. This is achieved by alerting

trout of the turbine presence, providing more time to select an avoidance pathway. More evidence is needed to fully understand the effect that increased visibility and colour may have on passage and behaviour and which colours most enhance visibility of the turbine and whether this is species dependent. Orange compared to white turbine blades decreased trout interactions with the turbine whilst not significantly affecting the ability of the trout to pass the turbine or swim freely through the working area. Therefore, modifying the appearance of the turbine has the potential to be an effective and low-cost solution to reduce turbine collisions and benefit fish welfare. By introducing different visual cues to the turbine and assessing the behavioural response of the fish, this chapter explored a potential mitigation measure for these turbines meeting thesis objectives 2 and 6.

Chapter 9. General Discussion

9.1 Synthesis

In a global landscape of increasing river fragmentation (Grill et al., 2019; Belletti et al., 2020) and the associated decline in biodiversity (Fahrig, 2003; Wu et al., 2019; Deinet et al., 2024), protecting the migration pathways and habitats of freshwater fish is increasingly important. To do this, fish passes are a key component, especially since the removal of a barrier is often impractical. Fish passes must be adapted not only to the type of hydraulic structure but also to the specific site of implementation and the range of fish species present (Boubée et al., 1999; Franklin et al., 2022). In addition, fish passage solutions, especially for small but frequently present migration barriers, must be cost effective if large-scale remediation of fragmentation is to be achieved. Past solutions to protect fish have been expensive and species targeted, making implementation difficult and only protecting some species of interest (van Puijenbroek et al., 2019). This thesis focused on experimentally assessing emerging anthropogenic barriers, evaluating current levels of protection offered by the existing technology and guidance, and finding new applications for existing technology as passes for multiple fish species in a set of laboratory trials using recirculating open channel flumes. In particular, this thesis assessed hydrokinetic turbines as an emerging technology and potential threat but also a possible way of remediating their negative effects, the use of existing eel tile designs as flow velocity reduction structures for velocity barriers, and the effectiveness of the current UK eel screening regulations.

Current eel screening regulations are designed to achieve 'Best Achievable Eel Protection' (Environment Agency, 2020) and aim to help the overall recovery of the critically endangered European eel (IUCN, 2024) in line with the eel regulations (UK Government, 2009). The regulations establish a range of permissible screen apertures, angles and approach velocities to prevent impingement and entrainment, but in previous tests the escape velocity has been measured around 0.1 m or more away from the screen (Environment Agency, 2020). This may be too far from the screen to capture the velocity and turbulence experienced by small fish on the screen and surrounding the process of releasing and swimming away from the screen's surface so PIV was used to quantify the near screen hydrodynamics. These analyses in Chapter 2 revealed that screen angle to the bank dominates the sweeping and escape velocities on the screen with the flow deviation caused by the screen playing a secondary role. Overall, there were not high levels of turbulence near

the screen surfaces and flow accelerations only started appearing to affect fish behaviour when the bypass was half the depth of the water column making a full depth bypass the best solution. The screens under the current regulations, however, did not produce any impingement or entrainment which only occurred at higher velocities than the regulations allow. The findings of Chapter 2 showed promising results for the current level of protection under the regulations but this was the case within a flume with no debris or sediment and low Reynolds numbers compared to realistic conditions. Understanding the hydrodynamics surrounding key aspects of fish protection and passage has allowed an understanding of dynamics of eel release from screens and how the flow deviated by the screen played a minor role.

Eel tiles were tested in Chapters 3, 4, and 5 as potential passage solutions for fish at high velocity barriers. Chapter 3 evaluated this potential by the quantification of the flow dynamics over and around the tiles. The tiles worked well to create a flow velocity reduction within and around them that could produce flows around 0.05 ms-1 but also caused an increase in turbulence, most notably by producing horizontal and vertical shear layers where slow flow met fast flow above the tiles and at the interface with the open channel. This turbulence had the advantage of only creating a localised low velocity area in the channel whilst not affecting the rest of the channel, leaving it free for fish with high swimming performance to use. Eels tested in the tiles showed higher passage rates, lower swimming effort, and were able to rest within the tiles allowing even eels with poor swimming performance to pass upstream (Chapter 4). The artificial substrate provided good passage conditions and resting spots for benthic fish at high velocity barriers and eels were able to adapt their swimming gait to make the most of the low velocity area by utilising the shear layer. Eels, however, can use the cylindrical protrusions of the tiles as a climbing substrate (which is the original concept of the tiles) but other fish species cannot. Three-spined sticklebacks are smaller than most fish and have relatively low comparative swimming performance (Taylor and McPhail, 1986) as well as swimming in a completely different mode, using pectoral fins instead of the caudal fin (Blake et al., 2005). They were therefore chosen to examine the potential of the tiles as a cross-species solution in Chapter 5. The tiles helped the sticklebacks make upstream progress but the presence of other shoalmates caused the biggest increase in passage compared to fish swimming as individuals. Encouragingly, many of the advantages of the tiles were found to be the same for sticklebacks as for eels but evidently the presence of shoalmates is a key component in stickleback passage success.

It was unclear, however, which of the many advantages of shoaling, including social and hydrodynamic (Larsson, 2012), contributed to the increase in passage, especially when swimming in the tiles and individuals divided by the protrusions thus making hydrodynamic interactions between fish unlikely. Chapter 6 examines the shoaling dynamics of sticklebacks in a bare flume to find how sticklebacks shoal in an open channel and if there is a hydrodynamic advantage. Shoaling sticklebacks experienced an overall reduction in fin beat frequency and a were able to beat their pectoral fins lower angular acceleration. This was also found to be the case for the shoal leader, showing some hydrodynamic advantage is also available for fish in front. Despite some evidence for shoaling fish showing that they need to correct more often using their caudal fins, shoaling was always beneficial suggesting that some hydrodynamic advantages exist to allow a reduced fin beat frequency at the same flow speeds, in line with findings from past studies (Partridge and Pitcher, 1979; Johansen et al., 2010; Hemelrijk et al., 2015; Marras et al., 2015; Ligman et al., 2024). Due to the comparative low complexity of flow in an empty flume juxtaposed with flow around eel tiles, some of the hydrodynamic advantages of shoaling in an open channel could be lost, and since the sticklebacks within the tiles could be separated by the cylindrical protrusions, other benefits of shoaling probably contributed to the higher passage success on top of the hydrodynamic benefits.

The effects of hydrokinetic turbines on fish behaviour and passage have previously been investigated for individual fish (Müller et al., 2023), but as established in Chapters 5 and 6, shoaling can modify fish behaviour in a range of flows so Chapter 7 evaluated the behaviour and passage of individuals and shoals of rainbow trout juveniles around different arrangements of hydrokinetic turbines. Shoaling did not change the tailbeat frequency of the fish but it did help to reduce resting time and increase boldness, again showing a social component to the benefits of shoaling. Swimming in the turbine wake reduced tailbeat frequency of the trout, particularly when the wake had lower velocities in treatments with pairs of turbines (instead of a single turbine). Passage past the turbines remained unaffected by the presence of other fish or by turbines in a channel that was wide comparative to the space taken by the turbines. In narrower channels, turbines do limit fish passage (Hammar et al., 2013; Müller et al., 2023), and due to the spatial confinement, turbine strikes are possible. Chapter 8 explored the possibility of using turbine blade colour as a behavioural deterrent to avoid collisions. Orange blades reduced turbine interactions compared to white but did not affect passage. The orange colour increased turbine visibility whereas with white

blades the fish were more likely to swim towards the turbine and only displayed avoidance behaviour when very close to the rotor. The benefits of the orange blades were linked to increased visibility rather than response to the specific colour, allowing fish to choose a turbine free pathway upstream from further away.

The findings of this thesis highlight how fish passage and protection in rivers has many potential solutions that can work for multiple species and that new directions of producing power from rivers (hydrokinetic turbines) are much more favourable in terms of fish passage than traditional HPPs. The hydrodynamics of passage play an important role in how fish adapt and use these solutions and can inform future designers to produce more efficient passes. The behavioural aspect of fish passage should not be overlooked, shoaling was a factor that was always beneficial to fish, either by producing a hydrodynamic advantage or for other reasons, and should therefore be considered more frequently in fish passage studies.

The aim and objectives of this thesis were met through chapters 2-8 as detailed below:

1. The effect of shoaling was assessed for different flow complexities revealing how in uniform flow (Chapter 6) there are highly detectable hydrodynamic, energetic, and behavioural benefits of shoaling in sticklebacks. In complex flows (Chapters 5 and 7), the behavioural benefits remained apparent increasing boldness for trout and increasing passage for sticklebacks whilst the hydrodynamic benefits were not detected. Shoaling proved an important factor in fish passage research and should be integrated more widely in future studies.

2. Through a detailed quantification of hydrodynamics (Chapters 2 and 3), and behavioural and kinematic analyses of the fish, new swimming techniques and adaptations to complex flows were discovered. Energetic and performance benefits were linked to the ability of fish to adapt their kinematics to the complex hydrodynamics and the underlying mechanisms used by the fish to exploit the screens, turbines, and tiles were found.

3. Eel tiles were found to bring benefits to European eels and three-spined sticklebacks at velocity barriers based on these flume studies for these two very morphologically and behaviourally different species (Chapters 3-5). The tiles are potentially a low cost solution that has very little effect on the overall conveyance of the channel and only modify flow in their vicinity.

4. The underlying angle dependant mechanisms of escape from a screen surface were found through a combination of hydrodynamic and kinematic analyses and a management tool was proposed to evaluate escape and sweeping velocities for wedge wire screens. Chapter 2 also confirmed the current screening regulations as appropriate for eels of the tested size.

5. Hydrodynamic analyses of passage solutions and fish protection measures (Chapter 2 and 3) were produced with fine spatial resolution to evaluate large and small scale effects of the flow and relate them to effects that may deter fish or make the conditions too harsh for them to swim in. These analyses are therefore not exclusively valid for the tested species but can also be used to pre-evaluate these solutions for other species whose swimming preferences and capabilities are known.

6. Scaled vertical axis turbines did not present a passage barrier in a relatively unconfined setting but when swimming in shoals and when the wake of the turbines produced beneficial flow conditions to lower swimming cost, the trout were emboldened towards the turbines and interacted with the turbines in ways that may be detrimental at a full scale turbine. To mitigate this risk, the colour of the blades was changed and provided better contrast to the background leading to reduced near turbine interactions whilst not affecting passage (Chapters 7 and 8).

9.2 Future research and limitations

All the experimental work presented in this thesis was conducted in laboratory flumes, this has the advantage of allowing researchers to control most variables while using live fish. Such an environment, however, inevitably fails to portray the conditions of a real river in multiple ways. Flows in flumes are tightly controlled whereas they are much more turbulent in nature, the water in the flumes is also clear and unpolluted in contrast to many freshwater environments (Wen et al., 2017). The fish in the experiments were also not in their natural environment, in part this was remedied by acclimating them to flume conditions but a flume cannot faithfully reproduce a natural river with all its complexities. A further limitation of how the experiments were conducted in terms of collecting high speed images and fine scale behaviours, is that the experiments had a fixed timescale. This was most evident as a limitation in the case of the eel tile experiments where fish that were steadily but slowly making progress upstream did not formally 'pass' upstream due to the expiration of the experimental period, leading to a likely underestimation of the benefits of the tiles.

Ideally, passage solutions should be tested with as many fish species and life stages as possible due to the large inter-species variations in swimming and behaviour (Clough et al., 2004). Future research should aim to address this by considering a variety of species for each passage solution representing the major migratory groups of species but also smaller river resident species. Other factors that affect fish behaviour and swimming could also be considered as future directions for research, this includes temperature, lighting, turbidity, heterospecific shoals and /or a wider range of flow conditions. For the eel tiles and eel screens, the flume presented clean operating conditions but did not consider (except theoretically) the effects of debris and sediment. In the case of the eel tiles, culverts often produce scour of sediment at their downstream end producing an overhang which is hard for fish to overcome and the tiles can potentially help remediate this but sediment could also clog the tiles and a future study could address this knowledge gap. Similarly, debris in rivers can block fish screens causing spots of lower or higher velocity through the screens modifying the hydrodynamics. How different screen orientations tested in Chapter 2 deal with debris accumulation and how that may impact the fish is therefore another knowledge gap for future research. Some of the chapters in this thesis required the repeated use of fish in treatments. This allowed for the reduction in total number of fish used but introduced unwanted pseudo-replication effects. These were accounted for with statistical tests, however some of these effects were difficult to test for. To validate the findings of flume studies, field studies should be performed to create a link between lab and field and evaluate higher Reynolds numbers and realistic flow conditions.

References

Agostinho, A. A., Agostinho, C. S., Pelicice, F. M., & Marques, E. E. (2012). Fish ladders: Safe fish passage or hotspot for predation? Neotropical Ichthyology, 10(4). https://doi.org/10.1590/S1679-62252012000400001

Albayrak, I., Maager, F. and Boes, R.M. 2020. An experimental investigation on fish guidance structures with horizontal bars. Journal of Hydraulic Research 58(3). doi: 10.1080/00221686.2019.1625818.

Algera, D.A. et al. 2020. What are the relative risks of mortality and injury for fish during downstream passage at hydroelectric dams in temperate regions? A systematic review. Environmental Evidence 9(1). doi: 10.1186/s13750-020-0184-0.

Amaral, S., Perkins, N., Giza, D. and McMahon, B. 2011. Evaluation of Fish Injury and Mortality Associated with Hydrokinetic Turbines. Manager.

Amaral, S. V., Bevelhimer, M.S., Čada, G.F., Giza, D.J., Jacobson, P.T., McMahon, B.J. and Pracheil, B.M. 2015. Evaluation of Behavior and Survival of Fish Exposed to an Axial-Flow Hydrokinetic Turbine. North American Journal of Fisheries Management 35(1). doi: 10.1080/02755947.2014.982333.

Ashraf I., Godoy-Diana R., Halloy J., Collignon B. and Thiria B. 2016Synchronization and collective swimming patterns in fish (*Hemigrammus bleheri*). J. R. Soc. Interface.1320160734 http://doi.org/10.1098/rsif.2016.0734

Ben Ammar, I., Cornet V., Houndji, A., Baekelandt, S., Atipine, S., Sonny, D., Mandiki, S., Kestemont P. 2021. Impact of downstream passage through hydropower plants on the physiological and health status of a critically endangered species: The European eel *Anguilla anguilla*. Comparative Biochemistry and Physiology -Part A : Molecular and Integrative Physiology 254. doi: 10.1016/j.cbpa.2020.110876.

Anderson, R. 2022. ICES Scientific Reports Rapport Scientifiques du CIEM. Available at: http://doi.org/10.17895/ices.pub.20418840.

Andersson, E., Nilsson, C. and Johansson, M.E. 2000. Effects of river fragmentation on plant dispersal and riparian flora. River Research and Applications 16(1). doi: 10.1002/(sici)1099-1646(200001/02)16:1<83::aid-rrr567>3.0.co;2-t.

El Aoula, R., Mhammdi, N., Dezileau, L., Mahe, G. and Kolker, A.S. 2021. Fluvial sediment transport degradation after dam construction in North Africa. Journal of African Earth Sciences 182. doi: 10.1016/j.jafrearsci.2021.104255.

Arai, T., Ueno, D., Kitamura, T. and Goto, A. 2020. Habitat preference and diverse migration in threespine sticklebacks, *Gasterosteus aculeatus* and *G. nipponicus*. Scientific Reports 10(1). doi: 10.1038/s41598-020-71400-4.

Ardekani, R., Greenwood, A.K., Peichel, C.L. and Tavaré, S. 2013. Automated quantification of the schooling behaviour of sticklebacks. EURASIP Journal on Image and Video Processing 2013(1). doi: 10.1186/1687-5281-2013-61.

Armstrong, G.S., Aprahamian, M.W., Fewings, A., Gough, P.J., Reader, N.A. and Varallo, P.V. 2020. Fish Pass Manual: Guidance Notes On The Legislation, Selection and Approval Of Fish Passes In England And Wales.

Badrul Salleh, M., Kamaruddin, N.M. and Mohamed-Kassim, Z. 2019. Savonius hydrokinetic turbines for a sustainable river-based energy extraction: A review of the technology and potential applications in Malaysia. Sustainable Energy Technologies and Assessments 36. doi: 10.1016/j.seta.2019.100554.

Baker, N.J., Boubée, J., Lokman, P.M. and Bolland, J.D. 2020. Evaluating the impact of hydropower on downstream migrating anguillid eels: Catchment-wide and fine-scale approaches to identify cost-effective solutions. Science of the Total Environment 748. doi: 10.1016/j.scitotenv.2020.141111.

Baltazar-Soares, M. et al. 2014. Recruitment collapse and population structure of the european eel shaped by local ocean current dynamics. Current Biology 24(1). doi: 10.1016/j.cub.2013.11.031.

Barber, I. and Ruxton, G.D. 2000. The importance of stable schooling: Do familiar sticklebacks stick together? Proceedings of the Royal Society B: Biological Sciences 267(1439). doi: 10.1098/rspb.2000.0980.

Barbin, G.P. and Krueger, W.H. 1994. Behaviour and swimming performance of elvers of the American eel, *Anguilla rostrata*, in an experimental flume. Journal of Fish Biology 45(1). doi: 10.1111/j.1095-8649.1994.tb01290.x.

Bates, D., Mächler, M., Bolker, B.M. and Walker, S.C. 2015. Fitting linear mixed-effects models using lme4. Journal of Statistical Software 67(1). doi: 10.18637/jss.v067.i01.

Battin, J. (2004). When good animals love bad habitats: Ecological traps and the conservation of animal populations. In Conservation Biology (Vol. 18, Issue 6). https://doi.org/10.1111/j.1523-1739.2004.00417.x

Beck, C. 2020. Fish protection and fish guidance at water intakes using innovative curved-bar rack bypass systems. In: VAW-Mitteilung, vol 257.

Beck, C. et al. 2020a. Swimming behavior of downstream moving fish at innovative curved-bar rack bypass systems for fish protection at water intakes. Water (Switzerland) 12(11). doi: 10.3390/w12113244.

Beck, C., Albayrak, I., Meister, J. and Boes, R.M. 2020b. Hydraulic performance of fish guidance structures with curved bars–Part 2: flow fields. Journal of Hydraulic Research 58(5). doi: 10.1080/00221686.2019.1671516.

Behrmann-Godel, J. and Eckmann, R. 2003. A preliminary telemetry study of the migration of silver European eel (*Anguilla anguilla* L.) in the River Mosel, Germany. Ecology of Freshwater Fish 12(3). doi: 10.1034/j.1600-0633.2003.00015.x.

Belletti, B., Garcia de Leaniz, C., Jones, J. et al. 2020. More than one million barriers fragment Europe's rivers. Nature 588(7838). doi: 10.1038/s41586-020-3005-2.

Bender, A., Langhamer, O., Francisco, F., Forslund, J., Hammar, L., Sundberg, J. and Molander, S. 2023. Imaging-sonar observations of salmonid interactions with a vertical axis instream turbine. River Research and Applications. Available at: https://onlinelibrary.wiley.com/doi/10.1002/rra.4171.

Berg, R. 1986. Fish passage through Kaplan turbines at a power plant on the River Neckar and subsequent eel injuries. Vie Milieu 36(4).

Berry & Escott Ltd. 2023. Eel Tiles. Available at: https://www.berryescott.co.uk/product/product-2-2/ [Accessed: 13 December 2023].

Berry, M., Sundberg, J. and Francisco, F. 2019. Salmonid response to a vertical axis hydrokinetic turbine in a stream aquarium. In: Proceedings of the 13th European Wave and Tidal Energy Conference. Naples, Italy. Available at: https://tethys.pnnl.gov/sites/default/files/publications/Berry-et-al-2019-EWTEC.pdf [Accessed: 21 July 2022].

De Bie, J. 2017. Quantification of the collective response of fish to hydrodynamics for improving downstream fish passage facilities. p. 175.

de Bie, J., Manes, C. and Kemp, P.S. 2020. Collective behaviour of fish in the presence and absence of flow. Animal Behaviour 167. doi: 10.1016/j.anbehav.2020.07.003.

de Bie, J., Peirson, G. and Kemp, P.S. 2018. Effectiveness of horizontally and vertically oriented wedge-wire screens to guide downstream moving juvenile chub (*Squalius cephalus*). Ecological Engineering 123. doi: 10.1016/j.ecoleng.2018.07.038.

de Bie, J., Peirson, G. and Kemp, P.S. 2021. Evaluation of horizontally and vertically aligned bar racks for guiding downstream moving juvenile chub (*Squalius cephalus*) and barbel (*Barbus barbus*). Ecological Engineering 170. doi: 10.1016/j.ecoleng.2021.106327.

Black, J. 2019. The science behind fish recovery and return (FRR) screens. In: Eel regulations conference.

Blake, R.W. 1979. The Mechanics of Labriform Locomotion I. Labriform Locomotion in the Angelfish (*Pterophyllum Eimekei*): An Analysis of the Power Stroke . Journal of Experimental Biology 82(1). doi: 10.1242/jeb.82.1.255.

Blake, R.W. 1981. Influence of pectoral fin shape on thrust and drag in labriform locomotion. Journal of Zoology 194(1). doi: 10.1111/j.1469-7998.1981.tb04578.x.

Blake, R.W., Law, T.C., Chan, K.H.S. and Li, J.F.Z. 2005. Comparison of the prolonged swimming performances of closely related, morphologically distinct three-spined sticklebacks *Gasterosteus* spp. Journal of Fish Biology 67(3). doi: 10.1111/j.0022-1112.2005.00788.x.

Blumstein, D.T. and Daniel, J.C. 2007. Quantifying behavior the JWatcher way. Sinauer Associates. doi: https://doi.org/10.1093/icb/icn005.

Blumstein, D.T., Daniel, J.C. and Evans, C.S. 2000. JWatcher. Available at: https://www.jwatcher.ucla.edu/ [Accessed: 13 December 2023].

Boes, R., Beck, C., Meister, J., Peter, A., Kastinger, M. and Albayrak, I. 2022. Effect of bypass layout on guidance of downstream moving fish at bar rack bypass systems. doi: 10.3850/iahr-39wc252171192022537.

Bolland, J. and Wright, R. 2009. REDEEMing pumping stations for eels.

Borazjani, I. and Sotiropoulos, F. 2009. Why don't mackerels swim like eels? The role of form and kinematics on the hydrodynamics of undulatory swimming. In: Physics of Fluids. doi: 10.1063/1.3205869.

Boubée, J., Jowett, I., Nichols, S. and Williams, E. 1999. Fish passage at culverts : a review, with possible solutions for New Zealand indigenous species. (December).

Boubée, J.A., Mitchell, C.P., Chisnall, B.L., West, D.W., Bowman, E.J. and Haro, A. 2001. Factors regulating the downstream migration of mature eels (*Anguilla* spp.) at Aniwhenua Dam, Bay of Plenty, New Zealand. New Zealand Journal of Marine and Freshwater Research 35(1). doi: 10.1080/00288330.2001.9516982.

Boubée, J.A.T. and Williams, E.K. 2006. Downstream passage of silver eels at a small hydroelectric facility. Fisheries Management and Ecology 13(3). doi: 10.1111/j.1365-2400.2006.00489.x.

Bouska, W.W. and Paukert, C.P. 2010. Road Crossing Designs and Their Impact on Fish Assemblages of Great Plains Streams. Transactions of the American Fisheries Society 139(1). doi: 10.1577/t09-040.1.

Briand, C., Fatin, D. and Legault, A. 2002. Role of eel odour on the efficiency of an eel, *Anguilla anguilla*, ladder and trap. Environmental Biology of Fishes 65(4). doi: 10.1023/A:1021172803705.

Bromley, R., Coyle, S., Hawley, K., Anderson, K. and Turnpenny, A.W.H. 2013. UK Best Practice fish screening trials study. doi: 10.2495/978-1-84564-849-7/008.

Brown, E., Sulaeman, S., Quispe-Abad, R., Müller, N. and Moran, E. 2023. Safe passage for fish: The case for in-stream turbines. Renewable and Sustainable Energy Reviews 173. doi: 10.1016/j.rser.2022.113034.

Brown, G.L. and Roshko, A. 1974. On density effects and large structure in turbulent mixing layers. Journal of Fluid Mechanics 64(4). doi: 10.1017/S002211207400190X.

Brown, L. and Castro-Santos, T. 2009. Three-dimensional movement of silver-phase American eels in the forebay of a small hydroelectric facility. In: Eels at the Edge: Science, Status, and Conservation Concerns.

Bruijs, M.C.M. and Durif, C.M.F. 2009. Silver Eel Migration and Behaviour. In: Spawning Migration of the European Eel. doi: 10.1007/978-1-4020-9095-0_4.

Bult, T.P. and Dekker, W. 2007. Experimental field study on the migratory behaviour of glass eels (*Anguilla anguilla*) at the interface of fresh and salt water. In: ICES Journal of Marine Science. doi: 10.1093/icesjms/fsm105.

Buysse, D., Mouton, A.M., Baeyens, R. and Coeck, J. 2015. Evaluation of downstream migration mitigation actions for eel at an Archimedes screw pump pumping station. Fisheries Management and Ecology 22(4). doi: 10.1111/fme.12124.

Buysse, D., Mouton, A.M., Stevens, M., Van den Neucker, T. and Coeck, J. 2014. Mortality of European eel after downstream migration through two types of pumping stations. Fisheries Management and Ecology 21(1). doi: 10.1111/fme.12046.

Cairns, D. K., Chaput, G., Poirier, L. A., Avery, T. S., Castonguay, M., Mathers, A., Casselman, J. M., Bradford, R. G. G., Pratt, T. C., Verreault, G., Clarke, K. D., Veinott, G., & Bernatchez, L. (2014). Recovery potential assessment for the American eel (Anguilla rostrata) for eastern Canada: description and quantification of threats. DFO Can. Sci. Advis. Sec. Res. Doc. 2013/134, August.

Calles, O., Karlsson, S., Hebrand, M. and Comoglio, C. 2012. Evaluating technical improvements for downstream migrating diadromous fish at a hydroelectric plant. Ecological Engineering 48. doi: 10.1016/j.ecoleng.2011.05.002.

Calles, O., Olsson, I.C., Comoglio, C., Kemp, P.S., Blunden, L., Schmitz, M. and Greenberg, L.A. 2010. Size-dependent mortality of migratory silver eels at a hydropower plant, and implications for escapement to the sea. Freshwater Biology 55(10). doi: 10.1111/j.1365-2427.2010.02459.x.

Carey, V.J. and Wang, Y.-G. 2001. Mixed-Effects Models in S and S-Plus. Journal of the American Statistical Association 96(455). doi: 10.1198/jasa.2001.s411.

Carolli, M. et al. 2023. Impacts of existing and planned hydropower dams on river fragmentation in the Balkan Region. Science of the Total Environment 871. doi: 10.1016/j.scitotenv.2023.161940.

Caroppi, G., Gualtieri, P., Fontana, N. and Giugni, M. 2018. Vegetated channel flows: Turbulence anisotropy at flow–rigid canopy interface. Geosciences (Switzerland) 8(7). doi: 10.3390/geosciences8070259.

Carr, J.W. and Whoriskey, F.G. 2008. Migration of silver American eels past a hydroelectric dam and through a coastal zone. In: Fisheries Management and Ecology. doi: 10.1111/j.1365-2400.2008.00627.x.

Carter, K.L. and Reader, J.P. 2000. Patterns of drift and power station entrainment of 0 + fish in the river trent, England. Fisheries Management and Ecology 7(5). doi: 10.1046/j.1365-2400.2000.00224.x.

Carter, L.J., Collier, S.J., Thomas, R.E., Norman, J., Wright, R.M. and Bolland, J.D. 2023. The influence of passive wedge-wire screen aperture and flow velocity on juvenile European eel exclusion, impingement and passage. Ecological Engineering 192. doi: 10.1016/j.ecoleng.2023.106972.

Cartner, S.C., Farmer, S.C., Kent, M.L., Eisen, J.S., Guillemin, K.J. and Sanders, G.E. 2019. The zebrafish in biomedical research: Biology, husbandry, diseases, and research applications. doi: 10.1016/C2016-0-02488-9.

Castro-Santos, T. and Haro, A. 2013. Survival and Behavioral Effects of Exposure to a Hydrokinetic Turbine on Juvenile Atlantic Salmon and Adult American Shad. Estuaries and Coasts 38(1). doi: 10.1007/s12237-013-9680-6.

Charmant, J. 2022. Kinovea. Available at: https://www.kinovea.org/ [Accessed: 13 December 2023].

Chaudhari, S., Brown, E., Quispe-Abad, R., Moran, E., Müller, N. and Pokhrel, Y. 2021. In-stream turbines for rethinking hydropower development in the Amazon basin. Nature Sustainability 4(8). doi: 10.1038/s41893-021-00712-8.

Chen, Z., Ortiz, A., Zong, L. and Nepf, H. 2012. The wake structure behind a porous obstruction and its implications for deposition near a finite patch of emergent vegetation. Water Resources Research 48(9). doi: 10.1029/2012WR012224.

Clough, S.C., Lee-Elliott, I.E., Turnpenny, A.W.H., Holden, S.D.J. and Hinks, C. 2004. Swimming Speeds in Fish : phase 2. Environment Agency R&D Technical Report W2-049/TR1.

Clough, S.C., Teague, N. and Webb, H. 2013. Even finer bar spacing, how low can you go? doi: 10.2495/978-1-84564-849-7/005.

Clough, S.C. and Turnpenny A W H. 2001. Swimming Speeds in Fish: phase 1. Available at:
https://assets.publishing.service.gov.uk/government/uploads/system/uploads/attachment_data/file/290589/sw2-026-tr1-e-e.pdf [Accessed: 16 March 2023].

Clough, S.C. and Turnpenny, A.W.H. 2001. Swimming speeds in fish : phase 1. Environment Agency.

Consuegra, S., O'Rorke, R., Rodriguez-Barreto, D., Fernandez, S., Jones, J. and Garcia de Leaniz, C. 2021. Impacts of large and small barriers on fish assemblage composition assessed using environmental DNA metabarcoding. Science of the Total Environment 790. doi: 10.1016/j.scitotenv.2021.148054.

Coombs, S., Peter, G. and Münz, H. 1989. The mechanosensory lateral lateral line: Neurobiology and Evolution.

Couto, T.B.A., Messager, M.L. and Olden, J.D. 2021. Safeguarding migratory fish via strategic planning of future small hydropower in Brazil. Nature Sustainability 4(5). doi: 10.1038/s41893-020-00665-4.

Cresci, A. 2020. A comprehensive hypothesis on the migration of European glass eels (*Anguilla anguilla*). Biological Reviews 95(5). doi: 10.1111/brv.12609.

Currier, M., Rouse, J. and Coughlin, D.J. 2021. Group swimming behaviour and energetics in bluegill *Lepomis macrochirus* and rainbow trout *Oncorhynchus mykiss*. Journal of Fish Biology 98(4). doi: 10.1111/jfb.14641.

Cushing, D.H. and Jones, F.R.H. 1968. Why do fish school? Nature 218(5145). doi: 10.1038/218918b0.

Daghooghi, M. and Borazjani, I. 2015. The hydrodynamic advantages of synchronized swimming in a rectangular pattern. Bioinspiration and Biomimetics 10(5). doi: 10.1088/1748-3190/10/5/056018.

Dainys, J., Stakėnas, S., Gorfine, H. and Ložys, L. 2018a. Mortality of silver eels migrating through different types of hydropower turbines in Lithuania. River Research and Applications 34(1). doi: 10.1002/rra.3224.

Dainys, J., Stakėnas, S., Gorfine, H. and Ložys, L. 2018b. Mortality of silver eels migrating through different types of hydropower turbines in Lithuania. River Research and Applications 34(1). doi: 10.1002/rra.3224.

Dalziel, A.C., Vines, T.H. and Schulte, P.M. 2012. Reductions in prolonged swimming capacity following freshwater colonization in multiple threespine stickleback populations. Evolution 66(4). doi: 10.1111/j.1558-5646.2011.01498.x.

David, L., Chatellier, L., Courret, D., Albayrak, I. and Boes, R.M. 2022. Fish Guidance Structures with Narrow Bar Spacing: Physical Barriers. In: Novel Developments for Sustainable Hydropower. doi: 10.1007/978-3-030-99138-8_7.

Dean, E.M., Infante, D.M., Yu, H., Cooper, A., Wang, L. and Ross, J. 2023. Cumulative effects of dams on migratory fishes across the conterminous United States: Regional patterns in fish responses to river network fragmentation. River Research and Applications 39(9). doi: 10.1002/rra.4173.

Dębowski, P., Bernaś, R., Skóra, M. and Morzuch, J. 2020. Route selection, migration speed, and mortality of silver eel passing through two small hydroelectric facilities. Fisheries & Aquatic Life 28(3). doi: 10.2478/aopf-2020-0016.

DEFRA. 2022. ENV15 - Water abstraction tables for England. Available at: https://www.gov.uk/government/statistical-data-sets/env15-water-abstraction-tables#full-publication-update-history [Accessed: 9 February 2024].

Deinet, S. et al. 2024. The Living Planet Index (LPI) for migratory freshwater fishes 2024 update. The Netherlands.

Dekker, W. 2003. Status of the European Eel Stock and Fisheries. In: Eel Biology. doi: 10.1007/978-4-431-65907-5_17.

Deleau, M. 2018. Impacts of Anthropogenic Sound on Fish Behaviour. University of Southampton.

Deleau, M.J.C., White, P.R., Peirson, G., Leighton, T.G. and Kemp, P.S. 2020a. The response of anguilliform fish to underwater sound under an experimental setting. River Research and Applications 36(3). doi: 10.1002/rra.3583.

Deleau, M.J.C., White, P.R., Peirson, G., Leighton, T.G. and Kemp, P.S. 2020b. Use of acoustics to enhance the efficiency of physical screens designed to protect downstream moving European eel (*Anguilla anguilla*). Fisheries Management and Ecology 27(1). doi: 10.1111/fme.12362.

Deng, J. and Shao, X. ming. 2006. Hydrodynamics in a diamond-shaped fish school. Journal of Hydrodynamics 18(1). doi: 10.1007/BF03400483.

Desrochers, D. 1995. Suivi de la Migration de L'Anguille D'Amerique (*Anguilla rostrata*) au Complexe Beauharnois: 1994.

DG ENER. 2022. Renewable Energy Directive - Non paper on complementary economic modelling. Available at: https://www.irena.org/media/Files/IRENA/Agency/Publication/2020/Nov/IRENA_Green_ Hydrogen_breakthrough_202.

Dorratcague, D.E., Leidy, G.R. and Ott, R.F. 1986. Fish screens for hydropower developments. ((ed.), New York, U.S.A., Am. Soc. Civ. Engrs., 1986, pp.1825-1834. (ISBN 0-87262-536–2)).

Drazin, P.G. 2002. Introduction to Hydrodynamic Stability. doi: 10.1017/cbo9780511809064.

Drouineau, H., Rigaud, C., Laharanne, A., Fabre, R., Alric, A. and Baran, P. 2015. Assessing the Efficiency of an Elver Ladder Using a Multi-State Mark-Recapture Model. River Research and Applications 31(3). doi: 10.1002/rra.2737.

Drucker, E.G. and Lauder, G. V. 2000. A hydrodynamic analysis of fish swimming speed: Wake structure and locomotor force in slow and fast labriform swimmers. Journal of Experimental Biology 203(16). doi: 10.1242/jeb.203.16.2379.

Duarte, G., Segurado, P., Haidvogl, G., Pont, D., Ferreira, M.T. and Branco, P. 2020. Damn those damn dams: Fluvial longitudinal connectivity impairment for European diadromous fish throughout the 20th century. Science of the Total Environment. doi: 10.1016/j.scitotenv.2020.143293.

Ebel, G. 2016. Fish Protection and Downstream Passage at Hydropower Plants Handbook of Bar Rack and Bypass Systems. 2nd ed. Büro für Gewässerökologie und Fischereibiologie.

Egg, L., Mueller, M., Pander, J., Knott, J. and Geist, J. 2017. Improving European Silver Eel (*Anguilla anguilla*) downstream migration by undershot sluice gate management at a small-scale hydropower plant. Ecological Engineering 106. doi: 10.1016/j.ecoleng.2017.05.054.

Elvidge, C.K., Ford, M.I., Pratt, T.C., Smokorowski, K.E., Sills, M., Patrick, P.H. and Cooke, S.J. 2018. Behavioural guidance of yellow-stage American eel *Anguilla rostrata* with a lightemitting diode device. Endangered Species Research. doi: 10.3354/esr00884.

Enders, E.C., Gessel, M.H. and Williams, J.G. 2009. Development of successful fish passage structures for downstream migrants requires knowledge of their behavioural response to accelerating flow. Canadian Journal of Fisheries and Aquatic Sciences 66(12). doi: 10.1139/F09-141.

Energy Institute. 2024. Statistical Review of World Energy. Available at: https://www.energyinst.org/statistical-review [Accessed: 16 July 2024].

Enstipp, M.R., Grémillet, D. and Jones, D.R. 2007. Investigating the functional link between prey abundance and seabird predatory performance. Marine Ecology Progress Series 331. doi: 10.3354/meps331267.

Environment Agency. 2009. Elver and Eel Passes: A Guide to the Design and Implementation of Passage Solutions at Weirs, Tidal Gates and Sluices. p. 97.

Environment Agency. 2020. Screening at intakes: measures to protect eel and elvers. Available at: www.environment-agency.gov.uk.

Erkinaro, J., Erkinaro, H. and Niemelä, E. 2017. Road culvert restoration expands the habitat connectivity and production area of juvenile Atlantic salmon in a large subarctic river system. Fisheries Management and Ecology 24(1). doi: 10.1111/fme.12203.

Etminan, V., Lowe, R.J. and Ghisalberti, M. 2017. A new model for predicting the drag exerted by vegetation canopies. Water Resources Research 53(4). doi: 10.1002/2016WR020090.

European Commission. EU. 2020. COMMISSION STAFF WORKING DOCUMENT EVALUATION of Council Regulation (EC) No 1100/2007 of 18 September 2007 establishing measures for the recovery of the stock of European eel.

Eurostat. 2022. EU overachieves 2020 renewable energy target.

Fahrig, L. 2003. Effects of Habitat Fragmentation on Biodiversity. Annual Review of Ecology, Evolution, and Systematics 34. doi: 10.1146/annurev.ecolsys.34.011802.132419.

Fjeldstad, H.P., Pulg, U. and Forseth, T. 2018. Safe two-way migration for salmonids and eel past hydropower structures in Europe: A review and recommendations for best-practice solutions. Marine and Freshwater Research. doi: 10.1071/MF18120.

Flores Martin, N., Leighton, T. G., White, P. R., & Kemp, P. S. (2021). The response of common carp (*Cyprinus carpio*) to insonified bubble curtains . The Journal of the Acoustical Society of America, 150(5). https://doi.org/10.1121/10.0006972

Ford, M.I. et al. 2018. Preferences of age-0 white sturgeon for different colours and strobe rates of LED lights may inform behavioural guidance strategies. Environmental Biology of Fishes 101(4). doi: 10.1007/s10641-018-0727-1.

Ford, M.I., Elvidge, C.K., Patrick, P.H., Sills, M. and Cooke, S.J. 2019. Coloured LED light as a potential behavioural guidance tool for age 0 and 2 year walleye Sander vitreus. Journal of Fish Biology 95(5). doi: 10.1111/jfb.14124.

Franke, G.F. et al. 1997. Development of Environmentally Advanced Hydropower Turbine System Design Concepts. Voith Hydro Inc. Report No. 2677-0141, Prepared for the U.S. Department of Energy, Idaho Operations Office, Idaho Falls, Idaho.

Franklin, P.A., Baker, C.F. and Reeve, K.A. 2021. A comparison of passage efficiency for native and exotic fish species over an artificial baffled ramp. Journal of Fish Biology 99(6). doi: 10.1111/jfb.14899.

Franklin, P.A., Sykes, J., Robbins, J., Booker, D.J., Bowie, S., Gee, E. and Baker, C.F. 2022. A national fish passage barrier inventory to support fish passage policy implementation and estimate river connectivity in New Zealand. Ecological Informatics 71. doi: 10.1016/j.ecoinf.2022.101831.

Fraser, S., Williamson, B.J., Nikora, V. and Scott, B.E. 2018. Fish distributions in a tidal channel indicate the behavioural impact of a marine renewable energy installation. Energy Reports 4. doi: 10.1016/j.egyr.2018.01.008.

Fuller, M.R., Doyle, M.W. and Strayer, D.L. 2015. Causes and consequences of habitat fragmentation in river networks. Annals of the New York Academy of Sciences 1355(1). doi: 10.1111/nyas.12853.

Gagnon, K., Gräfnings, M. and Boström, C. 2019. Trophic role of the mesopredatory three-spined stickleback in habitats of varying complexity. Journal of Experimental Marine Biology and Ecology 510. doi: 10.1016/j.jembe.2018.10.003.

Ghisalberti, M. 2002. Mixing layers and coherent structures in vegetated aquatic flows. Journal of Geophysical Research 107(C2). doi: 10.1029/2001jc000871.

Ghisalberti, M. and Nepf, H. 2005. Mass transport in vegetated shear flows. Environmental Fluid Mechanics 5(6). doi: 10.1007/s10652-005-0419-1.

Ghisalberti, M. and Nepf, H. 2006. The structure of the shear layer in flows over rigid and flexible canopies. Environmental Fluid Mechanics 6(3). doi: 10.1007/s10652-006-0002-4.

Gibson, R.J., Haedrich, R.L. and Wernerheim, C.M. 2005. Loss of Fish Habitat as a Consequence of Inappropriately Constructed Stream Crossings. Fisheries 30(1). doi: 10.1577/1548-8446(2005)30[10:lofhaa]2.0.co;2.

Gillis, G.B. 1998. Environmental effects on undulatory locomotion in the American eel *Anguilla rostrata*: Kinematics in water and on land. Journal of Experimental Biology 201(7). doi: https://doi.org/10.1242/jeb.201.7.949.

Van Ginneken, V., Durif, C., Balm, S.P., Boot, R., Verstegen, M.W.A., Antonissen, E. and Van Den Thillart, G. 2007. Silvering of European eel (*Anguilla anguilla* L.): Seasonal changes of morphological and metabolic parameters. Animal Biology 57(1). doi: 10.1163/157075607780002014.

Gosset, C., Travade, F., Durif, C., Rives, J. and Elie, P. 2005. Tests of two types of bypass for downstream migration of eels at a small hydroelectric power plant. River Research and Applications 21(10). doi: 10.1002/rra.871.

Gray, B.Y.J. 1936. Studies in Animal Locomotion: IV. The Neuromuscular Mechanism of Swimming in the Eel. Journal of Experimental Biology 13(2).

Grill, G. et al. 2019. Mapping the world's free-flowing rivers. Nature 569(7755), pp. 215–221. doi: 10.1038/s41586-019-1111-9.

Grill, G., Lehner, B., Lumsdon, A.E., Macdonald, G.K., Zarfl, C. and Reidy Liermann, C. 2015. An index-based framework for assessing patterns and trends in river fragmentation and flow regulation by global dams at multiple scales. Environmental Research Letters 10(1). doi: 10.1088/1748-9326/10/1/015001.

Guerra, M. and Thomson, J. 2019. Wake measurements from a hydrokinetic river turbine. Renewable Energy 139. doi: 10.1016/j.renene.2019.02.052.

Gulyás, M., Bencsik, N., Pusztai, S., Liliom, H. and Schlett, K. 2016. AnimalTracker: An ImageJ-Based Tracking API to Create a Customized Behaviour Analyser Program. Neuroinformatics 14(4). doi: 10.1007/s12021-016-9303-z.

Hadderingh, R.H. and Bakker, H.D. 1998. Fish mortality due to passage through hydroelectric power stations on the Meuse and Vecht Rivers. In: Fish Migration and Fish Bypasses.

Hadderingh, R.H., Van der Stoep, J.W. and Habraken, J.M.P.M. 1992. Deflecting eels from water inlets of power stations with light. Irish Fisheries Investigations. Serie A: Freshwater 36.

Halvorsen, S., Korslund, L., Gustavsen, P. and Slettan, A. 2020. Environmental DNA analysis indicates that migration barriers are decreasing the occurrence of European eel

(*Anguilla anguilla*) in distance from the sea. Global Ecology and Conservation 24. doi: 10.1016/j.gecco.2020.e01245.

Hammar, L., Andersson, S., Eggertsen, L., Haglund, J., Gullström, M., Ehnberg, J. and Molander, S. 2013. Hydrokinetic turbine effects on fish swimming behaviour. PLoS ONE 8(12). doi: 10.1371/journal.pone.0084141.

Hanson, C.H.J.R.W. and H.W.L. 1977. Entrapment and impingement of fishes by power plant cooling-water intakes: An overview. Marine Fisheries Review 39(10).

Harbicht, A.B. et al. 2022. Guiding migrating salmonid smolts: Experimentally assessing the performance of angled and inclined screens with varying gap widths. Ecological Engineering 174. doi: 10.1016/j.ecoleng.2021.106438.

Haro, A., Castro-Santos, T. and Boubee, J. 2000. Behavior and passage pf silver-phase American eels, *Anguilla rostrata* (LeSueur), at a small hydroelectric facility. Dana 12.

Haro, A., Castro-Santos, T., Whalen, K., Wippelhauser, G. and McLaughlin, L. 2003. Simulated effects of hydroelectric project regulation on mortality of american eels. In: American Fisheries Society Symposium.

Harrison, A.J., Walker, A.M., Pinder, A.C., Briand, C. and Aprahamian, M.W. 2014. A review of glass eel migratory behaviour, sampling techniques and abundance estimates in estuaries: implications for assessing recruitment, local production and exploitation. Reviews in Fish Biology and Fisheries 24(4). doi: 10.1007/s11160-014-9356-8.

Harvey, S.T., Muhawenimana, V., Müller, S., Wilson, C.A.M.E. and Denissenko, P. 2022. An inertial mechanism behind dynamic station holding by fish swinging in a vortex street. Scientific reports. 12(1), p. 1. doi: 10.1038/s41598-022-16181-8.

Hawryshyn, C.W., Arnold, M.G., Chaisson, D.J. and Martin, P.C. 1989. The ontogeny of ultraviolet photosensitivity in rainbow trout (*Salmo gairdneri*). Visual Neuroscience 2(3). doi: 10.1017/S0952523800001164.

Hawryshyn, C.W. and Hárosi, F.I. 1994. Spectral characteristics of visual pigments in rainbow trout (*Oncorhynchus mykiss*). Vision Research 34(11). doi: 10.1016/0042-6989(94)90137-6.

Heisey, P.G., Mathur, D., Phipps, J.L., Avalos, J.C., Hoffman, C.E., Adams, S.W. and De-Oliveira, E. 2019a. Passage survival of European and American eels at Francis and propeller turbines. Journal of Fish Biology 95(5). doi: 10.1111/jfb.14115.

Heisey, P.G., Mathur, D., Phipps, J.L., Avalos, J.C., Hoffman, C.E., Adams, S.W. and De-Oliveira, E. 2019b. Passage survival of European and American eels at Francis and propeller turbines. Journal of Fish Biology 95(5). doi: 10.1111/jfb.14115.

Hemelrijk, C.K., Reid, D.A.P., Hildenbrandt, H. and Padding, J.T. 2015. The increased efficiency of fish swimming in a school. Fish and Fisheries 16(3). doi: 10.1111/faf.12072.

Herrera-R, G.A. et al. 2020. The combined effects of climate change and river fragmentation on the distribution of Andean Amazon fishes. Global Change Biology 26(10). doi: 10.1111/gcb.15285.

Heydarnejad, S.S., Parto, M. and Pilevarian, A.A. 2013. Influence of light colours on growth and stress response of rainbow trout (*Oncorhynchus mykiss*) under laboratory conditions. Journal of Animal Physiology and Animal Nutrition. doi: 10.1111/j.1439-0396.2011.01243.x.

Holleran, C. 2023. Water abstraction statistics: England, 2000 to 2018. Available at: https://www.gov.uk/government/statistics/water-abstraction-estimates/water-abstraction-statistics-england-2000-to-2018#:~:text=In%202018%2C%20the%20most%20recent,at%2010.4%20billion%20cubic%20metres. [Accessed: 9 February 2024].

Holzner, M. 1999. Untersuchungen über die Schädigung von Fischen bei der Passage des Mainkraftwerks Dettelbach. Technische Universität München.

Hughes, K. 2024. The Mekong's Forgotten Fishes and the Emergency Recovery Plan to save them. Gland, Switzerland.

Hydrolox. 2024. Series 1800 Debris Removal / Fish Exclusion Screen.

ICES. 2020. Joint EIFAAC/ICES/GFCM Working Group on Eels (WGEEL). ICES Scientific Reports 2(85). doi: https://doi.org/10.17895/ices.pub.5982.

ICES. 2022. JOINT EIFAAC/ICES/GFCM WORKING GROUP ON EELS (WGEEL). doi: https://doi.org/10.17895/ices.pub.20418840.v1.

IUCN. 2024. The IUCN Red List of Threatened Species. Version 2024-1. Available at: https://www.iucnredlist.org [Accessed: 25 August 2024].

Jacoby, D. and Gollock, M. 2015. *Anguilla anguilla*, European Eel. Available at: http://dx.doi.org/10.2305/IUCN.UK.2014-1.RLTS.T60344A45833138.en.

Jansen, H.M., Winter, H. V., Bruijs, M.C.M. and Polman, H.J.G. 2007. Just go with the flow? Route selection and mortality during downstream migration of silver eels in relation to river discharge. In: ICES Journal of Marine Science. doi: 10.1093/icesjms/fsm132.

Jellyman, P.G., Bauld, J.T. and Crow, S.K. 2017. The effect of ramp slope and surface type on the climbing success of shortfin eel (*Anguilla australis*) elvers. Marine and Freshwater Research 68(7). doi: 10.1071/MF16015.

Jepsen, N., Klenke, R., Sonnesen, P. and Bregnballe, T. 2010. The use of coded wire tags to estimate cormorant predation on fish stocks in an estuary. Marine and Freshwater Research 61(3). doi: 10.1071/MF09038.

Jesus, J., Teixeira, A., Natário, S. and Cortes, R. 2019. Repulsive effect of stroboscopic light barriers on native salmonid (*Salmo trutta*) and cyprinid (*Pseudochondrostoma duriense* and *Luciobarbus bocagei*) species of iberia. Sustainability (Switzerland). doi: 10.3390/su11051332.

Johansen, J.L., Vaknin, R., Steffensen, J.F. and Domenici, P. 2010. Kinematics and energetic benefits of schooling in the labriform fish, striped surfperch *Embiotoca lateralis*. Marine Ecology Progress Series 420. doi: 10.3354/meps08885.

Johnson, P.N., Bouchard, K. and Goetz, F.A. 2005. Effectiveness of Strobe Lights for Reducing Juvenile Salmonid Entrainment into a Navigation Lock. North American Journal of Fisheries Management 25(2), pp. 491–501. doi: 10.1577/m04-073.1.

Jones, J. et al. 2019. A comprehensive assessment of stream fragmentation in Great Britain. Science of the Total Environment 673. doi: 10.1016/j.scitotenv.2019.04.125.

Jones, P.E. et al. 2021. Selective effects of small barriers on river-resident fish. Journal of Applied Ecology 58(7). doi: 10.1111/1365-2664.13875.

Jones, P.E., Svendsen, J.C., Börger, L., Champneys, T., Consuegra, S., Jones, J.A.H. and De Leaniz, C.G. 2020. Research article One size does not fit all: Inter- And intraspecific

variation in the swimming performance of contrasting freshwater fish. Conservation Physiology 8(1). doi: 10.1093/conphys/coaa126.

Katopodis, C. 1992. Introduction to fishway design. Oceans (January).

Kelvin, L. 1871. Hydrokinetic Solutions and Observations. Philadelphia Magazine 10, pp. 155–168.

Kemp, P.S. 2016. Meta-analyses, Metrics and Motivation: Mixed Messages in the Fish Passage Debate. River Research and Applications 32(10). doi: 10.1002/rra.3082.

Kemp, P.S. and O'Hanley, J.R. 2010. Procedures for evaluating and prioritising the removal of fish passage barriers: A synthesis. Fisheries Management and Ecology 17(4). doi: 10.1111/j.1365-2400.2010.00751.x.

Kempema, E.W. and Ettema, R. 2016. Fish, Ice, and Wedge-Wire Screen Water Intakes. Journal of Cold Regions Engineering 30(2). doi: 10.1061/(asce)cr.1943-5495.0000097.

Kerr, J.R., Karageorgopoulos, P. and Kemp, P.S. 2015. Efficacy of a side-mounted vertically oriented bristle pass for improving upstream passage of European eel (*Anguilla anguilla*) and river lamprey (*Lampetra fluviatilis*) at an experimental Crump weir. Ecological Engineering 85. doi: 10.1016/j.ecoleng.2015.09.013.

Kibel, P. 2008. FISHTEK consulting Archimedes Screw Turbine Fisheries Assessment . Phase II : Eels and Kelts .

Kirk, R.S. 2003. The impact of Anguillicola crassus on European eels. Fisheries Management and Ecology 10(6). doi: 10.1111/j.1365-2400.2003.00355.x.

Knapp, M., Montgomery, J., Whittaker, C., Franklin, P., Baker, C. and Friedrich, H. 2019. Fish passage hydrodynamics: insights into overcoming migration challenges for small-bodied fish. Journal of Ecohydraulics 4(1). doi: 10.1080/24705357.2019.1604091.

Kondolf, G.M. 1997. PROFILE: Hungry Water: Effects of Dams and Gravel Mining on River Channels. Environmental Management 21(4), pp. 533–551. doi: 10.1007/s002679900048.

Kondolf, M.G.; and Schmitt, R.J. 2018. Dams, Sediment discontinuity, and management responses. Hydrolink.March. Available at: https://hdl.handle.net/20.500.11970/109415 [Accessed: 10 September 2024].

Koukouvinis, P. and Anagnostopoulos, J. 2023. State of the Art in Designing Fish-Friendly Turbines: Concepts and Performance Indicators. Energies 16(6). doi: 10.3390/en16062661.

Kuznetsova, A., Brockhoff, P.B. and Christensen, R.H.B. 2017. lmerTest Package: Tests in Linear Mixed Effects Models. Journal of Statistical Software 82(13). doi: 10.18637/JSS.V082.I13.

Larinier, M. 2002a. Baffle Fishways. Bulletin Français de la Pêche et de la Pisciculture (364 supplément). doi: 10.1051/kmae/2002109.

Larinier, M. 2002b. Fish Passage Through Culverts, Weirs, and Estuarine Obstructions. Bulletin Français de la Pêche et de la Pisciculture (364 supplément). doi: 10.1051/kmae/2002097.

Larinier, M. 2002c. Fishways - General considerations. Bulletin Français de la Pêche et de la Pisciculture (364 supplément). doi: 10.1051/kmae/2002104.

Larinier, M. 2002d. Location of Fishways. Bulletin Français de la Pêche et de la Pisciculture (364 supplément). doi: 10.1051/kmae/2002106.

Larinier, M. 2008. Fish passage experience at small-scale hydro-electric power plants in France. In: Hydrobiologia. doi: 10.1007/s10750-008-9398-9.

Larinier, M. and Travade, F. 1998. Small-scale hydropower schemes and migratory fish passage. Houille Blanche 53(8). doi: 10.1051/lhb/1998093.

Larinier, M. and Travade, F. 2002. Downstream Migration: Problems and Facilities. Bulletin Français de la Pêche et de la Pisciculture (364 supplément). doi: 10.1051/kmae/2002102.

Larinier, M. and Travade, F. 2002. Downtsream Migration: Problems and Facilities. Bulletin Français de la Pêche et de la Pisciculture (364 supplément). doi: 10.1051/kmae/2002102.

Larsson, M. 2012. Why do fish school? Current Zoology 58(1). doi: 10.1093/czoolo/58.1.116.

Lauder. 1995. Speed effects on midline kinematics during steady undulatory swimming of largemouth bass, Micropterus salmoides. The Journal of experimental biology 198(Pt 2). doi: DOI: 10.1242/jeb.198.2.585.

Lauder, G. V. and Tytell, E.D. 2005. Hydrodynamics of Undulatory Propulsion. Fish Physiology 23(C). doi: 10.1016/S1546-5098(05)23011-X.

Leandro Velázquez-Luna, Eusebio Ventura-Ramos and Josept David Revuelta-Acosta. 2016. Effectiveness of Gabions Dams on Sediment Retention: A Case Study. Journal of Environmental Science and Engineering A 5(10). doi: 10.17265/2162-5298/2016.10.004.

de Leaniz, C.G. 2008. Weir removal in salmonid streams: implications, challenges and practicalities. Hydrobiologia 609. DOI: 10.1007/s10750-008-9397-x

Lemkecher, F., Chatellier, L., Courret, D. and David, L. 2022. Experimental study of fish-friendly angled bar racks with horizontal bars. Journal of Hydraulic Research 60(1). doi: 10.1080/00221686.2021.1903587.

Lemkecher, F., David, L., Courret, D. and Chatellier, L. 2018. Field measurements of the attractivity of bypasses for fishfriendly trashrack. In: E3S Web of Conferences. doi: 10.1051/e3sconf/20184003039.

Lenihan, E.S., McCarthy, T.K. and Lawton, C. 2019. Use of an acoustic camera to monitor seaward migrating silver-phase eels (*Anguilla anguilla*) in a regulated river. Ecohydrology and Hydrobiology 19(2). doi: 10.1016/j.ecohyd.2018.07.001.

Liao, J.C. 2006. The role of the lateral line and vision on body kinematics and hydrodynamic preference of rainbow trout in turbulent flow. Journal of Experimental Biology 209(20), pp. 4077–4090. doi: 10.1242/jeb.02487.

Liao, J.C. 2007. A review of fish swimming mechanics and behaviour in altered flows. Philosophical Transactions of the Royal Society B: Biological Sciences 362(1487). doi: 10.1098/rstb.2007.2082.

Liao, J.C., Beal, D.N., Lauder, G. V. and Triantafyllou, M.S. 2003. The Kármán gait: Novel body kinematics of rainbow trout swimming in a vortex street. Journal of Experimental Biology 206(6). doi: 10.1242/jeb.00209.

Lieber, L., Nimmo-Smith, W.A.M., Waggitt, J.J. and Kregting, L. 2019. Localised anthropogenic wake generates a predictable foraging hotspot for top predators. Communications Biology 2(1). doi: 10.1038/s42003-019-0364-z.

Ligman, M., Lund, J. and Fürth, M. 2024. A comprehensive review of hydrodynamic studies on fish schooling. Bioinspiration and Biomimetics 19(1). doi: 10.1088/1748-3190/ad1335.

Lindsey, C.C. 1978. Form, function, and locomotory habits in fish. In: Fish Physiology. doi: 10.1016/S1546-5098(08)60163-6.

Liu, C., Shan, Y. and Nepf, H. 2021. Impact of Stem Size on Turbulence and Sediment Resuspension Under Unidirectional Flow. Water Resources Research 57(3). doi: 10.1029/2020WR028620.

Lou, S., Chen, M., Ma, G., Liu, S., Zhong, G. and Zhang, H. 2021. Modelling of stem-scale turbulence and sediment suspension in vegetated flow. Journal of Hydraulic Research 59(3). doi: 10.1080/00221686.2020.1780491.

Luchiari, A.C. and Pirhonen, J. 2008. Effects of ambient colour on colour preference and growth of juvenile rainbow trout *Oncorhynchus mykiss* (Walbaum). Journal of Fish Biology 72(6). doi: 10.1111/j.1095-8649.2008.01824.x.

Lundin, S., Forslund, J., Goude, A., Grabbe, M., Yuen, K. and Leijon, M. 2016. Experimental demonstration of performance of a vertical axis marine current turbine in a river. Journal of Renewable and Sustainable Energy 8(6). doi: 10.1063/1.4971817.

Lundqvist, H., Rivinoja, P., Leonardsson, K. and McKinnell, S. 2008. Upstream passage problems for wild Atlantic salmon (*Salmo salar* L.) in a regulated river and its effect on the population. Hydrobiologia 602(1). doi: 10.1007/s10750-008-9282-7.

Magaju, D., Montgomery, J., Franklin, P., Baker, C. and Friedrich, H. 2021. Spoiler baffle patch design for improved upstream passage of small-bodied fish. Ecological Engineering 169. doi: 10.1016/j.ecoleng.2021.106316.

Marras, S., Killen, S.S., Lindström, J., McKenzie, D.J., Steffensen, J.F. and Domenici, P. 2015. Fish swimming in schools save energy regardless of their spatial position. Behavioral Ecology and Sociobiology 69(2). doi: 10.1007/s00265-014-1834-4.

May, R., Nygård, T., Falkdalen, U., Åström, J., Hamre, Ø. and Stokke, B.G. 2020. Paint it black: Efficacy of increased wind turbine rotor blade visibility to reduce avian fatalities. Ecology and Evolution 10(16). doi: 10.1002/ece3.6592.

Mayer, P.C. 2010. Economic models of fish shoal (school) size: A near comprehensive view of single species shoaling strategy. Journal of Bioeconomics 12(2). doi: 10.1007/s10818-010-9084-7.

McCleave, J.D. 1980. Swimming performance of European eel (*Anguilla anguilla* (L.)) elvers. Journal of Fish Biology 16(4). doi: 10.1111/j.1095-8649.1980.tb03723.x.

McDowall, R.M. 1992. Diadromy: Origins and Definitions of Terminology. Copeia 1992(1). doi: 10.2307/1446563.

Mehlis, M., Thünken, T., Bakker, T.C.M. and Frommen, J.G. 2015. Quantification acuity in spontaneous shoaling decisions of three-spined sticklebacks. Animal Cognition 18(5). doi: 10.1007/s10071-015-0884-y.

Meister, J. 2020. Fish protection and guidance at water intakes with horizontal bar rack bypass systems. doi: https://doi.org/10.3929/ethz-b-000455545.

Meister, J., Fuchs, H., Beck, C., Albayrak, I. and Boes, R.M. 2020a. Head losses of horizontal bar racks as fish guidance structures. Water (Switzerland) 12(2). doi: 10.3390/w12020475.

Meister, J., Fuchs, H., Beck, C., Albayrak, I. and Boes, R.M. 2020b. Velocity fields at horizontal bar racks as fish guidance structures. Water (Switzerland) 12(1). doi: 10.3390/w12010280.

Miller M, Sharkh SM, Kemp PS. 2024. Laying the foundations for selective-fish guidance using electricity: multi-species response to pulsed direct currents. PeerJ. Sep 16;12:e17962. doi: 10.7717/peerj.17962.

Motyka, R. et al. 2024. Downstream passage performance of silver eel at an angled rack: effects of behavior and morphology. Hydrobiologia. doi: 10.1007/s10750-024-05530-5.

Mouton, A.M., Stevens, M., Den Neucker, T. Van, Buysse, D. and Coeck, J. 2011. Adjusted barrier management to improve glass eel migration at an estuarine barrier. Marine Ecology Progress Series 439. doi: 10.3354/meps09325.

Muhawenimana, V. et al. 2021. Temperature surpasses the effects of velocity and turbulence on swimming performance of two invasive non-native fish species. Royal Society Open Science 8(2). doi: 10.1098/rsos.201516.

Muhawenimana, V., Wilson, C.A.M.E., Ouro, P. and Cable, J. 2019. Spanwise Cylinder Wake Hydrodynamics and Fish Behavior. Water Resources Research 55(11). doi: 10.1029/2018WR024217.

Muhlfeld, C.C. et al. 2019. Global Status of Trout and Char: Conservation Challenges in the Twenty-First Century. Trout and Char of the World: Global Status of Trout and Char: Conservation Challenges in the Twenty-First Century (September).

Müller, S., Muhawenimana, V., Sonnino-Sorisio, G., Wilson, C.A.M.E., Cable, J. and Ouro, P. 2023. Fish response to the presence of hydrokinetic turbines as a sustainable energy solution. Scientific Reports 13(1), p. 7459. Available at: https://www.nature.com/articles/s41598-023-33000-w.

Müller, S., Muhawenimana, V., Wilson, C.A.M.E. and Ouro, P. 2021a. Experimental investigation of the wake characteristics behind twin vertical axis turbines. Energy Conversion and Management 247. doi: 10.1016/j.enconman.2021.114768.

Müller, S., Wilson, C.A.M.E., Ouro, P. and Cable, J. 2021b. Experimental Investigation of Physical Leaky Barrier Design Implications on Juvenile Rainbow Trout (*Oncorhynchus mykiss*) Movement. Water Resources Research 57(8). doi: 10.1029/2021WR030111.

Müller, U.K., Smit, J., Stamhuis, E.J. and Videler, J.J. 2001. How the body contributes to the wake in undulatory fish swimming: Flow fields of a swimming eel (*Anguilla anguilla*). Journal of Experimental Biology 204(16). doi: https://doi.org/10.1242/jeb.204.16.2751.

Musa, M., Hill, C., Sotiropoulos, F. and Guala, M. 2018. Performance and resilience of hydrokinetic turbine arrays under large migrating fluvial bedforms. Nature Energy 3(10). doi: 10.1038/s41560-018-0218-9.

Mussalli, Y.G., Taft, E.P. and Larsen, J. 1980. OFFSHORE WATER INTAKES DESIGNED TO PROTECT FISH. ASCE J Hydraul Div 106(11).

Myrvold, K.M., Mawle, G.W., Andersen, O. and Aas, O. 2019. The Social, Economic and Cultural values of wild Atlantic salmon: A review of the literature for the period 2009-2019 and an assessment of changes in values. Available at: file:///C:/Users/c1517253/Downloads/1668.pdf [Accessed: 21 July 2022].

National Oilwell Varco. 2016. Mono Screens and extraction packages.

NatureServe. 2019. *Gasterosteus aculeatus*, Threespined Stickleback. Available at: http://dx.doi.org/10.2305/IUCN.UK.2019-2.RLTS.T8951A58295405.en.

Nepf, H. and Ghisalberti, M. 2008. Flow and transport in channels with submerged vegetation. Acta Geophysica 56(3). doi: 10.2478/s11600-008-0017-y.

Nepf, H.M. 2011. Flow and transport in regions with aquatic vegetation. Annual Review of Fluid Mechanics 44. doi: 10.1146/annurev-fluid-120710-101048.

Nepf, H.M. 2012. Hydrodynamics of vegetated channels. Journal of Hydraulic Research 50(3). doi: 10.1080/00221686.2012.696559.

Nepf, H.M. and Vivoni, E.R. 2000. Flow structure in depth-limited, vegetated flow. Journal of Geophysical Research: Oceans 105(C12). doi: 10.1029/2000jc900145.

Newbold, L.R., Hockley, F.A., Williams, C.F., Cable, J., Reading, A.J., Auchterlonie, N. and Kemp, P.S. 2015. Relationship between European eel *Anguilla anguilla* infection with non-native parasites and swimming behaviour on encountering accelerating flow. Journal of Fish Biology 86(5). doi: 10.1111/jfb.12659.

Newbold, L.R., Karageorgopoulos, P. and Kemp, P.S. 2014. Corner and sloped culvert baffles improve the upstream passage of adult European eels (*Anguilla anguilla*). Ecological Engineering 73. doi: 10.1016/j.ecoleng.2014.09.076.

NOAA. 2015. Diadromous Fish Passage: A Primer on Technology, Planning, and Design for the Atlantic and Gulf Coasts. p. 83.

NRW. 2024. Licenced Water Abstractions. Available at: https://datamap.gov.wales/layers/geonode:nrw_water_resource_permits [Accessed: 9 February 2024].

Ohms, H. A., Chargualaf, D. N., Brooks, G., Hamilton, C., Palkovacs, E. P., & Boughton, D. A. (2022). Poor downstream passage at a dam creates an ecological trap for migratory fish. Canadian Journal of Fisheries and Aquatic Sciences, 79(12). https://doi.org/10.1139/cjfas-2022-0095

Olsen, A.H. and Tullis, B.P. 2013. Laboratory Study of Fish Passage and Discharge Capacity in Slip-Lined, Baffled Culverts. Journal of Hydraulic Engineering 139(4). doi: 10.1061/(asce)hy.1943-7900.0000697.

Olsén, K.H., Petersson, E., Ragnarsson, B., Lundqvist, H. and Järvi, T. 2004. Downstream migration in Atlantic salmon (*Salmo salar*) smolt sibling groups. Canadian Journal of Fisheries and Aquatic Sciences 61(3). doi: 10.1139/f04-067.

Ouro, P., Runge, S., Luo, Q. and Stoesser, T. 2019. Three-dimensionality of the wake recovery behind a vertical axis turbine. Renewable Energy 133, pp. 1066–1077. doi: 10.1016/j.renene.2018.10.111.

Ouro, P. and Stoesser, T. 2017. Wake Generated Downstream of a Vertical Axis Tidal Turbine. In: 12th European Wave and Tidal Energy Conference (EWTEC).

Padgett, T.E., Thomas, R.E., Borman, D.J. and Mould, D.C. 2020. Individual-based model of juvenile eel movement parametrized with computational fluid dynamics-derived flow fields informs improved fish pass design. Royal Society Open Science 7(1). doi: 10.1098/rsos.191505.

Parasiewicz, P. et al. 2023. Over 200,000 kilometers of free-flowing river habitat in Europe is altered due to impoundments. Nature Communications 14(1). doi: 10.1038/s41467-023-40922-6.

Parkyn, D.C. and Hawryshyn, C.W. 2000. Spectral and ultraviolet-polarisation sensitivity in juvenile salmonids: A comparative analysis using electrophysiology. Journal of Experimental Biology 203(7), pp. 1173–1191.

Partridge, B.L. and Pitcher, T.J. 1979. Evidence against a hydrodynamic function for fish schools. Nature 279(5712). doi: 10.1038/279418a0.

Pauwels, I.S., Baeyens, R., Toming, G., Schneider, M., Buysse, D., Coeck, J. and Tuhtan, J.A. 2020. Multi-species assessment of injury, mortality, and physical conditions during downstream passage through a large archimedes hydrodynamic screw (Albert canal, Belgium). Sustainability (Switzerland) 12(20). doi: 10.3390/su12208722.

Pedersen, M.I., Jepsen, N., Aarestrup, K., Koed, A., Pedersen, S. and Økland, F. 2012. Loss of European silver eel passing a hydropower station. Journal of Applied Ichthyology 28(2). doi: 10.1111/j.1439-0426.2011.01913.x.

Peraza, J. and Horne, J. 2023. Conditional probabilistic encounter-impact model for fish-turbine interactions. Proceedings of the European Wave and Tidal Energy Conference 15. doi: 10.36688/ewtec-2023-214.

Pike, C., Crook, V. and Gollock, M. 2020. *Anguilla anguilla*, European eel The IUCN Red List of Threatened Species TM. Available at: https://dx.doi.org/10.2305/IUCN.UK.2020-2.RLTS.T60344A152845178.en.

Pinheiro, J., Bates, D., DebRoy, S., Sarkar, D., Heisterkamp, S. and Van Willigen, B. 2020. Package nlme: Linear and Nonlinear Mixed Effects Models. R package.

Piper, A. and Wright, R. 2017. Understanding fish and eel behaviour to improve protection and passage at river structures. http://www.gov.uk/government/organisations/environment-agency

Piper, A.T., Manes, C., Siniscalchi, F., Marion, A., Wright, R.M. and Kemp, P.S. 2015. Response of seaward-migrating European eel (*Anguilla anguilla*) to manipulated flow fields. Proceedings of the Royal Society B: Biological Sciences 282(1811). doi: 10.1098/rspb.2015.1098.

Piper, A.T., Rosewarne, P.J., Wright, R.M. and Kemp, P.S. 2018a. The impact of an Archimedes screw hydropower turbine on fish migration in a lowland river. Ecological Engineering 118. doi: 10.1016/j.ecoleng.2018.04.009.

Piper, A.T., Rosewarne, P.J., Wright, R.M. and Kemp, P.S. 2018b. The impact of an Archimedes screw hydropower turbine on fish migration in a lowland river. Ecological Engineering 118. doi: 10.1016/j.ecoleng.2018.04.009.

Piper, A.T., Svendsen, J.C., Wright, R.M. and Kemp, P.S. 2017. Movement patterns of seaward migrating European eel (*Anguilla anguilla*) at a complex of riverine barriers: implications for conservation. Ecology of Freshwater Fish 26(1). doi: 10.1111/eff.12257.

Piper, A.T., White, P.R., Wright, R.M., Leighton, T.G. and Kemp, P.S. 2019. Response of seaward-migrating European eel (*Anguilla anguilla*) to an infrasound deterrent. Ecological Engineering 127. doi: 10.1016/j.ecoleng.2018.12.001.

Piper, A.T., Wright, R.M. and Kemp, P.S. 2012. The influence of attraction flow on upstream passage of European eel (*Anguilla anguilla*) at intertidal barriers. Ecological Engineering 44. doi: 10.1016/j.ecoleng.2012.04.019.

Popper, A.N. and Hastings, M.C. 2009. The effects of anthropogenic sources of sound on fishes. Journal of Fish Biology 75(3). doi: 10.1111/j.1095-8649.2009.02319.x.

Porcher, J.P. 2002. Fishways For Eels. Bulletin Français de la Pêche et de la Pisciculture (364 supplément). doi: 10.1051/kmae/2002099.

Posa, A. 2019. Wake characterization of coupled configurations of vertical axis wind turbines using Large Eddy Simulation. International Journal of Heat and Fluid Flow 75. doi: 10.1016/j.ijheatfluidflow.2018.11.008.

Posa, A. 2020. Dependence of the wake recovery downstream of a Vertical Axis Wind Turbine on its dynamic solidity. Journal of Wind Engineering and Industrial Aerodynamics 202. doi: 10.1016/j.jweia.2020.104212.

Pottinger, T.G., Carrick, T.R. and Yeomans, W.E. 2002. The three-spined stickleback as an environmental sentinel: Effects of stressors on whole-body physiological indices. Journal of Fish Biology 61(1). doi: 10.1111/j.1095-8649.2002.tb01747.x.

Pracheil, B.M., DeRolph, C.R., Schramm, M.P. and Bevelhimer, M.S. 2016. A fish-eye view of riverine hydropower systems: the current understanding of the biological response to turbine passage. Reviews in Fish Biology and Fisheries 26(2). doi: 10.1007/s11160-015-9416-8.

Przybilla, A., Kunze, S., Rudert, A., Bleckmann, H. and Brücker, C. 2010. Entraining in trout: A behavioural and hydrodynamic analysis. Journal of Experimental Biology 213(17). doi: 10.1242/jeb.041632.

van Puijenbroek, P.J.T.M., Buijse, A.D., Kraak, M.H.S. and Verdonschot, P.F.M. 2019. Species and river specific effects of river fragmentation on European anadromous fish species. River Research and Applications 35(1). doi: 10.1002/rra.3386.

Pujolar, J.M. et al. 2012. Surviving in a toxic world: Transcriptomics and gene expression profiling in response to environmental pollution in the critically endangered European eel. BMC Genomics 13(1). doi: 10.1186/1471-2164-13-507.

Puzdrowska, M. and Heese, T. 2019. Turbulent kinetic energy in fish passes of various types of construction. WIT Transactions on Ecology and the Environment 234. doi: 10.2495/RBM190091.

R Core Team. 2022. R: A language and environment for statistical computing. Available at: https://www.R-project.org/. [Accessed: 13 December 2023].

Von Raben, K. 1957. Uber turbininen und ihre schadliche wirkung auf fische.

Rahn, A.K., Hammer, D.A. and Bakker, T.C.M. 2015. Experimental infection with the directly transmitted parasite *Gyrodactylus* influences shoaling behaviour in sticklebacks. Animal Behaviour 107. doi: 10.1016/j.anbehav.2015.07.004.

Rajaratnam, N., Katopodis, C., Sadeque, M.A.F. and Pokharel, N. 2010. Turbulent Flow near Vertical Angled Fish Screen. Journal of Hydraulic Engineering 136(11). doi: 10.1061/(asce)hy.1943-7900.0000269.

Ralph, A.L., Berli, B.I., Burkhardt-Holm, P. and Tierney, K.B. 2012. Variability in swimming performance and underlying physiology in rainbow trout (*Oncorhynchus mykiss*) and brown trout (*Salmo trutta*). Comparative Biochemistry and Physiology - A Molecular and Integrative Physiology 163(3–4). doi: 10.1016/j.cbpa.2012.07.007.

Ramadan, A., Hemida, M., Abdel-Fadeel, W.A., Aissa, W.A. and Mohamed, M.H. 2021. Comprehensive experimental and numerical assessment of a drag turbine for river hydrokinetic energy conversion. Ocean Engineering 227. doi: 10.1016/j.oceaneng.2021.108587.

Raptis, C.E., Van Vliet, M.T.H. and Pfister, S. 2016. Global thermal pollution of rivers from thermoelectric power plants. Environmental Research Letters 11(10). doi: 10.1088/1748-9326/11/10/104011.

Raupach, M.R., Finnigan, J.J. and Brunet, Y. 1996. Coherent eddies and turbulence in vegetation canopies: the mixing-layer analogy. Boundary-Layer Meteorology 78(3–4). doi: 10.1007/BF00120941.

Raut, S., Gupta, N., Nautiyal, P., & Everard, M. (2020). Re-establishment of fish passage for conserving threatened migratory species of West-Indian Himalayas. River Research and Applications, 36(2). https://doi.org/10.1002/rra.3577

Raynal, S., Chatellier, L., Courret, D., Larinier, M. and David, L. 2013. An experimental study on fish-friendly trashracks - Part 2. Angled trashracks. Journal of Hydraulic Research 51(1). doi: 10.1080/00221686.2012.753647.

Read, D.A., Hover, F.S. and Triantafyllou, M.S. 2003. Forces on oscillating foils for propulsion and maneuvering. Journal of Fluids and Structures 17(1). doi: 10.1016/S0889-9746(02)00115-9.

Ren, K., Yu, J., Chen, Z., Li, H., Feng, H. and Liu, K. 2023. Numerical investigation on energetically advantageous formations and swimming modes using two self-propelled fish. Ocean Engineering 267. doi: 10.1016/j.oceaneng.2022.113288.

Reyes, M.L. and Baker, J.A. 2016. Prolonged swimming performance within the threespine stickleback (*Gasterosteus aculeatus*) adaptive radiation and the effect of dietary restriction. Evolutionary Ecology Research 17(4).

Richard Seaby. 2023. The impact of mesh size on numbers of fish impinged or entrained in power station cooling water systems. In: First International Fish Impingement and Entrainment Conference. Liverpool: IFM, pp. 49–52.

Righton, D. et al. 2021. Important questions to progress science and sustainable management of anguillid eels. Fish and Fisheries 22(4). doi: 10.1111/faf.12549.

Río, G.E.N. Del, Camacho, R.G.R., Filho, N.M., de Oliveira, W. and Angulo, T.M.A. 2024. A Methodology for Designing a Fish-Friendly Turbine Rotor Applied to High-Power Generation. Journal of Applied Fluid Mechanics 17(1). doi: 10.47176/jafm.17.1.1927.

Ritchie, H. and Rosado, P. 2020. Electricity Mix. Available at: https://ourworldindata.org/electricity-mix [Accessed: 16 July 2024].

Rodgers, E.M., Heaslip, B.M., Cramp, R.L., Riches, M., Gordos, M.A. and Franklin, C.E. 2017. Substrate roughening improves swimming performance in two small-bodied riverine fishes: Implications for culvert remediation and design. Conservation Physiology 5(1). doi: 10.1093/conphys/cox034.

Romero-Gomez, P. and Richmond, M.C. 2014. Simulating blade-strike on fish passing through marine hydrokinetic turbines. Renewable Energy. doi: 10.1016/j.renene.2014.05.051.

Rominger, J.T. and Nepf, H.M. 2011. Flow adjustment and interior flow associated with a rectangular porous obstruction. Journal of Fluid Mechanics 680. doi: 10.1017/jfm.2011.199.

Rose, B.P. and Mesa, M.G. 2012. Effectiveness of common fish screen materials to protect lamprey ammocoetes. North American Journal of Fisheries Management 32(3). doi: 10.1080/02755947.2012.678965.

Russon, I.J. and Kemp, P.S. 2011. Experimental quantification of the swimming performance and behaviour of spawning run river lamprey Lampetra fluviatilis and European eel *Anguilla anguilla*. Journal of Fish Biology 78(7). doi: 10.1111/j.1095-8649.2011.02965.x.

Russon, I.J., Kemp, P.S. and Calles, O. 2010. Response of downstream migrating adult European eels (*Anguilla anguilla*) to bar racks under experimental conditions. Ecology of Freshwater Fish 19(2). doi: 10.1111/j.1600-0633.2009.00404.x.

Rytwinski, T., Algera, D.A., Taylor, J.J., Smokorowski, K.E., Bennett, J.R., Harrison, P.M. and Cooke, S.J. 2017. What are the consequences of fish entrainment and impingement associated with hydroelectric dams on fish productivity? A systematic review protocol. Environmental Evidence 6(1). doi: 10.1186/s13750-017-0087-x.

Santo, V. Di, Goerig, E., Wainwright, D.K., Akanyeti, O., Liao, J.C., Castro-Santos, T. and Lauder, G. V. 2021. Convergence of undulatory swimming kinematics across a diversity of fishes. Proceedings of the National Academy of Sciences of the United States of America 118(49). doi: 10.1073/pnas.2113206118.

Scharsack, J.P., Schweyen, H., Schmidt, A.M., Dittmar, J., Reusch, T.B.H. and Kurtz, J. 2012. Population genetic dynamics of three-spined sticklebacks (*Gasterosteus aculeatus*) in anthropogenic altered habitats. Ecology and Evolution 2(6), pp. 1122–1143. doi: 10.1002/ece3.232.

Schramm, M.P., Bevelhimer, M. and Scherelis, C. 2017. Effects of hydrokinetic turbine sound on the behavior of four species of fish within an experimental mesocosm. Fisheries Research 190. doi: 10.1016/j.fishres.2017.01.012.

Schweizer, P.E., Cada, G.F. and Bevelhimer, M.S. 2011. Estimation of the Risks of Collision or Strike to Freshwater Aquatic Organisms Resulting from Operation of Instream Hydrokinetic Turbines.

Seliger, C. and Zeiringer, B. 2018. River Connectivity, Habitat Fragmentation and Related Restoration Measures. In: Riverine Ecosystem Management. doi: 10.1007/978-3-319-73250-3_9.

Seppälä, O., Karvonen, A. and Valtonen, E.T. 2008. Shoaling behaviour of fish under parasitism and predation risk. Animal Behaviour 75(1). doi: 10.1016/j.anbehav.2007.04.022.

SETIS. 2013. Hydropower Factsheet. pp. 6–9. Available at: https://setis.ec.europa.eu/system/files/Technology_Information_Sheet_Hydropower.pdf.

Shaw, E.A., Lange, E., Shucksmith, J.D. and Lerner, D.N. 2016. Importance of partial barriers and temporal variation in flow when modelling connectivity in fragmented river systems. Ecological Engineering 91. doi: 10.1016/j.ecoleng.2016.01.030.

Sheikh, S.R. et al. 2021. A low-cost sustainable energy solution for pristine mountain areas of developing countries. Energies 14(11). doi: 10.3390/en14113160.

Shepherd, M.A., Labay, A., Shea, P.J., Rautiainen, R. and Achutan, C. 2016. Operational, water quality and temporal factors affecting impingement of fish and shellfish at a Texas coastal power plant. Global Ecology and Conservation 5. doi: 10.1016/j.gecco.2015.11.006.

Sheppard, J. and Block, S. 2013. Monitoring Response of Diadromous Populations to Fish Passage Improvements on a Massachusetts Coastal Stream. Journal of Environmental Science and Engineering 2.

Sheridan, S. et al. 2011. Screening at intakes and outfalls: measures to protect eel (*Anguilla anguilla*).

Shiau, J., Watson, J.R., Cramp, R.L., Gordos, M.A. and Franklin, C.E. 2020. Interactions between water depth, velocity and body size on fish swimming performance: Implications for culvert hydrodynamics. Ecological Engineering 156. doi: 10.1016/j.ecoleng.2020.105987.

Shoele, K. and Zhu, Q. 2009. Fluid-structure interactions of skeleton-reinforced fins: Performance analysis of a paired fin in lift-based propulsion. Journal of Experimental Biology 212(16). doi: 10.1242/jeb.030023.

Shoele, K. and Zhu, Q. 2010. Numerical simulation of a pectoral fin during labriform swimming. Journal of Experimental Biology 213(12). doi: 10.1242/jeb.040162.

Silva, A.T., Katopodis, C., Tachie, M.F., Santos, J.M. and Ferreira, M.T. 2016. Downstream Swimming Behaviour of Catadromous and Potamodromous Fish Over Spillways. River Research and Applications 32(5). doi: 10.1002/rra.2904.

Smith, D.L., Goodwin, R.A. and Nestler, J.M. 2014. Relating Turbulence and Fish Habitat: A New Approach for Management and Research. Reviews in Fisheries Science and Aquaculture 22(2). doi: 10.1080/10641262.2013.803516.

Smith, D.R., Fackler, P.L., Eyler, S.M., Villegas Ortiz, L. and Welsh, S.A. 2017. Optimization of decision rules for hydroelectric operation to reduce both eel mortality and unnecessary turbine shutdown: A search for a win–win solution. River Research and Applications 33(8). doi: 10.1002/rra.3182.

Smits, A.J. 2019. Undulatory and oscillatory swimming. Journal of Fluid Mechanics 874. doi: 10.1017/jfm.2019.284.

Solomon, D. and Beach, M. 2004a. Fish Pass design for Eel and Elver (*Anguilla anguilla*).

Solomon, D. and Beach, M. 2004b. Fish Pass design for Eel and Elver (*Anguilla anguilla*). Available at: https://assets.publishing.service.gov.uk/media/5a7f6ace40f0b6230268f5fe/sw2-070-tr1-e-e.pdf [Accessed: 13 December 2023].

Sonnino Sorisio, G., Müller, S., Wilson, C.A.M.E., Ouro, P. and Cable, J. 2023. Colour as a behavioural guide for fish near hydrokinetic turbines. Heliyon, p. e22376. doi: 10.1016/j.heliyon.2023.e22376.

Sonnino Sorisio, G., Wilson, C.A.M.E., Don, A. and Cable, J. 2024. Fish passage solution: European eel kinematics and behaviour in shear layer turbulent flows. Ecological Engineering 203, p. 107254. Available at: https://linkinghub.elsevier.com/retrieve/pii/S0925857424000788.

Sornes, K. 2010. Small-scale Water Current Turbines for River Applications. Zero Emission Resource Organization (January).

Spinti, R.A., Condon, L.E. and Zhang, J. 2023. The evolution of dam induced river fragmentation in the United States. Nature Communications 14(1). doi: 10.1038/s41467-023-39194-x.

Spurgeon, J.J., Paukert, C.P., Healy, B.D., Kelley, C.A. and Whiting, D.P. 2015. Can translocated native fishes retain their trophic niche when confronted with a resident invasive? Ecology of Freshwater Fish 24(3). doi: 10.1111/eff.12160.

Stewart, A., Hunt, R., Mitchell, R., Muhawenimana, V., Wilson, C.A.M.E., Jackson, J.A. and Cable, J. 2018. The cost of infection: *Argulus foliaceus* and its impact on the swimming performance of the three-spined stickleback (*Gasterosteus aculeatus*). Journal of the Royal Society Interface 15(147). doi: 10.1098/rsif.2018.0571.

Stewart, W.J., Tian, F.B., Akanyeti, O., Walker, C.J. and Liao, J.C. 2016. Refuging rainbow trout selectively exploit flows behind tandem cylinders. Journal of Experimental Biology 219(14). doi: 10.1242/jeb.140475.

Stocks, J.R., Walsh, C.T., Rodgers, M.P. and Boys, C.A. 2019. Approach velocity and impingement duration influences the mortality of juvenile Golden Perch (*Macquaria ambigua*) at a fish exclusion screen. Ecological Management and Restoration 20(2). doi: 10.1111/emr.12347.

Tack, N.B., Du Clos, K.T. and Gemmell, B.J. 2021. Anguilliform locomotion across a natural range of swimming speeds. Fluids 6(3). doi: 10.3390/FLUIDS6030127.

Taguchi, M. and Liao, J.C. 2011. Rainbow trout consume less oxygen in turbulence: The energetics of swimming behaviors at different speeds. Journal of Experimental Biology 214(9). doi: 10.1242/jeb.052027.

Tamario, C., Calles, O., Watz, J., Nilsson, P.A. and Degerman, E. 2019. Coastal river connectivity and the distribution of ascending juvenile European eel (*Anguilla anguilla* L.): Implications for conservation strategies regarding fish-passage solutions. Aquatic Conservation: Marine and Freshwater Ecosystems 29(4). doi: 10.1002/aqc.3064.

Tamario, C., Degerman, E., Donadi, S., Spjut, D. and Sandin, L. 2018. Nature-like fishways as compensatory lotic habitats. River Research and Applications 34(3). doi: 10.1002/rra.3246.

Tanino, Y. and Nepf, H.M. 2008. Lateral dispersion in random cylinder arrays at high Reynolds number. Journal of Fluid Mechanics 600. doi: 10.1017/S0022112008000505.

Taylor, E.B. and McPhail, J.D. 1986. Prolonged and burst swimming in anadromous and freshwater threespine stickleback, *Gasterosteus aculeatus* . Canadian Journal of Zoology 64(2). doi: 10.1139/z86-064.

Teichert, N., Tétard, S., Trancart, T., Feunteun, E., Acou, A. and de Oliveira, E. 2020. Resolving the trade-off between silver eel escapement and hydropower generation with simple decision rules for turbine shutdown. Journal of Environmental Management 261. doi: 10.1016/j.jenvman.2020.110212.

Teunen, L., Bervoets, L., Belpaire, C., De Jonge, M. and Groffen, T. 2021. PFAS accumulation in indigenous and translocated aquatic organisms from Belgium, with translation to human and ecological health risk. Environmental Sciences Europe 33(1). doi: 10.1186/s12302-021-00477-z.

Thandiackal, R. and Lauder, G. V. 2023. In-line swimming dynamics revealed by fish interacting with a robotic mechanism. eLife 12. doi: 10.7554/eLife.81392.

The Council of The European Union. 2007. COUNCIL REGULATION (EC) No 1100/2007. European Union. Available at: https://eur-lex.europa.eu/legal-content/EN/TXT/PDF/?uri=CELEX:32007R1100 [Accessed: 13 February 2024].

The MathWorks Inc. 2024. MATLAB.

Thielicke, W. and Sonntag, R. 2021. Particle Image Velocimetry for MATLAB: Accuracy and enhanced algorithms in PIVlab. Journal of Open Research Software 9. doi: 10.5334/JORS.334.

Thielicke, W. and Stamhuis, E. 2010. Pivlab-time-resolved digital particle image velocimetry tool for matlab. … under the BSD license, programmed with MATLAB.

Van Den Thillart, G., Van Ginneken, V., Körner, F., Heijmans, R., Van Der Linden, R. and Gluvers, A. 2004. Endurance swimming of European eel. Journal of Fish Biology 65(2). doi: 10.1111/j.0022-1112.2004.00447.x.

Thorncraft, G. and Harris, J.H. 2000. Fish Passage and Fishways in New South Wales: A Status Report. Crcfe 1(June).

Tien, J.H., Levin, S.A. and Rubenstein, D.I. 2004. Dynamics of fish shoals: Identifying key decision rules. Evolutionary Ecology Research 6(4).

Trancart, T., Carpentier, A., Acou, A., Charrier, F., Mazel, V., Danet, V. and Feunteun, É. 2020. When "safe" dams kill: Analyzing combination of impacts of overflow dams on the migration of silver eels. Ecological Engineering 145. doi: 10.1016/j.ecoleng.2020.105741.

van Treeck, R., Radinger, J., Noble, R.A.A., Geiger, F. and Wolter, C. 2021. The European Fish Hazard Index – An assessment tool for screening hazard of hydropower plants for fish. Sustainable Energy Technologies and Assessments 43. doi: 10.1016/j.seta.2020.100903.

Triantafyllou, M.S., Triantafyllou, G.S. and Yue, D.K.P. 2000. Hydrodynamics of fishlike swimming. Annual Review of Fluid Mechanics 32. doi: 10.1146/annurev.fluid.32.1.33.

Tritico, H.M. and Cotel, A.J. 2010. The effects of turbulent eddies on the stability and critical swimming speed of creek chub (*Semotilus atromaculatus*). Journal of Experimental Biology 213(13). doi: 10.1242/jeb.041806.

Tudorache, C., Blust, R. and De Boeck, G. 2007. Swimming capacity and energetics of migrating and non-migrating morphs of three-spined stickleback *Gasterosteus aculeatus* L. and their ecological implications. Journal of Fish Biology 71(5). doi: 10.1111/j.1095-8649.2007.01612.x.

Turnpenny, A. 2013. Trials and tribulations of fish recovery and return. 71, pp. 111–123. doi: 10.2495/978-1-84564-849-7/010.

Turnpenny, A., Blay, S., Carron, J. and Clough, S. 2001. Literature Review Swimming Speeds in Fish. Available at: www.environment-agency.gov.r.rk.

Turnpenny, A. and O'Keefe, N. 2005. Screening for intakes and outfalls: a best practice guide.

Tytell, E.D. 2004a. Kinematics and hydrodynamics of linear acceleration in eels, *Anguilla rostrata*. Proceedings of the Royal Society B: Biological Sciences 271(1557). doi: 10.1098/rspb.2004.2901.

Tytell, E.D. 2004b. The hydrodynamics of eel swimming II. Effect of swimming speed. Journal of Experimental Biology 207(19). doi: 10.1242/jeb.01139.

Tytell, E.D. 2005. Experimental hydrodynamics of swimming in fishes.

Tytell, E.D., Borazjani, I., Sotiropoulos, F., Baker, T.V., Anderson, E.J. and Lauder, G. V. 2010. Disentangling the functional roles of morphology and motion in the swimming of fish. In: Integrative and Comparative Biology. doi: 10.1093/icb/icq057.

Tytell, E.D. and Lauder, G. V. 2004. The hydrodynamics of eel swimming: I. Wake structure. Journal of Experimental Biology 207(11). doi: 10.1242/jeb.00968.

UK Government. 2009. The Eels (England and Wales) Regulations 2009 No. 3344. Available at: http://www.defra.gov.uk/foodfarm/fisheries/.

UNEP. 2023. Why does energy matter? UN Environment Program.

Unigarro Villota, S., Ghisalberti, M., Philip, J. and Branson, P. 2023. Characterizing the Three-Dimensional Flow in Partially Vegetated Channels. Water Resources Research 59(1). doi: 10.1029/2022WR032570.

Venables, W.N. and Ripley, B.D. 2002. Modern Applied Statistics with S Fourth edition. Springer, New York, NY. doi: https://doi.org/10.1007/978-0-387-21706-2_7.

Verhelst, P., Buysse, D., Coeck, J., Reubens, J.T., Vincx, M. and Mouton, A. 2014. Estuarine behaviour of European silver eel (*Anguilla anguilla*) in the Scheldt Estuary. Book of abstracts – VLIZ Young Scientists' Day. Brugge, Belgium, 7 March 2014 (1100).

Vermaak, H.J., Kusakana, K. and Koko, S.P. 2014. Status of micro-hydrokinetic river technology in rural applications: A review of literature. Renewable and Sustainable Energy Reviews 29. doi: 10.1016/j.rser.2013.08.066.

Vezza, P., Libardoni, F., Manes, C., Tsuzaki, T., Bertoldi, W. and Kemp, P.S. 2020b. Rethinking swimming performance tests for bottom-dwelling fish: the case of European glass eel (*Anguilla anguilla*). Scientific Reports 10(1). doi: 10.1038/s41598-020-72957-w.

Videler, J.J. 2019. Fish locomotion. In: Encyclopedia of Ocean Sciences. doi: 10.1016/B978-0-12-409548-9.04099-9.

Viehman, H.A. and Zydlewski, G.B. 2014. Fish Interactions with a Commercial-Scale Tidal Energy Device in the Natural Environment. Estuaries and Coasts 38(1). doi: 10.1007/s12237-014-9767-8.

Vowles, A.S., Don, A.M., Karageorgopoulos, P. and Kemp, P.S. 2017. Passage of European eel and river lamprey at a model weir provisioned with studded tiles. Journal of Ecohydraulics 2(2). doi: 10.1080/24705357.2017.1310001.

Vowles, A.S., Don, A.M., Karageorgopoulos, P., Worthington, T.A. and Kemp, P.S. 2015. Efficiency of a dual density studded fish pass designed to mitigate for impeded upstream passage of juvenile European eels (*Anguilla anguilla*) at a model Crump weir. Fisheries Management and Ecology 22(4). doi: 10.1111/fme.12128.

Vowles, A.S., Kemp, P.S. 2021. Artificial light at night (ALAN) affects the downstream movement behaviour of the critically endangered European eel, Anguilla anguilla, Environmental Pollution, Volume 274, 116585, ISSN 0269-7491, https://doi.org/10.1016/j.envpol.2021.116585.

Walker, J.A. and Westneat, M.W. 2002. Performance limits of labriform propulsion and correlates with fin shape and motion. Journal of Experimental Biology 205(2). doi: 10.1242/jeb.205.2.177.

Walter, T. and Couzin, I.D. 2020. TRex, a fast multi-animal tracking system with markerless identification, 2D body posture estimation and visual field reconstruction. bioRxiv.

Wang, M. et al. 2024. A triple increase in global river basins with water scarcity due to future pollution. Nature Communications 15(1). doi: 10.1038/s41467-024-44947-3.

Ward, A.J.W., Duff, A.J., Krause, J. and Barber, I. 2005. Shoaling behaviour of sticklebacks infected with the microsporidian parasite, *Glugea anomala*. Environmental Biology of Fishes 72(2). doi: 10.1007/s10641-004-9078-1.

Warren, M.L. and Pardew, M.G. 1998. Road Crossings as Barriers to Small-Stream Fish Movement. Transactions of the American Fisheries Society 127(4). doi: 10.1577/1548-8659(1998)127<0637:rcabts>2.0.co;2.

Watz, J., Nilsson, P.A., Degerman, E., Tamario, C. and Calles, O. 2019. Climbing the ladder: an evaluation of three different anguillid eel climbing substrata and placement of upstream passage solutions at migration barriers. Animal Conservation 22(5). doi: 10.1111/acv.12485.

Webb, P.W. 1984. Form and Function in Fish Swimming. Scientific American 251(1). doi: 10.1038/scientificamerican0784-72.

Webb, P.W. and Cotel, A.J. 2011. Assessing possible effects of fish-culture systems on fish swimming: The role of stability in turbulent flows. Fish Physiology and Biochemistry 37(2). doi: 10.1007/s10695-011-9497-9.

Wei, C., Hu, Q., Li, S. and Shi, X. 2023. Hydrodynamic interactions and wake dynamics of fish schooling in rectangle and diamond formations. Ocean Engineering 267. doi: 10.1016/j.oceaneng.2022.113258.

Weihs, D. 1973. Hydromechanics of fish schooling. Nature 241(5387). doi: 10.1038/241290a0.

Wen, Y., Schoups, G. and Van De Giesen, N. 2017. Organic pollution of rivers: Combined threats of urbanization, livestock farming and global climate change. Scientific Reports 7. doi: 10.1038/srep43289.

White, B.L. and Nepf, H.M. 2007. Shear instability and coherent structures in shallow flow adjacent to a porous layer. Journal of Fluid Mechanics 593. doi: 10.1017/S0022112007008415.

White, B.L. and Nepf, H.M. 2008. A vortex-based model of velocity and shear stress in a partially vegetated shallow channel. Water Resources Research 44(1). doi: 10.1029/2006WR005651.

Wild Trout Trust. 2020. Raibow Trout. Available at: https://www.wildtrout.org/content/rainbow-trout#:~:text=The%20rainbow%20trout%20is%20native,(not%20far%20from%20Alaska). [Accessed: 21 July 2022].

Wilkinson, L. 2011. ggplot2: Elegant Graphics for Data Analysis by WICKHAM, H. Biometrics 67(2). doi: 10.1111/j.1541-0420.2011.01616.x.

Williams, J.E., Isaak, D.J., Imhof, J., Hendrickson, D.A. and McMillan, J.R. 2015. Cold-Water Fishes and Climate Change in North America. In: Reference Module in Earth Systems and Environmental Sciences. doi: 10.1016/b978-0-12-409548-9.09505-1.

Wilson, R.W. and Wood, C.M. 1992. Swimming performance, whole body ions, and gill Al accumulation during acclimation to sublethal aluminium in juvenile rainbow trout

(*Oncorhynchus mykiss*). Fish Physiology and Biochemistry 10(2). doi: 10.1007/BF00004526.

Winemiller, K.O. et al. 2016. Balancing hydropower and biodiversity in the Amazon, Congo, and Mekong. Science 351(6269). doi: 10.1126/science.aac7082.

Winter, H. V., Jansen, H.M. and Breukelaar, A.W. 2007. Silver eel mortality during downstream migration in the River Meuse, from a population perspective. In: ICES Journal of Marine Science. doi: 10.1093/icesjms/fsm128.

WMO. 2023. State of Global Water Resources 2022.

Wright, G. V., Wright, R.M. and Kemp, P.S. 2015. Impact of Tide Gates on the Migration of Adult European Eels, *Anguilla anguilla*. Estuaries and Coasts 38(6). doi: 10.1007/s12237-014-9931-1.

Wright, R.M. et al. 2022. First direct evidence of adult European eels migrating to their breeding place in the Sargasso Sea. Scientific Reports 12(1). doi: 10.1038/s41598-022-19248-8.

Wu, H. et al. 2019. Effects of dam construction on biodiversity: A review. Journal of Cleaner Production 221. doi: 10.1016/j.jclepro.2019.03.001.

Würsig, B., Greene, C.R. and Jefferson, T.A. 2000. Development of an air bubble curtain to reduce underwater noise of percussive piling. Marine Environmental Research 49(1). doi: 10.1016/S0141-1136(99)00050-1.

Yoshida, T., Furuichi, D., Williamson, B.J., Zhou, J., Dong, S., Li, Q. and Kitazawa, D. 2022. Experimental study of fish behavior near a tidal turbine model under dark conditions. Journal of Marine Science and Technology (Japan) 27(1). doi: 10.1007/s00773-021-00850-w.

Yoshida, T., Zhou, J., Park, S., Muto, H. and Kitazawa, D. 2020. Use of a model turbine to investigate the high striking risk of fish with tidal and oceanic current turbine blades under slow rotational speed. Sustainable Energy Technologies and Assessments 37. doi: 10.1016/j.seta.2020.100634.

Zeileis, A., Kleiber, C. and Jackman, S. 2008. Regression models for count data in R. Journal of Statistical Software 27(8). doi: 10.18637/jss.v027.i08.

Zha, W., Zeng, Y., Katul, G., Li, Q., Liu, X. and Chen, X. 2021. Laboratory study on behavioral responses of hybrid sturgeon, *Acipenseridae*, to wake flows induced by cylindrical bluff bodies. Science of the Total Environment 799. doi: 10.1016/j.scitotenv.2021.149403.

Zhang, J., Kitazawa, D., Taya, S. and Mizukami, Y. 2017. Impact assessment of marine current turbines on fish behavior using an experimental approach based on the similarity law. Journal of Marine Science and Technology (Japan) 22(2). doi: 10.1007/s00773-016-0405-y.

Zhang, Y. and Lauder, G. V. 2024. Energy conservation by collective movement in schooling fish. eLife 12. doi: 10.7554/eLife.90352.

Zhao, T. and Nepf, H.M. 2021. Turbulence Dictates Bedload Transport in Vegetated Channels Without Dependence on Stem Diameter and Arrangement. Geophysical Research Letters 48(21). doi: 10.1029/2021GL095316.

Zheng, T., Niu, Z., Sun, S., Shi, J., Liu, H. and Li, G. 2020. Comparative study on the hydraulic characteristics of nature-like fishways. Water (Switzerland) 12(4). doi: 10.3390/W12040955.

Zielinski, D.P. and Sorensen, P.W. 2016. Bubble Curtain Deflection Screen Diverts the Movement of both Asian and Common Carp. North American Journal of Fisheries Management 36(2). doi: 10.1080/02755947.2015.1120834.

Appendix A

Measurements of the European eels from Chapter 2

Fish ID	Total length (mm)	Head width (mm)	Head depth (mm)	Head length (mm)	Mass (g)
1	141	6.6	6.5	17.5	6.2
2	153	8.0	7.8	19.0	11.8
3	184	8.9	9.1	22.5	13.4
4	216	10.7	10.6	28.5	18.6
5	187	10.3	7.7	21.1	13.8
6	145	6.9	6.8	19.1	11.3
7	159	7.5	6.9	21.5	9.7
8	188	8.9	NA	22.2	12.9
9	136	8.0	7.4	18.4	9.7
10	157	7.6	7.8	18.4	9.3
11	145	7.5	7.0	16.9	8.7
12	153	8.2	6.7	17.1	12.2
13	171	8.0	8.0	21.6	12.9
14	175	9.6	8.7	22.7	14.4
15	156	8.3	7.5	20.5	12.6
16	163	9.0	7.6	20.3	12.3
17	160	7.0	7.0	18.4	12.1
18	171	9.0	8.3	21.2	15.1
19	183	8.2	7.8	25.5	16.1
20	165	9.0	8.4	22.2	11.4
21	157	6.5	7.1	18.4	11.2
22	177	10.2	8.4	22.8	14.8
23	167	9.2	8.2	23.3	13.8
24	179	8.7	8.5	21.8	13.8
25	176	8.9	8.6	22.0	14.7
26	176	8.4	8.4	21.8	13.8
27	196	7.4	8.2	24.3	15.5
28	165	8.3	8.5	21.4	12.1
29	145	7.3	8.1	17.3	9.6
30	159	7.4	7.9	18.3	11.6
31	203	9.1	9.7	27.3	17.1
32	187	9.8	9.5	25.0	15.0

Appendix B

All velocity plots for all screens for all tested velocities

0.3

239
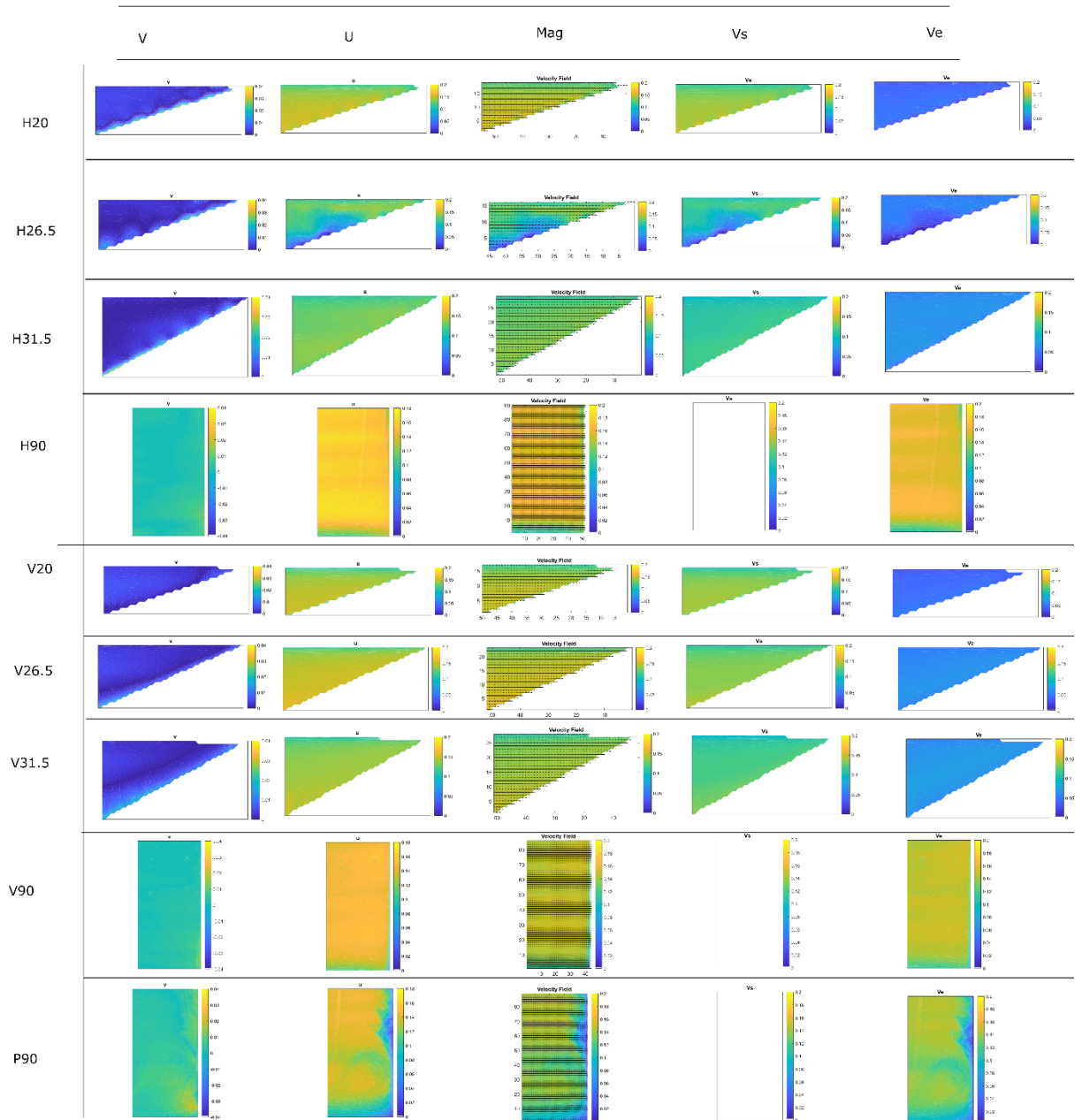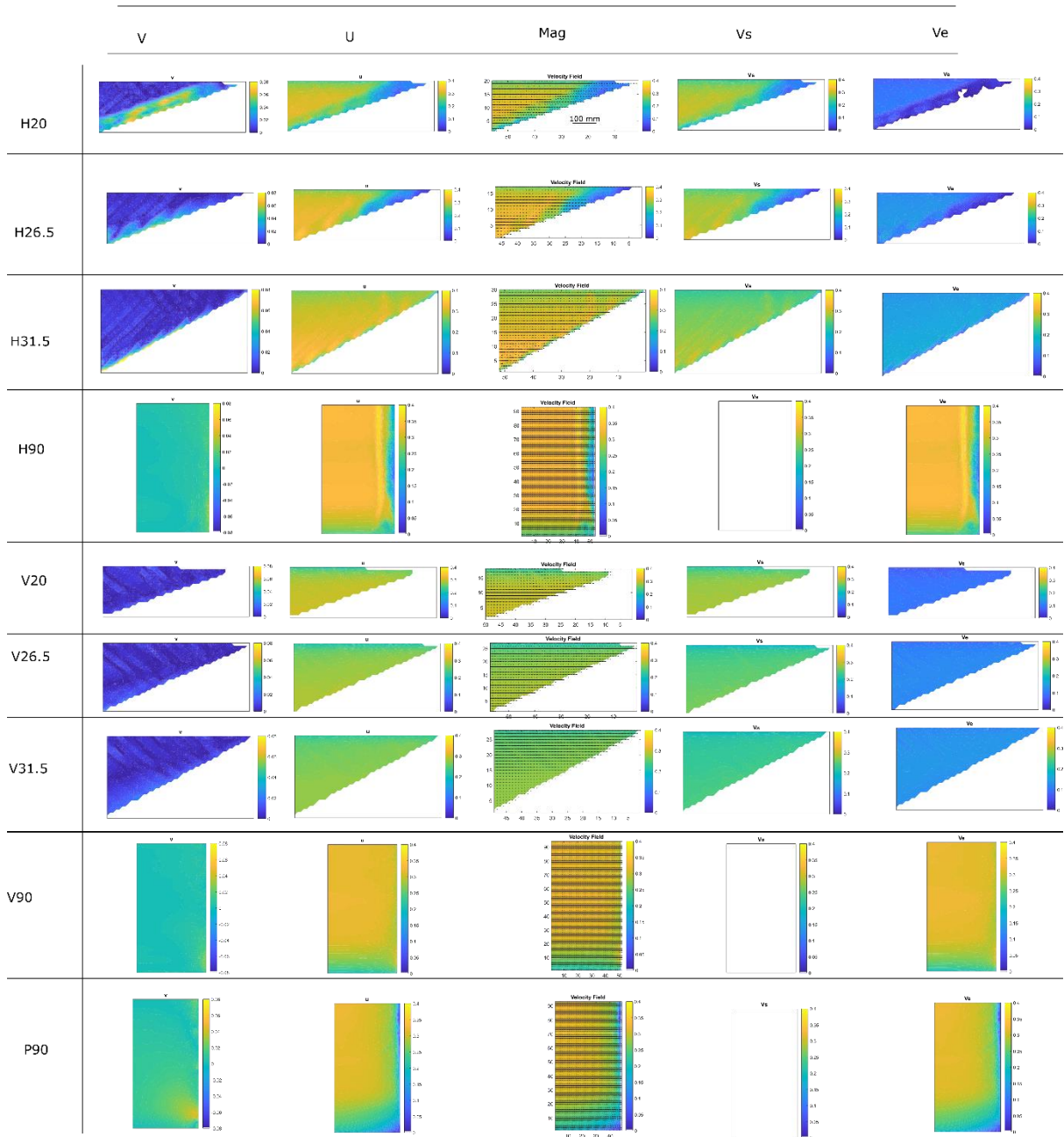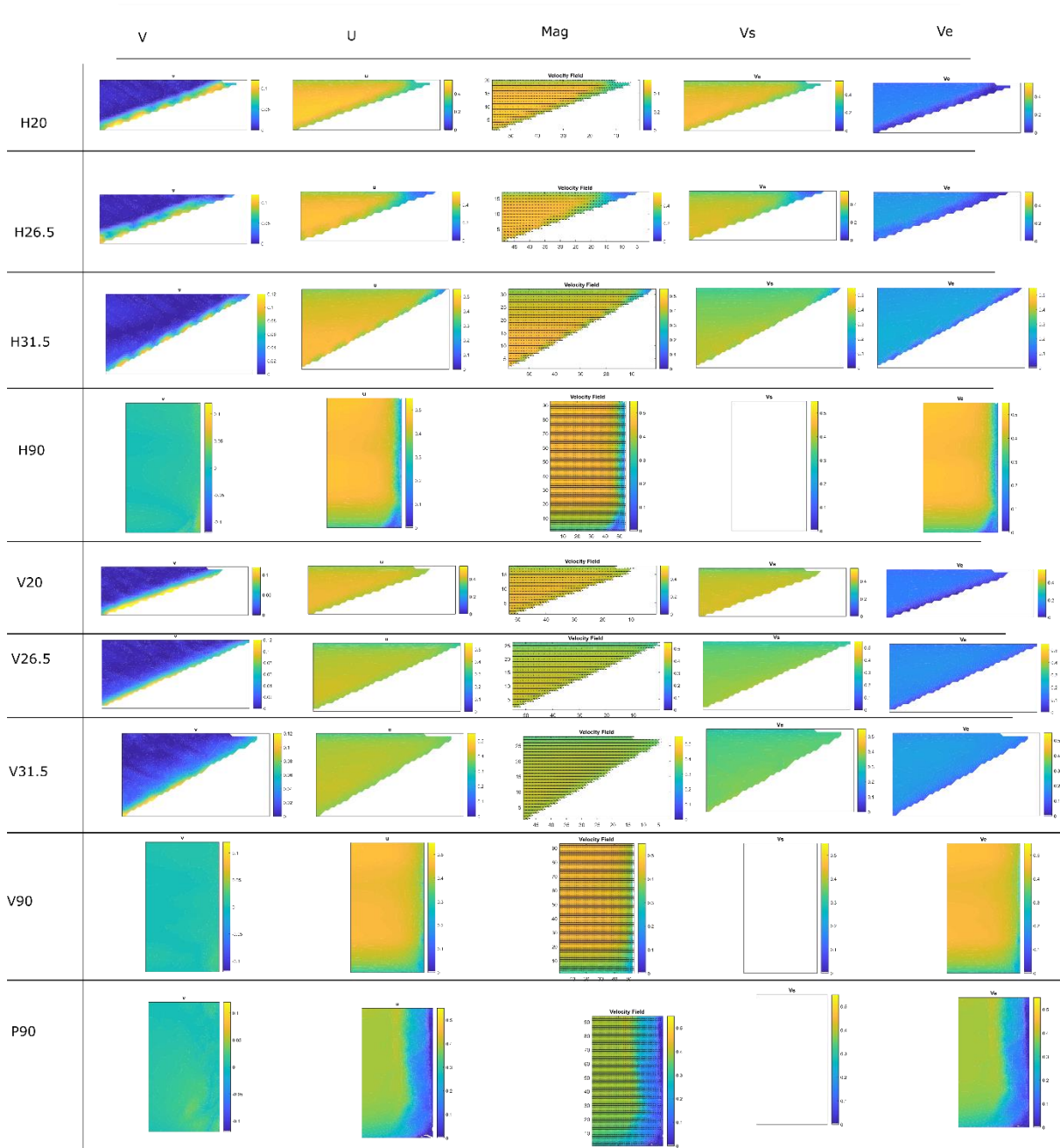
Plots showing the vorticity and velocity in the bottom bypass configuration.
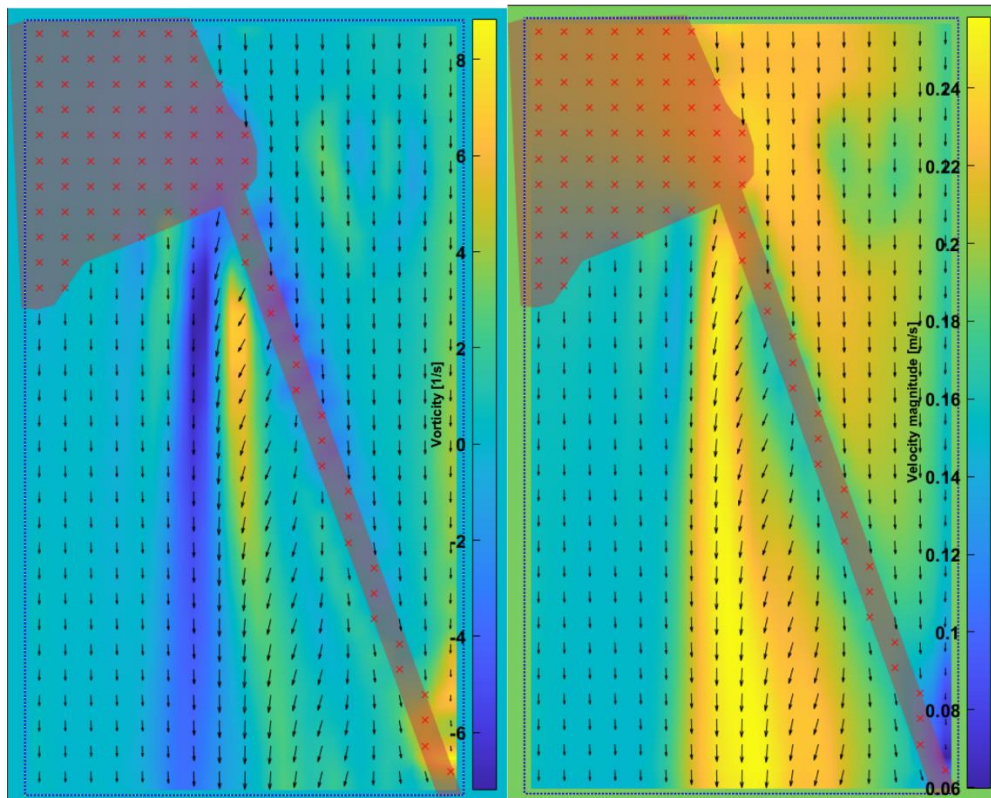
Appendix C

PIV image of the eel tiles
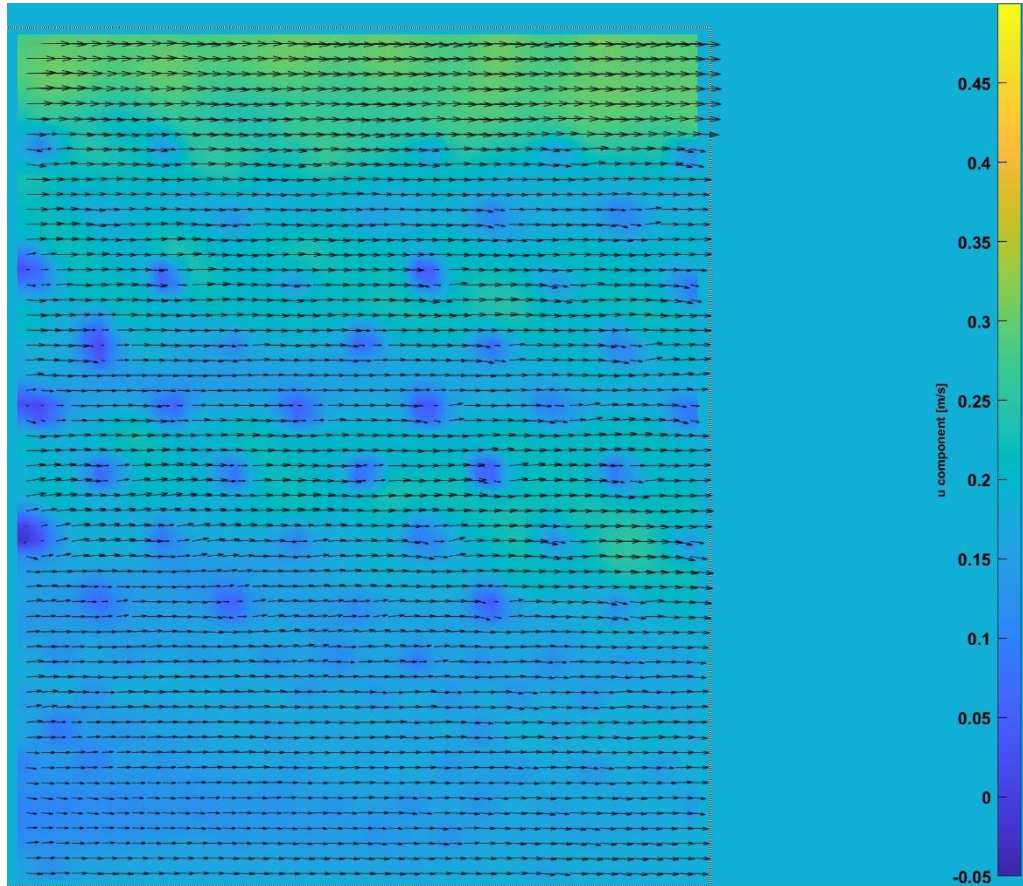
Appendix D

All measurements made of the sticklebacks in Chapter 7:

Single fish

Single Fish	SL (mm)	TL (mm)	W (g)	Pectoral Base (mm)	Pectoral Trailing edge (mm)	Pectoral Length (mm)	Caudal Base (mm)	Caudal Trailing edge (mm)	Caudal length (mm)	Caudal peduncle (mm)	m/f
1	31.2	36.4	0.538	2.1	6.2	5.1	2.5	6.8	4.6	1.2	f
2	39.6	45.3	0.806	2.8	6.9	5.8	3.1	11.4	5.5	1.7	f
3	34.8	39.7	0.731	3	6.4	5.3	2.8	8.3	4.9	1.3	f
4	37.7	5.3	0.767	2.9	7.1	6.7	2.8	10	5.8	1.6	f
5	42.3	48.7	1.081	3.1	10.1	6.5	3.3	10.7	5.7	1.8	f
6	33.9	37.9	0.648	2.4	6	4.9	2.7	6	3.6	1.3	f
7	33.1	39.1	0.607	2.7	7.4	5.4	2.5	6.6	4.9	1.4	f
8	41.3	45.8	1.072	3.3	7.2	5.7	2.5	11.9	5	1.9	m
9	37.7	42.8	0.689	2.5	8.1	6.6	3.3	10.6	4.9	1.5	f
10	44.2	50.7	1.168	3.1	8.1	5.8	3.7	12.2	5.7	1.9	f
11	45.1	52.7	1.101	3.2	8.3	6.5	3.6	11.4	5.6	2	m
12	38.3	43.8	0.83	3.7	8.6	6.6	3.4	12.9	5.2	2.1	m
13	32.7	37.7	0.386	damaged			2	7.1	4.8	1.2	f
14	37	42.4	0.736	2.6	8.7	6	2.6	10.3	4.7	1.4	f
15	41.6	49.1	1	3	5.7	5.5	2.3	5.3	7.7	1.5	f
16	40	46.5	0.91	3.6	7.2	7	2.6	6.9	6.8	1.4	m
17	38.8	44.3	0.61	3	5.7	5.5	2.3	6.5	5.9	1.2	f
18	46.7	53.8	1.348								m
19	36.4	42.8	0.87	3.1	6.8	5.6	2.7	11	5.5	1.6	m
20	40.1	46.2	0.828	2.5	8.5	5.8	3.4	10.3	5.1	1.7	f

Shoals:

Shoal	Fish	SL (mm)	TL (mm)	W (g)	Pectoral Base (mm)	Pectoral Trailing edge (mm)	Pectoral Length (mm)	Caudal Base (mm)	Caudal Trailing edge (mm)	Caudal length (mm)	Caudal peduncle (mm)	m/f
1	1.1	38	43.8	0.658	3.1	7.2	5	3.3	9.2	4.9	1.4	m
	1.2	43.6	49.8	1.146	3.1	8.2	6.8	3.8	10.7	5.5	1.8	f
	1.3	39.5	45.6	0.864	3	7.5	5.8	2.9	11.8	5.3	1.6	f
	1.4	44.5	51	0.996	3.0	8.4	6.9	3.6	11.9	5.9	1.7	f
	1.5	40.5	47.3	1.116	3.3	7.5	6.3	3.1	10.4	5.2	1.6	f
2	2.1	37.7	43	0.882	2.7	7	4.5	3	7.8	5.1	1.6	f
	2.2	35.2	50.3	0.606	2.7	6.2	5.6	3.1	6.2	4.5	1.2	f
	2.3	33.6	39.8	0.711	2.7	6.1	4.5	2.3	7.7	4.7	1.2	m
	2.4	35.8	43.1	0.76	2.4	6.1	4.8	2.7	8.8	5.0	1.3	m
	2.5	37	43.8	0.721	3.1	6.5	5.4	2.7	9.1	4.9	1.3	f
3	3.1	49.8	57.5	2.089	3.9	8.7	7.4	4.6	11.1	7.2	2.4	m
	3.2	50.1	56.6	1.768	3.7	10.1	6.7	3.9	10.2	6.3	2.5	m
	3.3	49.6	55.7	1.809	3.5	9.4	8.0	4.4	13.4	6.5	2.1	
	3.4	48.9	56.3	1.756	3.4	9.6	7.6	4.4	14.0	6.3	2.3	

	3.5	50.3	56.4	1.932	3.9	10.0	7.9	4.5	13.8	6.4	2.3	
4	4.1	33	39.3	0.488	2.7	5.3	4.3	2.2	7.9	4.6	1.2	f
	4.2	39	44.9	0.894	2.6	6.9	5.4	3.2	9.5	4.9	1.4	f
	4.3	34.5	39.5	0.6	2.5	6.0	5.2	2.9	8.0	4.9	1.3	f
	4.4	35.9	42.6	0.587	2.7	6.3	5.5	2.8	8.5	4.9	1.3	m
	4.5	35.9	42.4	0.695	2.8	6.0	5.1	2.9	8.5	4.6	1.3	f
5	5.1	47.7	55.9	1.578	3.3	11.2	8.5	3.5	11.7	6.4	1.8	f
	5.2	45.7	51.4	1.467	3.4	11.6	7	4.2	9.5	6	2.2	m
	5.3	42.8	50.6	1.186	3.2	8.1	6.2	3.6	11.6	5.5	1.8	f
	5.4	49.4	58.7	1.832	3.4	9.7	7.9	4.0	14.4	6.8	2.3	f
	5.5	48.4	57.1	1.78	3.6	9.1	7.4	4.2	13.8	6.2	2.2	f
6	6.1	27	31.3	0.291	1.8	3.8	3.3	1.5	2.1	3.9	0.8	f
	6.2	36.4	43.4	0.592	2.9	6.6	5.3	2.7	9.4	4.9	1.4	f
	6.3	30.8	36.5	0.416	2.4	5.3	4.2	2.3	6.9	4.4	1.0	f
	6.4	34.8	41.3	0.685	2.9	6.3	5.0	2.5	8.2	4.9	1.3	f
	6.5	28.9	35.3	0.359	2.4	4.3	3.9	2.2	6.2	4.0	0.9	f
7	7.1	33.2	39.5	0.518	2.2	5.7	4.6	2.2	8.0	4.2	1.2	f
	7.2	35.5	41.3	0.652	2.5	6.3	5.2	2.5	8.2	5.0	1.3	f
	7.3	38.2	44.2	0.835	2.7	6.8	5.8	2.7	9.1	5.3	1.5	m
	7.4	40	47.1	0.81	3.2	7.0	5.8	3.4	10.2	5.4	1.6	f
	7.5	29.1	35.2	0.325	2.0	4.8	3.6	1.7	6.0	4.0	0.9	f
8	8.1	36	42.9	0.65	2.4	6.1	5.5	2.6	9.1	4.8	1.4	f
	8.2	37.6	43.8	0.83	3.1	6.8	5.6	2.8	9.3	5.0	1.5	m
	8.3	34	39.4	0.556	2.9	6.1	4.9	2.3	7.5	4.6	1.2	f
	8.4	35.3	41.1	0.715	2.8	6.0	5.3	2.7	8.4	4.7	1.3	f
	8.5	36.4	42.3	0.752	3.0	6.6	5.2	3.1	8.8	5.1	1.4	f
9	9.1	38.8	46.6	0.91	2.6	6.8	5.7	3.1	10.1	5.1	1.5	m
	9.2	40.1	47	1.045	2.9	7.4	5.8	2.9	10.2	5.3	1.6	f
	9.3	37.5	43.4	0.744	3.0	6.7	5.7	3.1	9.1	5.3	1.4	f
	9.4	36.9	43.5	0.699	2.8	6.3	5.6	3.2	9.3	4.9	1.4	f
	9.5	45.9	53.7	1.256	3.6	8.5	6.9	3.7	12.9	6.4	2.0	f
10	10.1	31.8	37.3	0.649	2.2	5.2	4.2	2.5	7.0	4.2	1.1	f
	10.2	30.7	34.8	0.463	2.2	5.2	4.1	2.3	5.9	3.8	1.0	f
	10.3	33.5	40	0.545	2.4	5.9	4.7	2.4	7.8	4.6	1.2	m
	10.4	31.8	38	0.625	2.4	5.6	4.2	2.0	7.1	4.0	1.1	m
	10.5	36.7	42	0.652	2.9	6.8	5.2	2.6	8.4	5.1	1.4	f
11	11.1	40.1	46.2	0.984	3.0	7.4	5.8	3.5	10.4	5.3	1.6	f
	11.2	41.5	48.5	1.084	3.1	7.9	5.9	3.4	11.1	5.8	1.7	f
	11.3	35.6	41.7	0.602	2.4	6.6	5.1	2.6	8.6	5.0	1.3	f
	11.4	36.1	43.4	0.638	2.6	6.1	5.0	2.7	9.0	4.9	1.4	m
	11.5	33.8	38.8	0.585	2.5	6.1	4.6	2.3	7.2	4.6	1.2	f
12	12.1	30	35.5	0.458	2.3	4.7	4.1	2.3	6.2	4.1	1.0	f
	12.2	38.5	46.7	1.024	3.2	7.1	5.8	2.9	10.4	5.2	1.5	m
	12.3	35.1	40.7	0.589	2.7	5.8	4.9	3.0	8.2	4.9	1.3	f
	12.4	33.4	39.4	0.634	2.4	5.8	4.9	2.4	8.0	4.5	1.2	f
	12.5	38.1	44	0.895	2.7	6.8	5.4	2.7	9.1	5.3	1.6	f
13	13.1	33.3	39.6	0.57	2.8	5.6	4.7	2.7	7.9	4.6	1.2	f
	13.2	34	40.6	0.66	2.8	5.8	5.1	2.4	8.0	4.8	1.2	f
	13.3	31.8	37.7	0.515	2.6	5.0	4.7	2.0	7.1	4.0	1.2	f
	13.4	33.4	38.8	0.55	2.9	6.0	4.5	2.8	7.5	4.1	1.3	f
	13.5	31.4	36.7	0.5	2.6	5.3	4.3	2.6	6.9	3.9	1.2	f
14	14.1	47.3	56.7	1.717	3.4	9.0	7.6	3.9	13.9	5.9	2.3	m
	14.2	34.7	40.3	0.575	2.6	5.9	5.1	2.8	7.9	4.6	1.3	f
	14.3	36.2	41.9	0.745	2.8	6.5	5.4	2.5	8.8	5.0	1.4	
	14.4											
	14.5											

15	15.1	36.9	44.3	0.87	2.8	6.4	5.4	2.9	9.1	4.7	1.5	m
	15.2	26.8	31.1	0.339	1.8	4.4	3.7	1.8	5.0	3.7	0.8	f
	15.3	37.5	43.4	0.898	2.7	6.5	5.4	2.8	9.2	4.7	1.4	m
	15.4	38.9	46	0.807	2.9	6.9	5.4	3.2	10.0	5.1	1.5	f
	15.5	43.4	50	1.112	3.4	8.3	6.4	3.9	11.3	5.7	1.8	m
16	16.1	38.1	45.7	0.791	2.8	6.6	5.7	3.3	9.8	4.8	1.5	f
	16.2	43	50	1.223	3.4	8.0	6.4	3.2	11.6	5.4	1.9	f
	16.3	45.6	52.8	1.441	3.3	8.8	7.3	3.5	12.3	6.1	2.0	m
	16.4	43.8	50.9	1.145	3.4	8.4	6.7	3.4	11.8	5.7	1.9	f
	16.5											
17	17.1	44.1	51.9	1.297	3.5	8.5	6.8	3.8	12.3	5.5	1.9	f
	17.2	51.1	59.5	1.705	3.5	10.4	8.4	4.6	14.9	6.4	2.3	f
	17.3	43.5	50	1.021	3.2	8.5	6.8	3.6	11.7	5.5	1.8	m
	17.4	42.8	49.5	1.022	3.1	8.3	6.3	3.2	11.5	5.8	1.8	m
	17.5											
18	18.1	36.5	43.9	0.751	3.1	6.2	5.1	3.0	9.3	4.6	1.4	f
	18.2	37.7	43.9	0.745	2.7	6.6	5.2	2.9	9.3	4.7	1.5	f
	18.3	37.7	45	0.642	3.2	7.0	5.3	3.3	9.4	5.2	1.6	m
	18.4	38.7	45.4	0.643	3.1	7.1	5.7	3.4	10.0	5.4	1.6	f
	18.5											
19	19.1	34.4	40.1	0.558	2.7	5.9	5.0	2.6	7.8	4.8	1.2	f
	19.2	35.5	42.1	0.459	2.7	6.3	4.8	2.5	8.4	5.0	1.3	m
	19.3	32.5	39.7	0.558	2.2	5.3	4.4	2.5	7.7	4.4	1.1	f
	19.4	34.5	39.2	0.526	2.8	5.9	4.8	2.9	7.4	4.9	1.3	m
	19.5	38.1	44.4	0.883	3.2	7.2	5.6	2.7	9.4	4.8	1.5	f
20	20.1	47.2	56.1	1.445	3.5	9.3	7.6	4.2	13.7	5.9	2.1	f
	20.2	47.9	55.8	1.618	3.5	9.3	7.6	3.9	13.7	6.6	2.3	f
	20.3	49.8	58	1.705	3.4	9.6	7.9	4.6	14.2	6.8	2.2	m
	20.4	50.9	60.9	1.955	3.6	9.9	8.3	4.1	15.1	6.5	2.3	f
	20.5	46.1	53.5	1.488	3.2	8.7	6.9	4.0	12.5	6.4	2.0	m

Appendix E

Cluster analysis and principal component analysis plots from Chapter 7.

Hierarchical Clustering Dendrogram

PCA Plot Logjam clusters